Universidade do Minho

Escola de Arquitectura

Paulo Lopes Lago de Carvalho

**(De)materializing Detail: Technology, Structure, Design
Development of a reinforced glass connection technique**

Doctoral Thesis

Architecture /Construction and Technology

Supervisor:

Prof. Paulo J. S. Cruz

Co-supervisor:

Dr. ir. Frederic A. Veer

April 2014

Name: Paulo Lopes Lago de Carvalho

Email address: paulo.carvalho@arquitectura.uminho.pt.com

Title of thesis:

(De)materializing Detail: Technology, Structure, Design.

Development of a reinforced glass connection technique

Supervisors: Professor Paulo J. S. Cruz and Dr. ir. Frederic A. Veer

Year of conclusion: 2014

University of Minho, 15th of April 2014

Signature: _____

To Susana and Martinha

Acknowledgements

Abstract

(De)materializing Detail: Technology, Structure, Design.
Development of a reinforced glass connection technique

This dissertation is motivated by the desire to investigate the impact of innovative materials and construction techniques on the materiality of the architectural object. In particular it intends to question the contribution of the structural use of glass on the redefinition of the constructed limit, focusing on the detail of the connection between panels.

The recent ability to reinforce glass with metal elements, similarly to what happened with the concrete in the past, offers important advantages, compensating the inevitable brittleness of glass. Contrary to concrete, the transparent qualities of glass determine that both the acts of *reinforcing* and *connecting* transcend the simple technical scope. It is considered that a close combination with other materials may provide additional conceptual and phenomenological value if conceived through an integrated approach.

This research proposes to extend the concept of reinforced glass to the scope of the connection in order to *dematerialize* it. The goal is to develop a reinforced glass connection technique that is structurally efficient and industrially feasible. The investigation is based on an integrated design approach applying two complementary experimental methods - laboratorial and industrial. Developed in parallel, they comprise on one hand a set of laboratorial tests to investigate the structural behaviour of the several load transfer mechanisms, on the other hand a direct contact with the various processing technologies of the materials that compose the system.

Among the several sell-supporting structural configurations achievable with the *connecting through the reinforcement* system (prerequisite to ensure the transparent condition of the solution) the *folded* typology was selected for development and construction of a full-scale prototype. The final version of the detail results in a visually faded connection, not only for being composed entirely by transparent materials, but also for the rigorous simplicity of configuration and disposition between the parts. It demonstrates the capacity to *dematerialize* the connection element at the same time that selectively reinforces and *materializes* the glass panels.

Resumo

Detalhe (Des)materializante: Tecnologia, Estrutura, Design.
Desenvolvimento de uma técnica de ligação de vidro reforçado

Esta dissertação é motivada pelo desejo de investigar o impacto de materiais e técnicas construtivas inovadoras na materialidade do objecto arquitectónico. Em particular pretende questionar o contributo da utilização estrutural do vidro para a redefinição do limite construído, a partir do detalhe de ligação entre painéis.

A recente capacidade de reforçar o vidro com elementos metálicos, à semelhança do que aconteceu com o betão no passado, oferece vantagens importantes, compensando a inevitável fragilidade do vidro. Ao contrário do betão, as qualidades transparentes do vidro determinam que ambos os atos de *ligar* e *reforçar* transcendem o simples âmbito técnico. Considera-se que uma combinação estreita com outros materiais poderá proporcionar valor conceptual e fenomenológico adicional se concebida através de uma abordagem integrada.

A presente investigação propõe estender o conceito de reforço do vidro para o âmbito da ligação com o intuito de a *desmaterializar*. O objectivo é desenvolver uma técnica de ligação de vidro reforçado que seja estruturalmente eficiente e industrialmente realizável. A investigação baseia-se numa abordagem de design integrado aplicando duas metodologias experimentais complementares - laboratorial e industrial. Desenvolvidas paralelamente, compreendem por um lado um conjunto de ensaios laboratoriais para investigar o comportamento estrutural dos vários mecanismos de transferência de carga, por outro um contacto direto com as várias tecnologias de transformação dos materiais que compõem o sistema.

Das várias configurações estruturais autoportantes realizáveis com o sistema de *ligação através do reforço* (pré-requisito para garantir a condição transparente da solução) foi selecionada a tipologia *dobrada* para desenvolvimento e construção de um protótipo à escala real. A versão final do detalhe resulta numa ligação visualmente desvanecida, não apenas por ser composta integralmente por materiais transparentes, mas também pela rigorosa simplicidade da configuração e disposição entre as partes. Demonstra a capacidade de *desmaterializar* o elemento de ligação ao mesmo tempo que *materializa* e reforça seletivamente os painéis de vidro.

Table of Contents

x

List of abbreviations

Al - Aluminium

An - Annealed (glass)

EVA - Ethylene-Vinyl Acetate

ETFE - PolyTetraFluoroEthylene

FT - Fully Tempered (glass)

HS - Heat Strengthened (glass)

IGU - Insulating Glass Unit

LVDT - Linear Variable Differential Transformer

PA6 - Polyamide 6 or *Nylon* 6

PC - Polycarbonate

PMMA - PolyMethyl MethAcrylate or *Acrylic*

POM - PolyOxyMethylene

PVB - PolyVinyl Butiral

SG - SentryGlas

T_g - Glass transition temperature

UV - Ultraviolet

I Introduction

1 Introduction to the research

1.1   Background and motivation

The recent acknowledgment of the structural qualities of glass has had a significant impact on its connection detail. The opportunity to avoid the traditional opaque frame to hold the glass element in place freed the architectural object from the inevitability of a materially defined limit, further enhancing the ability to dematerialize its presence.

Despite the growing confidence on the structural application of glass, based on an increasing knowledge on its mechanical behaviour as well as the continuous improvement on manufacturing and transformation technologies, it remains an unsafe structural material. Its brittle behaviour determines that when overstressed it breaks without warning. Contrary to other structural materials, glass doesn't deform plastically before failure. Concrete, before being reinforced, suffered from similar limitations. Both materials behave well in compression but poorly in tension. When steel rods were added to the original mixture of sand, aggregates and cement, reinforced concrete was created offering a composite material that behaves well both in compression and tension. An analogous principle may be applied to glass. If a reinforcing material with high tensile strength is integrated and efficiently connected to the glass by means of an intermediate bond, it is possible to achieve significant post-breakage resistance. In the event of breakage, glass takes the compressive stress whilst the reinforcement assumes the tensile stress.

Contrary to concrete, the transparent quality of glass determines that both the act of connecting and reinforcing transcends the pure technical scope. The combination of another material may deliver additional conceptual and phenomenological value if properly integrated. Several reinforcement solutions apply porous semi-transparent materials like perforated steel plates, that when embedded in the glass do not interrupt the desired capacity to *see through*. The present investigation proposes to extend the concept of reinforced glass to the connection technique in order to dematerialize it. The question is *how a thin steel perforated plate may play an active role in a connection mechanism?*

Extending the reinforcement outwards of the glass panel and mechanically fixing it creates a load path. However its considerable slenderness restricts it contribution to tensile loads. Similarly to the concept of *reinforced glass*, a significant part of the loads must be transferred through the glass itself. A third material with appropriate softness must be added in order to intermediate the glass-to-glass contact.

The effectiveness of the connection system relies on the combination of three load transfer mechanisms: 1) *Adhesive* between glass and steel perforated plate by means of adhesive interlayers; 2) *Mechanical* between the perforated steel plate and an intermediary soft material, using steel bolts and nuts; and 3) *Contact* between glass and an intermediary soft material with the aid of silicone for sealing purpose. The combination of the three-load transfer mechanisms is expected to allow an even load transfer. In the end, the distributed stress and the visual dematerialization become conceptually congruent.

However, this is still a concept that needs to be validated and developed. The technological feasibility and mechanical behaviour are not fully investigated. These are considered essential aspects to integrate in the design development. The challenge is to develop a *reinforced glass connection technique* that is structurally effective, industrially feasible and visually faded within the transparent vocabulary that leads to dematerialization.

1.2   Methodology

The development of the *reinforced glass connection technique* is based on an integrated design approach applying two complementary experimental methodologies:

- *Experimental investigation in an industrial setting* to develop an insight based on contact with the several technologies that intervene in the fabrication process of the connection system. It included analysis, execution and evaluation of the several steps within the transformation work of the materials (glass, steel and polymers). In the glass transformation case, where most of the investigation took place, it was possible to take contact with the whole production sequence from material supply to final delivery.

- *Experimental investigation in a laboratory environment* - to scientifically collect and analyse data about the structural behaviour of the different materials and interfaces that compose the connection system. It included the tensile behaviour of thin steel plates ("the strong link"), the adhesive behaviour of embedded thin steel plates ("the weak link"), the compressive behaviour of intermediate layers in contact with glass ("in between") and the bending behaviour of the connection ("testing the concept"). In a later phase of the connection development, in the scope of the full-scale prototype, the experimental investigation included the analysis of the out-of-plan compressive behaviour of a folded structure.

Concerning the first type of experimental investigation, the work developed within the glass transformation industry included the preparation phase, namely glass cutting, grinding, polishing, cleaning and layering; and the actual lamination phase, using a silicone blanket lamination system combined with an autoclave, where most of the technological challenges were expected to arise. The close contact with the full production sequence was very important to enrich our knowledge of glass and associated materials by learning from experts. Additionally, the possibility to monitor and sometimes execute the work enabled a clear understanding of the material's transformation limits, determined by the material itself or by the technologies involved along the development stages. Understanding the freedom of action was important to push the boundaries of the design work without compromising the feasibility and available time for the research. Concerning the polymers and steel transformation industries, the experimental work was more intense in the later phase of the research concerning the connection design development and execution. It included contact with production techniques namely CNC machining, laser cutting, and polishing in the case of the polymers; cutting and folding in the case of the steel transformation industry.

Concerning the second type of experimental investigation, a broad set of techniques and parameters were selected to collect the data about the mechanical behaviour as described above:

The *tensile behaviour of thin steel plates* was investigated by means of *tensile* tests and the parameters included were "perforated and non perforated" steel plate and "direction of load application" related to the perforation pattern (open-pattern and closed-pattern direction);

The *adhesive behaviour of embedded thin steel plates* was investigated by means of *pull-out* tests and the parameters included were "perforated and non-perforated" steel plate, "adhesive interlayer" type (soft PVB or stiff SG), "embedment depth" of the steel insert (20 mm and 40 mm) and high temperature (40 °C and 75 °C - only on SG specimens);

The *compressive behaviour of glass in contact with different substrates* was investigated by means of *custom setup compression tests* and the parameters included were the "type of glass" (annealed, heat strengthened and fully tempered) and the "type of intermediate layer" (Al, PMMA, PC, POM, PTFE and PA6);

The *bending behaviour of the connection* was investigated by means of *four point bending tests* and the parameters included were "assembly type", "high temperature" (45 °C and 70 °C) and "time of loading".

The out-of-plan compressive behaviour of the folded reinforced glass structure was investigated by a custom setup compression test.

From the conceptual phase, through the development and final validation, the design process received continual feedback from the parallel experimental investigations. The combination of an empirical *hands-on learning by doing process* developed in the industrial setting with the methodologically scientific investigation supported by laboratorial equipment revealed to be critical in the accomplishment of the integrated approach.

Also important for the integrated design development was the possibility to execute several prototypes during the research, which were found to be a very useful tool to critically evaluate the design intermediary decisions. On the one hand it allowed the anticipation of new problems, clarifying the necessary changes to solve them; on the other hand it allowed controlling and improving the constructional and aesthetic quality of the connection that led to the execution of the full-scale prototype.

1.3 Objective

The main goal of this investigation is to increase the number of available constructional means to dematerialize an architectural object by designing an improved reinforced glass connection technique. In this regard it is also a goal of this investigation to contribute to the current knowledge on the technological and structural aspects of glass embedded connections.

1.4 Outline of the thesis

The thesis is divided in five sections comprising a total of twelve chapters. The first section corresponds to the preceding and current text and presents the *Introduction* of the thesis. Here the investigation problem is explained, the methodology is defined, the objective is clarified and the structure of the thesis is presented.

The second section addresses the *Theoretical Framework* that supports the investigation. Chapter 2 *Transparencies* discusses contemporary theories on the dematerialization of the architectural object focusing on redefined concepts of lightness and transparency. The renewed perception of specific historical references is also discussed. Chapter 3 *Structure and detail* describes the relationship between structure and transparent surfaces produced on the scope of this contemporary approach, focusing on the ability of structural glass to confound this distinction. It also addresses the critical importance of detailing on the design of dematerialized shapes, introducing recent technological evolutions that will inform the design. Chapter 4 introduces the investigation *Concept* of *connecting through the reinforcement*. Firstly the theory of reinforced glass is clarified, then the investigation concept is presented, illustrating the different load transfer mechanisms that guarantee the effectiveness of the connection technique, and finally the work of other researchers investigating similar concepts is discussed. Chapter 5 presents the *Materials* included in the investigation, namely glass, polymers and stainless steel.

The third section presents and discusses the *Experimental investigation* conducted to validate the concept and support the development of the connection technique. Chapter 6 presents the experimental investigation on the *Fabrication* of reinforced glass elements, focusing on the specific technological challenge of laminating with protruded pieces. Chapter 7 presents the experimental investigation conducted on the *Structural behaviour*. Initially the load transfer mechanisms were investigated separately - *the strong link* (tensile behaviour of thin steel plates), *the weak link* (adhesive behaviour of embedded thin steel plates) *and in-between* (compressive behaviour of glass in contact with different substrates). Then, the concept is tested and validated by investigating the *bending behaviour of the connection*. Chapter 8 addresses the *Potential problems* related to the influence of external factors on the structural behaviour of polymeric materials that are integrated into the connection. The effect of increased *temperature* is tested on the adhesive and bending behaviour, and the effect of *time* of loading is tested on the bending behaviour of the connection.

The fourth section addresses the several stages of the *Design* development. Chapter 9 addresses the *Design of the connection detail,* starting by discussing the relevant information gathered from previous chapters that critically inform the design possibilities and limitations. Both the technical requirements and morphological possibilities and applications are presented. The design development focuses then on the specific folded geometry connection technique, clarifying the boundary conditions and necessary improvements on the lamination technology. The evolution of the folded detail is described, discussing the main problems and solutions that led to the final detail. The five main versions of the detail are addressed corresponding to the same connection prototypes. Chapter 10 presents the fabrication and construction of a *folded reinforced glass* structure full scale *Prototype* using the investigated connection technique. Previously the results of the experimental investigation on the structural behaviour of an intermediate scale *folded reinforced glass* structure are presented and validated.

The fifth section presents the main *Conclusions and Recommendations* of the investigation comprising Chapters 11 and 12 respectively.

II Theoretical framework

2 Transparencies

2.1   Processes of dematerialization

"What interests me about the transparency is the idea of evaporation. Ever since man became man, he has fought against fate, against the elements, against matter. He started off building stone by stone, then made windows with small pieces of oiled paper, then learned how to do other things. There is a kind of architectural "Darwinism" at work, which is an evolutionary process through which man attempts to cover the maximum amount of space, the largest surface, insulate the most but with the least amount of material, without looking like he did anything. There's been a tremendous push forward that still isn't over and never will be. We can summarize it as follows: how can we resolve the most material problems with the greatest amount of elegance? It evolves the domination of matter". (Jean Nouvel in: Baudrillard and Nouvel 2005, 63)

The progressive dematerialization of the architectural object has been a continuous process, pushed by specific moments in history when knowledge and technique combined to improve the art of building. The XIX century and the consequences of industrial revolution was such a moment. Materials could be tailored to the exact needs by an emerging scientific knowledge. The new born engineering discipline gained its autonomy, investigating new structural solutions out of the new materials. Glass and iron emerged as ever-available solutions that when combined, proved to profoundly transform the architectural morphology. The construction of the Crystal Palace in 1851 by Joseph Paxton created a great impact on society, giving shape to the new era that was emerging (see Figure 2.1). For the first time a large building "obliterated the old opposition of light and shadow, which had formed the proportions of past architecture" (...) creating instead a "room of shadowless light" (Hilberseimer in: Gannon 2002, 23).
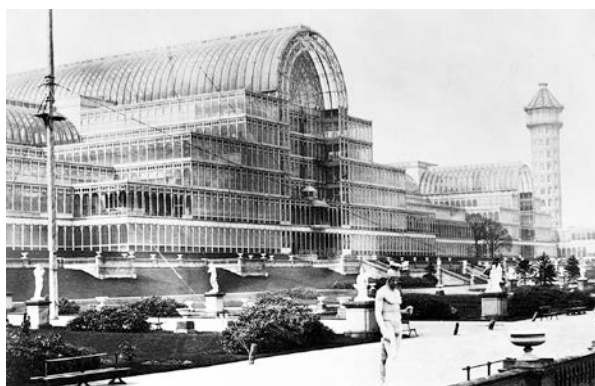
(a)   (b)

Figure 2.1. Crystal Palace (1851) exterior (a) and interior view (b).

Following this landmark a long period of debate concerning the use of iron and glass in architecture took place, particularly the considerable dematerialization that it implied. Semper considered iron to be an "invisible material" since its "tectonic truth or constructional perfection leaded to slenderness cables and ribbons", resulting in a reduced surface to be visually displayed (Georgiadis 1995, 8). The main point of discussion was the alleged incompatibility of dematerialized forms with the monumentality required for institutional buildings (ibid.) along with its acceptance and even encouragement for non-institutional buildings such as railroads and markets. Also the fact that this new construction method proposed an inversion of support and load feelings (see Figure 2.2) caused some strangeness to the traditional onlooker: "Instead of the rigid balance of support and load characteristic of the stone, iron demands a more complex and fluid balance of forces" (Giedion 1995, 102).

This long debate was essential for the maturation of the technique but more importantly and consequential, for the emerging of transparency as an operative architectural concept. The event of the Eiffel tower turned out to be a turning point. Its broad acceptance as a permanent and legitimate cultural landmark of Paris led to the certainty that "invisibility was not the characteristic" - since the Eiffel tower was "the most visible structure in Paris" - but rather transparency (Georgiadis 1995, 35).

Importing transparency to traditional building typologies, and investigating its constructional and spatial consequences was significant for the creation of the architecture of the modern movement. Replacing walls by frames, the space flowed and extended to the landscape. Glass gains a growing importance supported by a continuous technological advancement to provide larger, stronger and clearer glass panes.

(a)   (b)

Figure 2.2. Invertion of support and load feelings in Palais de Machine in Paris (1889) (a) and Pont Transbordeu in Marseille (1905) (b).

"What would concrete be, what steel without plate glass? The ability of both to transform space would be limited, even lost altogether, it would remain only a vague promise. Only a glass skin and glass walls can reveal the simple structural form of the skeletal frame and ensure its architectonic possibilities. (...) These are truly architectural elements forming the basis for a new art of building. They permit us a degree of freedom in the creation of space that we will no longer deny ourselves. Only now can we give shape to space, open it, and link it to the landscape. It now becomes clear once more just what walls and openings are, and floors and ceilings. Simplicity of construction, clarity of tectonic means, and purity of materials have about them the glow of pristine beauty" (Mies van der Rohe in: Kenneth Frampton 1995, 175).

Separation between structure and facade results in the creation of the curtain wall. With it, *transparency*, *simultaneity* and *superimposition*, both in architecture as in art, emerge as the desired modern aesthetics, summarized and appraised by Giedion in the corner of the workshop wing of the Bauhaus in Dessau by Walter Gropius: "In this case it is the interior and the exterior of a building which are presented simultaneously. The extensive transparent areas, by dematerializing the corners, permit the hovering relations of planes and the kind of *overlapping* which appears in the contemporary painting (Giedion 1967, 495). These principles were developed and refined by the following modernist masters, such as Le Corbusier and Mies van der Rohe, until the 1960s when the modern premises begin to be called into question. Post-modernism elects transparency as one of its targets, and several strategies are developed in order to *rematerialize* the architectural object and re-approach it to the complexity of traditional architecture.

The paired images presented by Giedion to illustrate the concept of Space, Time and Architecture (see Figure 2.3(a)) are latter included in Colin Rowe and Robert Slutzky rhetoric of the influential article "Transparency: Literal and Phenomenal" (Rowe and Slutzky 1963).

(a)   (b)
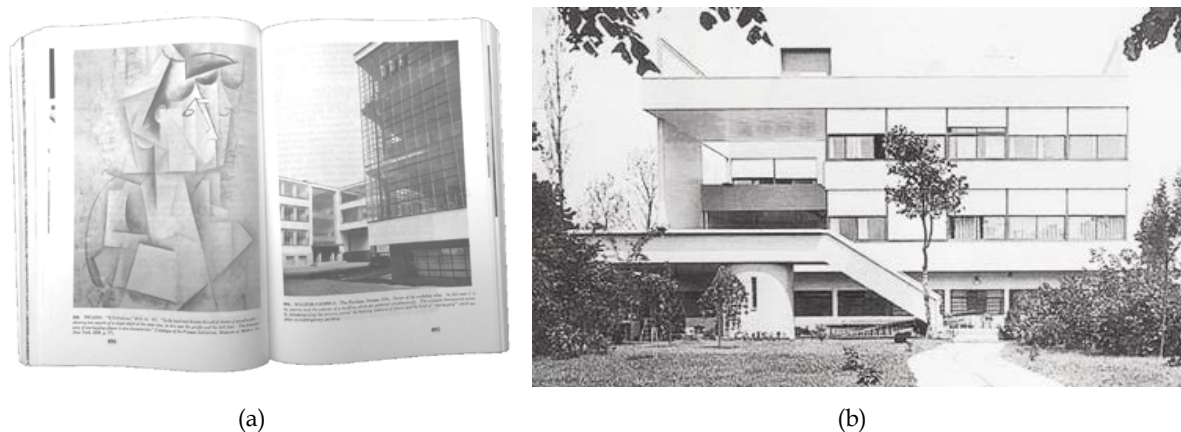
Figure 2.3. Paired image of Space, Time and Architecture showing Picassos L'Arlesienne and Bauhaus Dessau workshop wing (a) and front view of Villa Stein by Le Corbusier (b).

This important publication suggested a redefinition of the modern concept of transparency, with considerable influence in the generations to come. They proposed to distinguish between *literal transparency*, "an inherent quality of substance" (ibid., p. 161) that allows one to see through it that they associated with Siegfried Giedion illustration of the Bauhaus (1925-26) in Space, Time and Architecture (Giedion 1967, 495); and *phenomenal transparency*, "a quality of (spatial) organization" (ibid.) applied to the facade of Le Corbusier's Villa Stein in Garches (1926) (see Figure 2.3 (b)). This second privileged definition was borrowed from Georgy Képes "Language of Vision":

> "*If one sees two or more figures overlapping one another, and each of them claims for itself the common overlapped part, then one is confronted with a contradiction of spatial dimensions. To resolve this contradiction one must assume the presence of a new optical quality. The figures are endowed with transparency: that is, they are able to interpenetrate without an optical destruction of each other.*" (Kepes 1969, 77)

The impact of this formulation was significant and influenced the architectural discourse, particularly in the United States. Meanwhile, as Blau argues "the categorical distinction between two kinds of transparency was strategic. It served to privilege one form of modernism, that of Le Corbusier, over another kind, that of Gropius, and was part of a larger effort to recover a more complex and compelling modernism for architectural practice in the 1950s (when the article was written but not published yet) than the *corporate functionalism* that dominated American practice at the time" (Blau 2007, 51).

In the following years, the architectural practice gradually departed from the modern conception of transparency and its *see through* aesthetics. Important to notice that during this period of probation, significant technological advancements occurred in the glass industry, partially pushed by the parallel industries of automotive and aeronautic.

As we approached the end of the century, a renewed interest for modern transparency re-emerged marked by two parallel tendencies (Vidler 1992, 221). One that sought to recover the modern principles and beliefs, and further develop the capacity of materials to dematerialize using available technical means, and the other which while recalling the use of transparent materials of early modern structures, problematizes its premises and re-evaluates the contemporary concept of transparency.

2.2   Transparency as *Light Construction*

Light Construction exhibition held at the Museum of Modern Art (MoMA) in 1995, is considered by several authors as the first critical framework of the recent re-emergence of transparent architecture. Many of the architects included in the exhibition (Rem Koolhaas, Herzog and de Meuron, Kazuyo Sejima, Jean Nouvel, among others), were at an early stage of a career of great relevance in todays architectural panorama.

Before addressing the actual content of the exhibition, it is important to focus on the curatorial approach by Terence Riley that led to the selection criterion. In previous exhibitions on architecture held at the MoMA, such as the 1932's "International Style" curated by Philip Johnson and Henry-Russel Hitchcock (Hitchcock and Johnson 1997), the 1988 "Deconstructive Architecture" by Philip Johnson and Mark Wigley (Johnson and Wigley 1988), the works were collected based on a set of formal rules that once aggregated would define a new style. In *Light Construction*, rather than the specific components of a style, what was emphasized was an *emergent sensibility*, comprising a more indefinite and intentionally vague stance. In Riley's words "in recent years a new architectural sensibility has emerged, one that not only reflects the distance of our culture from the machine aesthetics of the early twentieth century but marks a fundamental shift in emphasis after decades when debate about architecture focused on issues of form" (Riley 1995, 9). The importance of this approach was that by organizing the exhibition in terms of sensibility rather than style, Riley intentionally "shifted the attention from form and organization into the realm of perception, emotion and affects" (Gannon 2002, 17).

Visual phenomena are a central topic on the exhibition. The works presented applied a wide variety of materials, most of them exhibiting what can be considered *non-literal* or *mediated* transparencies. Among others, there were multi-layered planes of clear, translucent and reflective glass, perforated metal screens, corrugated and translucent plastic sheathings, metal and fabric wires, etc. The richness of surfaces offered by these materials demonstrated to be particularly qualified to capture light and establish with it complex relationships. When extensively and innovatively applied, as in the facades of the exhibited projects, a common feature was discernible. These newly formulated architectural skins were used not to *reveal*, as the modern paradigm, but to *veil*. It is proposed to redefine the relationship of the observer and the object by interposing veiling membranes. The goal is to establish a subjective relationship, one capable of instigating psychological effects on the observer, as Picon states, "transparency is now associated with filtering. It is no longer a passive quality, it represents a proactive behaviour" (Picon 2009, 70).

To explain his thesis, Riley resorted on a literary metaphor articulated by Jean Starobinsky, a Swiss literary critic, in which he refers to an episode of Montaigne about the Poppaea's veil[1]: "Why did Poppaea think of masking the beauties of her face, except to enhance them to her admirers?" (Starobinsky 1989, 231). Poppaea was a mistress of the emperor Nero. Being one among many women trying to capture the emperor's attention, she wore a veil to distinguish herself from the competition. The veil works as a mechanism of desire by the mystery that it creates. As Starobinsky refers "in dissimulation and absence there is a strange force that compels the spirit to turn toward the inaccessible" (ibid.). The veil has the capacity to be both "obstacle and interposed sign" (ibid.), feeding ones imagination about what remains on the other side. A balancing state between accessibility and blockage towards knowledge is a critical feature of the veiling act.

 Starobinsky makes an instructive distinction between the act of vision and that of gaze[2]. While the first referred to the immediate act of seeing, the second dealt with the more durational act of "expectation, concern, watchfulness, and consideration". As he referred, "the gaze does not exhaust itself immediately. It evolves perseverance, doggedness, as if animated by the hope of adding to its discovery or reconquering what is about to escape." Contrary to the act of vision where a collection of a number of images occurs (nowadays with an exponential increase) gaze develops, as Starobinsky refers, "a more complex faculty of establishing relations" (ibid., p.232).

The concept of a mediated relationship between the observer and a distanced space is clearly patent on the Saishunkan Seiyaky Women's dormitory (1991) by Kazuyo Sejima (see Figure 2.4 (a)) and Fumihiko Maki's project for a Congress Centre in Salzburg (1992) (see Figure 2.4 (b)), both integrated in the exhibition. The first was conceived as a building to receive employees of a local enterprise, to share this space during their first years of practice. The building's program is organized around a communal living space, which is proposed to be used as an extension of the private rooms. This communal area was designed to be spacious and bright, offering a partial view to the outside road, necessary to keep its privacy assured. The movable walls of the individual rooms leading to the communal area are made of frosted glass, the several skylights are sheeted by corrugated plastic and the facade is covered in most of its area by finely perforated metal screens. The ambient light is repeatedly filtered, acquiring a delicate softness while "the various screened materials (...) impose limitations on vision" (Riley 1995, 11).

---

[1] The title of this essay and the first citation refers to a passage of another essay "That difficulty increases desire", from Michel de Montaigne, a XVI century french philosopher.
[2] Derived from the French word "regard". Also applied by the French philosopher Jacques Lacan in psychoanalitical context to describe the anxious state derived from the moment of personal awareness that one can be viewed, leading to a lost of a degree of autonomy upon realizing that he or she has an external appearance.

<div align="center">(a)   (b)</div>
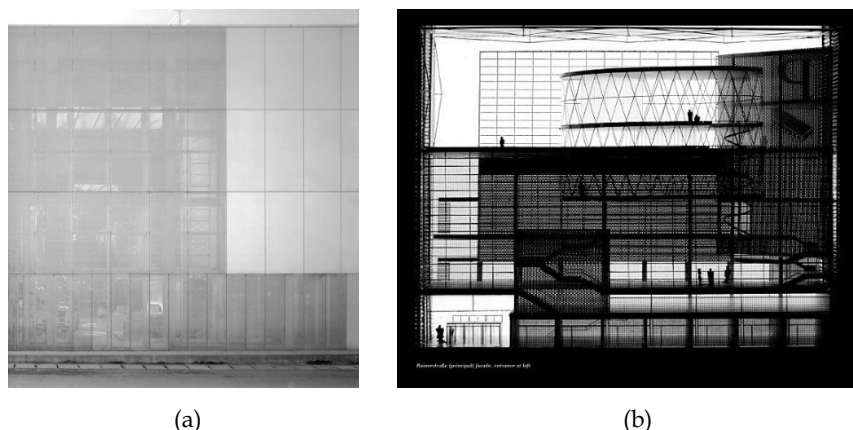
Figure 2.4. Detail of the north facade of the Saishunkan Seiyaky Women's dormitory by Kazuyo Sejima (1991) (a) and model view of the main facade of the Congress hall Centre in Salzburg by Fumihiko Maki (1992) (b).

Maki's project was a Congress Hall competition centre that was never built. The size of the building was significant, comprising a complex program freely distributed through eleven stories. The idea was to conceive it as a permeable volume, materialized through the combination and superimposition of panes of glass, louvers and perforated metal with the actual steel skeletal frame. There was an intention to communicate the interior activities to the outside and use it as part of the architectural expression. In this case it would achieve an extreme complexity by consisting on a simultaneous perception through the transparent layers of plan and section. Although more open than the previous example, the "distance between the viewer and the space is no less rigorously maintained"(ibid.).

Earlier, Antony Vidler also theorized in comparable terms about the psychological effects of a veiling skin, referring to the Rem Koolhaas entry for the Paris National Library competition (1989) (see Figure 2.5). Designed as a 100 m high block raised off the ground, it is "interpreted as a solid block of information, a repository of all forms of memory - books, laser disks, microfiche, computers and databases" (Koolhass 1998, 616). Within this block would be the public spaces contained inside multiple volumes, freely disposed in relation to the overall structure and establishing visual relations with the city. The facade would be materialized with varying degrees of transparency, applying partial silkscreens with irregular white patterns. In Vidler's words, "here transparency is conceived of as solid not as void, with the interior volumes carved out of a crystalline block, so as to float within it, in amoebic suspension. These are then represented on the surface of the cube as shadowy presences, their three-dimensionality displayed ambiguously and flattened, superimposed on one another, in a play of amorphous densities" (Vidler 1992, 221).

(a)   (b)
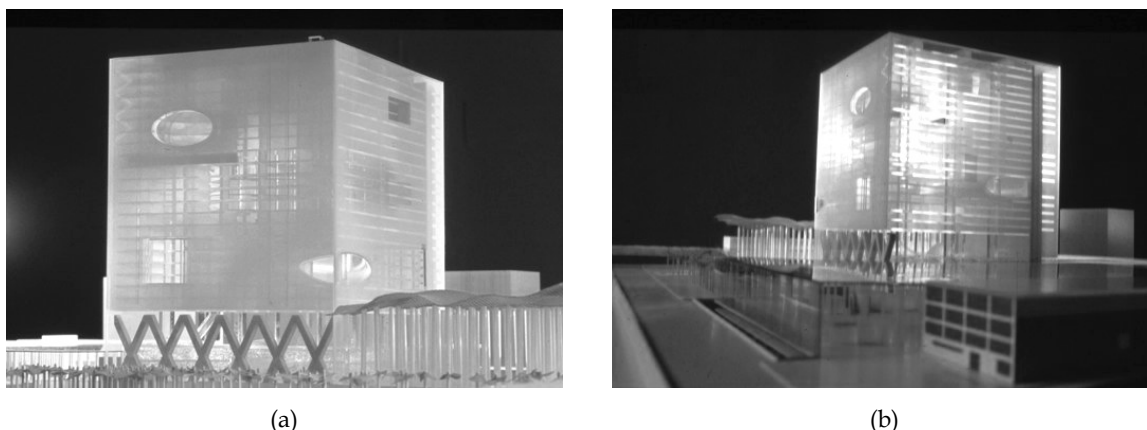
Figure 2.5. Different exterior perspectives of the Paris National Library competition entry model by Rem Koolhaas (OMA).

Translucency, a state here defined between the experience of absolute transparency and its opposite of reflection, may exhibit according to Vidler some *qualities of estrangement*. These are essential to psychologically instigate the observer in similar ways as the uncanny effect of the mirrors. The subject facing the translucent cube "is suspended in a difficult moment between knowledge and blockage, thrust into an experience of density and amorphism, even if it is left before an external surface that is, to all intents and purposes, nothing more than a two-dimensional simulacrum of interior space" (ibid.).

Vidler supported his statement on Freudian and Lacanian interpretation of mirrors, specifically the importance of anxiety and the *space of the sudden* to create the presence of the uncanny. At the end, as Milheiro refers, what interests Vidler on this renewed concept is the capacity of transparency to self-reference in order to "reconquer a fleshy visibility" (Milheiro 2007). Glass can be then worked as "thick, almost palpable substance" (Vidler 1992, 225) approaching it self from traditional architecture.

Conceiving the architectural surface as a screen is understood in the scope of "Light Construction" theorization as an important link to contemporary culture of electronic media. These works positively embrace contemporary culture of images, assuming its abundance and the resulting over-stimulation as an opportunity to investigate new possibilities that may "lead to new forms of artistic engagement" (Gannon 2002, 20). A positive contamination of parallel practices of film, television, video has a clear impact on the constructed materiality. The exhibited works demonstrate an increasing "sensibility to light, movement, and information" (Riley 1995, 22), confidently investigating on the territory of the immaterial thus "increasingly challenging the traditional appearance of permanence" (Tschumi 1995, 53).

The significance of the visual thickening of a surface, in the scope of the painting, was comprehensively defined years ago by the Spanish philosopher Ortega Y Gasset:

> "*The depth dimension, whether spatial or of time, visual or auditory, always appears in a surface. So the surface, strictly speaking, possesses two values: one when we take it as what it is materially, the other when we see it in its second, virtual life. In the latter case, without ceasing to be a surface, it expands in a deep sense. This is what is known as foreshortening. Foreshortening is the organ of visual depth; in it we find an extreme case where simple vision is fused with a purely intellectual act*" (Ortega y Gasset in: Segura 2003, 18).

The consideration about a material and virtual value of the surface has significant pertinence in today's transparent architecture. The Cartier Foundation designed by Jean Nouvel in 1998, materializes this duality in an expressive way. Implemented with considerable distance from the street front, at the exact footprint of an existing building, as mandated by local inhabitants, Nouvel created a building defined by two large glass and steel planes. One of the planes is placed in the continuity of the street façade with the exact same height of the neighbouring buildings and the other is placed back attached to the building volume itself.

Both glazed planes were extended to the sides beyond the necessary length to enclose the building. This extra material assertively employed enables a detachment of the screens, necessary to assume its role as mirroring devices. With it, fractured reflections of the surroundings are produced in order to create what Nouvel defines as "*environmental design*, a mechanism to reengage the contemporary city actively in its controlled and uncontrolled states: a morphology of static material and moving imagery" (Fierro 2003, 110). In-between the two glass planes there is a garden, further reverberating real and virtual images of the trees, which assume significant relevance in the final materiality of the building (see Figure 2.6).

Figure 2.6. Complex superimposition of reflections as seen through the glass planes of the Cartier Fondation captured by the photographer Jordi Bernadó (1998).

The profound effect of the building when mirroring and registering the immediate urban surrounding of the Boulevard Raspail is highly dependent on delicate manipulations of the glass screens. The detailing of these planes has a decisive importance on the overall effect, particularly in the capacity of the building to dissipate into the context.

Also included on the exhibition was the work of several artists whose installations share the same attitude towards perception and construction. Among them Dan Graham's work is particularly interesting for the discussion. From the early 1980s, Dan Graham developed public architectural installations which he called *pavilions*. Intentionally blurring the line between art and architecture, Graham's pavilions usually comprise steel and two way mirror glass to create diverse optical effects: "the inside and outside views are both quasi-reflective and quasi-transparent, and they superimpose inter-subjective images of inside and outside viewers bodies and gazes along with the landscape" (Graham 1999, 174). The pavilions are conceived to be observed from the outside as well as from the inside: "People entering or observing Dan Graham's pavilions are able to look at a specific site and their place within it. Any change in the lighting conditions, provokes a change in the relative reflectivity or transparency of the pavilions' two way mirror glass, putting the relationship between people and their surroundings into constant flux" (Pimlott 1997, 53).

In recent works such as "Two-way Mirror Punched Steel Hedge Labyrinth" (1996), "Greek Cross Labyrinth" (2001) or "Performance Café with Perforated Sides" (2010) (see Figure 2.7), Graham introduced the perforated metal in his vocabulary. The result is an intensified experience of the pavilions, since each individual viewer when looking through the overlapping steel panels perceives a *moiré pattern*. The interference of this visual effect further calls for individual participation.

(a)   (b)

Figure 2.7. Interior view of "Greek Cross Labyrinth" pavilion (2001) (a) and exterior view of "Performance Café with Perforated Sides" (2010) (b) by Dan Graham.

Transparency conceived as *Light Construction* recurrently refers to the contemporary requirement of direct experience to artistic understanding. This tendency produces art objects which "do not passively await the contemplation of connoisseurs; instead, they act dramatically, engaging experts and laypersons alike on material, emotional, and conceptual levels" (Gannon 2002, 19). Ultimately, as Vattimo refers "the focal point of art (...) is no longer the work, but the experience" (ibid., p. 20).

An important contribution to the understanding of this tendency is given by Rosalind Krauss when proposing a phenomenological reading of minimalist art. It refutes the classical reading in which the works achieve their meaning by becoming manifestations or expressions of a hidden centre, arguing that its geometric shape is instead entirely context dependent: "far from having what we could call the fixed and enduring centers of a kind of formulaic geometry, Minimalism produces the paradox of a centerless because shifting geometry (Krauss 1994, 134). The tendency of minimalism to shift from form to surface, as lodging the meaning in the thin surface of the object strengthens the interest in reflective materials to exploit the play of natural light.

2.3   Revisionist readings of the architectural history

In the previous chapter, a recent method of theorizing design was described, in which a phenomenological approach is valued over traditional formal emphasis. Following and contributing to this tendency, several critics have developed revisionist readings of the architectural history. It not only allowed to re-include and valorise forgotten "master pieces" of architecture, which didn't fit the modern rhetoric, and were therefore overlooked; but also to re-interpret the work of the modern canonical masters, such as Mies van der Rohe, uncovering hidden intentions that prove the complexity and deepness of avant-garde practices.

Designed by Pierre Charreau and built in 1932, the *Maison de Verre* was regarded as *other* compared to the ongoing practice. Although referred in some publications of that time, with a special number from the Architecture d'Aujord'hui (Nelson 1933), the fact that it was filled with ambiguity, materialized through an overlap of transparencies and translucencies, alternating clear and obscured views, was considered by the critics as "anathema to the fresh air and hygiene of the mainstream Modern Movement" (Kenneth Frampton 1986, 380).

It was only in the late 1960s that Kenneth Frampton, aware of the historical blank, embarked with his students on a profound study of the house, from the background to the minor details, leading to a relevant publication (Kenneth Frampton 1969). Before this edition, little information about the house was of public knowledge, particularly the construction drawings, which significance is referred by Blanchet as being "one of the key enabling to understand the singular conception of the house" (Futagawa, Bauchet, and Vellay 1988)..

Starting from the particular attitude towards the site and implementation of the house, it already denoted the distance from modern thinking. The initial will to demolish the totality of an existing house to build a new one, was precluded by an old tenant living on the top third floor who refused to leave. The privileged location on the intellectual and social neighbourhood of St. Germain des Prés district in Paris, led to the solution of completely demolishing the two lowest floors to give room to the desired new building. This *tour de force* insertion consisted on the underpinning of the remaining structure in place using a steel structure. The question of bringing light into a house set back on a narrow courtyard was also determining, revealing Charreau's pragmatism:

"I had to build between two party walls, and the plans called for a division of space according to the needs and tastes of modern living habitats. There was only one-way to get the maximum of light: build entirely translucent facades. I began experimenting in 1927, using large and thick plates of glass, frosted on one side. This first attempt didn't satisfy me at all though. At any rate, and given the fact that the ventilation and heating problems had been solved in a very special way, the principle of doing away with windows was adopted: there would be only small windows for security. At this stage, giving up the idea of using large glass blocks, we began looking for elements which, once assembled, could make unlimited surfaces, but without creating the gaping holes of large glass plates. It was out of the question to think of new materials for such a modest experiment. Among those already existing, I chose Nevada-type glass lens since they seemed to correspond to the conditions of the problem" (Charreau in: Futagawa, Bauchet, and Vellay 1988).

The creation of an uninterrupted glass facade was the ambition, whose type and size of application was a novelty at that time. It was completely filled by industrially produced bricks without openings to courtyard, offering an image of complete uncommon simplicity and sobriety. Previously known structures with glass lenses as the main element of the building skin were reduced to the Bruno Taut's glass pavilion. This delay of over twenty years denounced as Frampton refers "a certain technical insecurity" (ibid.), especially from the manufacturers who are referred as having refused to give a guarantee for such large applications of glass bricks in facades. The problem of the increasing weight towards the lower layers of bricks, which could lead to breakage, was surpassed by an inventive solution comprising a steel grid measuring four blocks wide and six blocks high, directly supported by the main structure (see Figure 2.8). This module turned out as being the basic element of the project's arrangement, defining with refined abstractness the body of the facade.
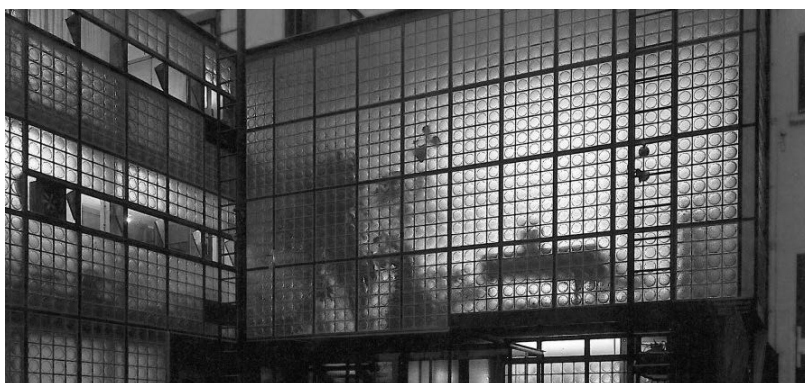
Figure 2.8. Main facade of the Maison de Verre (1932).

Together with the novelty of extending the glazing to the limits of the building, the application of the same coating cement both on the lenses joints and the steel frame of the façade was determinant to materialize a surface "devoid of a chassis, as if unlimited" (Futagawa, Bauchet, and Vellay 1988). The capacity of concave frosted blocks to shimmer as light passes further increased the insubstantial essence of the facade. The view to the inside is limited. It acts as a screen, "showing only what one wishes and leaving the imagination to complete an image of what is behind it" (Segura 2003). Paralleling to Ortega Y Gasset thoughts on the double value of surface, Segura states that the *screeneness* of the Maison de Verre has also a double read: "its own, that which derives from the quality of its surface, texture and weave, and that of constituting a membrane which, by allowing glimpses of light and movement, provides a sketch of the life taking place within it." (ibid.) This characterization reveals a significant proximity to the *light construction* examples. As Riley refers, "Vidler's description of façades that reveal *shadowy presences* could equally be applied to Charreau's master piece" (Riley in: Davidson 1994, 36).

Moving to the interior, Charreau proved that the façade's attitude was by no means a *superficial* accident. Most of the interior partitions are conceived as screens, spanning from floor to ceiling and taking many forms being folding, pivoting, rotating or rolling; materialized to be transparent, translucent or visually opaque depending on light or view point. The necessity to give shape to a demanding program comprising a doctoral practice on the first floor, social living on the second floor and private rooms on the third floor, and the desire to combine it with spatial fluidity triggered the inventiveness for an alternative attitude in which "everything is rational but different" (Banham 1996, 261). The solution developed for the separation of the main staircase is of particular interest. A series of vertical translucent glass panels, framed but elevated from the floor, culminate in a pivoting glazed curved door that separates the private area. It is made of three panels of transparent glass, vertically unframed, to which perforated metal screens are hinged, allowing to subtly manipulate both the view and the light conditions (see Figure 2.9).

| (a) | (b) | (c) |
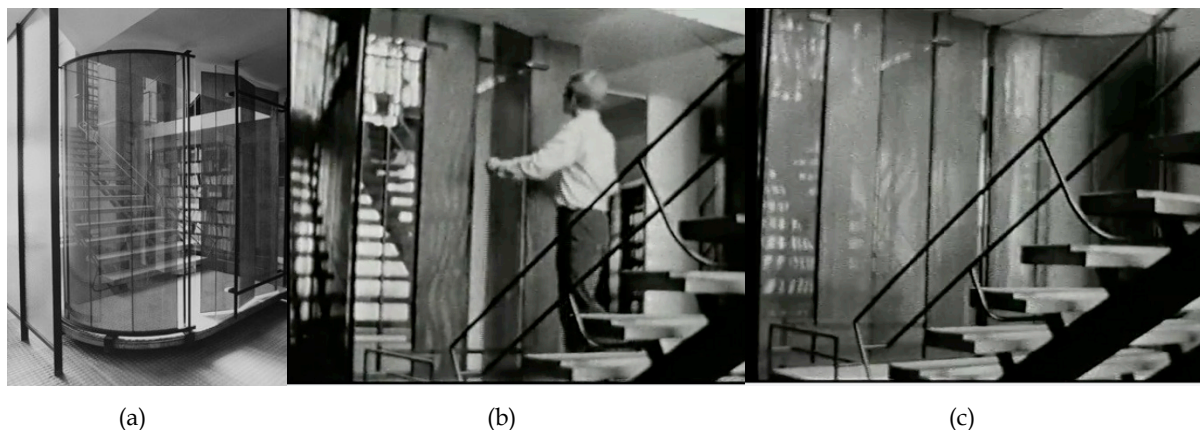
Figure 2.9. View to the main staircase of the Maison de Verre (a) and view to the public corridor with opened (b) and closed (c) movable perforated metal screen.

This solution condenses the will for transformability in which the house in enmeshed, proposing "operations that range from pure necessity to subtle poetic variation" (Segura 2003, 20). The staircase results as both visible and inaccessible, managing privacy issues in a subtle yet thoroughly efficient way. When speaking about the recently inaugurated house, Charreau considered it as being "a model made by artisans with a view towards standardization" (Futagawa, Bauchet, and Vellay 1988, 6).

The 25th anniversary of the Toronto Dominion Centre, designed by Mies van der Rohe in 1967, was regarded as an opportunity to re-approach Mies's body of work and interpret it in an alternative way. Detlef Mertins[1] proposed to focus mainly on its *presence* (Mertins 1994). A building complex composed of six towers and a pavilion covered in bronze-tinted glass and black painted steel that drastically changes its appearance from opaque to transparent, determined by the light and context, reveals as Mertins refers an identity that is both "stable and unstable", "autonomous and contingent" (ibid., p. 23) (see Figure 2.10). This approach challenges received readings of Mies's work, in which the formal issues, as defined by the *International Style*, were considered to be essential. Mies's architecture was frequently described as being governed by an extreme constructional discipline, responsible for the creation of what was considered the self-referential and transcendental modernist object. This interpretation was partially sustained by the classical formal ramifications that the constructive language denounced, regarded as supreme laws that, once followed would lead to an "absolute integrity of form" (Giedion 1967, 607). The appraisal of such a univocal character was severely attacked by post-modern critics, such as Lewis Mumford who pejoratively defined it as a "shoe-box" (Jencks 1977, 40). Several authors have recently opened Mies's work to new questions and hypothesis in a necessary and relevant work of updating and framing its legacy in contemporary practice, "how might critical transformations of Mies's architecture serve for new work appropriate to our own time?" (Mertins 1994, 23).

---

[1] Detlef Mertins was the organizer of "The Presence of Mies" symposium in 1992 together with Brigitte Shim, and Editor of the publication with the same name following the symposium.

Figure 2.10. Sequence of photographs of Toronto Dominion Center from the initial pages of "Presence of Mies" book.

| (a) | (b) | (c) | (d) |
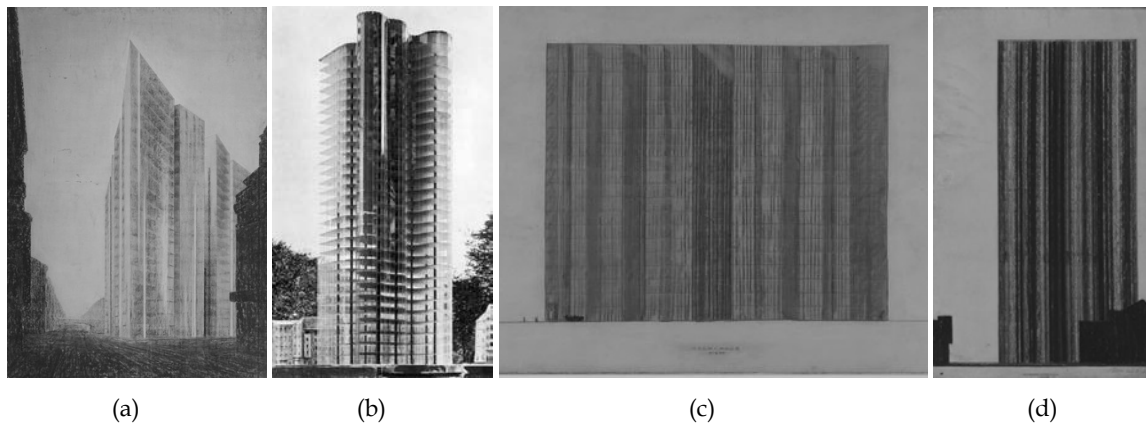
Figure 2.11. Friedrichstrasse Skyscraper Project (1921) exterior perspective (a) and elevation study (c); Glass Skyscraper Project (1922) model view (b) and elevation study (d).

> "*I discovered by working with actual glass models that the important thing is the play of reflections and not the effect of light and shadows as in ordinary buildings. The results of these experiments can be seen in the second scheme published here. At first glance, the curved outline of the plane seems arbitrary. These curves however, were determined by three factors, sufficient illumination of the interior, the massing of the building from the street and lastly the play of reflections. I proved in the glass model that calculations of light and shadow do not help in designing an all glass building*" (Mies van der Rohe in: K Frampton 2007, 195)

The series of radical experiments developed by Mies van der Rohe for skyscraper competitions in the 1920s resulted in several important representations in the form of drawings and montages (see Figure 2.11). They reveal a strong interest about the complexity of glass phenomenology, serving as tools to investigate the reflections when revealed under changing conditions of light. Together they disclose Mies's concerns about the "substitution of glass for mass" as well as "the effect of glass on the observer" (Mertins 1994, 53). Although the structure was a very important expressive element, it is evident that its perception would be accomplished behind a layer of mutable skin. According to Frampton, the delicate attention towards its specific materiality led Mies to treat glass as if it was "a kind of transparent stone". In fact, the same representation technique of charcoal and wax, that he used to investigate the reflective nature of glass (see Figure 2.11 (c) and (d)) was applied by Mies to render the tactility of a subsequent concrete office building, turning clear that what was in question was "a tectonic proposition rather than a gratuitous aesthetic speculation" (Kenneth Frampton 1995, 161)

Figure 2.12. Lake Shore Drive 860 facades.

During these years Mies was in contact with the expressionists movement that had brought in Germany after the First World War, particularly with Bruno Taut and his "Glass Chain". Both skyscrapers proposals were in fact published in the last issue of the Taut's magazine *Fruhlicht,* confirming its relevance in the scope of 1914 *Glasarchitektur* of Paul Scheebart (Scheerbart 2000).

Later in his career, Mies returned to the problem of designing a glass skyscraper with the possibility to actually build it. His sensibility towards the materials was combined with strong research into the possibilities of the dematerialized skin, following studies in dynamic form conducted during his active role at the Bauhaus (Mertins 1994, 59). The result was the departure from the rhetoric of the all glass volume to the diaphanous membrane of glass and steel. On the Lake Shore Drive 860 facades (see Figure 2.12) "the structural frame and its glass infill become architecturally fused, each losing a part of its particular identity in establishing the new architectural reality" (Peter Carter in: Kenneth Frampton 1995, 192). Significant for the discussion is also the perceptual dynamic character of the facade, constantly challenging the observer about its specific materiality: "As one moves around this rotational composition, the projecting mullions either open out to reveal the full extent of the infill glazing or close up to present the illusion of being a twenty-six-story relief construction in opaque steel" (ibid. , p.193).

When describing the fundamental basis of Mies work, Frampton argues that it derived from a "constant struggle between three divergent factors: the technological capacity of the epoch, the aesthetics of avant-gardism, and the tectonic legacy of classical romanticism". Mies's competence on integrating all the three depended to a large extent on the phenomenology of glass and the ability to simultaneously express "transparency and corporeality. The dichotomy revealed itself most sublimely in his attitude to glass, which he used in such a way as to allow it to change under light from the appearance of a reflective surface to the disappearance of the surface into pure transparency: on one hand the apparition of nothing, on the other, an evident need for support." (ibid., p.283)

(a)   (b)   (c)
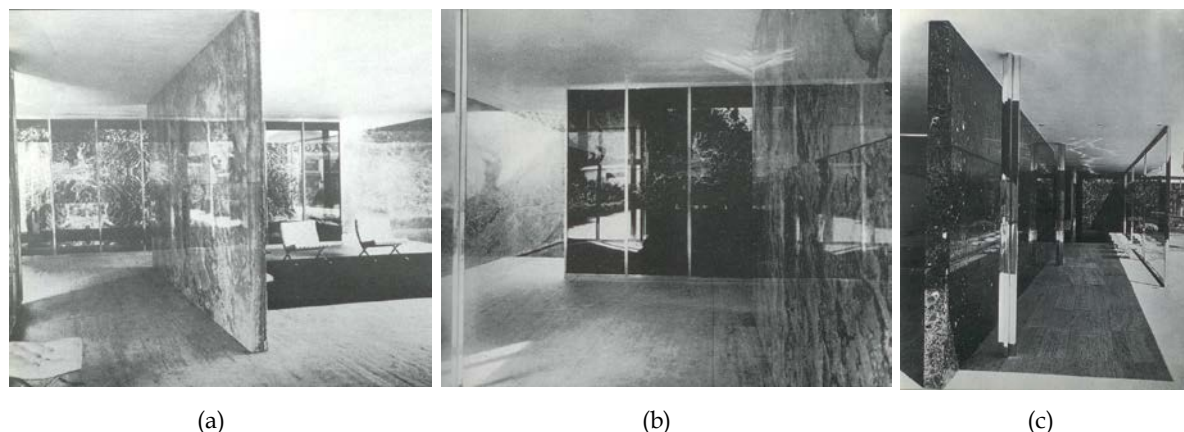
Figure 2.13. Different perspectives of the interior spaces of the Barcelona Pavilion by Mies van der Rohe (1929).

The Barcelona Pavilion has become one of the central buildings around which the discussion of this "new Mies" has been triggered. Built as a temporary construction in 1929, it was thoroughly disclosed through numerous publications after it's dismantling until it was reconstructed in 1986. At the end three pavilions existed for the collective memory, two real and one virtual. This timely fragmented experience and the paradox of rebuilding a temporary pavilion more than 50 years later encouraged an updated critic. Absent in these recent approaches to the Barcelona Pavilion, is the classical connotation towards the regular and visible structure as well as the free flow of space around the neoplasticist asymmetrical planes made of rare and quality materials. Instead, the focus changed to the perception of space and the optical illusions offered to the visitor. Rosalind Krauss argues in fact that the phenomenological approach, advocated as the most appropriate methodology to approach minimalist art, is being imported to the architectural criticism. As she refers, these contemporary evaluations describe the pavilion focusing on the contingence of "every material assuming, chameleon-like, the attributes of something else not itself (...) columns dissolving into bars of light, or glass walls becoming opaque and marble ones appearing transparent due to their reflectivity" (Krauss 1994, 134) Figure 2.13).

Particularly influential for the discussion was the book "Fear of Glass" by the catalan critic Josep Quetglas (Quetglas 2001). It proposed a completely new approach to the pavilion, one that forces an active role of interpretation inviting the viewer to become an actor. As Moneo refers Quetglas writings "helps us to understand the new rules of the game by showing us how we are to understand, elaborate, and live the materials which artists and architects offer us" (Moneo 2001, 9). Describing the pavilion's structure, Quetglas is assertive in claiming its transparent character. As he explains, Mies "masked his pillars optically, covering them with reflections, undefining them. They are transparent" (Quetglas 2001, 84).

Following all these reformulated perceptions of Mies's work, emphasizing the "difficult and contradictory" features with special care about the "contingencies of materiality and perception" in which it operated and was fully immersed, several authors claimed that Mies could actually be considered the "modern patriarch of Light Construction" (Gannon 2002, 20).

The investigation of the modernist avant-garde concept of transparency is nowadays regarded with a renewed interest for its complexity and trans-disciplinary significance. In the early 1920s László Moholy-Nagy assumed, invited by Gropius, the preliminary course and the metallurgical workshop coordination at the Bauhaus. Together with his students he developed what he defined as "exceptional visual experiences" (László Moholy-Nagy 1956, 84). Those were exercises of visual analysis of spaces and forms, where the senses were stimulated using a great diversity of industrial materials like glass, polished metal, perforated plates, acrylics, etc. Those were considered fertile materials in terms of transparency and reflection phenomena, necessary to develop perceptual experiences that challenged the traditional observation. As Nagy referred, what interested him was not "the reproduction of known fields and ways of perception but the production of as yet unknown ones (...) a hitherto unexplored depth of vision" (Laszlo Moholy-Nagy 1933, 688), a depth of vision that Moldering parallels to what Walter Benjamin defined as "the optical unconscious[1]".

There was the conviction that the new visual media (photography, film, etc.) could increase visual knowledge and with it become a decisive progress weapon of the modern man: "Likewise there is a progress in the process of thinking there is also an evolution in the sensory comprehension (...) the vision development not only allows to extend the comprehension of the native but also the progressive development of the human sensitivity, with which more profound and ample human experiences can be made (Kepes 1969, 101). Through his investigation, both pedagogical and artistic, Nagy searched the production of "new optical knowledge", considering that it depended on the capacity to educate the eye in terms "abstract seeing" (Blau 2007, 52).

---

[1] The expression «optical unconscious» derives from the acknowledgement by German philosopher Walter Benjamin of the absolutely original contribution of photography and cinema towards the enrichment of human perception. These new technical images helped discover hitherto unknown - i.e. unacknowledged and analysed by perception and therefore restricted to the space of the unconscious or, as he called it, of an «optical unconscious» - movements and dimensions of reality (Victor Flores).

Figure 2.14. X-ray image used by Mies to illustrate the *skin and bone* concept for the skyscraper competition.

Great advancements were taking place on photography during these years, particularly, the invention of the x-ray photography, a novelty that despite its medical purpose, triggered great artistic interest: "the x-ray photography opened up a new aspect of the visible world. Things that until then were occult to the human eye may be penetrated and seen. Here transparency has a new meaning since the objects depth is evaluated also by its optical density" (Kepes 1969, 80). With the x-ray photographs a simultaneous vision of the inside and the outside is allowed combining the outline and structure in a gradation of transparency, something completely new at that time. It also influenced other artists and architects such as Mies, who deliberately used an image of a human head rendered through x-ray photography to illustrate his concept of *skin and bone* for the referred proposal of a skyscraper in the 1920s (see Figure 2.14).

Nagy methodology to investigate the *new vision* consisted on the combination of two opposed techniques (Molderings 2009, 38): "scientific" (like the x-ray) and "faulty", a technique defined as if the photography was taken by an amateur. In this case, non-conventional points of view were applied, combined with a series of techniques capable of creating a "deliberate impairment of perception" such as "exaggerated perspectives, harsh contrasts, optical deformations, cast shadows that overly darken the subject, false tonal values, etc" (ibid.).

The perceptual capacity of these techniques was initially tested in the scope of a collaboration with Siegfried Giedion to conceive the visual arguments for the 1928 influential book "Building in France, Building in Iron, Building in Ferroconcrete" (Giedion 1995). The book addressed the aesthetic and spatial relationship between the introduction of the new materials and construction methods derived from the industrial production, the great engineering constructions of the XIX century, and the modernist avant-garde architecture of Gropius, Le Corbusier or Mies van der Rohe. Giedion and Moholy-Nagy were capable of, as Georgiadis argues, inventing "an aesthetics of engineering and made it coincide with that of the modern architecture" (Georgiadis 1995, 43).

(a)   (b)   (c)
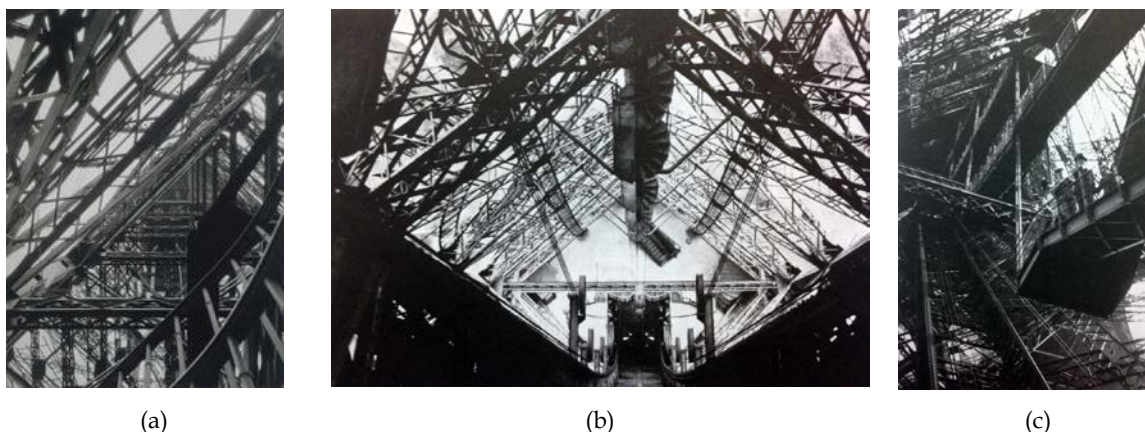
Figure 2.15. Different perspectives of the Eiffel Tower photographed by Giedion in collaboration with Moholy-Nagy.

In the photographs of the Eiffel tower for example (see Figure 2.15), assertive framings were favoured to overall perspectives, combined with negative exposures to "reduce forms to lines, surfaces and volumes, and with that reach such a degree of abstraction that the observer is seduced into abandoning the conventional *perspectival view* and adopting a *cinematographic view*" (ibid.).

Concerning the method of using scientific techniques, as already mentioned, the x-ray photography was a central topic, however it was a technique too costly and complicated for use by amateurs. Nagy developed a method to produce x-ray effects avoiding the need of special apparatus. It consisted on cameraless photographs or *photograms*, based on the positive-negative process to record the varying intensities of light, as Nagy explained: "practically, this is nothing more than a photo negative, produced by laying objects on the emulsion-covered surface. Opaque objects contacting this surface block out all light leaving this part of the sheet unexposed, i.e. white. Shadows of these objects caused by lighting during the exposure result in varying gray-values depending upon the density of the shadows. Areas flooded with light, that is, fully expose, become black" (László Moholy-Nagy 1956, 188). The resulting images (see Figure 2.16) were "diagrammatic records of motion of light translated into black and white and gray values". Its significance rested on the capacity to "grasp new types of spatial relationships and spatial renderings" (ibid., p. 189).
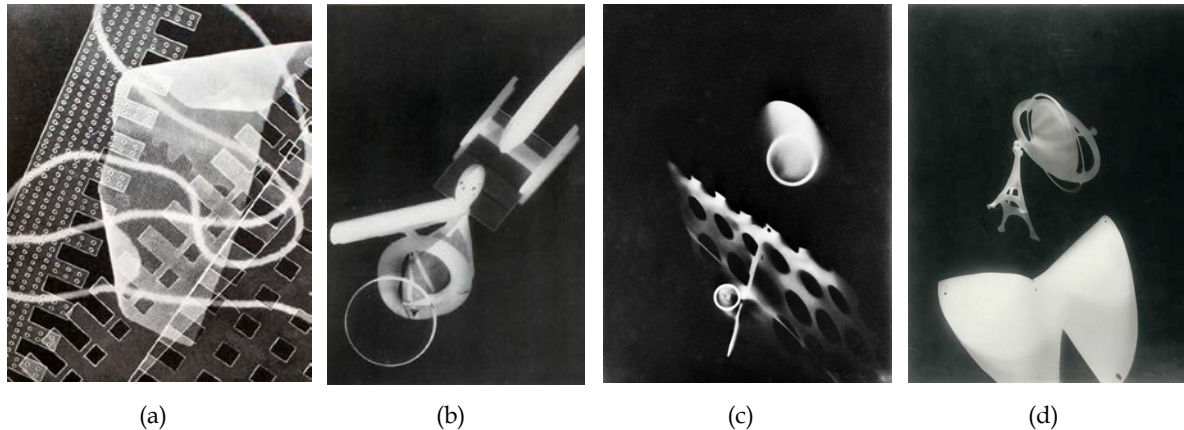
Figure 2.16. Photograms by L. Moholy-Nagy: Untitled 1922 (a), Untitled 1923 (b), Untitled 1925 (c) Fotogramm mit Eiffelturm und Kreisel 1928 (d).

Later, Nagy focused on the capacity of new technologies to enable him working with the light. Once again he develop the means to achieve the goal of "painting with light" and not be limited to the space of the canvas. At the Paris exhibition in 1930 Moholy-Nagy presented the "Light Prop for an Electrical Stage" (1930) (see Figure 2.17), a motorized moving sculpture comprising glass, polished metal pieces such as meshes, wires and perforated plates, encased within a box and illuminated by coloured bulbs. These individual surfaces, prolific light modulators, when moving in close positions, produced an overlapping of light and shadows, continuously changing shape, hue and colour. With this complex apparatus, Moholy-Nagy was successful in translating into space and movement his previous static photograms. The impact was significant in its capacity to transform space by the moving projections of light and shadows. In this case architecture was conceived and influenced by its sensory perception. As Blau refers, "for Moholy-Nagy transparency was a function of projection beyond the object itself: the generation of a spatial phenomenon that is experienced optically, but is invisible. In other words, the object generates space and *spatial effect* but it is not conterminous with the space; it does not inhabit the space, it does not contain space, it instead expresses space" (Blau 2007, 55).
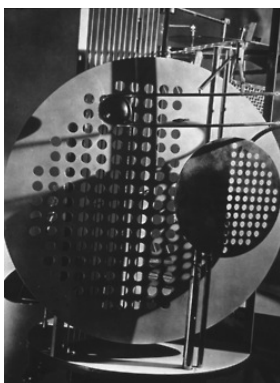
Figure 2.17. Light Prop for an Electrical Stage by Moholy-Nagy (1930).

According to Eve Blau, this conception of transparency as *projection* and its capacity to create space is currently being investigated and expanded by SANAA. In 2006, Sejima and Nischizawa were challenged to design a pavilion as an extension to the existing Toledo glass museum. In a city once considered a major centre of glass production, it constituted a privileged opportunity for SANAA to continue their growing investigation on the concept of transparency in architecture[1]. The program to be hosted by the pavilion, although not very complex, consisted of spaces with very different characteristics: five exhibition spaces, two glass fabrication hot shops, a multipurpose room, a café and other auxiliary spaces.

To architecturally resolve the commission, a special attention was directed to the "idea of the wall and its relationship with space". As Sejima explains: "one wall has two sides, so if you define the shape of the wall, this will affect two adjacent spaces ... we decided to make a wall with two thin membranes not necessarily linked together, and we found that this created a kind of double wall between these two spaces and marked the independence of each room. Both are closed and you can perceive one from the other, but they keep their independence" (Kazuyo Sejima in: Moreno and Grinda 2004, 19).

From a technical point of view, the creation of this *buffer space*, was an inventive solution to solve the great thermal amplitude caused by the ovens inside the hot shops and the exterior climate. This continuous temperature controlled and ventilated airspace, only accessible for maintenance and cleaning, ended up evolving all the interior spaces. However, the architectural impact is much substantial. An autonomous glass wall defines each interior space, leaving in-between a space that is purely relational. This determines that spaces are at the same time independent (physically) and interconnected (visually) (see Figure 2.18).

| (a) | (b) |

Figure 2.18. Different views through the glass layers of the Toledo Glass Pavilion by SANAA.

---

[1] Sejima's work before joining Ruyo Nischizawa to form SANAA was included in the "Light Construction" exhibition.

Although the glass is fully transparent "there are so many curved layers that the building has an opaque feeling to it. You cannot grasp if the reflection is from one layer of glass or another, or whether you are just seeing the other side of the museum. The building produces a completely different feeling of transparency. You can see through it, but it is opaque." (ibid.)

Previously in 2008, SANAA was able to test this concept at a reduced scale when they were invited to design an artistic installation to be installed at the referred Mies's Barcelona Pavilion. The proposal consisted on the creation of a transparent curtain to be implemented at the core of the pavilion. The authors described it as "an acrylic (that) stands freely on the floor and is shaped in a calm spiral. The curtain softly encompasses the spaces within the pavilion and creates a new atmosphere" (see Figure 2.19). They also referred that they "imagined an installation design that leaves the existing space of the Barcelona Pavilion undisturbed" (Sejima and Nishizawa 2010). Despite the *softly* attitude, simple in its arrangement and materiality, the new element establishes a strong confrontation with the previous order. As they state, perceptually the spaces change dramatically, since "the view through the acrylic will be something different from the original with soft reflections slightly distorting the pavilion" (ibid.). The idea of building a pavilion inside the Mies pavilion was also an opportunity to produce "a reflection on their own appropriation of Mies's aesthetic vision"(Moravánszky 2010). In this case, as in the Toledo Glass Pavilion, the overlapping of several layers of glass with different degrees of curvature, constituted an optical device that reflects, refracts but "far more importantly, project spaces onto, through and beyond each other (...) In other words, transparency operates here in terms of projection, generating space beyond the object itself, which is experienced optically but which is immaterial" (Blau 2009, 33).

(a)   (b)

Figure 2.19. Different views of the SANAA's installation at the Barcelona Pavilion.

3 Structure and detail

3.1   Strategies of perceptual dissipation

Contemporary theorization of transparency is characterized by being more inclusive, diverse and thus more complex. At the same time that absorbs a broad set of new *materialities* that operate on the spectrum between total transparency and opacity, proposes to redefine the relationship between the observer and the architectural object. The facade becomes a predominant mediation element that at the same time hides and reveals, triggering subjective interpretations. This new formulation of transparency implies a tension between the observer and the object that parallels the tension between structure and surface of the building itself. As Blau refers "transparency claims to define a new relationship between structure and surface that privileges appearance over form and language" (Blau 2009, 30). The consequence is a perceptual relativization of the building's structure. In Riley words "the structure, while providing support in a straight forward manner, has a diminished potential to determine the appearance of the building" (Riley 1995, 20).

A clear example of the exposed definition is the Goetz Collection building designed by Herzog and de Meuron (1992) (see Figure 3.1 (a)). Its reinforced concrete supporting structure is encased between two layers of translucent glass, which comprise the inner and outer surfaces of the facade. The result is that the middle height volume of the building, opaque with its birch veneer panels, seems to float over the dematerialized lower volume. Similarly, the Kunsthaus in Bregenz (1997), designed by Peter Zumthor, also display a concrete structure that when covered by a continuous translucent facade, results in a *ghost-like* appearance, both during the daylight and when lit from behind (see Figure 3.1 (b)).

(a)   (b)

Figure 3.1. Goetz collection building by Herzog and de Meuron (1992) (a) and Kunstahus Bregenz by Peter Zumthor (1997) (b).

In both cases, the facade sections are conceived with significant depth. It relates to the emergent topic of climate control, which these buildings positively embrace. Besides the generous thickness of these sections, they usually integrate several materials to fulfil multiple technical tasks. Due to this fact, the surface acquires a pronounced depth, comprising an opportunity to increase the visual complexity in the mediated relationship between inside and outside. As Riley refers, "the extravagance of these efficiencies reminds us that isolation is not a simply functional goal in these structures, but a visual and ultimately cultural one" (Riley 1995, 17).

The Cartier Foundation designed by Jean Nouvel pursues a similar goal of relativizing structure towards the observer perception, however, contrary to the previous examples, avoids the translucent dissipation. Applying large panels of transparent glass, it seeks to use multiple reflections in order to destabilize the visual coherence of the structure (see Figure 3.2). Similar formal treatment is conceived both to the detached structure of the street facade and to the one behind, corresponding to the actual building facade. Everything is reduced to perfectly orthogonal abstract grids. When reflected in the diverse panels, a multiplication effect is created leading to a visual superimposition of different geometrical markings, which merge the grid into an undefined amalgam. As Fierro refers, in this case "the structure of the building is put at the service of desired illusionary effects" (Fierro 2003, 110) to an extent of actually causing a weakening of the structure, since the exclusion of diagonal members to brace the structure, as desired by Nouvel to avoid disturbing the visual abstraction of the orthogonal grid, proved to be the cause of a later excessive structural deformation caused by the wind[1].

| (a) | (b) |

Figure 3.2. General view of the different planes of the Fondation Cartier facade (a) and detailed view of the visual merging of real and reflected images on the facade surfaces (b).

---

[1] Diagonal bracings were added later on the ground floor level to prevent further deformation.
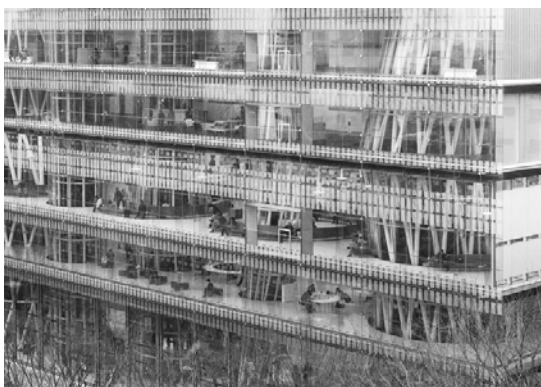
Figure 3.3. Sendai Mediatéque south facade by Toyo Ito (1995).

Toyo Ito project for the Sendai Mediatéque used a different strategy. The structure is concentrated on thirteen large *tree-like tubes* that vertically penetrate the different floors in a continuous movement. This materialization follows the principle investigated by Ito of an *architecture with diffused limits* to answer contemporary condition of floating subjects, as he explains*:* "the aspiration to an architectonic mark, in contemporary language a hardware, that enables a software, the interchangeable program along time, implies a commitment on dematerialization of the building, bind to the elimination of matter through electronic means" (Ito 2006, 29). The structure is based on new calculation methods, which enables to parameterize its constitution, acquiring a formless shape according to the received load requests. Nevertheless, it is considered that in this case, the structure maintains a certain degree of protagonism, which defines the perception of the object (see Figure 3.3).

More recently, the transparency concept investigated at the Toledo Glass Pavilion by SANAA, led to question the relationship of the structure towards the partitions. A deprivation of its visual force was investigated by proposing tubular profiles of just 100 mm diameter painted in white. These are arranged in an apparently random order, removing any possibility of an ordered set, and thus contributing to its dissolution in the layers of reflection and transparency produced by the curved glass (see Figure 3.4). Even the joints between glass panels, conceived to the minimum, are easily confused with the pillars. The result leads some people to assume that is the glass that supports the ceiling, which is not the case (Nordeson 2009, 72).

(a)   (b)
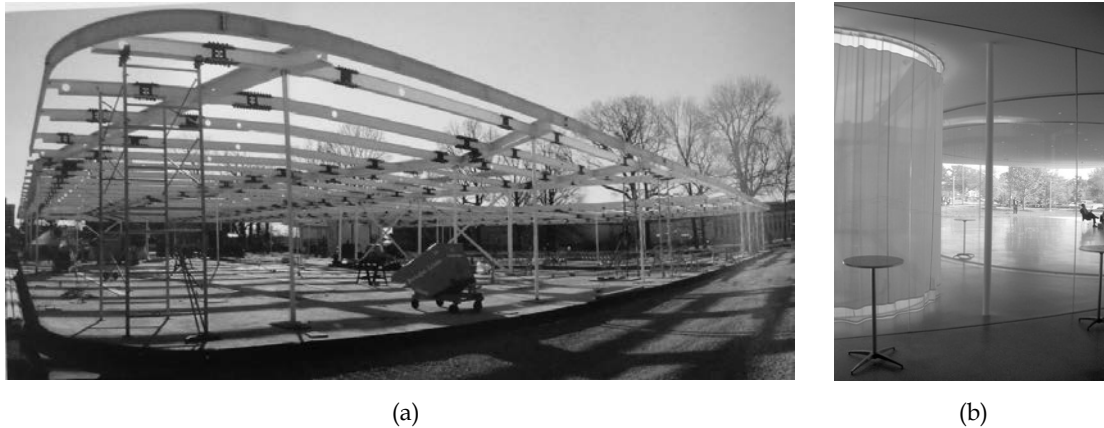
Figure 3.4. View of the structure during construction (a) and view a singular 100 mm diameter pillar behind the glass (b)

In a previously designed proposal for the new Campus Centre for the Illinois Institute of Technology (1997-1998), in which SANAA proposed a similar exercise of fading the structure, the intentions were clear and anticipates the Toledo attitude: "we selected a very small, thin column and very thick glass for the partitions. We wanted to study the idea of reducing the usual hierarchy between structure and partition, where the structure comes first and partitions are infill. So we tried to make the structure disappear and the partitions very thick and heavy" (Kazuyo Sejima in: Moravánszky 2010).

3.2   Glass as structure - erasing the boundary

The commission for the Glass Video Gallery in Groningen (1990) designed by Bernard Tschumi asked for the design of a space to display pop-music videos. Tschumi took this opportunity to "articulate an architectural manifesto about the nature of viewing" (Tschumi 2012, 369). The gallery space is defined entirely by glass planes, exploiting the possibility of making the entire envelope - walls, fins, roof and beams - with structural glass (see Figure 3.5). No material distinction is made between what encloses and what gives stability. In fact, this was the only building exhibited at *light construction* in which glass was applied as load bearing material. The structure gives priority to reflected images by erasing the boundary between support and surface. The resulting phenomenological richness decisively contributes for the purpose of the pavilion as Tschumi refers: "the monitors inside provide unstable facades, while the glass reflections create mirages that suggest limitless space. At night, the space becomes an ensemble of mirrors and reflections, and questions both what is real and what is virtual, and whether the envelope is an actual structure or an illusionistic spectacle" (Tschumi 2013).

The ability of glass to perform structural roles in the building produces a significant shift in the traditional tectonic assumption. However, contrary to common sense, the use of structural glass dates back from the early XIX century when conservatories were built, functioning as laboratories for an informed, yet still intuitive, practice. The description of Loudon, an important figure in the dissemination of this type of structures, concerning the construction steps of the 1827 Large Conservatory at Breton Hall in Yorkshire, sets out the key principle of its design: "there were no rafters or principle ribs for strengthening the roof besides the common wrought-iron sash bar ... this causes some anxiety, for when the iron work was put up, before it was glazed, the slightest wind put the whole of it in motion from the base to the summit ... as soon as the glass was put in, however, it was found to be perfectly strong" (Loudon in: Wigginton 1996, 35).
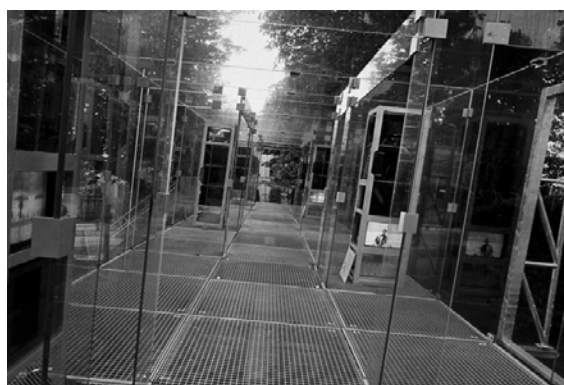
(a)   (b)

Figure 3.5. General view (a) and interior view (b) of the Glass Video Gallery in Groningen.

As Wigginton refers, in this passage Loudon is describing a stressed skin, "in which the apparently fragile transparent membrane is the element which gives strength and stability to the frame. This "minimal and fine detail of an iron-framed membrane" (ibid.) demonstrated to be a clear advancement compared to the previous solutions that inevitably blocked the light.

Another *living* example of this approach is the palm house at Bicton (1840) (see Figure 3.6). It exhibits an extremely slender metal structure to which glass is coupled in perfect harmony. There is no apparent main structure, just a slim top horizontal cover to where the glass stripes converge. The structure resumes to slender arches of iron and very slim columns, so elegant that it is very hard to grasp and gets visually dissolved. It seems like it is inflated from within, an invisible inner pressure moulding the envelope in equilibrium.

(a)   (b)

Figure 3.6. Interior view (a) and facade detailed view of the palm house at Bicton (1840).

3.3   Detailing for dematerialization

Designing towards immateriality is increasingly supported by new synthetic materials, which broaden the available vocabulary of *non-literal transparencies*. Additionally, the way these materials are applied produces significant effect on its perception. As Riley refers, nowadays "architects are dealing with issues of transparency as an attitude towards detail" (Riley in: Davidson 1994, 47). Far more critical that the inherent qualities of the material, is how the material is applied, it's detailing.

A comprehensive discussion about the impact of these new transparencies highly depends on approaching the *discourse of the details*, a discourse as Fierro explains, "where detail assumes a status typically accorded to other conventionally primary aspects - planimetric syntax, spatiality of the interior, or structural order, for example - in configuring and describing the entity of the architectural work" (Fierro 2003, XII). The frame of Fierro's study was the French *grand projects* of the 1990s, to which some *light constructed* buildings are related and included. An interesting conclusion of this study concerns the opposed tendencies in ideologically charged transparent construction between "expressive intents" and "available resources". As soon as the principle that "physical construction might be endowed with the potential, through the medium of transparent skins, simultaneously to heighten, transcend and make literal a political construed metaphor of accessibility" (ibid.), revealed to be difficult to implement, detailing of the transparent medium was the focus of attention: "as the meanings incumbent in the glass accrue out of control, the physical elements are simultaneously pared down to their most minimal. Every centimetre between glass and support, every decision to weld rather than screw, every chemical additive to the surface coating of the glass becomes extravagantly significant" (ibid.).

Nouvel's interventions in Paris, also addressed in Fierro's study, were frontally critical to the existing political agendas of full accessibility. Deliberate manipulation of reflections in the Cartier Foundation Building denounces Nouvel's affinity with contemporary culture of images, in this case the image of the city. The construction of the conceptual argument also demonstrated to be highly dependent on the detailing of the facades. As discussed earlier, the Cartier Foundation materializes Nouvel's image of contemporary condition: "it is a metaphor of the lack of limits between the real and the virtual and a reference to the permanent versatility of all shapes and spaces according to the light and reflections that are receiving" (Solà-Morales 2003, 147).

<div align="center">(a)   (b)</div>
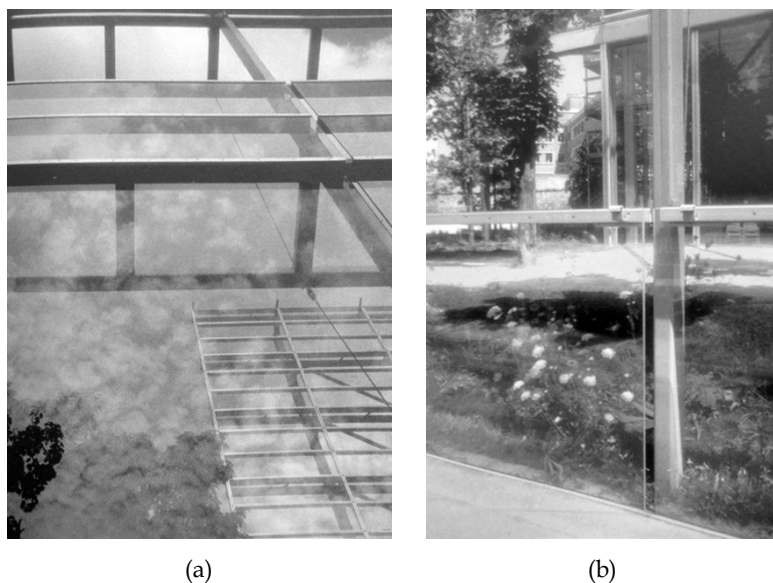
Figure 3.7. Details of Cartier Foundation facades.

Nouvel designed the planes of the facades as autonomous entities that once perceived together tend to visually merge. The multiplying reflected images are interposed with actual real images of the close surroundings, offered by moments of visual silence where the reflective matter is supressed. The detailing of the facade was decisive, making it difficult to distinguish each plane as well as what is inside and what is outside.

Firstly, the already referred geometrical abstraction, achieved by the perfectly orthogonal grid of the screen's structural frame and the actual frame of the building. When both get reflected, an overlap of similar geometric patterns occurs. Additionally, the detailing of the mullions seeks to increase uncertainty between several screens and spaces. The mullion is similarly detailed whether covering interior space or positioned outside on the projected area.

On the freestanding screen, the glass panes are just mechanically fixed instead of adhesively bonded with structural silicone. The vertical joints are left open keeping the same gap between the glass panes (see Figure 3.7). The final reading of the whole results unpredictable and indefinite, efficiently dissipating its presence in the Parisian landscape. Detail has the capacity, as Fierro refers, "to assume a pivotal role in conceptual structures embedded deeply within the building's cultural agendas" (Fierro 2003, 283).

At the Kunsthaus in Bregenz the translucent glass skin that covers the whole building produces a strong material unity. It follows Zumthor's design philosophy demonstrated in several previous projects, in which the building is the result of a search for the essential nature of the materials. Instead of exposing the technological means used to achieve the constructive ends, serenity is valued along the several design choices, with the goal of, as Achleitner refers, "liberate the view towards essential things" (Achleitner 1999, 54).

<center>(a)   (b)   (c)</center>
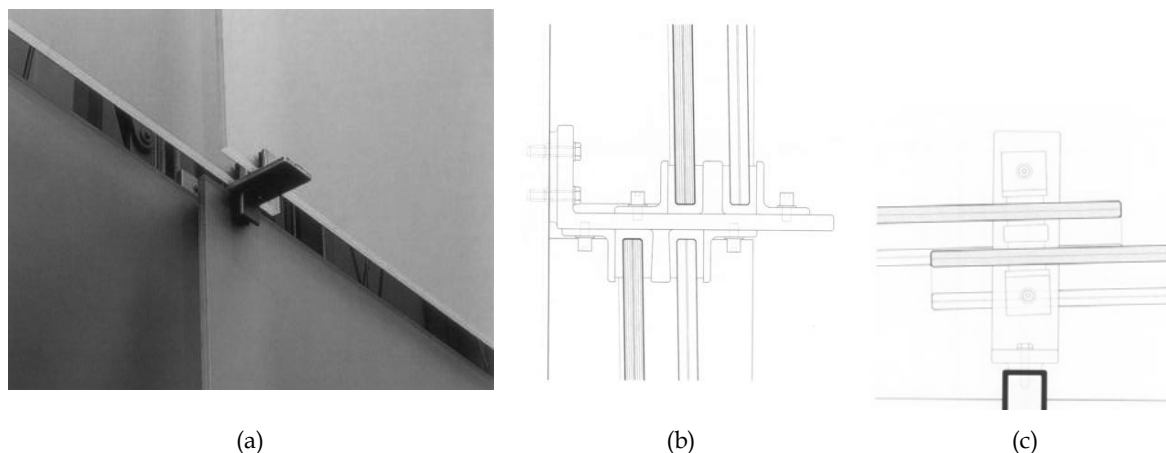
Figure 3.8. Close view (a), vertical section detail (b), and horizontal section detail (c) of the Kunsthaus Bregenz facade connection system.

The facade is composed by finely etched glass panels, all with the same size. These are disposed in a scale-like texture by horizonataly overlapping part of each glass body, in an uninterrupted movement around the building. Translucency combined with this gentle disposition of the glass panels grants it a soft sense, unusually strong in facades of this size. The simple and tactile detailing of the glass support performed a decisive role on this perception, since the panel's integrity turns evident the sensitive approach. The edges are fully exposed, however, no drilling or cutting was performed. The glass panes simply rest on metal consoles fixed with clamps. On each node, four glass panes meet and overlap, slightly resembling a wind propeller when closely observed (see Figure 3.8). The wind in fact penetrates the building skin through the open joints. The metal supports are designed to be condensed and avoid any visual connection to the inner structure. The geometric repetition of isolated metallic points along with the overlap of translucent plates, results in an abstract surface where both elements tend to dissolve into one entity.

At the Sendai Mediatéque a dematerialized structure is conceived with intentionally ambiguous limits. Particularly, the south side in which a double layer facade presents the exterior glass screen visibly detached. In similar terms as the Cartier Foundation, this gesture seeks to blur the limits by extending the facade beyond the actual enclosed volume without defining the edges. The space is prolonged and the boundary between the interior and the exterior results difficult to identify. The glass, instead of being framed along its edges, is just punctually fixed on the corners or edges. This metal element is attached to a transparent glass fin, further increasing the facade autonomy and detachment (see Figure 3.9).

Figure 3.9. Close view of the connection detail between glass panel and glass fin of the Sendai Mediateque south facade.

Some glass panes present translucent silk printed inscriptions along the surface with geometric patterns. It captures the light passing through, adding another layer to the depth of the dematerialized building, and filtering the view to the tree-like filigree structure. This detailing of the facade clearly takes advantage of the structural capacity of glass to assume itself part of the loads and actively dematerialize the structure, as seen both on the fins and facade plan. It enabled to reduce, as already seen in Bregenz, the connection between glass panes and between these and the structure, to isolated points.

3.4   Technology of the frameless - from bolts to bonds

The significant development of construction systems depends on a thorough knowledge of the materials involved. In the case of glass, it's detailing remained limited for a long time due to a generalized lack of information. It was assumed that brittleness was an insurmountable fact, which reduced the design hypotheses to a limited set of conventional framed solutions. However, from the moment in which the structural capacities of glass were explored, the hypotheses multiplied, enabling a considerable advancement on detailing possibilities.

The 1975 Willis and Faber Dumas building designed by Norman Foster, was considered innovative by the way its facade was conceived. Instead of hanged, glass was suspended from the roof, which had a decisive impact on the detailing. It consists on a vertical set of six glass panels, in which the first is fixed on the roof and each piece is hanged from the one above. The glass panels are connected by patch plate to join four glass panels at the corners by means of bolts (see Figure 3.10 (b)).

To compensate for the wind pressure half-height glass fins were added, to which the patch plate connects (see Figure 3.10 (a)). Applying glass this way demanded a high level of confidence and knowledge as Foster himself refers: "it was only by doing our own independent technical research and detailed drawings that we were able to convince a manufacturer that glazing without mullions really was achievable" (Foster 2013).

(a)   (b)
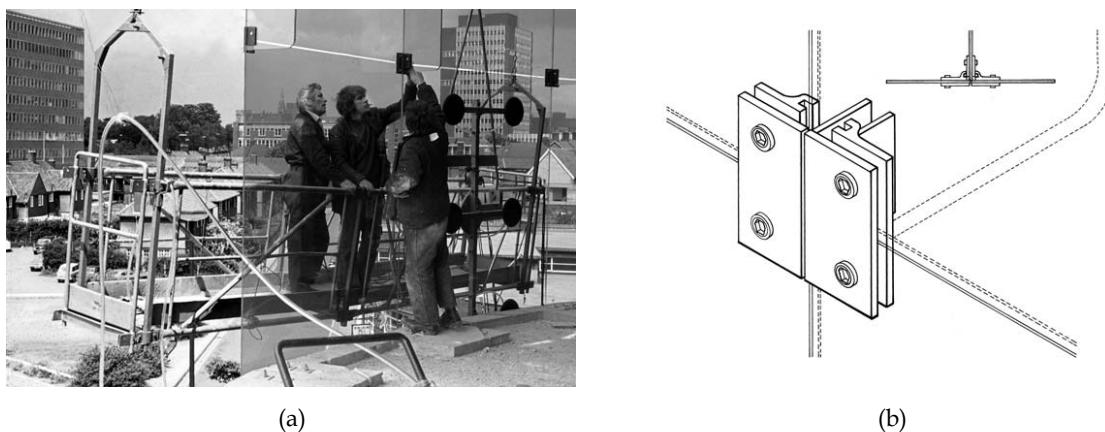
Figure 3.10. Willis Faber Dumas facade during instalation (a) and detailed view of the glass connector (b).

Transferring loads through bolted connections, penetrating the material body is a very common way of connecting other materials such as steel or timber. It has been historically appreciated due to its simplicity, ease of assembly and effectiveness. The ductility of these materials deals well with the unavoidable stress concentration caused by this kind of contact. On the contrary the brittleness of glass requires certain measures to be taken in order to safely use it. The glass pane must be toughened[1] to allow for the high stresses on the holes. These must also be finely ground to a smooth surface to which must be added a suitable compression ring (polymeric or aluminium) to avoid direct glass to steel contact.

Peter Rice delivered an important contribution in the development and dissemination of this type of connection. Departing from the principles applied at the Faber Dumas facade, and the existing technology commercially available by Pilkington (Planar System®), Rice developed an innovative bolted connection solution to be applied at the Cité des Sciences in Paris (see Figure 3.11). The design approach defined the desire to preserve as much as possible the "pure planar nature of the glass surface" (Rice and Dutton 1995, 16). Therefore Rice searched for the possibility to avoid any steel or aluminium profile on the plan, or any glass stiffening fins. As he explains: "the techniques of fixing glass and exploiting its structural capacity (...) allow structural elements to be eliminated from the glass plane. This has particular potential in architectural expression, because until recently the transparent or luminous surface has been dominated by the mullions or glazing bars that have been necessary to hold the glass in place" (ibid.).

Rice's solution increased the safety of this type of application by introducing the possibility of glass to slightly rotate. This is achieved by using an articulated bolt that is introduced in the fitting design, and is positioned in the plane of the glass (see Figure 3.11 (a)). It allowed preventing any bending or twisting stresses at or around the hole, significantly increasing the predictability of this kind of structures.

The influence of Rice on the detailing of glass went far beyond the technological innovation of the system. He was aware that this type of assembly systems tends to produce a sense of technical and industrial determinism that reduces empathy from the observer. To contradict it, he insisted on designing and fabricating the metal parts from cast steel to a more natural fluid shape, instead of using the conventional rectangular machined and welded wrought steel elements. This was found to be an essential step forward as observed in previous experiences on the Centre Pompidou or the Pyramid du Louvre. Metal parts were designed by Rice demonstrated a high sensitivity to the poetics of ontological expression (Fierro 2003, 282).

---

[1] Heat-stregnthened or fully tempered. See section 5.1.1.6.

<div align="center">(a)   (b)</div>
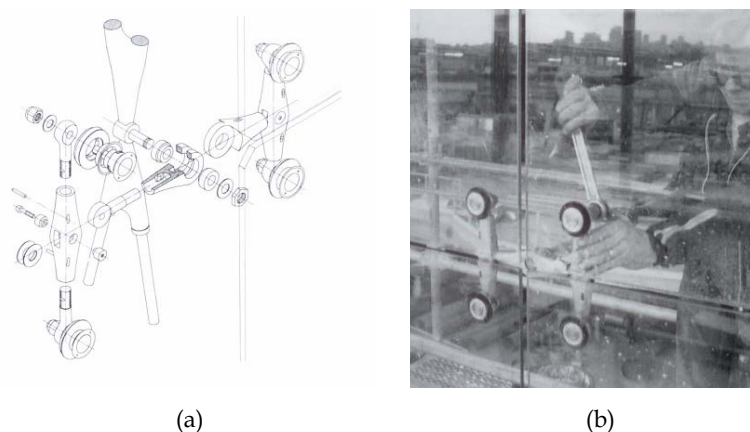
Figure 3.11. Broken apart perspective (a) and exterior view during assembly (b) of articulated bolt connection developed by Peter Rice.

The progress made by the chemical industry in the last century, resulted on the development of increasingly reliable adhesive solutions for the construction sector. These were thoroughly tested for a long time on more innovative sectors such as automotive or aeronautics. Assembling glass units in facades using structural silicone has been practiced in the US since the 1960s. The advantages have been noticed in terms of productivity of application, reducing assembly and sealing to only one step. More evident to the design practice was the avoidance of the mullion at the face of the glass. Transparency was meanwhile limited to the opaqueness of the silicone covering the mullion.

Recently, several fully transparent bonding techniques have become available, with increased adhesive capacities. Besides bonding glass to glass, which has been practiced since the invention of laminated glass, today it is possible to efficiently bond glass to metal. Epoxy glue, for example, due to its high stiffness and strength has been used to bond the surface of different layers of glass, allowing to connect column to beam without using any metal parts.

In the glass staircase detail for the Apple store in NY, designed by James O'Challaghan in 2002, the metal part is adhesively connected to the glass by the polymeric interlayer, which is used to laminate the glass panes (O'Callaghan 2007). The recently available ionomer interlayers (e.g. SentryGlas from Dupont), significantly stiffer and stronger than PVB, allowed to efficiently connect glass to metal. In this case the metal part is innovatively integrated within the glass thickness (see Figure 3.12). This type of connection relies on the adhesive resistance of the contact surface between metal and interlayer to transfer loads. It results more gradually due to the combination of adhesive and contact mechanisms.

(a)   (b)   (c)
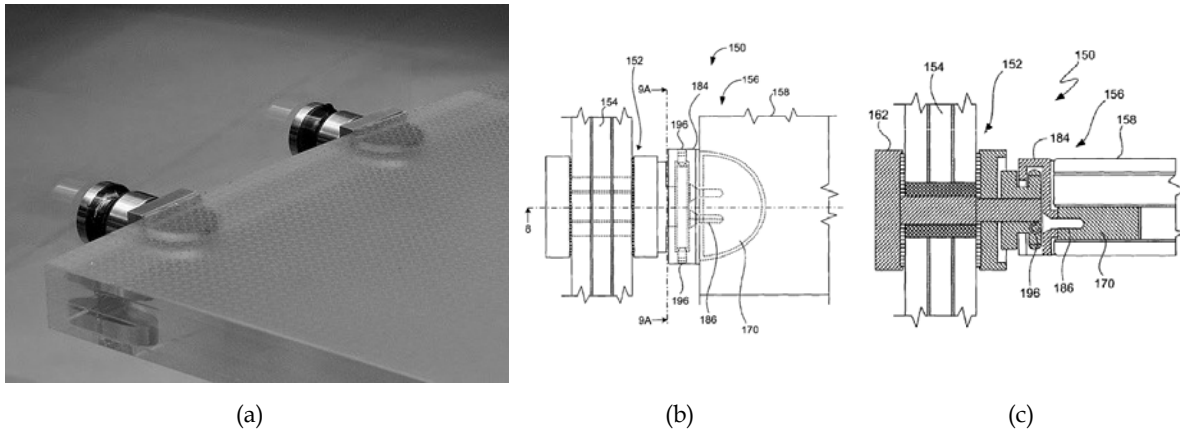
Figure 3.12. General view (a), detailed upper view (b) and detailed cross-section (c) of the Apple store glass staircase embedded connection developed by O'Challaghan.

This patented solution with semi-circular in-plane shape, to ease the build-up of local stresses around the metal insert, was laminated in the third layer of the tread laminate (see Figure 3.12). A compatibility issue is referred concerning the material used for the metal insert (O'Callaghan 2005). Different types of steel and aluminium caused cracking of treads during the lamination and autoclave process and in some cases even after assembly. Titanium was selected because its thermal expansion and conductance properties are much closer to glass, despite the higher cost. To simplify the lamination process and to allow for polishing afterwards, the titanium inserts were designed to be laminated shy of the glass edge.

With the increasing development in fabrication techniques, this detail was further developed in order to be applied in subsequent commissions. The challenge was to connect the glass panes through the laminated inserts and further refine its design in order to avoiding as much as possible the visibility of bolts and screws. In the case of the facade connector (see Figure 3.13 (a)) the solution consisted on hollowing the insert to allow a metal tab to rotate though the joint itself, which was then covered by the silicone, hiding all the mechanism (O'Callaghan and Bostick 2012).

Concerning the staircase connector, while the first version had one side of the fitting embedded in the laminate and the other done by a conventional bolted connection, the new simplified version enabled to laminate both sides of the fitting (Figure 3.13 (b)). The consequences are relevant since the surfaces result more smoothly reflective and simplified. Primacy is given to the essence of the material, instead of revealing constructional features.

<div align="center">(a)   (b)</div>
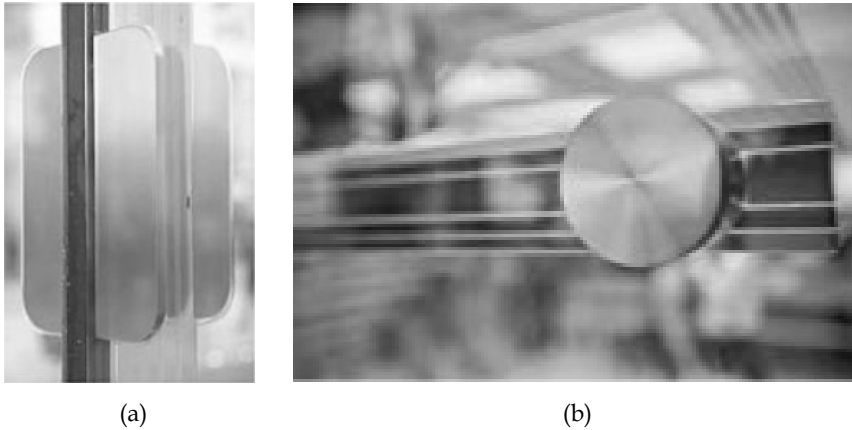
Figure 3.13 Details of the embedded connections of the facade (a) and stairs (b) of the second version of the Apple store in NY.

The design philosophy of the detail follows in a certain sense the tectonic sobriety that Mies van der Rohe advocated along his career. When detailing the steel structures, he consistently preferred to weld instead of bolting. As Frampton refers: "Mies tended to underemphasize the connectivity of the joint and its fabrication; a technical silence that attains its apotheosis perhaps in the flat welds of the Farnsworth House (Kenneth Frampton 1995, 204).

3.5   Embedding towards hybridization

The freedom to embed elements in the glass body has had a significant influence on the connection design, along with a growing awareness of the advantages of detailing glass as a hybrid entity. It is possible to embed porous materials in the laminate thickness, and with it, improve the thermal performance by acting as solar shading. One of the first manufacturers of this solution was the Japanese company Asahi Glass, released in 1989 with the commercial name Lamimetal®. According to the datasheet, this product also provides an enhanced resistance to penetration and splintering, compared with conventional laminated glass. It is presented as a solution suited for anti-theft applications, both in terms of resistance, as by the immediate visual perception through the presence of the perforated plate (Asahi Glass 2011). Lamimetal® consists of a perforated plate that is embedded between two adhesive interlayers and two glass panes (Figure 3.14 (c)). The plate thickness as well as the polymeric interlayer is not discriminated by the manufacturer.

One of the most emblematic buildings where Lamimetal® was applied is the Osaka Maritime Museum in Japan, designed by Paul Andreau and open to public in July 2000. The main part of the building was built over the sea at the Osaka bay, and consisted in a 35 m high glass dome (see Figure 3.14). The concept behind the building was the creation of a *bubble* in the sea, a condition referred by the architect, of "integration in the natural elements that would thus define it in an ever-changing way" (Andreau 2011).

The severe climatic characteristics of the site placed the challenge of ensuring the essential transparency to clarify the architectural concept and, at the same time, achieve satisfactory internal conditions for occupants and exhibition material. Several shading systems were considered including mobile solutions that would run along the facade following the solar movement however, besides the high cost, it was considered that would considerably change the desired result. The final solution was using the Lamimetal®, which by embodying a perforated metal plate laminated in-between two glass panes would control the amount of light through the size of the holes.

<table>
<tr><td>(a)</td><td>(b)</td><td>(c)</td></tr>
</table>
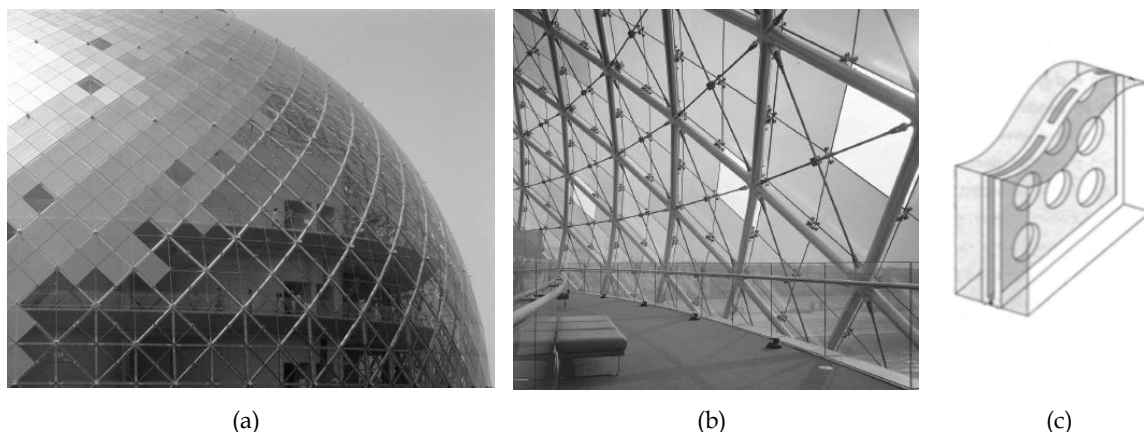
Figure 3.14. General exterior view (a) and interior view (b) of the Osaka Maritime Museum by Andreau; and detailed cross-section view of the Lamimetal® glass panel (c).

The fixation of the glass consists of a point support system without frame, in which the joints are filled with silicone. It was possible to avoid the insulated glass unit due to the fact that the winter periods were relatively short. To optimize this fixed solution, the annual solar route was analysed in relation to the surface of the dome, stating that where the solar gains would be significant, Lamimetal® would be almost opaque, while where negligible the glass would have a high degree of transparency (Dallard et al. 2001, 24). The final result privileged a gradual transition between opacity and transparency and a balance between visibility and comfort. At night the sphere surface fades away when lit from inside thus exposing the exhibition that inhabits the museum.

A similar solution in which a three-dimensional metal plate is embedded in the air space of an insulated glass unit was developed by the German manufacturer Okalux, with the commercial name Okatech® (see Figure 3.15). The main goal of this glazing solution is to conciliate a substantial solar protection with the provision of a certain degree of transparency. In its composition it is possible to apply different types of metallic meshes, expanded or perforated plates that play both functional and aesthetic roles. In addition the system is easy to clean and has low maintenance as the metal cannot get dirty.
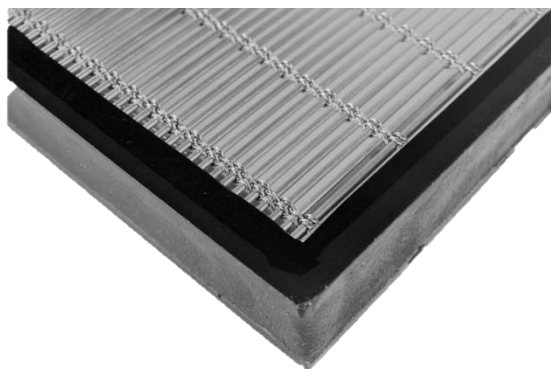
Figure 3.15. Sample of Okatech® by Okalux

The thickness and configuration of the metal layer's solids and voids formalize a three dimensional surface optimized for solar incidence throughout the year. In other words, they function as *micro-shades* that, in the summer virtually block all the sunrays, while in the winter the angle of incidence is lower, allowing the passage of the sunrays and consequent heating of interior spaces. In terms of visibility it works in a similar way, blocking views from superior or inferior angles, increasing transparency as the viewing angle decreases. The manufacturer refers that process of light passage through the unit characterizes by phenomena of refraction and reflection, which allows exploring diverse illumination effects.

Contrary to Lamimatel® this product derives from a current insulating glass unit (IGU) with an aluminium spacer, to which an additional plate of glass is added resulting in two air spaces. During the bonding process of the aluminium spacer, the metal layer is inserted into the air space closer to the exterior pane, together with a special air filling.

At the Seattle Central Library in USA, designed by Rem Koolhaas (OMA) and opened in May 2004, a specific solution for this product was developed, using expanded aluminium plates (see Figure 3.16). Responding to the critical lightning and thermal control requirements of a library, the solution allows to offer a space with a comfortable light for reading, functioning as a shading and anti-glare device. The facade becomes partially transparent, allowing that who is inside may see to the outside, preventing at the same time that who is outside may see to the inside. On the other hand, the solution allowed optimizing natural lightning, lessening the consumption of artificial light. During the day the expanded aluminium plate gives the outer skin a metallic sheen, while at night when lit from inside it becomes unnoticeable.

(a)   (b)

Figure 3.16. General view of the Seattle Central Library (a) and interior view through a hybrid glass facade panel (b).

(a)   (b)   (c)
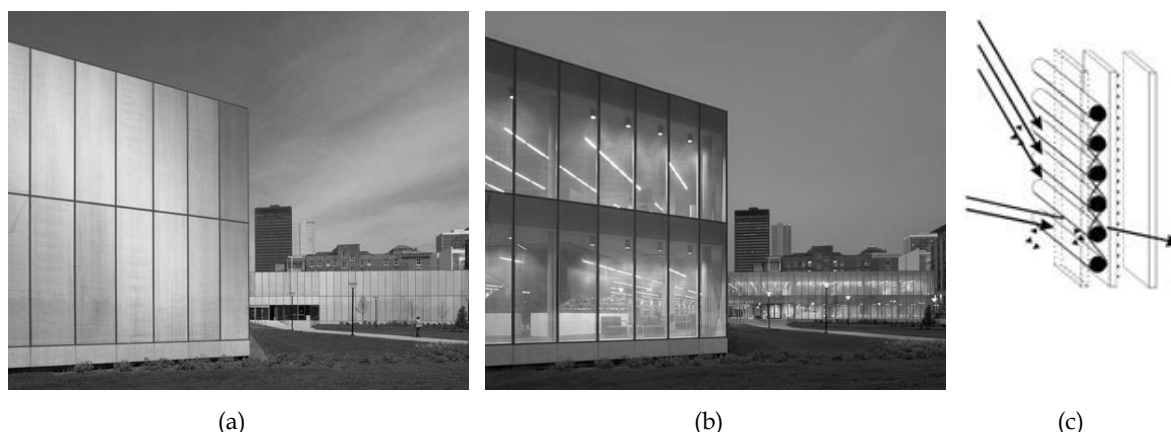
Figure 3.17. General view during the day (a) at nightfall (b) and functioning scheme of the Des Moines Public Library glazing system.

At the Des Moines Public Library, also in the USA, designed by David Chipperfield and opened to public in 2006, a similar solution was used in which the metal layer is a copper mesh. In this case the glass fixing was detailed with a hidden aluminium frame to which the glass is bonded with structural silicone, resulting that during the day when observed from the exterior, seems to be an opaque mass, glittering with a warm coppered tone, and during the night when lit from behind becomes more transparent (see Figure 3.17 (a) and (b)). Seen from inside a certain degree of transparency is always ensured, meeting the intention of offering to the library users a sensations of being at the park reading a book.

As can be observed on the scheme of the Figure 3.17 (c), similarly to the previous building, the metallic mesh blocks the summer sunrays, thus reducing heat gains, allowing at the same time to comfortably illuminate the interior spaces. The system provides certain flexibility in terms of composition, since on the one hand it is possible to insert any type of metallic interim, on the other hand the air space thickness may vary as required. In the Des Moines case, the system comprises, from exterior to interior, an 8 mm thick pane of glass, 2 mm air space with copper mesh in the interior, an 8 mm thick pane of glass with a low emissivity layer, a 16 mm thick air space and a laminated glass composed by two 5 mm thick glass panes forming the inner face. During the fabrication process a complete sealing of the air box that contained the mesh was mandatory to avoid unwanted oxidation and condensation.

4 Concept

4.1   Preliminary concepts

The increasing knowledge on the mechanical behaviour of glass as well as the continuous improvement on manufacturing and transformation processes has encouraged its broader use as a structural element. The unique combination of transparency with high stiffness and compressive strength is highly appreciated thus a number of strategies are being developed to counteract its brittleness. Recent investigations on the post breakage behaviour of glass focus on the consequences of failure rather than the probability of failure (Louter 2011, 5). Only achieving significant residual stability does the high safety factor commonly adopted for structural glass applications may be diminished, reducing the need for sacrificial layers and increasing the overall structural robustness. This state of the art design philosophy, which allows for the failure of individual components, while assuring the overall safety was originally adopted in the aeronautical engineering (Schittich and Balkow 1999, 97) with a practical aim to reduce weight and hence costs. A similar approach to glass behaviour is beneficial to make it more competitive compared to other structural materials.

4.1.1   Wired glass

When discussing the issue of reinforcing glass the reference to the traditional wired glass is common. It is a familiar image to most people since it was broadly used in many public buildings such as schools and libraries, mostly as an infill for corridor partition doors. This type of glass exists since the XIX century when the double rolling glass production process was invented. During the production of the flat glass according to this method, a thin wire mesh was set between two ribbons of glass prior to the passage through the roller. Once cooled, the two ribbons would fuse and create a mono-mass element with a wire mesh in it. For many years it was the only solution available to hold the glass pieces together in the event of breakage. It was the standard solution applied in public building where a large influx of people was expected, and in which the question of safety in terms of fire was considered critical. The wire mesh had the capacity to retard the breakage of glass due to high pressure of the increased temperature. It would guarantee an extended isolation of spaces, critical in the occurrence of a fire in order to delay the fire propagation and the circulation of toxic smokes. In the case of breakage, the several glass cracks remained retained in the wire, preventing the fall. It was also frequently used in skylights. It revealed in the meantime that the consequences of an impact were potentially serious, since the wounds would be caused both by the broken glass and the sharp edges of the wire. Today this solution is not permitted in many jurisdictions. This has led to the development of expensive fire resistant laminated glass systems.

<table>
<tr><td>(a)</td><td>b)</td></tr>
</table>
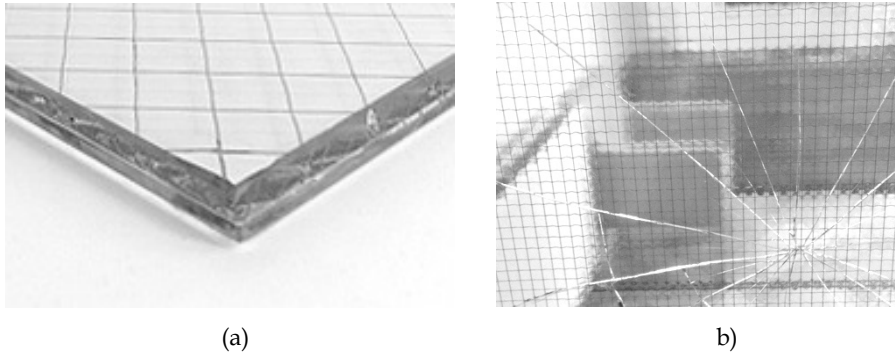
Figure 4.1. Sample of a wired glass pane (a) and image through a broken wired glass (b).

The wired glass exhibits a significant transparency. The reduced diameter of the wire granted a fine quadrangular pattern that from a small distance seizes to be perceptible (see Figure 4.1). The wired glass may have its surfaces textured, a possibility allowed by the production method by applying textured rolls. Wired glass is considered the weakest basic glass product, with the lowest mechanical strength. The glass mass is already damaged with the wire embedment, which results in considerably lower allowable stresses. Additionally it cannot be toughened. It is clear that the future existence of wired glass will depend on its decorative charm for interior design.

4.1.2 Laminated glass

The combination of at least two glass panels with polymeric adhesive interlayers in-between defines the laminated glass concept (see Figure 4.2). The elasticity and adhesive capacity of the interlayer provides a first measure to improve the post breakage behaviour of glass. At the event of a glass breakage it remains bonded to the other(s) and collapse is prevented. If all the glass panes break it is still possible to assure a certain residual structural capacity by means of an interlocking or arching effect. The load dispersal mechanisms and the effective structural capacity depend both on the size of the glass fragments and the type of adhesive interlayer. The larger the glass fragments and the stiffer the interlayer, the better the post breakage performance. The adhesion between interlayer and glass is obtained through a lamination process in which heat and pressure are combined (for more detailed information see chapter 6.3).

Figure 4.2. Sample of a laminated glass unit.

The most common type of interlayer is the PVB (Polyvinyl Butiral) foil[1]. It is estimated that over 95% of all laminated safety glass supplied nowadays employs PVB (I. Stelzer 2010). Created for the automotive industry several decades ago, it was then imported to the building construction sector. Another type of foil interlayer is the EVA (Ethyl Vinyl Acetate). It is mainly used for solar industry applications due to its flexibility and clarity. Recently the company Dupont provided a new type of interlayer considerably stronger and stiffer (Dupont 2009). The commercial name is Sentryglas® (SG) originally developed as an efficient solution for glazing in hurricane prone areas. For the experimental research PVB and SG were the chosen interlayer materials. Extended information about the composition and mechanical behaviour of the interlayers is presented in section 5.2.1.

4.1.3 *Reinforced glass*

Concrete and glass are two very distinct materials but concerning their mechanical characteristics it is possible to make a parallel. With similar density, both materials behave well in compression but poorly in tension. Additionally, the failure mechanism of both materials is essentially brittle. When steel rods were added to the original mixture of sand, aggregates and cement, reinforced concrete was created offering a composite material that behaves well both in compression and tension. An analogous principal can be applied to glass. If a reinforcing material with high tensile strength is integrated and efficiently connected to the glass by mean of an intermediate bond, it is possible to achieve significant post-breakage resistance. In the event of breakage, glass takes the compressive stress whilst the reinforcement assumes the tensile stress.

---

[1] It is possible to bond glass panels using adhesive resins instead of foils. It is a very specific type of lamination mainly used for special laminates such as glass panels with complex geometries. Additionally, the post breakage behaviour of resin-laminated glass is inferior compared with foil laminated glass.

There is a clear difference between reinforcing concrete and glass, which deals with the topic of transparency. The material combined with glass has always a visible presence beyond its structural role that must be attained. There is a wide range of suitable materials to reinforce glass. At a certain level, it has instigated the investigation of different solutions within the same concept.

Research conducted by Frederic Veer on the scope of the *Zappi* research project initiated in 1995 (F. Veer 2005), focused on a concept for a composite glass-polycarbonate segmented beam. The concept went through several stages until a final model was presented in 2003 (F. A. Veer et al. 2003), which combined overlapping glass segments with a polycarbonate foil in between the glass layers and a stainless steel angle embedded in the tension zone (see Figure 4.3). The different materials were bonded together using *photobond* 468 acrylate resin. This configuration showed an improved behaviour since after cracking of the glass occurred the stainless steel strip carried most of the tensile loads allowing a considerable post breakage resistance. With this configuration the cracked glass proved to be capable of taking the compressive loads.

glass

polycarbonate

stainless steel

(a)   (b)
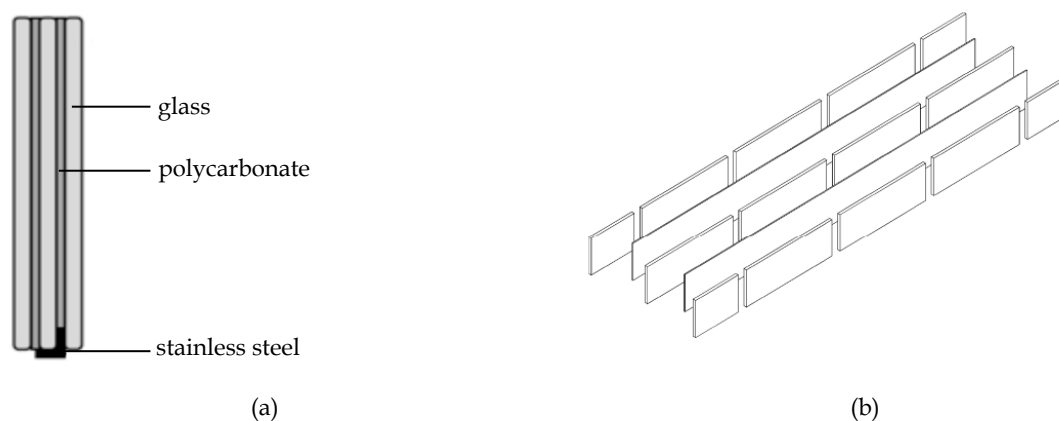
Figure 4.3. Reinforced segmented glass beam investigated by Veer et al. Schematic cross section (a) and segmentation scheme (b).

Further research on this reinforced glass beam concept was conducted by Louter, focusing on a specific beam layout (Louter 2011). It comprised three layers of annealed glass and a square stainless steel section embedded in the recessed intermediate layer. Both SG and adhesive resin were tested as bonding systems. According to Louter the effect of the reinforcement is twofold. It dissipates fracture energy when deformed thus halting the crack propagation, and transfers the tensile force over the crack and transfer it back into the glass through the intermediate bond (ibid., p. 22). Even if the three glass layers break, it is possible to carry a residual load. The experimental investigation addressed the effect of several parameters with significant influence on the structural performance such as temperature, humidity, load duration, reinforcement percentage, among others.
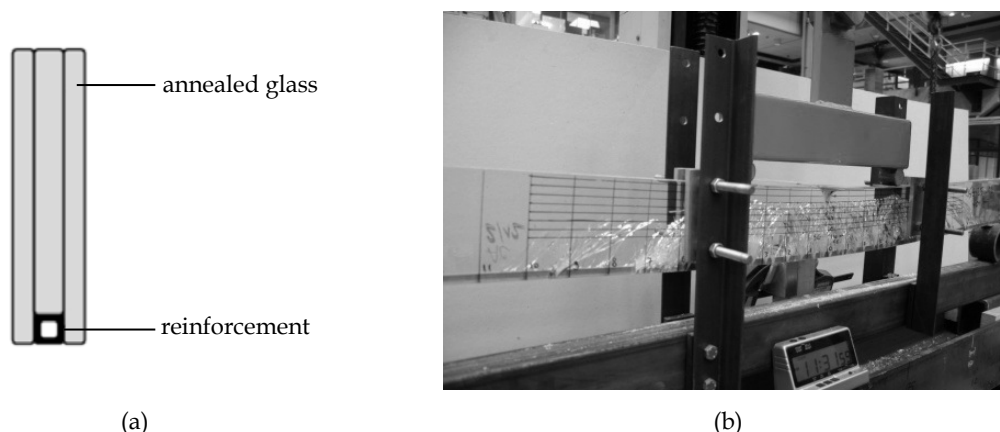
Figure 4.4. Reinforced glass beam investigated by Louter. Schematic cross section (a) and 1.5 m beam specimen during bending test (b).

Pequeno and Cruz investigated the benefits of combining timber with glass (Cruz and Pequeno 2008, 2009). The two materials were bonded using polymer, silicone and polyurethane adhesive. Panel shaped specimens were developed comprising two 6 mm PVB laminated annealed glass on each side and a 200 mm timber core (see Figure 4.5). A comparison was made between the timber panels and the composite glass-timber panels. Both types of panels were tested in vertical and horizontal position for wall and floor applications. The tests showed that composite panels present an enhanced resistance before initial failure and ductile behaviour afterwards.
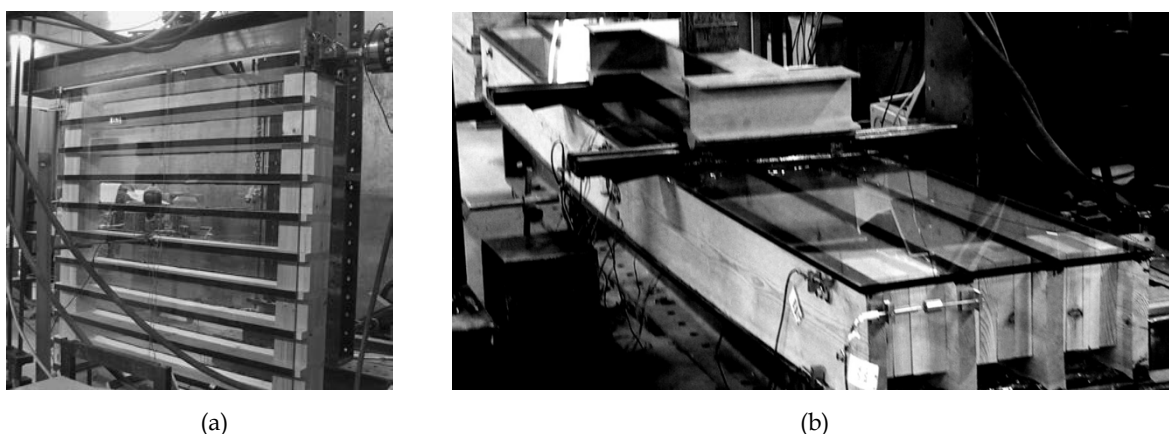
Figure 4.5. Glass-timber composite panels investigated by Pequeno and Cruz.

Reinforced glass investigated by Speranzini consists of glass coupled with one-directional sheets of fibre-reinforced polymers (Speranzini and Neri 2007) (see Figure 4.6). Three types of glass were experimentally investigated (annealed, fully tempered and laminated) with and without two types of FRP (Glass and Carbon). The compound elements consisted on glass with fibres on one side bonded with epoxy resin. The two types of fibres show different mechanical resistance being the carbon FRP superior but preventing any transparency, whilst glass FRP becomes translucent after the application of the resin.

Specimens were tested in three and four point bending to analyse the flexural behaviour. The compound elements showed superior strength before and after initial failure compared to single glass elements. An increase in the glass bearing capacity and ductile behaviour was thus achieved.

Figure 4.6. GFRP reinforced glass investigated by Speranzini et al.

To counteract the reduced residual strength of laminated glass plates specifically made out of fully tempered glass in unfavourable ambient conditions, Feirabend proposed to embed stainless-steel thin perforated metal sheets or fabrics of high tensile strength in the intermediate polymeric layer (Feirabend and Sobek 2009; Feirabend 2008, 2010) (see Figure 4.7). The high tensile and extensional stiffness of the reinforcement combined with a good adhesion by the synthetic interlayer material provided the possibility to increase the residual strength of glass plates in the damaged state. The investigation addressed the different types of glass (annealed, heat strengthened and fully tempered glass) and the influence of temperature and time of loading.

(a)   (b)
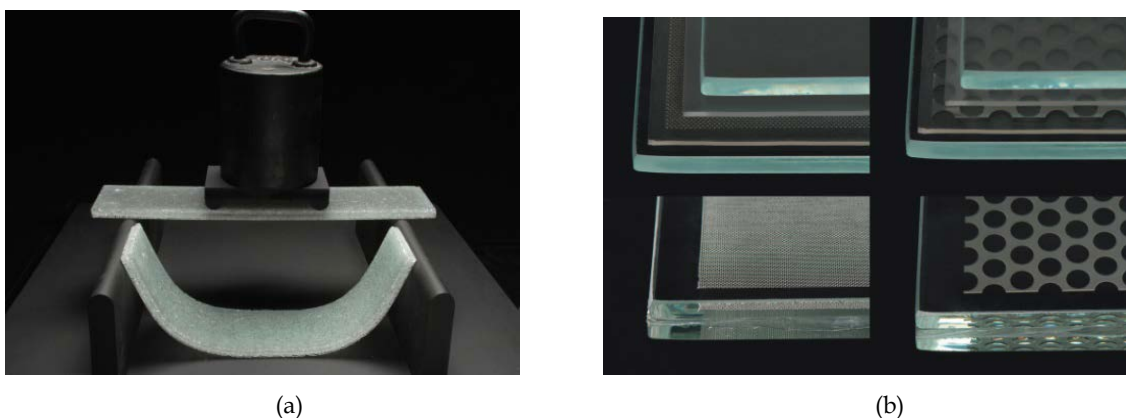
Figure 4.7. Reinforced glass plates investigated by Feirabend view with and without reinforcement (a) and different types of steel reinforcement (b).

4.2   *Connecting through the reinforcement* concept

When addressing the issue of structural connection the two essential characteristics of glass - transparency and brittleness - appear particularly incongruent. The inability of glass to absorb stress concentrations advises the use of large contact areas to evenly transfer the loads. Meanwhile the inevitable opaqueness of metal connection elements conflicts with the desire for transparency. The solution has been reducing the size of the metal element, greatly increasing the applied stress.

The concept of *connecting through the reinforcement* was developed in a different perspective. Instead of seeking to minimize the size of the opaque connection element, it is proposed to dematerialize it, replacing it by a thin perforated steel plate embedded in the laminate. Similarly to the concept of *reinforced glass,* this connection relies for its mechanical behaviour on the combination of the significant compressive strength of glass and the similarly significant tensile strength of steel. Besides extending the reinforcement to the outside of the laminate, the glass-to-glass contact must be intermediated by a suitable soft layer.

The effectiveness of the reinforced glass connection system relies on the combination of three load transfer mechanisms (see Figure 4.8 and 4.9):

- *Adhesive* between glass and steel perforated plate by means of at least two adhesive interlayers;
- *Mechanical* between the perforated steel plate and polymer (intermediary soft layer), using steel bolts and nuts;
- *Contact* between glass and polymer (intermediary soft layer) edges with the aid of silicone for sealing purposes;

The combination of the three-load transfer mechanisms will allow for an even load transfer. In the end, the distributed stress and the visual dematerialization become conceptually congruent.
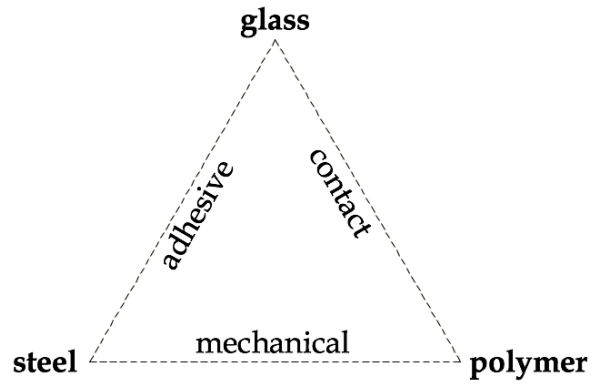
Figure 4.8. Scheme of the three main materials that compose the investigated connection and the correspondent three load transfer mechanisms.
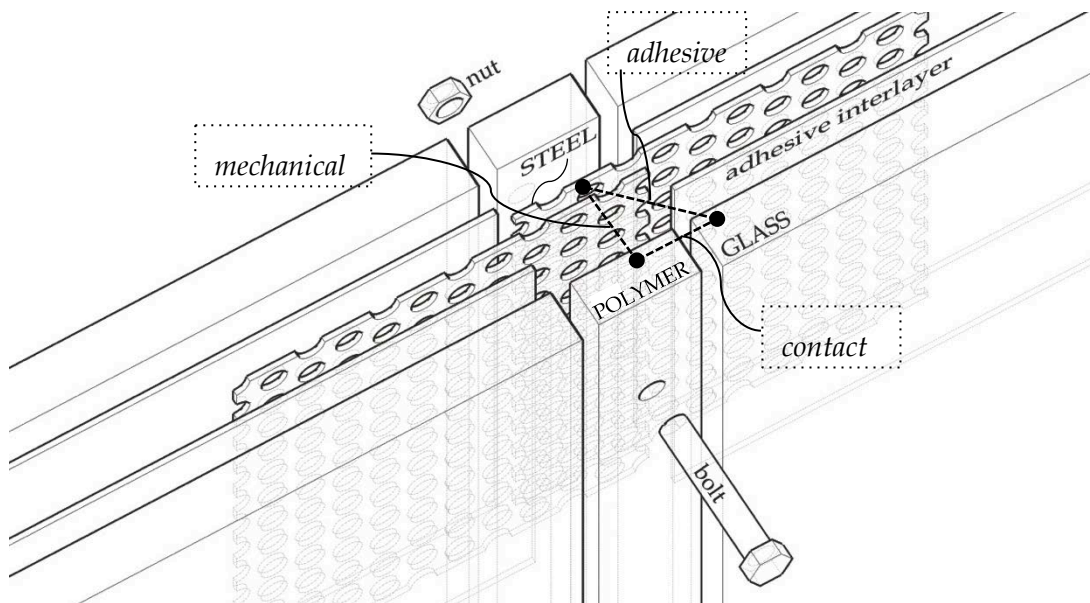
Figure 4.9. Broken apart perspective of the *connecting through the reinforcement* concept.

4.3   Similar concepts studied by others

Bagger et al. studied several types of connection details for plate shell structures of glass (Bagger, Jonsson, and Almegaard 2008; Bagger 2010; Bagger et al. 2007). The most promising connection mentioned by the author was the glued-in plate connection, which is a type of embedded adhesive connection. It consists of an aluminium plate embedded into the glass facet edge using a structural adhesive. The plate shell facets are built up by three layers of glass, laminated together using Sentryglas (Figure 4.10. Tested specimens had the inner thicker pane with an offset of 20 mm from the edge of the two other pans to create a peripheral canal where a continuous 4 mm aluminium plate, with a width of 50 mm, is glued using a structural adhesive. The rotational stiffness of the connection is referred to be adjustable by changing the thickness and material of the glued-in plate.

According to the author, there are several advantages in using this connection. The embedding of the entire detail prevents any extra height to the glass surfaces leaving just 10 - 20 mm width without glass. Its slenderness contributes not to read it as the main structure, and it can be improved by reducing the tested width of the connection. However, both the plate and structural silicone are opaque. The detail is ductile in bending due to deformation of the metal insert. Additionally, significant tolerances are possible to be absorbed in all directions. The main disadvantage deals with the construction method. Half of the connection has to be glued on site, becoming susceptible to adhesion problems. It is also very difficult to replace a broken facet. Finaly, the considerable thickness of the metal element obligates the use three layers of glass.

aluminium plate
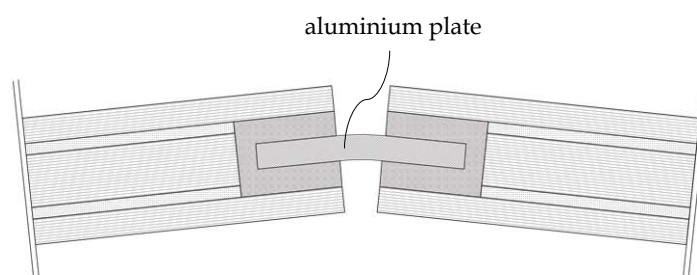
Figure 4.10. Glued-in plate connection investigated by Bagger et al.

perforated
aluminium
plate

(a)   (b)
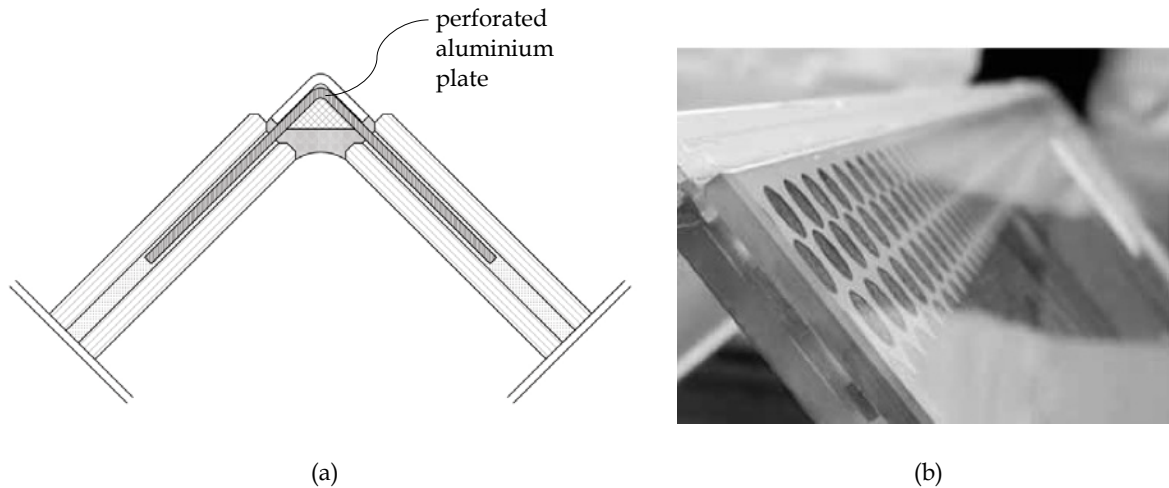
Figure 4.11. Cross-section view of the folded glass roof embedded connection developed by Willareth (a) and photo of prototype (b).

Willareth et al. developed an embedded connection solution for a new folding glass roof for the Historic City Swimming Hall in Zurich installed in 2012 (Willareth and Meyer 2011). Two laminated glass units comprising each two glass panes and Sentryglas interlayers are coupled by a perforated metal strip embedded in both laminates (see Figure 4.11). The coupled laminated glass panels were bent along a pre-perforated line on the metal strip after the lamination process. This gave the desired shape and prepared the folded glass unit to be installed on site where a final silicone joint would be applied. The bending resistance of the coupling metal strips was calculated with sufficient safety margin to provide the required resistance during service. This detail is restricted to a two-unit module, being applied on the upper corner of the folded structure. The lower corner is connected by the roof main structure. Over the connecting folded perforated aluminium plate, an aluminium angle is bonded to protect the connection elements.

Neugebauer developed a solution to increase the residual bearing capacity of glass elements in which a retention mechanism is incorporated. It is proposed to semi-embed a strip of fabric or steel wire mesh into a PVB laminated glass unit. One side of the fabric or mesh protrudes the glass to be fastened to a customized yet traditional frame. (Neugebauer 2005). In case of glass breakage, membrane forces increase, which tend to pull the glass out of the supporting system, forcing the connection to become effective. The goal is to assure that in case of total breakage of the laminated glass for overhead glazing, it remains fixed and is prevented from falling down. This same system may be used for blast resistant glass façade systems (Neugebauer 2013). In case of an explosion, the resulting load transfer of the shock wave to the supports cause the pulling of the glass. Additionally, the author mentions other advantages such as the possibility to increase the span length or to minimize the thickness of the glass, and the possibility to use all types of glass - annealed, heat strengthened and tempered.
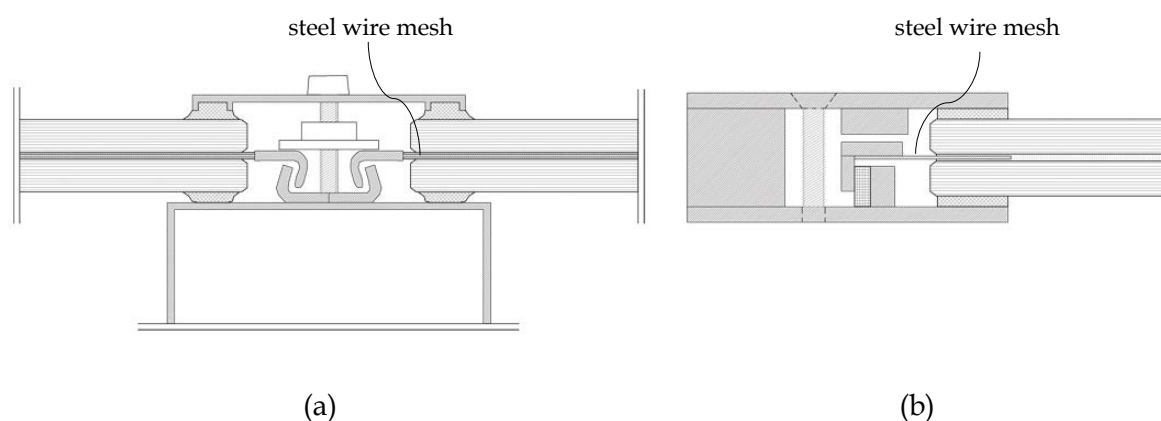
Figure 4.12. Cross-section view of retention mechanism investigated by Neugebauer for overhead glazing (a) and blast resistant glazing (b).

Also Wellershoff investigated an optimized solution for blast resistant facades in which a patented fitting-cable-connector is applied (Wellershoff 2011; Wellershoff et al. 2013). In this solution a perforated carbon-fibre is embedded in a PVB laminated unit and protruded to the outside. It is then connected to a conical fitting outside the laminate by means of flexible Kevlar fibres. This solution bases its retention mechanism just on the corners of the glass where the referred cones are clamped into the fitting (see Figure 4.13.).
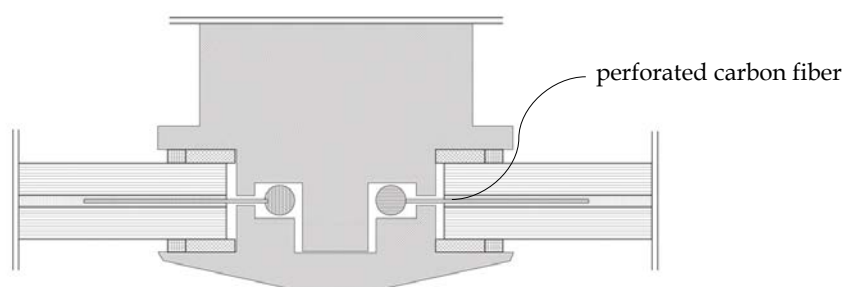
Figure 4.13. Cross-section view of fitting-cable-connector for blast resistant façades investigated by Wellershoff et al.

Puller et al. investigated the load transfer capacity of metal inserts embedded in glass-SG laminates by means of short-term pull-out tests at different temperatures (23 ºC, 40 ºC and 75 ºC) (K. Puller and Sobek 2012; Krestin Puller, Denonville, and Sobek 2011). The test specimen consisted of a 25 mm width high strength steel insert (Domex 700 MC D), embedded at 50 mm length (see Figure 4.14 (a) and (b)). For the tests at lower temperatures a 4,56 mm thick steel insert was used in order to isolate the interlayer deformations by avoiding the yield of the metal. At higher temperature it was not necessary reducing to just 1 mm thick.

Additionally, numerical simulations were performed in order to verify the material models and study the stress distribution inside the laminate. It was concluded that the load was transferred both through the embedded surface area and the edge of the insert, differently distributed according to the temperature. Due to the stiffness of the interlayer at 23 °C, most of the load is transferred through the embedded surface area causing a stress concentration close to the glass edge. On the contrary, at 75 °C the decreased stiffness of the SG led to stress concentration at the insert edge and neighbouring glass surfaces. In order to optimize the load carrying behaviour, adjusted insert geometries were investigated (K. Puller 2012, 86). A fingering geometry was introduced with the purpose of distending the metal body and increasing the edge contact surface (see Figure 4.14 (c)). It was concluded that when transferring load with this geometry a larger area of glass and SG was activated, considerably reducing stress concentrations under the same applied load and embedded metal area.

(a)	(b)	(c)
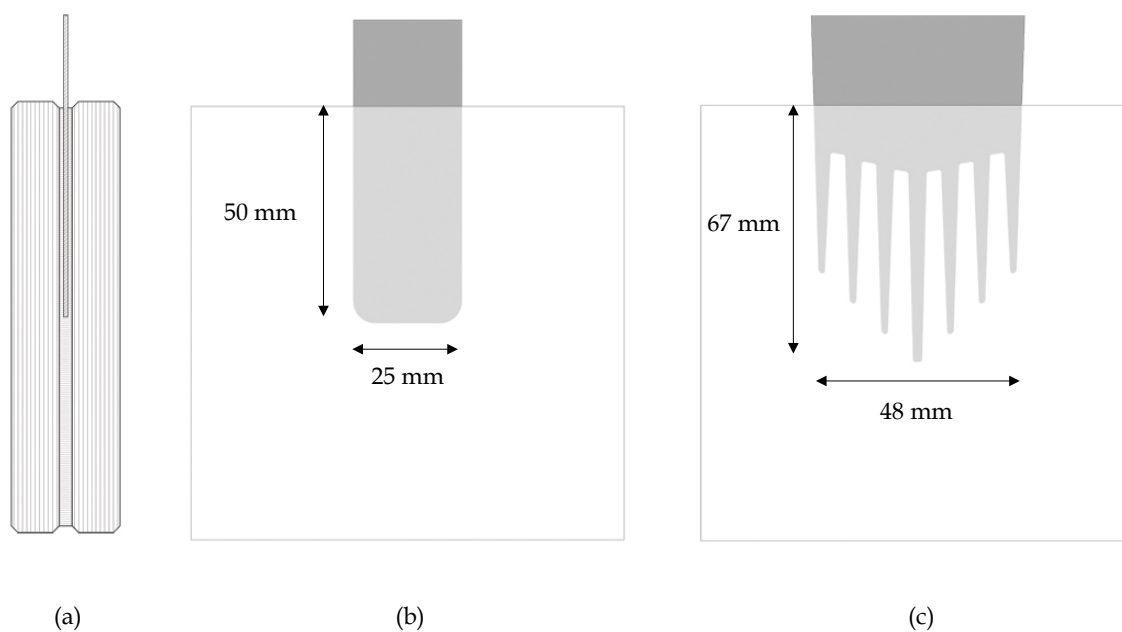
Figure 4.14. Embedded steel connection investigated by Puller et al: cross section (a) side view of initial insert geometry (b) and side view of proposed insert enhanced geometry (c).

Belis et al. studied the failure behaviour of a hybrid glass/steel beam developed by Absoluut Glastechniek (The Netherlands), which has an incorporated connection system (Belis et al. 2009). The hybrid segment is composed by a fully tempered two layer laminated glass core, to which a slender steel frame is bonded with structural sealant along the long edge. This element is responsible for adding ductility to the system, avoiding stress concentrations, and for bridging the tensile forces from one segment to another. In order to do so, a connection system was incorporated in the steel frame, consisting on a steel block placed on the short side of the beam. It is welded to the steel

strip and connected to a similar by means of a high precision rigid bolted joint (see Figure 4.15 (a)). This hybrid system was experimentally investigated in short and long term loading in order to be applied on the roof and facade of a building in The Hague in the summer of 2008 (see Figure 4.15 (b)).

(a)   (b)
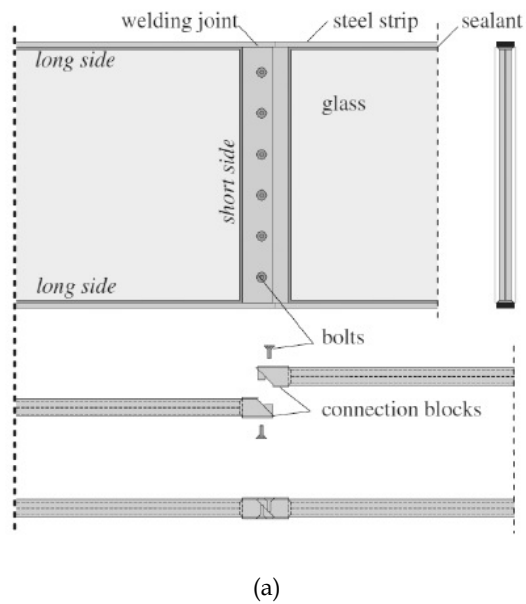
Figure 4.15. Integrated edge connection system between hybrid glass beams investigated by Belis et al.: detail view (a) and application on the roof and facade of a building in The Hague.

5 Materials

5.1   Glass

5.1.1   The molecular paradox behind transparency

Glass differs from most materials by combining substantial hardness and clear transparency. This valuable marriage is founded on a paradox between its chemistry and physical state. Definitions in the literature consider glass as a "supercooled liquid" (Haldimann, Luible, and Overend 2008; Wigginton 1996) contrary to the basic assumption of glass solidity. Looking at its molecular structure it is in fact similar to liquids, organized in a completely random or amorphous order. The ability to counteract the typically crystallized inner structure of a solid is the essential condition to allow light pass through it without scattering and thus achieve transparency.

Avoiding crystal formation is both a question of matter and technique. When a certain solid substance, with a typical crystalized molecular structure, is heated above a certain specific temperature, the intermolecular forces weaken, causing a phase change to the liquid state. That's what happens with water, for instance. When below 0°C, it has a crystallized molecular structure that guarantees its ice solid condition but when above 0°C, it liquefies becoming molecularly amorphous (see Figure 5.1). Silica, the main constituent of glass, also exhibits a crystalline structure when solid. Meanwhile, when heated above 1700 °C it doesn't immediately liquefy. Between the two typical states, it develops a condition defined as plastic-viscous (Haldimann, Luible, and Overend 2008). It is characterized by a slow amorphization of the crystal lattice and advances through a considered temperature range. This viscous state significantly reduces the molecular mobility, opening an *opportunity window* for the molecular paradox. If carefully cooled, the molecular re-arrangement and consequent crystal formation is prevented. This phenomenon is also described as a *freezing* of the atomic structure.

Theoretically glass can be produced from any material, but in practice only few exhibit the described extended viscosity that allows it, thus being called *glass formers* (Wigginton 1996). The most common is the oxide of silicon, but there are others such as oxide of boron, germanium, phosphorus or arsenic.

| ice | water | silica | glass |
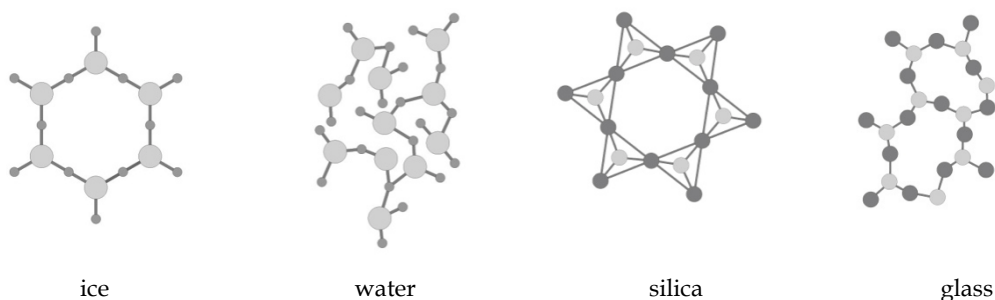
Figure 5.1: Representation of typical molecular structures of ice, water, silica and glass

5.1.2 The composition of soda lime silica glass

The composition of the glass widely used today in the building industry remains very similar from when it was discovered more than 2000 years ago (Wigginton 1996). The glass recipe empirically developed during the Roman Empire may be considered the first version of a slow and wise process of refinement. Based in silica sand as the main raw material, it culminated in the *soda-lime silica glass* standard composition, remarkable for its quality and consistency. Being a product of extraction, silica sand also has in its composition some impurities that are uneconomical to remove. Some of them are considered useful, such as iron oxide, which only 0,1% helps the melting process while giving glass its typical greenish tone. To this main constituent are added lime, soda, magnesia and alumina. The limits of each constituent on the composition according to the standard is described in Table 5.1:

Table 5.1: Chemical composition of soda-lime silica glass according to EN 572-1: 2004

Silica sand	Lime	Soda	Magnesia	Alumina	Others
69-74%	5-14%	10-16%	0-6%	0-3%	0-5%

Nowadays other glass compositions are available for specific uses. Low iron soda lime glass is a similar product in which the content of iron oxide is reduced. It is produced at a slightly superior cost and delivers a perfectly clear glass, without the green tint. For this reason it also provides lower heat absorption rate and high natural light transmittance.

5.1.3 The evolution of the flat glass production

The production of flat glass considerably evolved in the last 2000 years but remained grounded on three fundamental steps: *melting* the several compounds to guarantee a perfect mix; *forming* the molten mass once temperature drops and viscosity increases; and *cooling* in a controlled process to solidify glass, care being taken to avoid the crystal formation and to avoid residual stresses. *Forming* and *cooling* are two interdependent processes with crucial role on the final quality. Before industrialization had taken place in the XVIII century, these two steps were manually performed in a continuous movement by skilled artisans. Blowing and spinning were the main techniques used to produce flat glass after the original roman cast plate technique.

(a)   (b)
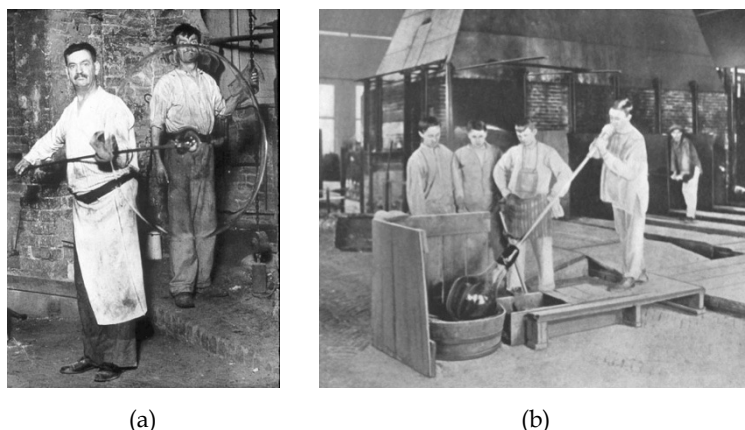
Figure 5.2: Spinning crown glass (a) and blown cylinder glass (b) manufacture techniques.

In the XIX century, scientific knowledge transformed the production of glass, both in its chemistry - becoming known, understood and reproducible - and in its fabrication, which became industrialized. In 1884 the rolling production method was patented, first in a single and then double solution. Flat glass produced according to this method resulted translucent due to the roughness of the surface in contact with the rollers. It had to be ground and polished. However, it triggered the production of patterned and wired glass. A thin wire mesh was set between two ribbons of glass prior to the passage through the roller.

At the beginning of the XX century, the drawing technique was invented. Several competing technologies co-existed, namely the Belgian Foucault method, the American Colburn/Libbey Owens method, and the Pittsburgh Plate Glass (PPG). The Foucault process (patented in 1904) resulted in the most competitive process to produce thin glass until the half of the XX century.

5.1.3.1   The float glass process

It was only in 1959 that the float glass process became available. Invented and developed by Sir Alastair Pilkington from Pilkington Glass Company, this process introduced an innovative solution to deal with the issues of forming and careful cooling. As the name denotes, the glass would float on top of a liquid to achieve two perfectly flat sides at once. No rigid bed would contact with glass during the challenging stages. In Pilkington's words: "Because the surface of the metal is dead flat, the glass is dead flat too. Natural forces of weight and surface tension bring it to an absolutely uniform thickness" (cited from: Wigginton 1996). Tin was chosen due to the complementary characteristics with glass, namely the lower melting point and the higher density that makes glass float. Initially only 6 mm thick glass was produced resulting from the equilibrium of forces. But the process was further developed and optimized, using techniques for damming and pulling the glass in order to achieve a much wider range of thicknesses from 2 to 25 mm.

Nowadays, most of the flat glass production for the building industry is made according to the float method, leading to a global spread of *float lines*. These are designed as a horizontal continuous process, comprising four main components (see Figure 5.3): a *melting tank* where the raw material is melted at around 1550°C; a *float bath* where the material is introduced at 1100°C and flows over the molten tin to form the perfectly shallow surfaces; the *annealing lehr*, where the controlled heating and cooling process takes place to release any installed stress, necessary for further processing without breakage; and finally the automatic *checking, cutting and storing*. It is a fully automated process running 24h a day and 365 days a year. The resulting scale of production led to a considerable reduction of cost.
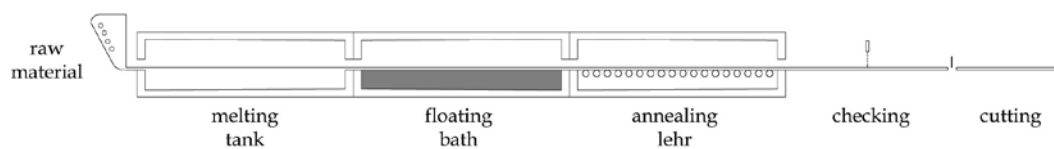
Figure 5.3: Schematic representation of the float glass process.

The floating process delivers high dimensional accuracy and geometrical precision. The perfectly flat surfaces considerably improved the overall strength compared with previous production methods. These exhibit a characteristic *brilliant fired quality* contrasting with the undisturbed optical quality of float glass. The standard size of float glass plates measures 6 m × 3,21 m. Due to recent market demands, some glass companies are already producing 9 m × 3,21 m glass as a standard size. Oversized glass panes are expected to become reality, turning transportation and handling as the main restrictions. In terms of thicknesses it is supplied in the range of 2 to 19 mm. For all these reasons the float method naturally became the leading process, replacing the other competing techniques in all the available thicknesses.

5.1.4 *Physical properties*

Glass is an isotropic material with a density similar to concrete. When a load is applied on the glass body it deforms in a perfect elastic manner until the maximum stress is reached, beyond which it fails in a brittle way (see Figure 5.4). Unlike other structural materials like steel, glass doesn´t deform plastically to dissipate stresses, which makes it extremely sensitive to stress concentrations. It's young's modulus is similar to aluminium's and its thermal expansion co-efficient is close to titanium's.
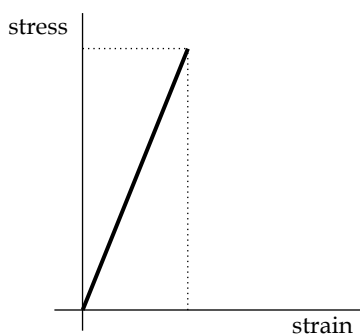
Figure 5.4. Stress-strain diagram of linear-elastic behaviour glass in tensile loading

The strength of glass is a very complex phenomenon. It is not considered a material constant and depends on several interrelated parameters. Theoretically, glass is considered to possess an extremely strong atomic structure but in practice it is a weak material [1]. The difference between theoretical and practical strength was first explained by Griffith referring to the inevitable existence of microscopic flaws randomly distributed on every glass surface. Known afterwards as Griffith flaws, they acted as stress concentrators from which the fracture initiates.

The high superficial hardness, presence of Griffith flaws and lack of plasticity reserves, causes glass panes to be particularly sensitive to contact with other materials. Additionally, during the process of handling, transport, assembly, use, etc., the damage of the surface is almost inevitable, causing scratches or flaws, usually more critical with superior size and depth, further reducing the practical strength of glass. For this reason, the tensile strength on the edges is generally inferior as on the surface of the glass pane. The damage inflicted during cutting and machining has a relevant role on crack initiation. A consistent edge treatment is very relevant since it may improve this condition. The dependence on the surface integrity is referred as being less critical when glass is loaded in compression (Wurm 2007, 37). In this case, the existing cracks tend to close and not propagate. The practical compressive strength is almost ten times higher than the tensile strength in bending, but still very far from the theoretical strength estimation.

Time induces further reduction of the practical tensile resistance of glass. Two interconnected phenomenon may be distinguished: one related to the age of the element, considering the inherent increase of surface degradation over time caused by corrosion, scratches, etc.; the other related to the duration of loading. Glass resistance for permanent loads is considerably inferior compared to instant loads (wind, use, etc). Permanent tensile stress combined with humidity gives rise to localized corrosion on the crack tip causing it to slowly propagate, weakening the glass.

---

[1] According to NRP EN572-1: 2004 the characteristic tensile bending strength is 45MPa.

5.1.5   Heat treatment

The glass strength dependence on its surface conservation is partially overcome with the application of a heat strengthening treatment[1]. By heating the whole mass of the glass above the fusion temperature and rapidly cooling it with cold air fans, it is possible to place the entire surface of the glass pane into compression. When in contact with the cold air the surface solidifies and contracts, while the interior mass is still in fusion. When it starts to slowly cool down, the consequent contraction is prevented by the already solidified surface.

According to the cooling velocity, it is possible to distinguish two levels: heat strengthened (HS) and fully tempered (FT). The FT glass is cooled faster thus creating superior internal stresses compared to HS glass. It is considered that the usable tensile resistance is increased precisely by the same amount of the installed stresses. It is necessary to overcome the pre-compression of the surface for the cracks to be susceptible to open and propagate. The two levels of pre-stressing give different surface pre-stresses, but also two completely different crack patterns (see Figure 5.5). On failure the stored energy of the pre-stress is released. In FT glass this energy release causes the total disintegration of the glass into small pieces. FT glass is also considered a safety glass[2] due to the bluntness of the resulting small pieces, which reduces the risk of human injuries in case of impact. The HS glass presents a crack pattern similar to the annealed glass, but with more branching. The cracks are also radial until the borders, but resulting in smaller fragment size.
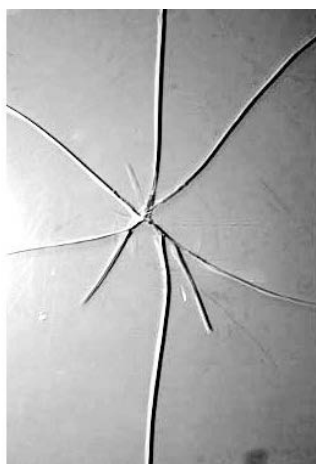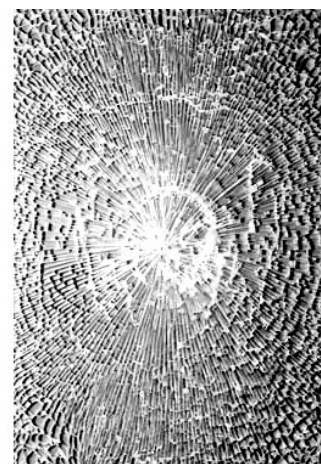
| Annealed | Heat-strengthened | Fully tempered |
| (45 MPa) | (70 MPa) | (120 MPa) |

---

[1] A chemical tempering process is also used for special applications. It consists on immerging the glass in a hot potassium chloride bath, causing the exchange of sodium ions in the glass surface by potassium ions. These are larger and induce a thin compressed layer.

[2] The term *safety glass* is increasingly being questioned in the scope of structural glass due to its residual post failure resistance.

Figure 5.5: Fracture pattern of annealed, heat- strengthened and fully tempered glass and correspondent characteristic tensile bending strength according to EN 572-1: 2004; prEN 13474-1: 1999.
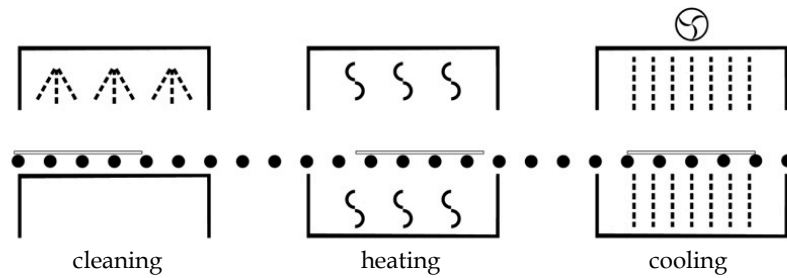
Figure 5.6: Schematic representation of the several stages comprising the process of thermal treatment of glass.

The process consists on moving the glass pane on rollers and at the same time raise the temperature of the whole glass element until around 650 °C followed by a rapid cooling of the surface using cold air fans (see Figure 5.6). The surface in contact with the cold air solidifies and compresses instantaneously while the core mass is still flexible. When it begins the cooling process, the resulting compression is prevented by the already solidified surface. The internal stresses of the glass are in equilibrium between the compressed surface and the tensioned core.

The toughening processes have an additional advantage of repairing some microscopic cracks, slightly improving the usable resistance and the structural behaviour (Schittich and Balkow 1999). As the surface is placed under compression to a certain depth this also prevents sub-critical cracks from growing. A minimum of 4 mm of thickness is required for the tension layers to form properly. In terms of maximum size it depends on the corresponding manufacturers furnace size. It is considered that the young's modulus of glass is unaffected by toughening while the thermal shock resistance is significantly improved. After toughening, no more mechanical work can be done on the glass, since it would interfere with the internal balance of tensioned and compressed zones (see Figure 5.7) causing the energy to be released and the disintegration of the glass.
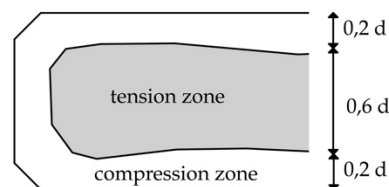
Figure 5.7: Schematic cross-section of heat-treated glass with tension and compression zones

There is a low probability of fully tempered glass to break spontaneously. This phenomenon is commonly considered to be caused by residual inclusions of nickel-sulphide particles in the glass mass. Invisible to the human eye, when heated these particles expand more than the surrounding glass causing its disintegration. Nowadays it is possible to check its existence prior to application and significantly reduce the probability of spontaneous failure[1].

Some optical distortions may rise when glass is toughened. Since the process consists on sliding fused panes of glass over ceramic rolls, it results on slight optical distortions in the glass surface. Additionally, when glass is toughened, it loses its initial isotropy, gaining fields of stress in its body. This resulting anisotropy has optical consequences, creating multiple reflections visible when observed in daylight at a sharp angle. The light is doubly refracted and becomes polarized. This effect may be minimized if the cooling stage is carefully controlled.

---

[1] The heat soak test, consists on heating the glass to cause the nickel sulphide expansion, is a destructive method that reduces the probability but doesn't eliminate it.

5.2   Polymers

Natural polymers such as rubber or cellulose have been applied in a variety of tasks until synthetic polymers were discovered and developed in the last century to meet the needs of the modern society. Polymers are described as a large molecule (macromolecule) composed of repeating structural units (Ehrenstein 2001). According to the internal structure, polymers can be classified as thermoplastics, thermosets and elastomers (ibid.). In this investigation only thermoplastics were used. This type of polymer differs from the others by softening above a specific temperature and returning to a rigid state when cooled. This occurs due to the fact that the molecular chains of thermoplastic polymers are connected by physical and not chemical bonds (ibid).

Temperature is one of several external factors that influence the mechanical behaviour of polymers. It behaves elastic, viscoelastic or viscous depending on the temperature. At the typical temperature range of building applications, viscoelastic behaviour is expected in most polymers. Additionally, the time of loading also affects the mechanical behaviour. When a certain stress is applied on a polymer over a period of time, a continuous change in the response of the material is predictable. It is expected that a polymer will creep under constant load and that relaxation will occur under enforced constant deformation. If the temperature increases these phenomena are accelerated.

The glass transition temperature (T_g) of each type of polymer defines the range of temperatures through which there is a transition from a glassy to a rubbery state. Below T_g or for high loading rates there is the tendency for a rigid and brittle behaviour, while at temperatures above glass transition temperature or for low loading rates polymers tend to exhibit a tough and ductile behaviour. Some polymers are applied in practice above their glass transition temperatures, and some are used below. The different polymers used in the experimental investigation are described in detail in the next pages, organized according to their role as adhesive interlayers and contact bars.

5.2.1   Adhesive interlayers

For the experimental investigation two types of adhesive interlayers were chosen: PVB and SG®. The first is the most common and widely used solution for laminated glass while the second is a relatively recent solution with enhanced mechanical properties. PVB as an adhesive foil was originally developed for the automotive industry at the beginning of the XX century, when there was a significant increase of cars driving on the roads and car accidents began to be a problem (Hinckley and Robinson 2005).
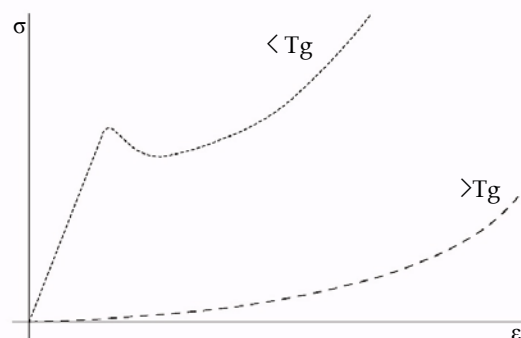
Figure 5.8. Influence of test temperature on the stress-strain curve of the intermediate layer in uniaxial tensile test (adapted from Feirabend 2010, p18).

The post-failure behaviour of car windshields had to be engineered to respond to specific requirements. Beside the impact resistance from external objects, it should have sufficient compliance to ensure minimal head trauma for a passenger that strikes the windshield (Bennison et al. 2001). It should also have the capacity to adhere to all the glass fragments and keep it in one piece.

PVB or Polyvinyl Butyral is an amorphous thermoplastic belonging to the chemical group of polyvinyl acetates. To produce adhesive foils from this relatively rigid compound, the addition of a significant quantity of plasticizers is needed. Its content increases the elasticity but also has a significant influence on the adhesion capacity and water absorption (Weller and Kothe 2011). The glass transition temperature of PVB is commonly referred as between 10 °C and 15° C (Kott and Vogel 2005) but some producers offer a PVB foil with higher T_g between 18°C and 23°C (Butacite from Dupont). At room temperature the PVB foil is considered a soft material with an elongation at break of over 200%. Meanwhile at reduced temperatures below 0 °C it becomes a rigid material. At higher temperatures and extended loading times its stiffness reduces considerably.

Below T_g the PVB foil in uniaxial tensile tests exhibits an approximately linear elastic behaviour yield, after which it starts to deform non-elastically. Above T_g the viscoelastic behaviour is visible exhibiting a non linear-elastic stress-strain curve (Feirabend 2010) (see Figure 5.8). PVB interlayers are produced on rolls with different widths and a thickness that is normally a multitude of 0.38 mm.

In 1998 Dupont commercially launched the SentryGlas® Plus (SGP) interlayer, in response to new hurricane performance standards adopted in certain regions of the United States of America. The enhanced characteristics of this interlayer led it to be used for several other purposes as improved bomb blast resistance, specially after 9/11 terrorist attacks, and in a wide structural applications (facades, overhead glazing, balustrades, glass floors & steps, etc.) In 2008 it returned to its original name SentryGlas® (SG®).

SG® interlayer is a semi-crystalline thermoplastic polymer (Bucak and Meissner 2005). It is composed of ethylene / methacrylic acid copolymers containing small amounts of metal salts that may be permanently bonded to glass (Ingo Stelzer, Bennison, and Qin 2008). Dupont currently defines it as an ionomeric material (I. Stelzer 2010). SG is mainly produced in sheets with 0,98 mm, 1,52 mm or 2,28 mm. Recently Dupont made available SG also on roll form, only for the lowest thickness.

Table 5.2. Main properties of PVB and SG interlayers at room temperatures (these values may slightly change according to different suppliers)

		PVB	SG
Density	(kg/m^3)	1070	950
Tensile strength	(N/mm^2)	> 20	34,5
Maximal elongation	(%)	> 250	400
Coefficient of thermal expansion	(10^{-6} k^{-1})	468	100-150
Glass transition temperature	(°C)	10-15	55

In Table 5.2 are compared the main properties of PVB and SG. Although both interlayers are polymers, SG has a totally different molecular architecture compared to PVB. It is significantly stiffer, tougher and chemically more robust than conventional PVB and displays elasto-plastic stress-strain behaviour. It is also more durable presenting excellent edge stability under extreme weather conditions and no tendency for yellowing as happens with PVB. SG has a stiffness up to 100 times higher than that of PVB (Dupont 2009). The mechanical properties of a stiff interlayer lead to benefits in glass strength, stiffness and creep resistance, both before and after glass breakage (Bennison et al. 2001)

5.2.2   Contact bars

Several types of polymers were selected for the experimental investigation in order to test its suitability as a contact bar for the connection. In Table 5.3 is shown a summary of the most important properties of each polymer.

Table 5.3. Summary of the most important properties of the selected polymers for contact bar purpose (GRANTA 2012).

		PC	PMMA	PA6	POM	PTFE
Density	(kg/m³)	1200	1180	1140	1410	2200
Young's modulus	(GPa)	2,0 - 2,4	2,2 - 3,8	2,6 - 3,2	2,5 - 5,0	0,4- 0,6
Compressive strength	(MPa)	69,0 - 86,9	72,4 - 131,0	55,0 - 104,0	74,9 - 124,0	16,5 - 27,5
Elongation	(% strain)	70,0 - 150,0	2,0 - 10,0	30,0 - 100,0	10,0 - 75,0	200,0 - 400,0
Hardness (vickers)	(HV)	17,7 - 21,7	16,1 - 21,9	25,8 - 28,4	14,6 - 24,8	5,9 - 6,5
Fracture toughness	(MPa.m^0.5)	2,1 - 4,6	0,7 - 1,6	2,2 - 5,6*	1,71 - 4,2	1,3 - 1,8*
Glass transition temp.	(ºC)	147,0	84,9 - 165	43,9 - 55,9	-18,2 - -8,2	107 - 123
Thermal exp. coeff.	(strain/ºC)	120,0 - 137,0	72,0 - 162,0	144,0 - 149,0	75,7 - 202,0	126 - 216
Transparency	(-)	opt. quality	opt. quality	translucent	opaque	translucent
Refractive index	(-)	1,5 - 1,6	1,5 - 1,6	1,5	-	1,3 - 1,4

Polycarbonate or PC is a transparent thermoplastic, known to have good mechanical properties. It exhibits very good optical transparency and good toughness and rigidity, even at relatively high temperatures. It is possible to improve the PC properties in terms of the flame retardation, refractive index and resistance to softening. Reinforcing it with glass fibres it is possible to improve the mechanical performance at higher temperatures. PC is usually processed by extrusion or thermoforming. Injection moulding is also possible. It is commonly used to produce helmets or riot shields.

PolyMethyl MethAcrylate or PMMA, also known as Acrylic, is a transparent thermoplastic with very good resistance to weathering. PMMA is considered to be hard and stiff. Meanwhile it is sensitive to stress concentrations and fails in a brittle manner, comparable to glass. It is possible to improve the impact resistance of PMMA by blending it with an acrylic rubber. It can be shaped by casting or extrusion. Very easy to mill and polish. Scratches may easily be removed by polishing or by heating the surface of the material. Laser cutting may be used to form intricate designs with very clean cut, since it vaporizes to gaseous compounds. Nowadays it is a very popular and economical solution with various uses. It is usually used as a lightweight substitute of glass. Its density is half that of glass, but it has an inferior scratch resistance compared with glass. Its impact strength is superior to glass but considerably inferior to PC.

Polyamide or PA, also known as Nylon is a thermoplastic with translucent quality, known for its toughness and low coefficient of friction. There are many categories of PA with different properties. For the experimental investigation the PA6 was selected. The density, strength and ductility of PA are considered in the average compared with unreinforced polymers. When reinforced with mineral, glass powder or glass fibres it is possible to increase its modulus, strength and density. PA is very flexible in terms of workability. It is easily injection moulded, machined and finished. It is used today in very diverse purposes.

PolyOxyMethylene or POM is an opaque thermoplastic similar to PA but with increased stiffness and fatigue resistance. It was first marketed by DuPont as Delrin in 1959. It also presents a good water resistance and low coefficient of friction. With a highly crystalline structure, POM is easily mouldable, has a goof fatigue resistance and stiffness. Normally POM is used in applications in which its natural lubricity is exploited.

PolyTetraFluoroEthylene or PTFE, also known as Teflon, is a high density translucent thermoplastic with extremely low coefficient of friction. It is a member of the fluoroplastic family presenting a translucent white appearance. It is also known to be water repellent and very stable. Its mechanical properties are inferior compared with previous polymers. Typical uses of PTFE are protective coatings, non-stick cooking products and water repellent fabrics.

5.3   Stainless steel

Stainless steel, also known as inox steel, is a high quality steel created to provide good performances in terms of corrosion and heat resistance. It is an alloy of iron with a minimum of 10.5% of chromium. It is considered non-rusting due to a protective layer that is created in its entire surface as a reaction to the contact with oxygen and moisture. When damaged, this oxide film self-repairs and assures a rapid and effective protection. The content of chromium (or manganese) improves the corrosion resistance, meanwhile its considerable cost has a strong impact in the price comparing with ordinary steels. For this reason it is only supplied in thin plates, or other small elements. There are several categories of stainless steels available today. In each category different grades exist according to the compositional range. For this research a specific grade was chosen designated as AISI[1] 304. It belongs to the class of austenitic stainless steels containing 18-25 % of chromium, 8-20 % of Nickel and 0,15% of carbon.

The mechanical behaviour of stainless steel is considered a critical topic for this research. Its typical tensile stress-strain is shown in Figure 5.9. In a first phase it exhibits a linear elastic behaviour until the yield strength is reached. It then shows plastic deformation with increasing strength until the maximum is reached. After this ultimate strength it typically doesn't fail, exhibiting a decrease in strength before fail.
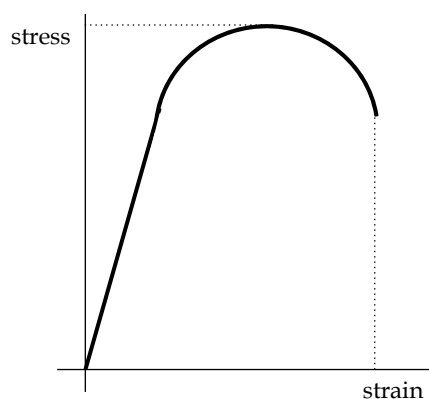
Figure 5.9 Typical tensile stress-strain diagram for stainless steels

Punching is the commonly used process for standard perforation of metal plates. It consists on a full width metal tool that inflicts the perforation in consecutive parallel rows, while the metal plate is carried at right angle. The position of the tool in each step is adapted to the required perforation pattern.

---

[1] AISI stands for American Iron and Steel Institute and relates to the American grading system frequently used in Europe for practical purposes. The official European designation for AISI 304 is X5CrNi18-10.
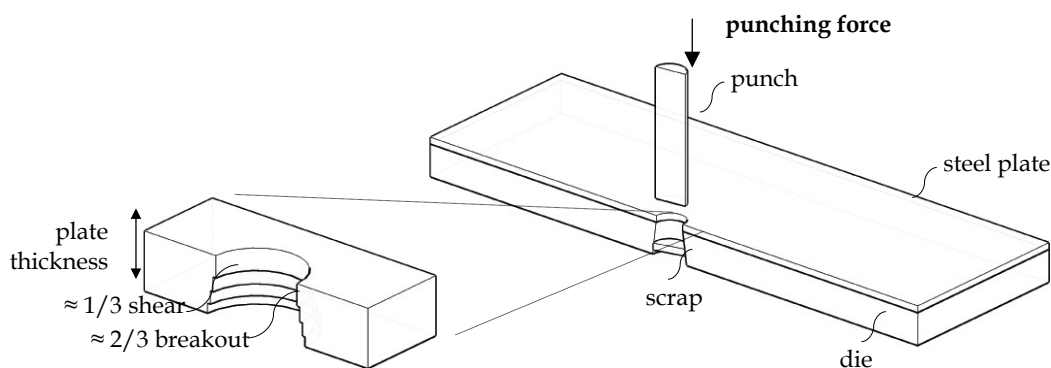
Figure 5.10. Punching of steel plates. Detailed view of irregular internal surface with approximatelly 1/3 of the hole is made by shear and the rest 2/3 by breakout of the material.

The punching process causes corrugation of the sheets due to the perforation energy. When punching, approximately l/3 of the thickness of perforation is done by shear and the other 2/3 is by breakout. The resultant hole in the metal shows an irregular cross-section with slightly conical shape (see Figure 5.10). It determines a punch side of the sheet with a smoother surface different from the rougher backside. It is straightened afterwards together with the edge treatment and the cut to size. This process is aided with the use of lubricants, which cover the final product and need to be removed before adhesive bonding is possible. For very thick or customized design solutions, other methods of perforation may be used such as milling, laser and water jet cut. These processes are more flexible concerning the available tools to be used, feed direction of the metal sheet and speed of perforation. For these reasons these are usually CNC controlled machines, allowing a superior freedom of movements hence perforations.

There are several standard perforations patterns with round, square, slot (running) and decorative motifs. These can be arranged in a straight (90 ºC) or staggered order. According to Industrial Perforators Association (IPA), the perforated metal with round holes arranged in a standard 60º staggered pattern ranging from 5 mm to 19 mm account for more than half of the perforating industry's production (IPA 1993), at least in the American context. It is considered the most versatile in its application providing a wide range of open areas and offering an optimized strength. The web width (c) to thickness ratio should always be greater than one to avoid breakage of the webs during punching. The hole diameter (w) must be at least twice the thickness of the plate to guarantee the final integrity and quality of the perforated plate. By determining the hole diameter (w) and the distance between its centres (t) the perforation percentage is defined. The pattern chosen for the perforated plate applied on experimental tests is the R5T8. It is characterized by having 5 mm diameter holes staggered at an angle of 60 º, and distancing 8 mm from centre to centre. This type of pattern has 35,4% of the surface perforated. The maximum perforation percentage available is 70%, beyond which it tends to distort.
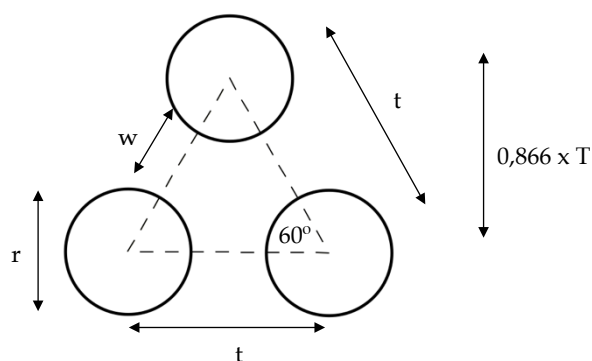
Figure 5.11. Round staggered RT pattern geometrical rules.

It is supplied in flat form and generally in rectangular shape. Standard dimensions of the sheets are 1000 mm x 2000 mm (small), but it can also be supplied in 1250 mm x 2500 mm (medium), 1500 mm x 3000 mm (large) and 1600 mm x 4000 mm (super). Standard thicknesses range from 0,5 mm to 10 mm for Aisi 304 stainless steel.

According to the standardized perforation procedure two distinctive axis are defined in the 60° pattern: the direction of the stagger is the short dimension or width of the sheet while the straight row of closely-spaced holes is parallel to the long dimension or length of the sheet. Relating to the pattern, on the width direction we have the "closed pattern", and on the other direction there is the "open pattern" (see Figure 5.12).

The mechanical behaviour of perforated plates is determined by the constituent material and strongly influenced by the size and arrangement of the holes. These are responsible for an anisotropic behaviour dependent on the direction of loading. The influence of the geometrical parameters and the parameters interdependences on the mechanical behaviour of perforated steel plates with staggered round holes was investigated by El-Magd et al. (El-Magd, Kranz, and Risch 2001). The orientation angle of the holes with respect to the direction of the applied tensile load influenced the modulus of elasticity, the breaking load and elongation curve of the sample.
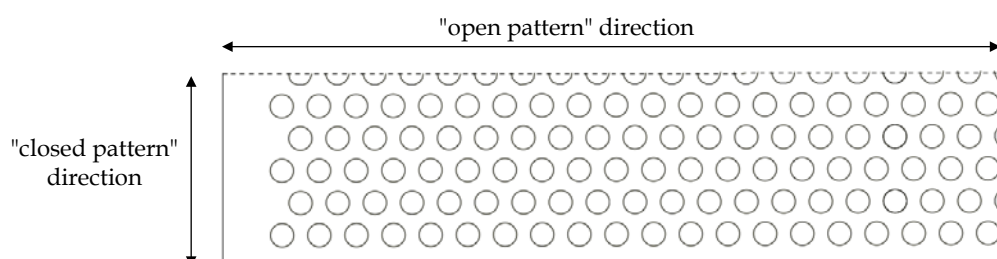
Figure 5.12. Open and closed pattern directions on a RT standard perforated plate.

III Experimental investigation

6 Fabrication technology

6.1 Glass processing

Float glass is normally supplied in standard sheets measuring 6 m × 3,21 m [1] that have to be processed to the required size. The most common method to separate different panes of glass is simply by inflicting a linear flaw on one side, that once stressed by pressuring the opposite side easily opens into a full thickness crack. This process of separation causes a removing of micro and macroscopic flakes of material resulting in an irregular edge surface. In non-structural framed applications it is not problematic. Meanwhile, when the glass edge is expected to be stressed, it may be critical since the presence of flaws in the edge surface results in a lower tensile strength. The quality of glass edge processing is relevant for structural applications. The several necessary steps are then described.

6.1.1 Cutting

The first step is cutting the glass pane to an intermediate size, usually 2 mm larger than the desired final dimension. A manual or CNC diamond or tungsten carbide tipped tool is used, advisably with lubricant oil to achieve a fine line of removed material from the surface. A mechanical weakening line is created on the glass surface that when slightly stressed, by bending the glass pane, drives the crack growth. The resulting cut edge is very irregular, clearly showing in a close look the first damage caused by the diamond (upper side) and the consequent break due to overstress with characteristic undulating waves or *Wallner* lines running transversely to the edge (see Figure 6.1).

Another process available to cut glass is the abrasive water jet, which consists on a high-pressure water jet to which abrasive grains are added. This method is more accurate when compared with the previous and offers an enhanced edge surface quality before any further processing. Meanwhile, it is considered a time and cost intensive process, which means that it can only be applied in special applications. An advantage is the much greater freedom of shape, including holes.
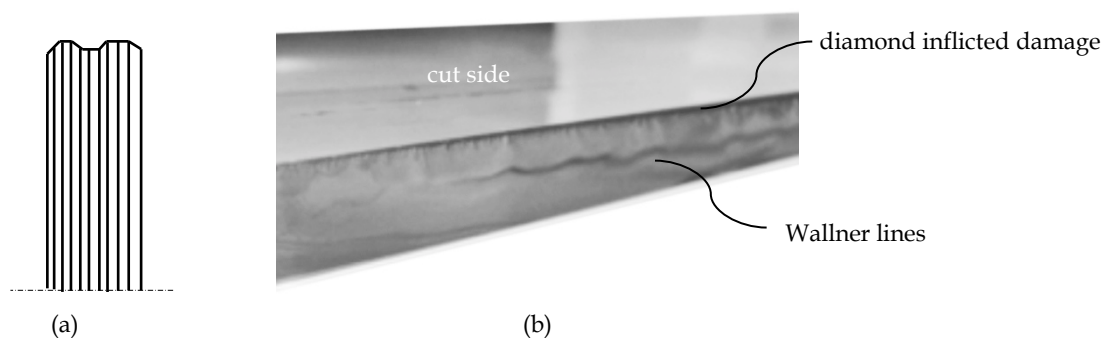
Figure 6.1. Diamond cut glass edge schematic representation (a) and view showing different side damage (b)

---

[1] Superior lengths are becoming ever common as standard float glass supplied in certain countries.

6.1.2   Grinding

Grinding is the process by which several layers of irregular material are mechanically removed from the cut edge until a flat surface is acquired. Usually a set of rotating tools coated with diamond or carborundum particles is used. The process comprises several consecutive stages of decreasing grain size. At the beginning of the process larger irregularities are removed using larger grinding particles. For the edges to be considered fully ground, avoiding blank spots in the edges surface, a minimum of 2 mm of material must be removed. The resulting edge is perfectly flat showing a matt surface. During the process, similar grinding tools are used in a 45° position for bevelling. The dimension of the bevel is adaptable but it is often around 1,5 mm. For a 10 mm thick glass, for example, only 7 mm is straight whilst the other 3 mm (2 x 1,5 mm) are bevelled.

(a)   (b)
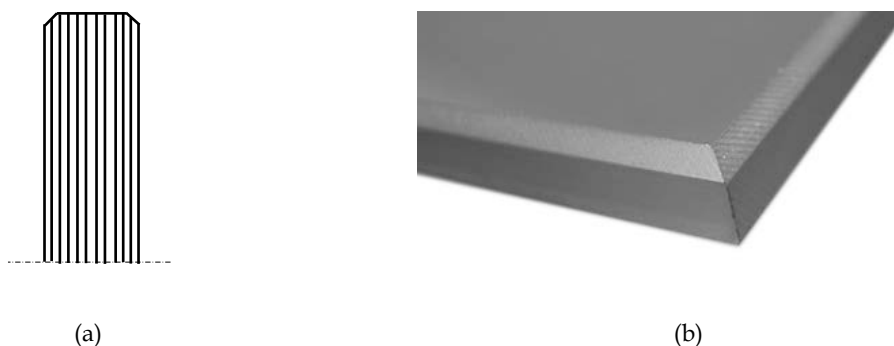
Figure 6.2. Grinded glass edge schematic representation (a) and close-up view (b)

6.1.3   Polishing

In order to have fully transparent edges, a final polishing stage must by carried out. It is usually performed in the same machine as grinding, consisting on a consecutive phase where similar rotating tools are used. Instead of diamond particle coating, the polishing rotating tools present a smoother polymeric surface. At the final of the process a significant transparency of the edge is achieved, more evident when low-iron glass is used, due to the inexistence of the greenish appearance of the typical soda lime silica glass edges. After polishing the edges, glass panes are pre-cleaned with water-based solution and dried with air blow and wipes in order to avoid deposits on the surface.

(a)   (b)
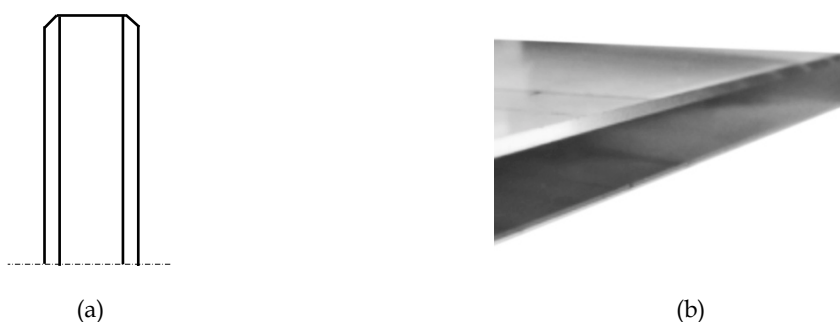
Figure 6.3. Polished glass edge schematic representation (a) and close-up view (b).

6.2 Preparation

The preparation work for the lamination process is of great importance since it has a significant influence in the quality of the adhesion between the different materials. A first condition to be assured, before the actual preparation process, refers to the storage of the polymeric interlayer. Both PVB and SG are hygroscopic before lamination, which means that the storage conditions of the foils are very strict. The packaging integrity must be maintained as much as possible, especially moisture proof bags (Van Russelt 1997). Excessive moisture in the interlayer will have a significant effect on adhesion, contributing to the appearance of defects such as partial delamination, air bubbles or excessive fluidity.

The assembly work was done in a clean room with controlled environment (see Figure 6.4 (a)) where the interlayer could be safely manipulated. Before being manipulated inside the clean room, both glass and metal elements were cleaned with a proper solvent (isopropyl alcohol e.g.) to eliminate all possible contaminants such as: oil, grease, finger prints, separating agent, dust, etc. First the tin and airside of the float glass individual panes were checked using a UV detector (see Figure 6.4 (b)) in order to laminate always with the same glass orientation. According to the interlayer manufacturers the adhesion is stronger when in contact with the tin side. Then the several interlayer foils were cut with a regular craft knife. Once all the pieces were available and ready, the assembly and positioning work was carried out. The pre-assembled laminate was fixed with heat resistant tape (see Figure 6.4. (c)).

(a)   (b)   (c)
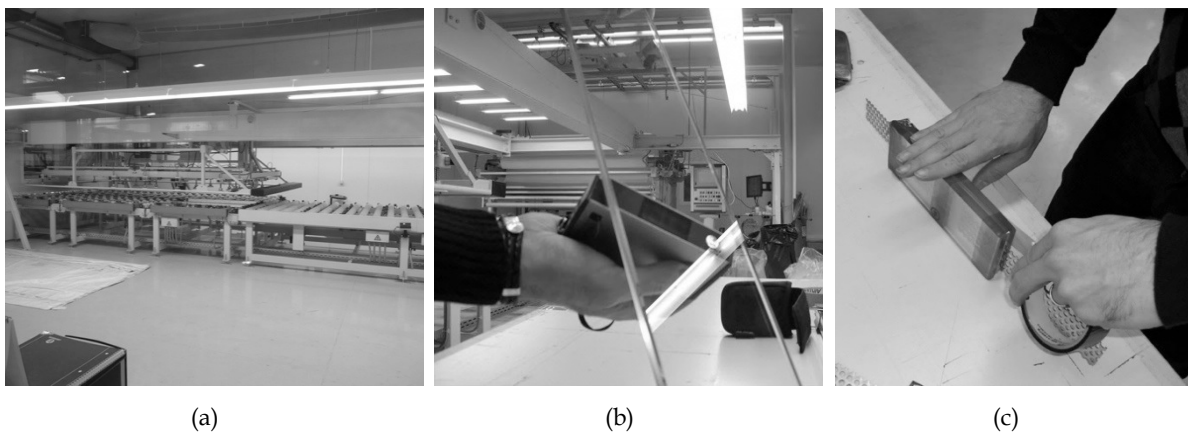
Figure 6.4. Clean room of Vicer where the preparation work took place (a), tin side of glass check with UV detector (b) and fixing of pre-assembled laminate with heat resistant tape (c).

6.3 Lamination

Lamination comprises the set of procedures through which adhesion of glass (and other elements) to the polymeric interlayer is achieved. There are several methods available to perform the lamination, sharing some common procedures that are briefly described. Firstly, the application of pressure is essential during the whole process in order to remove all the air inside the laminate and assure that no bubble remains after the final adhesion is achieved. It can be applied by vacuum, autoclave or a combination of both. This process is even more important and demanding when inserts with perforated bodies are integrated within the laminate. During the preliminary lamination tests, the combination of vacuum and autoclave proved to be the best solution. Vacuum was applied before, during and after the autoclave cycle, along the cooling process. It proved to be essential to avoid remaining air bubbles.

High temperature is another essential ingredient of the lamination process, necessary for the effective bonding to be achieved. It is during this process that the once translucent interlayer foil becomes transparent. It is applied according to rising steps until a maximum of around 130 °C. The high temperature allows the polymeric foils to become semi-fluid and flow to adapt to the glass surface and fill any void inside the laminate. The subsequent cooling process is very critical, also being carried out through staging steps. The several stages of the lamination process are schematically represented in Figure 6.5. During this investigation the silicone blanket and the vacuum bag systems were applied. Their specificities are described in detail in the following chapters.

| layering + positioning | vacuum | vacuum heat + atmospheric. pressure | vacuum cooling | finished laminate |
| (1) | (2) | (3) | (4) | (5) |
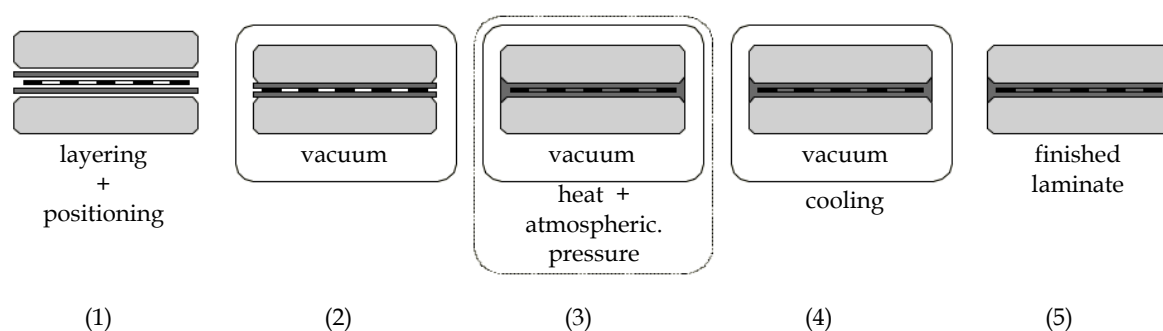
Figure 6.5. Schematic representation of the several stages comprising the optimized lamination procedure.

6.3.1 Silicon blanket lamination method

The silicone blanket system is a lamination method targeted for industrial use, known to offer very good productivity at low cost. The preparation work is very simple and there is almost no waste from the process, since the silicone blanket is re-usable (see Figure 6.6 (a)).

<table>
<tr><td>(a)</td><td>(b)</td></tr>
</table>
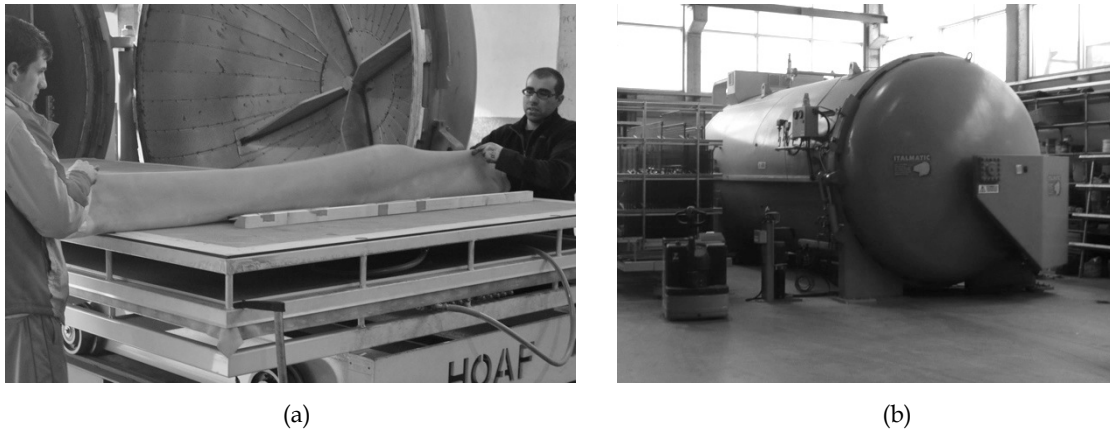
Figure 6.6. Re-usable silicone blanket (a) and autoclave (b)

Additionally, it can be optimized to be an autoclave free process, further reducing the costs. This requires the acquisition of a special oven fuelled with propane gas. During this investigation this special oven was not available and the system was used with an autoclave (see Figure 6.6 (b)).

The infrastructure comprises a set of stacked tables, where the several pre-assembled laminates are placed (see Figure 6.7 (a)). Once a table is full, a thick silicone foil is placed over to cover the whole surface (see Figure 6.7 (b)) and be sealed at the table edges by means of the stacked steel structure (see Figure 6.7 (c)). Special attention must be taken to the free space around each laminate unit, which must be adequate to avoid any localized over stress or insufficient flow of air. Between the laminates and the table surface a fibre wire net is disposed in order to allow an efficient flow of air under the laminate.

<table>
<tr><td>(a)</td><td>(b)</td><td>(c)</td></tr>
</table>
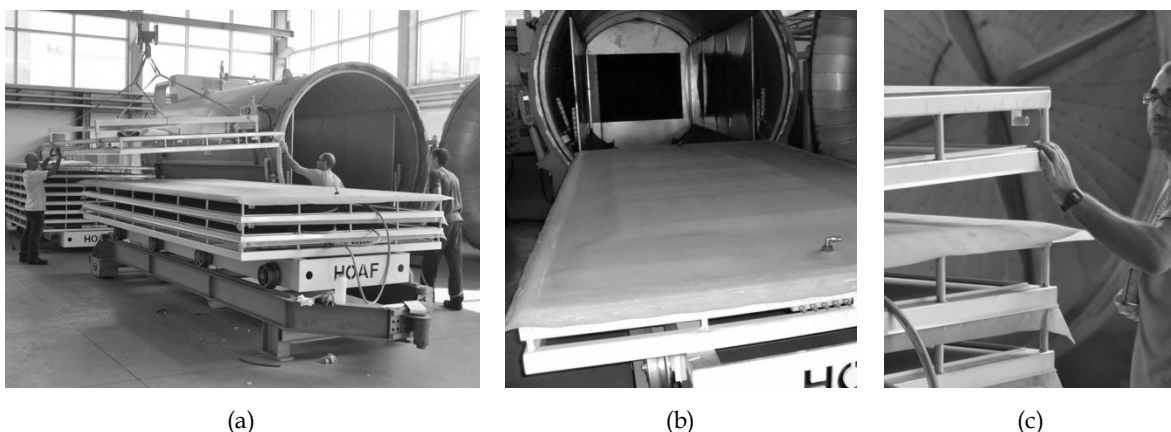
Figure 6.7 View of the stacked table structure (a), silicone blanket covering the table (b) and detailed view of the sealing mechanism performed by the steel angles on the edges of the tables (c).

(a)   (b)
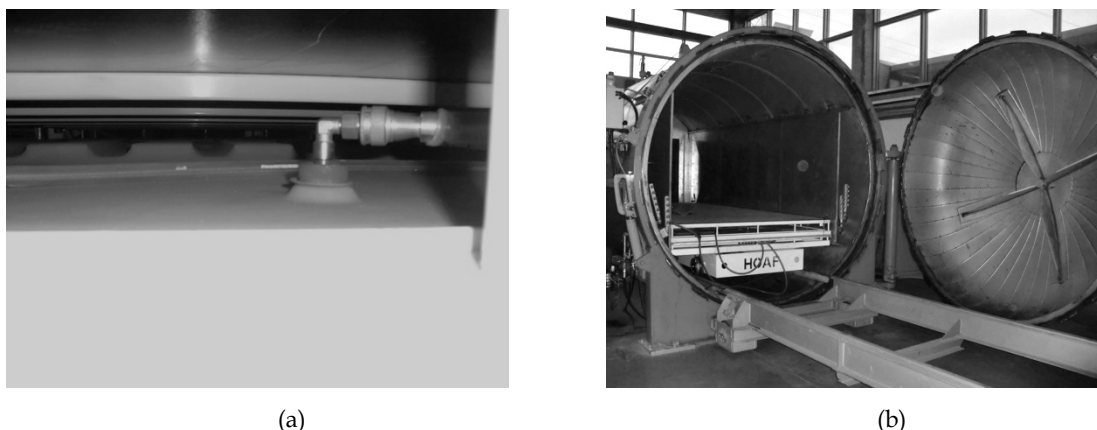
Figure 6.8 Close view of one pump valve applying vacuum (a) and table structure inside the autoclave (b).

The optimized calibration developed for the investigation laminates, predicted a vacuum period previous to the autoclave cycle. The silicone foil comprises two pump valves at the edges through which the air removal is carried out (see Figure 6.8 (a)). The first stage, carried outside of the autoclave, is meant to remove as much air as possible before the melting of the interlayer, but is also essential to assure that there is no leak of air, which could compromise the following cycle. Afterwards, the table structure is put inside the autoclave for the temperature and pressure cycle to be applied (see Figure 6.8 (b)).

As mentioned before, the silicone blanket lamination system allows reducing or even eliminating the use of autoclave for the application of atmospheric pressure. The good elasticity of the silicone blanket combined with the vacuum pressure results in a comparable effect to the atmospheric pressure achieved with the autoclave (see Figure 6.9). According to the lamination system manufacturer, this system is indicated to laminate complex assemblies such as the ones investigated with embedded perforated inserts. However, it was concluded that the heating process, although applied to the same degree, being from a different source from the propane gas, might have significant influence on the results. Several laminates consistently had remaining air bubbles. It was then decided that a small amount of atmospheric pressure was beneficial for assuring that no air bubble remained inside the perforated inserts.
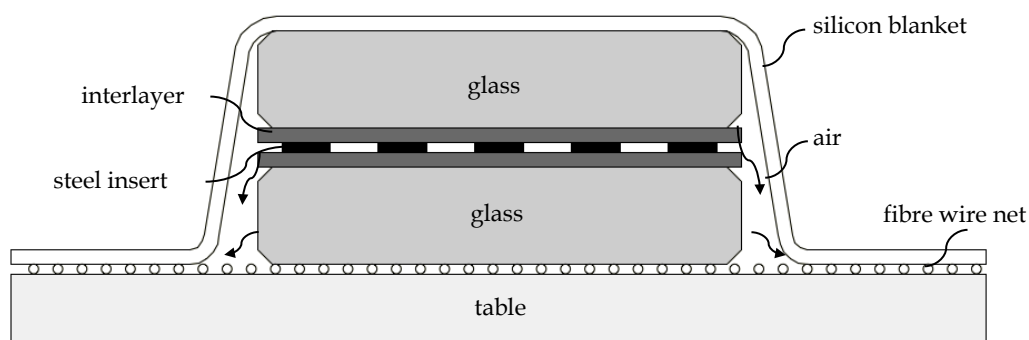
Figure 6.9. Cross section of a laminate inside a silicon blanket lamination system during vacuum stage.

6.3.2 Vacuum bag lamination method

The vacuum bag system is a very common lamination method specifically applied to complex laminates, in order to guarantee excellent quality results. It is a very flexible method being used both in industrial and laboratory scale. However, one of the major disadvantages compared to the previous method concerns with the non-reusable consumables necessary for each lamination cycle. Besides the inherent cost, it represents additional waste to the process. Furthermore, it is a time consuming process due to the elaborate preparation work necessary for each lamination cycle.

The lamination of specimens for this investigation using the vacuum bag method was performed at École Polytechnic Fédérale de Lausanne in June 2013 in collaboration with Mr. Manuel Santarsiero and Dr. Christian Louter. The several steps are briefly described above.

Firstly, the several layers of wrapping materials dispensed in rolls were cut to the correct size in order to efficiently evolve the pre-assembled laminates. It comprises the vacuum bag, the breather material and the perforated release material[1]. The last is wrapped individually in each laminate (see Figure 6.10).

| (a) | (b) |
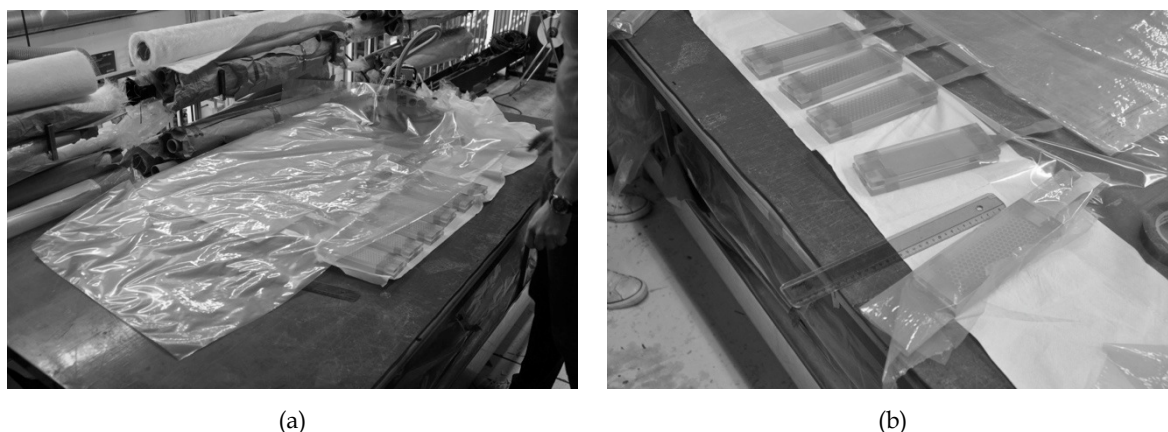
Figure 6.10. Vacuum bag consumables cutting (a) and wrapping of laminates with perforated release film (b)

---

[1] The perforated release material may also be applied in the sylicon blanket system

Then the several laminates are disposed with some space between each other and globally wrapped by the breather material (see Figure 6.11 (a)). Above it, two *waiting* discs were placed before the final close of the bag to help on the efficient seal of the connection to the pump valve. It is done with the aid of a mastic sealant tape, very resistant and adaptable to different substrates (see Figure 6.11 (b)).

| (a) | (b) |

Figure 6.11. Wrapping of the laminates with breather material (a) and closing of the bag with mastic sealant (b).

Once perfectly sealed along the edge, the bag is perforated on the area of the discs to allow the connection to the valve (Figure 6.12 (a)). Then the valve is screwed and sealed to the bag with mastic tape (Figure 6.12 (b)).

| (a) | (b) |

Figure 6.12. Perforation of the vacuum bag (a) and sealing of the pump valve connection (b)

The bag was then connected to the vacuum pumps and the preliminary removing of air was initiated. When it was assured that no air leak existed. the bag was inserted in the autoclave and the temperature and pressure was initiated (see Figure 6.13).

(a)   (b)

Figure 6.13. Connection of the bag to the vacuum pump (a) and introduction of the bag inside the autoclave (b)

Contrary to the silicone blanket, the vacuum bag lamination system is symmetrical in its structure, which enables greater equilibrium of forces inside the bag (see Figure 6.14). The influence is very significant when dealing with small size and complex units. In terms of atmospheric pressure inside the autoclave it is necessary to apply a considerably higher level to be efficient, compared with the level used in the previous method.
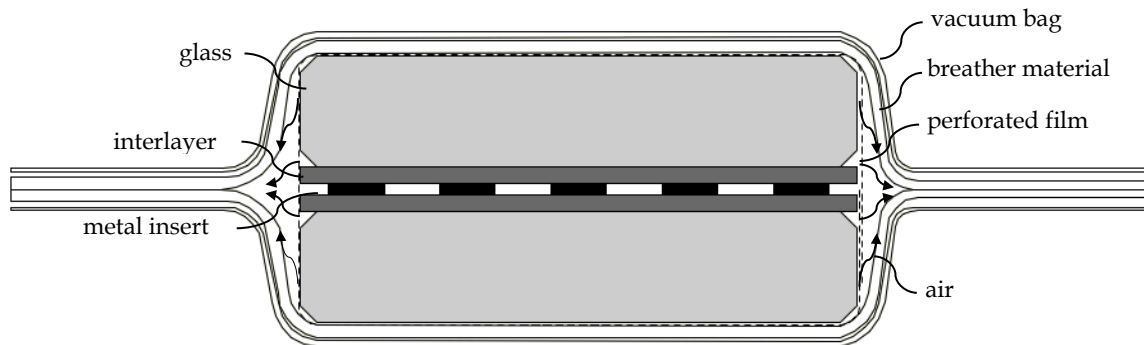
Figure 6.14. Cross section of a laminate inside a vacuum bag lamination system during the vacuum stage.

6.4   Experimental investigation

This section addresses the experimental investigation conducted to study the procedures necessary to efficiently laminate metal elements semi-embedded in glass. The method adopted was a typical *hands-on* learning process based on trial and error. According to the results obtained, possibilities were tested and parameters were adapted in close contact with technicians of both interlayer and lamination system companies. Most of the investigation was conducted at the Vicer Lda lamination facilities using the available silicon blanket lamination system with autoclave.

6.4.1   Preliminary tests

In a first stage a wide variety of parameters were tested in order to understand the possibilities and limitations of the technology. Concerning the adhesive interlayer, both PVB and SG were tested using different thicknesses; combined with perforated metal inserts of different kinds and finishes (galvanized, mild, stainless and lacquered), thicknesses and open areas (see Figure 6.15).
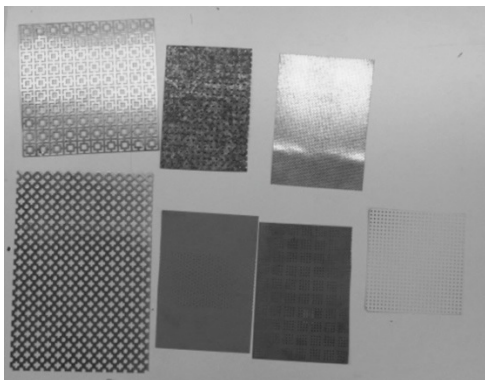
Figure 6.15. View of a sample of different types of metal inserts used during the preliminary tests

Although the results were satisfactory using both PVB and SG, several problems were detected and solutions to solve it were discussed. One problem that consistently appeared was the air bubble retention. As mentioned before, the existence of hollowed bodies inside the laminate hampers the process of removing all the trapped air inside the laminate. In Figure 6.16 three typical cases with correspondent cause for this phenomenon are shown. The first case (a) is the most common and easy to solve, corresponding to an insufficient vacuum during the lamination process. One solution was to increase the time of vacuum especially after the autoclave cycle. It is very important to keep the vacuum on until the temperature of the interlayer decreases below its T_g temperature. Another solution was to improve the flow of air during vacuum by increasing the space among the pieces when placed on the lamination table. The uneven flow of air caused in some cases the phenomena of localized trapped air.

The second case (b), identified right at the beginning, happened due to a chemical incompatibility of the galvanized steel and the PVB interlayer causing a visible chemical reaction, which resulted in small size bubbles spread over the surface. The third case (c) presumably happened due to excessive moisture content on the interlayer, which significantly increased its fluidity during the application of temperature and hampered the release of air, even when outside the laminate.

| (a) | (b) | (c) |
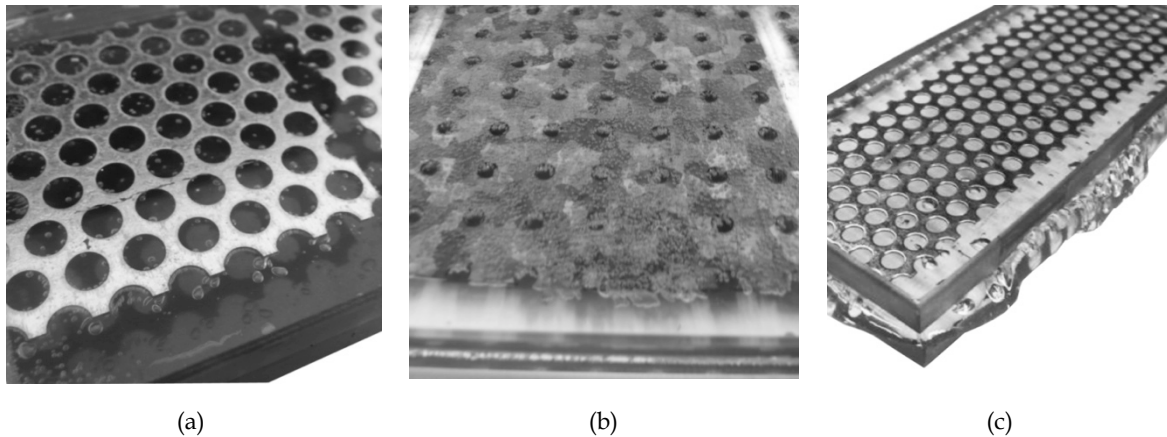
Figure 6.16. Retained air bubbles inside the laminate due to different causes: insufficient vacuum (a), chemical incompatibility with metal insert (b) and excessive moisture in the interlayer (c).

Another recurrent problem was the overflow of interlayer. Its first cause was the maximum temperature reached during the autoclave cycle, which proved to be high (see Figure 6.17 (a)). As previously discussed, the lamination process that leads to the effective adhesion is based on an equilibrium between temperature and pressure. This means that the decrease of temperature couldn't be considerable risking to compromise the adhesion process. One available solution to counteract the flow of interlayer was the application of the perforated removing film around each laminate. Additionally, another probable cause, already mentioned concerning the air bubbles, was the excessive moisture content, which significantly increased the fluidity of the interlayer (see Figure 6.17 (b)).

| (a) | (b) |
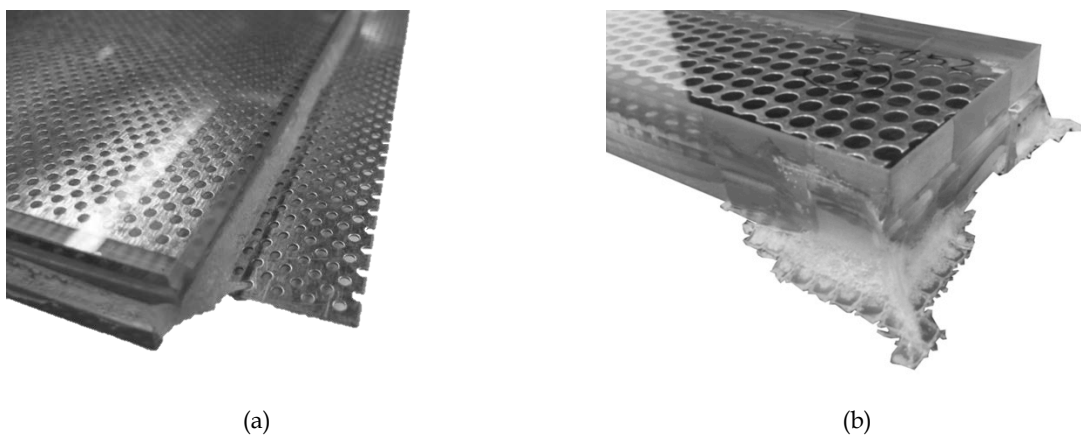
Figure 6.17. Leak of interlayer during autoclave cycle due to excessive temperature (a) and excessive moisture content on the laminate (b).

The considerable pressure applied during the lamination process caused some localized glass breakages (see Figure 6.18). Several causes contributed to it. Firstly, an asymmetrical assembly, in which the metal insert only covered part of the intermediate area, led to an overstress of the glass. To avoid it, a shim was introduced to equalize the forces. In rare occasions, the insufficient cleaning of the table resulted in solid deposits from previous breakages that caused local stress concentrations in the lower glass. Furthermore, the different thermal expansion of glass and steel is referred in the literature (O'Callaghan 2005) as a cause of overstressing that leads to glass breakage. The reduced thickness of the steel applied in this investigation together with the proportionally considerable thickness of the adhesive interlayer contributed to the avoidance of this phenomenon.
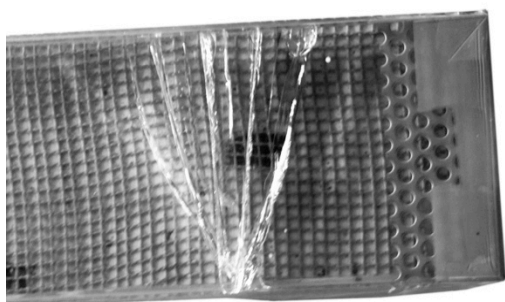
Figure 6.18. Glass breakage occurred during lamination.

6.4.2   Lamination of protruded steel elements

On a second phase, a more focused investigation was conducted to solve the problem of laminating protruded perforated steel plates with consistently good quality results. This specific type of lamination problem lacked standard procedures. Its inherent complexity and the need to fully calibrate its execution along with the development of the design of the connection detail (further discussed on this thesis, see chapters 9.4 and 10.3) led the current investigation to be prolonged during the whole research until the fabrication of the final prototype.

When laminating with the silicon blanket system, the protruded steel insert is compromised if unprotected, due to the applied pressure that would deform it. A shim was placed below the protruded steel element, with the smallest size possible to reduce its influence on the necessary flow of air around the laminates during the vacuum process. However, the correct thickness to be applied wasn't clear. Firstly a similar glass with the same thickness was placed to hold the steel plate and protect it from deforming. It showed to be insufficient, since the steel insert showed tendency to move down when the interlayer was warmed up. It resulted that the steel insert was embedded close to the lower glass pane with a reduced thickness of interlayer between the two (see Figure 6.19).
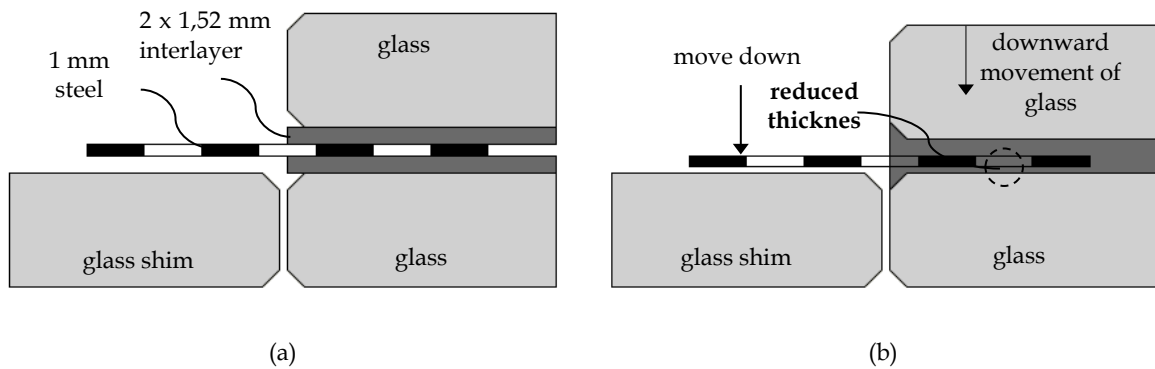
Figure 6.19. Position of protruded steel insert before (a) and after autoclave cycle (b), using a shim with the same thickness of the glass.

A second solution for the shim was conceived with the same thickness of the length from the base to the upper surface of the protruded steel, consisting on the combined thicknesses of glass and interlayer. The goal was to fix the steel insert to the shim in order to prevent it from moving and avoid differential settlements along the laminate. After the autoclave cycle it resulted that the fixed steel insert approached the upper glass pane when it adapted to fill the gap between the two interlayers (see Figure 6.20).
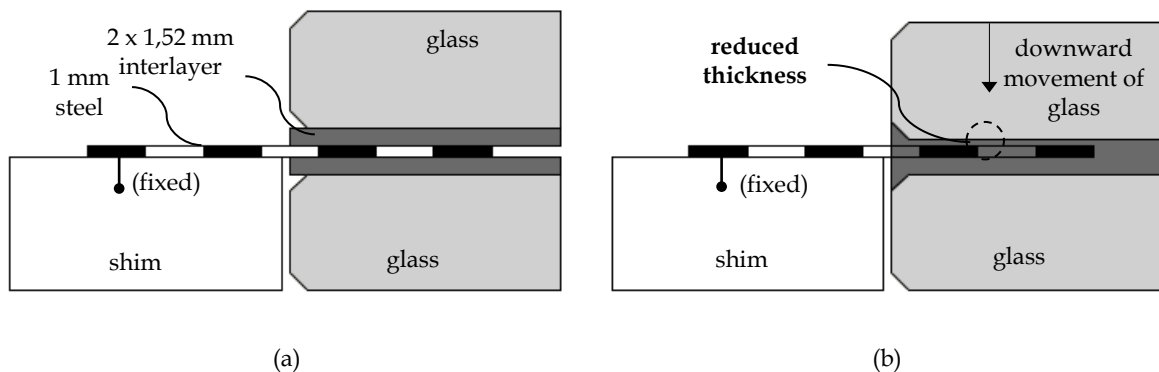
Figure 6.20. Position of protruded steel insert before (a) and after autoclave cycle (b), fixed to a shim with the same thickness of glass and interlayer (1,52 mm).

Changing the thickness of the interlayer, replacing the standard 1,52 mm thick by the recently available 0,89 mm thick, proved to be a good solution. This thickness is very similar to the steel plate, which means that the position of the protruded steel related to both upper and lower glass panes may remain similar before and after the autoclave cycle (Figure 6.21).
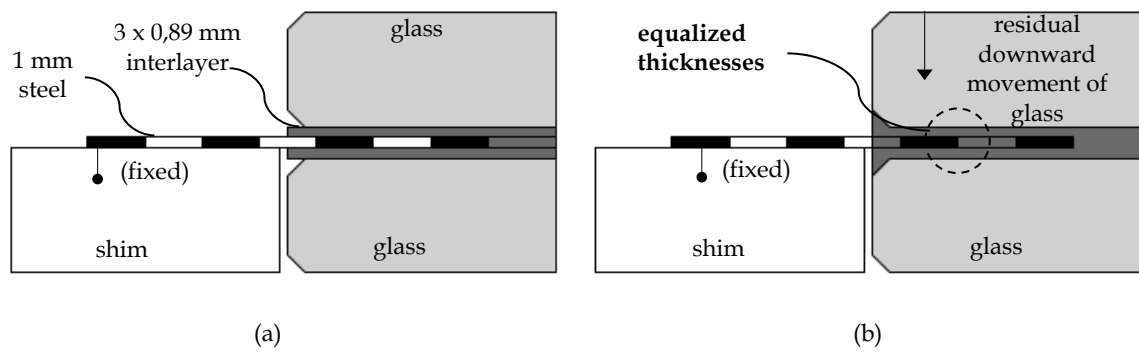
Figure 6.21. Position of protruded steel insert before (a) and after autoclave cycle (b), fixed to a shim with the same thickness of glass and interlayer (0,89 mm)

6.5   Conclusions

The fabrication of laminated glass with protruded steel embedded elements is a complex and delicate process with no standard laboratory or industrial procedures available to follow. For this reason an experimental investigation was conducted with particular focus on the positioning of the protruded steel embedded element before and after the autoclave cycle. From the experimental investigation it is concluded that it is possible to fabricate good quality laminated glass with protruded steel embedded elements (Figure 6.22). This requires following the basic good practices for lamination, calibrating the temperature and pressure (vacuum and atmospheric pressure) parameters to the specific constitution and size of the laminate, and level the support conditions in combination with laminate structure, in order to fix the position of the protruded steel before and after autoclave cycle, counteracting the deformation of the inner supporting conditions caused by the melting of the interlayer, necessary to adhere and fill the hollowed gaps of the perforated steel.
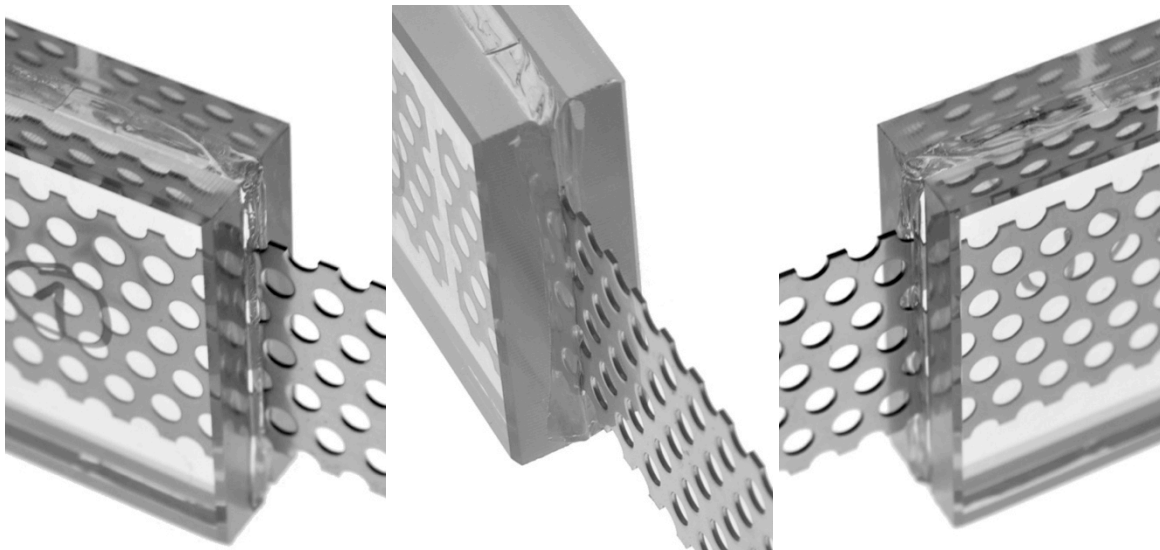
Figure 6.22. Different close-up views of successfully laminated glass with protruded steel embedded elements.

7 Structural behaviour

7.1   *The strong link* - **tensile behaviour of thin steel plates**

This section addresses the experimental investigation conducted to study the tensile behaviour of thin steel plates. The type of test applied is the tensile test. Several parameters have been selected as relevant, namely the perforation of the steel plate and the direction of load application concerning the perforation pattern. Specific research questions have been raised that this experimental investigation seeks to respond:

- How different is the tensile behaviour between a perforated and a non-perforated thin steel plate?

- What is the influence of the direction of load application in the tensile behaviour of a perforated steel plate?

Three types of test specimens were designed combining perforated and non-perforated steel with the same thickness. Both perforated specimens were cut from the same plate according to the *open* and *closed* direction of the RT pattern of perforation (see section 5.3).

7.1.1   Test procedure

7.1.1.1   Test specimens

Figure 7.1 shows the configuration of the non-perforated and perforated tensile test specimens.
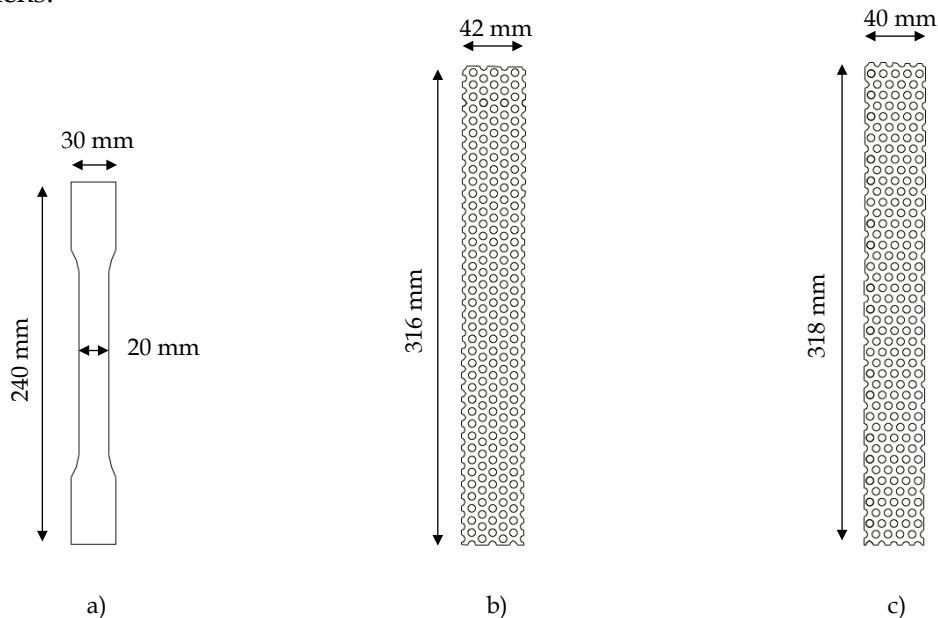
Figure 7.1.Tensile test specimens: non-perforated - *dumbbell* (a), perforated - *open pattern* (b) and perforated - *closed pattern* (c).

All the specimens are made of AISI 304 stainless steel and have a thickness of 1 mm. The non-perforated specimen is dumbbell shaped according to EN 10 002-1 and was cut using a laser machine. It has a total length of 240 mm and a width of 30 mm on the tops. The width on the middle section is reduced to 20 mm according to the dumbbell shape, presenting a 20 mm^2 cross section area.

The perforated steel specimens have a R5T8 perforation pattern, which is characterized by having 5 mm diameter holes disposed diagonally at an angle of 60 ^{o}, distancing 8 mm from centre to centre. This type of pattern has 35,4 % of the surface perforated. The open pattern perforated specimens have 316 mm length and 42 mm width, while the closed pattern perforated specimens have 318 mm length and 40 mm wide. The difference is due to the necessary alignment with the perforation hole centre to avoid the creation of weakened areas. It revealed to be critical in triggering early failures.

In order to guarantee that the breakage would occur at the central zone of the specimen and guarantee that both the types of perforated specimens had the same cross section area, one hole bar was manually cut on each side of the *open pattern* specimens, whilst on the closed pattern only half bar (as determined by the original cut line) was cut on each side (see Figure 7.2.). This way both specimens had 12 mm^2 of cross section area. For the *pull-out* tests, a total of 9 specimens were made resulting in three specimens for each type.

a)   b)
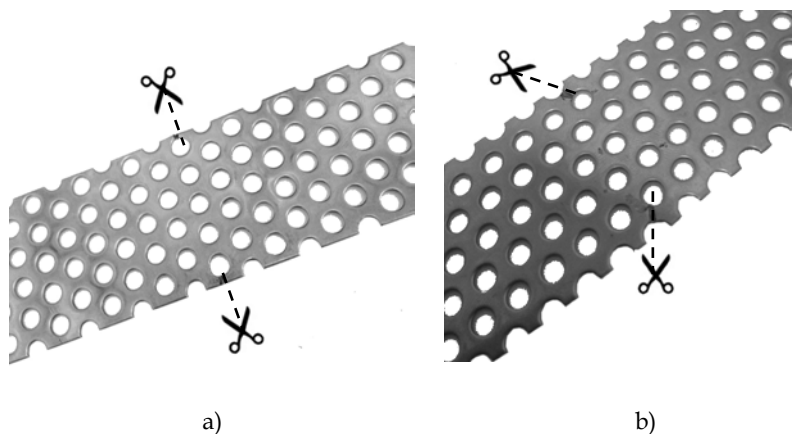
Figure 7.2. Preparation cut of perforated steel specimens: *closed pattern* (a) and *open pattern* (b).

7.1.1.2   Test setup

The *pull-out* tests have been performed using a Microtest EM1/50 universal machine of 50 kN maximum force. The specimens were fixed on the upper and lower bracket with 40 mm of embedment on each side (see Figure 7.3). The lower cross head was set to move downwards at a constant rate of 2 mm/minute, and stop when a 60 % drop in the applied load occurred. The temperature in the room during the tests was around 20 °C. The total displacement was measured using the internal system of the machine.
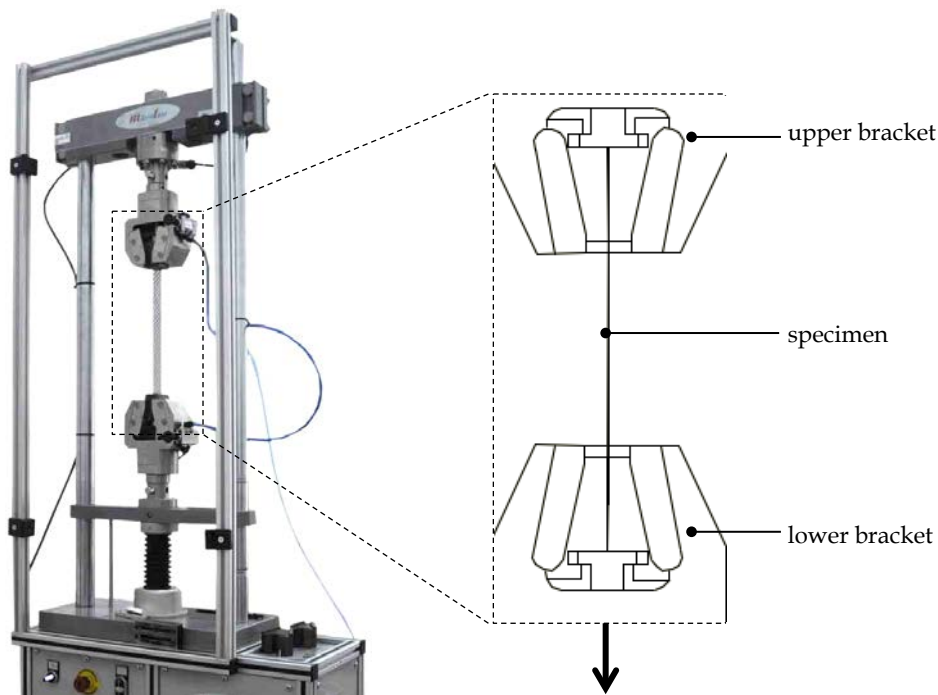
Figure 7.3. Tensile test setup

7.1.2   Test results

7.1.2.1   Perforated plate

In Table 7.1 are presented the results of the tensile tests on perforated steel specimens, and on Figure 7.4 are presented the correspondent load-displacement curves, of both open pattern and closed pattern types. The maximum loading, correspondent displacement and maximum nominal stresses are also presented.

Table 7.1. Results of the tensile tests on *open pattern* and *closed pattern* perforated steel specimens.

Type	$F_{máx}$ (kN)		$\sigma_{máx}$(MPa)*		Displacement - $F_{máx}$ (mm)	
		Mean		Mean		Mean
open pattern	8,70		725		26,40	
	8,59	**8,66**	716	**722**	25,11	**25,98**
	8,70		725		26,42	
closed pattern	8,18		682		10,39	
	8,71	**8,48**	726	**707**	18,49	**15,30**
	8,56		713		17,02	

(a)
open pattern

(b)
closed pattern
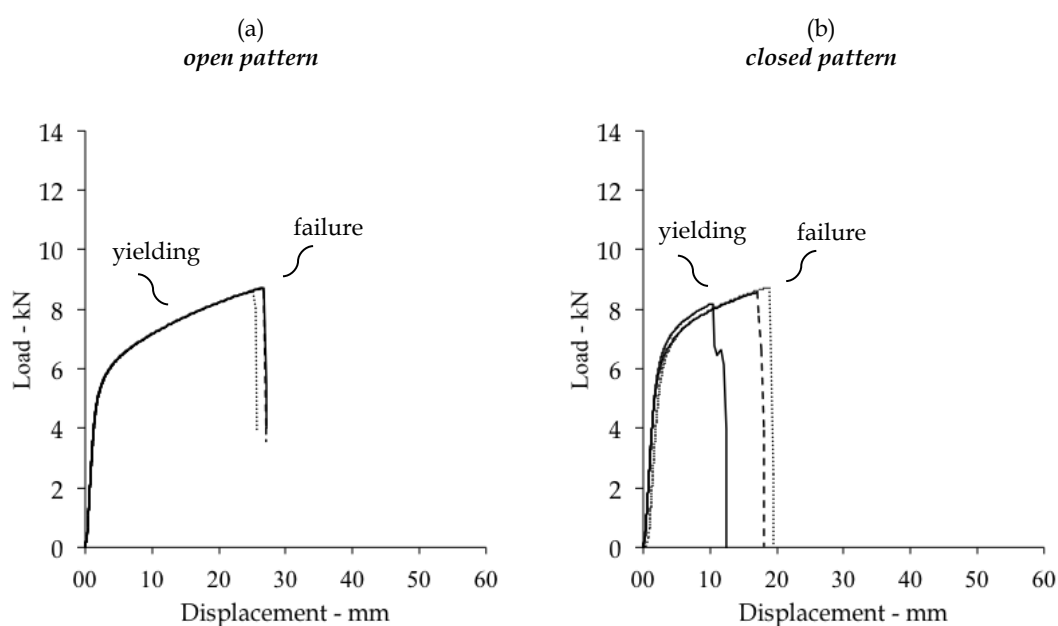
Figure 7.4. Load displacement diagrams of the tensile tests on perforated plates.

The tests on the perforated steel specimens loaded on the *open pattern* direction show a linear elastic behaviour until 4,0 kN, succeeded by the plastic deformation. It extends to an average maximum load of 8,7 kN, corresponding to an applied stress of 725 MPa. It occurred at a displacement of around 26 mm, when one of the hole's bar disrupted and triggered the complete failure of the specimen. The perforated steel plates loaded on the *closed pattern* direction show similar behaviour to the *open pattern*, however the elastic deformation extends until an average load of 5,0 kN. After the plasticization it breaks at an average maximum load of 8,5 kN or 707 MPa of applied stress. Although these values are very close to the observed on the *open pattern* specimens, in this case the maximum loading occurred at a considerably lower displacement of 15 mm.

7.1.2.2   Non-perforated plate

In Table 7.2 are presented the results of the tensile tests on non-perforated steel specimens, and on Figure 7.5 are presented the correspondent load-displacement curves. The maximum loading, correspondent displacement and maximum nominal stresses are also presented.

Table 7.2. Results of the tensile tests on non-perforated steel specimens.

Type	$F_{máx}$ (kN)		$\sigma_{máx}$(MPa)*		Displacement at $F_{máx}$ (mm)	
		Mean		Mean		Mean
non-perforated	12,31		616		64,12	
	12,50	**12,50**	625	**625**	63,56	**64,25**
	12,68		634		65,08	
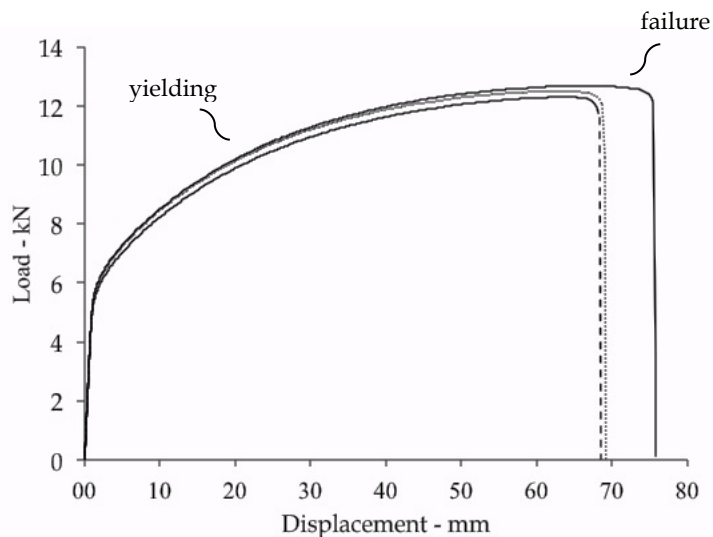
Figure 7.5. Load displacement diagrams of the tensile tests on non-perforated steel specimens.

The tests on the non-perforated steel specimens show a linear elastic behaviour until an average load of 5,0 kN, succeeded by the plastic deformation that extends to an average maximum load of 12,5 kN. It corresponds to a mean stress of 625 MPa, after which the steel disrupted. It occurred at an average displacement of 64 mm.

7.1.3 Discussion

The results of the tensile tests clearly showed a very similar behaviour of perforated and non-perforated specimens. Comparing the mean maximum stresses, there was small superiority of the perforated specimens results. Within this type of specimens, the maximum load obtained in the two directions of load application - *open pattern* and *closed pattern* - was almost the same.

However, it was clear that when loaded in the open-pattern direction, the steel specimens exhibited higher elongation at break. The increase was almost 70% compared with the closed-pattern specimens. This difference is justified by the geometrical arrangement of the perforations, noticeable in the failure pattern of each specimen. The *open pattern* fails diagonally according to a discontinuous line, which causes some plastic deformation of the neighbouring holes to happen before failure. On the contrary, the *closed pattern* fails transversally according to a straight line without initiating any deformation in the surrounding area (see Figure 7.6)

plastic deformation

discontinuous failure

straight failure

(a)   (b)   (c)
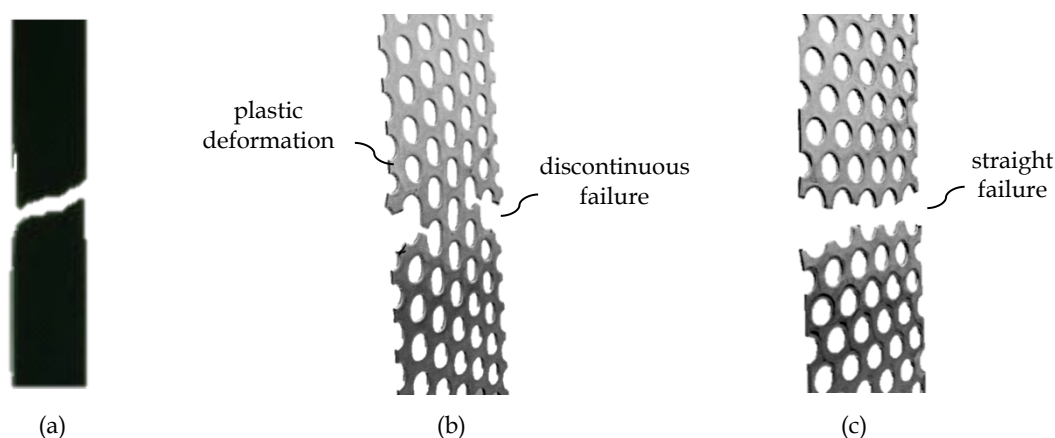
Figure 7.6. Close-up view of tested specimens at the zone of failure: non-perforated - dumbbell (a), perforated - *open pattern* (b) and perforated - *closed pattern* (c).

7.1.4 Conclusions

From the tensile tests it is possible to conclude that there is no significant difference on the tensile strength of perforated and non-perforated steel plates. Also the direction of loading in the perforated and non-perforated steel doesn't affect significantly the maximum load. A visible difference is noticeable in the elongation at break, which in the open pattern is considerably higher due to the failure behaviour, which is preceded by local plastic deformation.

7.2 *The weak link* - adhesive behaviour of embedded thin steel plates

This section addresses the experimental investigation conducted to study the adhesive behaviour of thin steel inserts embedded in laminated glass. The *pull-out* test has been selected as the appropriate method to address the shear strength of the bond between glass and the steel inserts. Several parameters have been selected as relevant, namely the type of interlayer, the perforation of the metal insert and the embedment depth. Specific research questions have been raised that this experimental investigation seeks to respond:

-How different is the adhesive capacity between glass and thin steel elements when using a soft or a stiff interlayer?

- How does the use of perforated metal affect the adhesive behaviour?

- What is the influence of the metal embedment depth in the adhesive behaviour?

The test specimens were designed in accordance, combining a soft interlayer and a stiff interlayer, perforated and non-perforated steel inserts and two embedment depths (20 mm and 40 mm). In order to allow a comparative analysis between the different types of specimens, some aspects were guaranteed: both types of interlayers have the same thickness, both steel insert types have the same cross section, and the embedded surface nominal area is similar both in perforated and non-perforated steel inserts.

7.2.1 Test procedure

7.2.1.1 Pull-out test specimens

The *pull-out* test specimen comprises two 10 mm thick rectangular shaped pieces of annealed float glass measuring each 70 mm x 200 mm. These are laminated with a thin steel plate in between, partially embedded to allow pulling. To compensate this extra thickness, an additional fully embedded perforated plate is added to all the laminates, guaranteeing an equalized pressure during the lamination process. Each specimen is laminated with two interlayer foils of 1,52 mm of thickness each, placed between the glass panes and steel insert. Two types of interlayers were used, a soft - polyvinyl butiral (PVB) and a stiff - ionomer SentryGlas® (SG).

For the semi-embedded plate, two types were used: perforated and non-perforated. Both are made of AISI 304 stainless steel and have 1 mm thickness. The perforated plate has a R5T8 perforation pattern, which is characterized by having 5 mm diameter holes disposed diagonally at an angle of 60 °, distancing 8 mm from centre to centre. This type of pattern has 35,4 % of the surface perforated. The non-perforated plate is dumbbell shaped according to EN 10 002-1. This is due to the necessity to match the cross section area and adhesive contact nominal area of both perforated and non-perforated steel plates.

The steel inserts were embedded according to two depths - 20 mm and 40 mm - defining two distinct adhesive areas. In order to assure nominal comparison between perforated and non-perforated specimens, both have to have the same adhesive area. The non-perforated plate is less wide, measuring only 27 mm, compared with the perforated plate, which measures 42 mm (see Figure 7.7). At the end, two nominal adhesive surface areas were determined, independent of the type of the steel plate. According to the embedment depth it was 10,8 cm² for 20 mm embedment and 21,6 cm² for 40 mm embedment.

The specimens were laminated using the silicone blanket system as described in the previous chapter. After the lamination process all the specimens were inspected and the total thickness was measured in the four corners. For the *pull-out* tests, a total of 24 specimens were made resulting in three specimens for each combination.
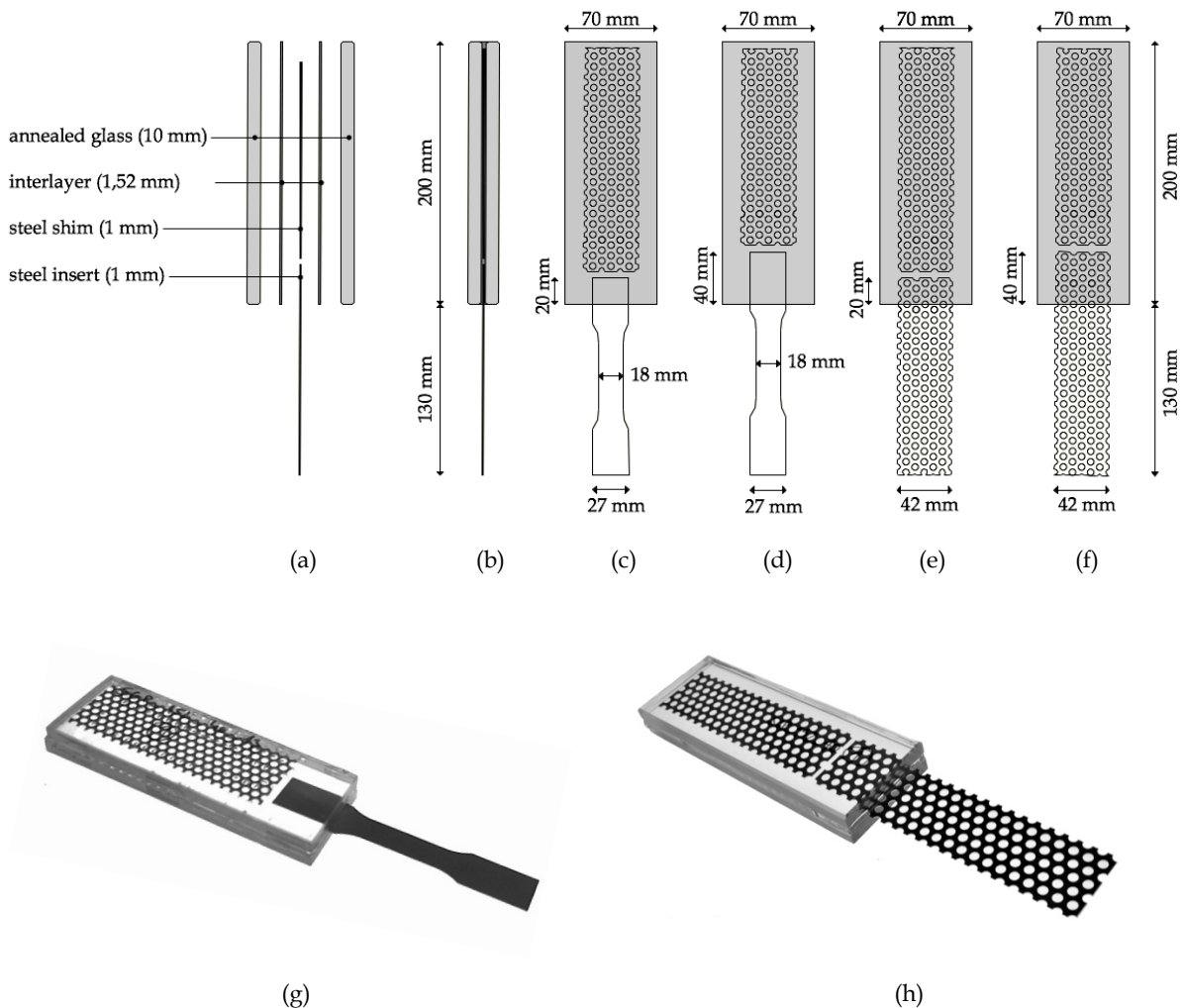
Figure 7.7: *Pull-out* adhesion test specimens: composition (a), cross section (b), 20 mm embedded non-perforated specimen front view (c), 40 mm embedded non-perforated specimen front view (d), 20 mm embedded perforated specimen front view (e), 40 mm embedded perforated specimen front view (f), 40 mm embedded non perforated specimen picture (g) and 40 mm embedded perforated specimen picture (h).

7.2.1.2   Pull-out test setup

The *pull-out* tests have been performed using a Microtest EM1/50 universal machine of 50 kN maximum force. To accommodate the specimens in place, two symmetrical custom-made steel profiles were fixed to the upper crosshead through an inner bolted steel bar. The space left between the two steel profiles allows the protruded steel element of the specimen to pass and get gripped by the lower crosshead, while holding in contact the glass edges. Aluminium bars were added to intermediate this contact and absorb any stress concentration (see Figure 7.8). The lower cross head was set to move downwards at a constant rate of 2 mm/minute, and stop when a 60 % of load decrease occurred. The temperature in the room during the tests was around 20 $^{\circ}$C. The total displacement of the connection was measured using the internal system of the machine.
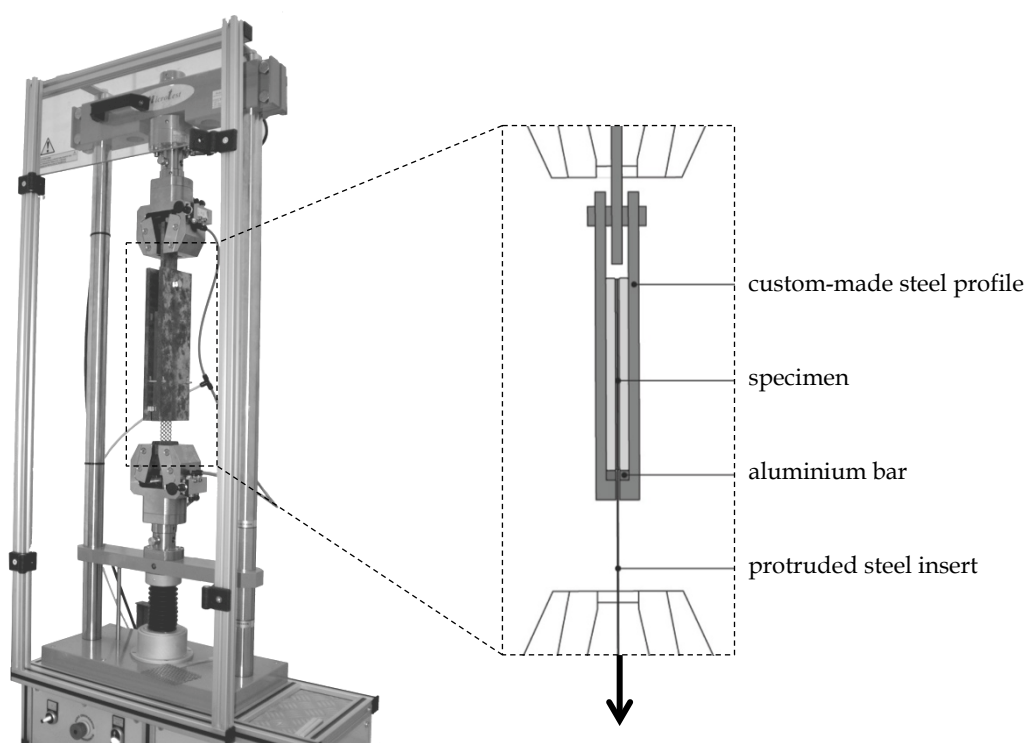
Figure 7.8: *Pull-out* test setup.

7.2.2   Test results

7.2.2.1   PVB laminated steel inserts

In Table 7.3 and Table 7.4 are presented the results of the *pull-out* tests on PVB laminated steel inserts, and on Figure 7.9 and Figure 7.10 are presented the correspondent load-displacement curves, of both non-perforated and perforated specimens with 20 and 40 mm of embedment. The maximum loading, correspondent displacement and maximum nominal stresses on the adhesion surface are presented. The failure of both glass and steel is also referred.

The tests on 40 mm embedded non-perforated plate specimens show an initial linear elastic behaviour until a maximum load is reached at an average of 6,5 kN. This maximum loading occurs at around 2,7 mm of displacement in the three specimens. Afterwards, the load decreases rapidly due to the slipping of the steel insert.

The 20 mm embedded non-perforated plate specimens show similar behaviour to the 40 mm, but carrying inferior loads. A similar linear elastic behaviour is clear at the beginning until an average load of 2,4 kN, at around 2,5 mm of displacement, corresponding to the maximum force applied in this case. At this force level the load suddenly decreases, interrupted by small increases, configuring an irregular and slow overall decreasing of final loading. In specimen #03 the displacement was very slow and long until a total slip of the plate occurs at 17,5 mm.

Table 7.3: Results of the *pull-out* tests on non-perforated steel PVB embedded inserts.

Embedment (mm)	$F_{máx}$ (kN)	Mean	$\tau_{máx}$ (MPa)*	Mean	Displacement $F_{máx}$ (mm)	Glass breakage	Steel failure
40	7,5		3,5		2,7		
	5,9	**6,5**	2,7	**3,0**	2,7	No	No
	6,1		2,8		2,7		
20	2,8		2,6		2,6		
	2,2	**2,4**	2,0	**2,2**	2,3	No	No
	2,1		1,9		2,5		

* Maximum nominal stress

(a)
40 mm embedment

(b)
20 mm embedment
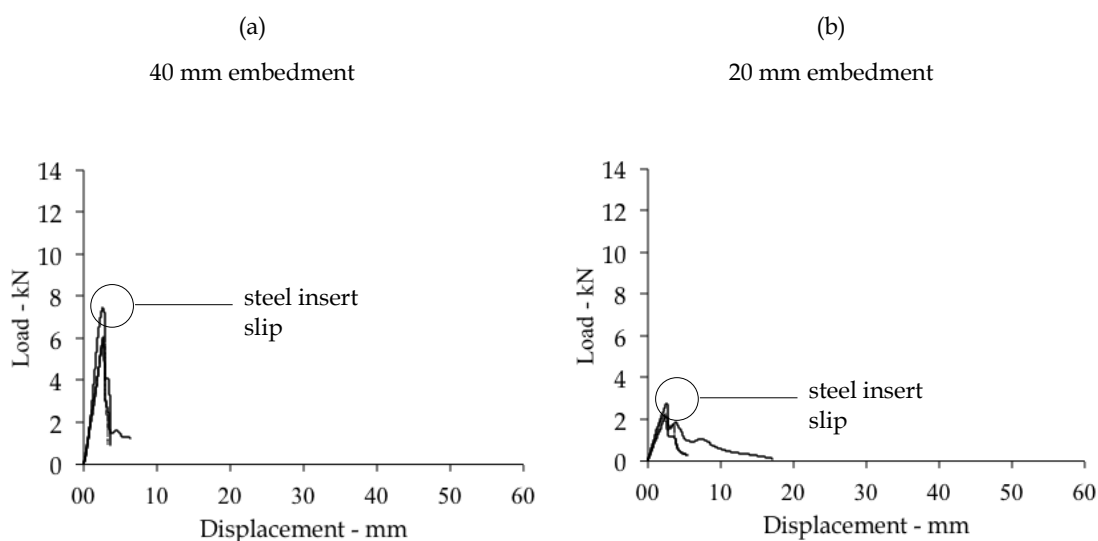
Figure 7.9: Load displacement diagrams of the *pull-out* tests on non-perforated steel PVB embedded inserts.

In the case of the perforated plate specimens, the 40 mm-embedded series exhibited elastic deformation until a first relative maximum load at around 1,5 mm of displacement. It is followed by an irregular increasing of load until an average maximum is reached at 5,7 kN. Afterwards, a progressive failure is visible in the three specimens followed by redistribution.

With similar behaviour but inferior load levels, the 20 mm embedded perforated plate specimens also exhibits a first relative maximum, followed by an irregular behaviour. The maximum average load of 2,6 kN happens at 4,2 mm of displacement, succeeded by a slow decrease of loading and considerable deformation.

Table 7.4: Results of the *pull-out* tests on perforated steel PVB embedded inserts.

Embedment (mm)	$F_{máx}$ (kN)	Mean	$\tau_{máx*}$ (MPa)	Mean	Displacement $F_{máx}$(mm)	Glass breakage	Steel failure
40	5,1		2,4		5,8		
	6,5	5,7	3,0	2,7	7,7	No	No
	5,6		2,6		5,6		
20	2,5		1,1		3,6		
	2,9	2,6	1,3	1,2	5,6	No	No
	2,5		1,1		3,5		

* Maximum nominal stress

(a)

40 mm embedment

(b)

20 mm embedment
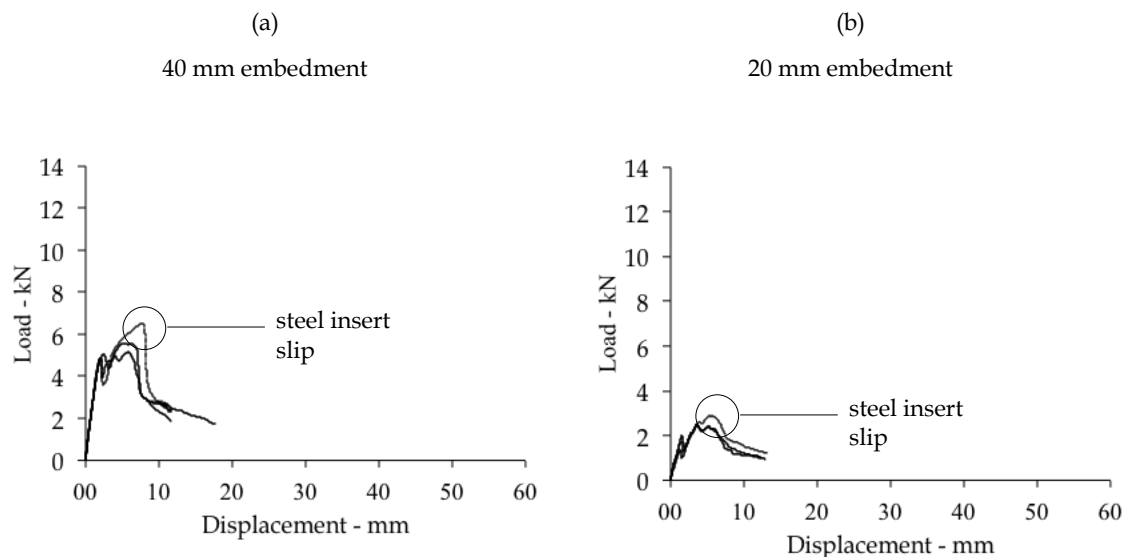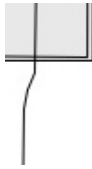
Figure 7.10: Load displacement diagrams of the *pull-out* tests on perforated steel PVB embedded inserts.

7.2.2.2   *SG laminated steel inserts*

In Figure 7.11 and Figure 7.12 are presented the results of the *pull-out* tests on SG laminated steel inserts in similar terms as the previous PVB tested specimens. After an initial elastic deformation, the 40 mm embedded non-perforated plate start to yield and deform in a plastic way. This transition occurs at a value close to 5,0 kN of load and is clearly visible in the load versus displacement curve. During the subsequent plastic deformation of the semi-embedded steel, the load continues to increase until a first crack occurs in the glass. It happened at distinct levels of load in all three specimens, in the range from 10,0 to 13,0 kN. Despite these cracks, which continued to increase coupled with the consequent rearrangement of the parts, the load capacity continued to increase. It only stopped when the glass breakage was such that the stiffness was lost and load decreased abruptly. The mean maximum load was 12,1 kN.

The 20 mm embedded non-perforated plate specimens behaved in a very similar way compared to the 40 mm, exhibiting a metal plasticisation after the initial elastic deformation of the connection. The glass of all the three specimens broke at a certain level of load but no increase of loading occurred. It happened at an average maximum load of 11,4 kN. Afterward a fast decrease of load is visible.

Table 7.5: Results of the *pull-out* tests on non-perforated steel SG embedded inserts.

| Embedment (mm)	$F_{máx}$ (kN)	Mean	$\tau_{máx}$ (MPa)	Mean	Displacement $F_{máx}$ (mm)	Glass breakage	Steel failure
40	13,2		6,1		53,0		
	12,5	**12,1**	5,8	**5,6**	42,3	Yes	No
	10,8		5,0		28,5		
20	11,8		10,9		35,0	Yes	
	11,3	**11,4**	10,5	**10,5**	31,7	Yes	No
	11,0		10,2		29,2	No	
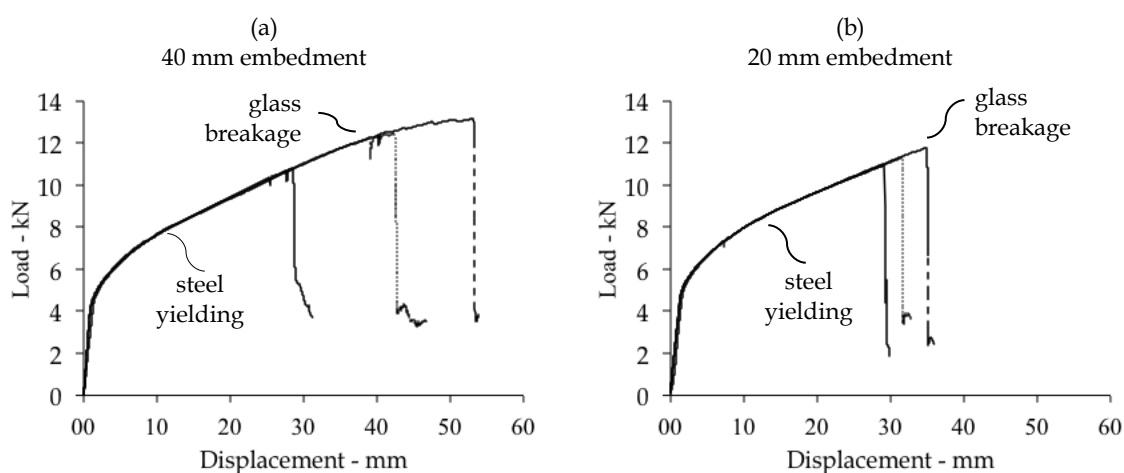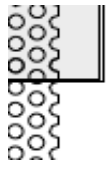
Figure 7.11: Load displacement diagrams of the *pull-out* tests on non-perforated steel SG embedded insert.

Concerning the specimens with perforated plate, the 40 mm embedment series consistently showed elastic deformation until 5,0 kN of load and consequent plastic deformation when the metal start to elongate until its failure at around 11,7 kN. Only one of the specimen's glass broke but it may have happened simultaneously with the metal failure, since there is no visible inflection in the load deformation curve, before the final decrease of load.

The 20 mm perforated plate specimens also show elastic-plastic transition at similar load level. The metal inserts start to deform until the occurrence of glass breakage. It happened with two specimens, one broke just one glass and exhibited some increase of load capacity afterwards, whilst the other specimen exhibited the breakage of the second glass, which prevented an increase of load capacity. It is visible in the load deformation curve and led to final failure.

Table 7.6: Results of the *pull-out* tests on perforated steel SG embedded inserts.

	Embedment (mm)	$F_{máx}$ (kN)		$τ_{máx}$ (MPa)		Displacement $F_{máx}$ (mm)	Glass breakage	Steel failure
			Mean		Mean			
	40	11,6		5,4		43,7	No	
		11,7	**11,7**	5,4	**5,4**	43,0	Yes	Yes
		11,7		5,4		45,3	No	
	20	10,0		9,3		24,1	Yes	
		9,9	**10,1**	9,2	**9,3**	24,4	No	No
		10,3		9,5		26,1	Yes	

(a)   (b)

40 mm embedment specimens   20 mm embedment specimens
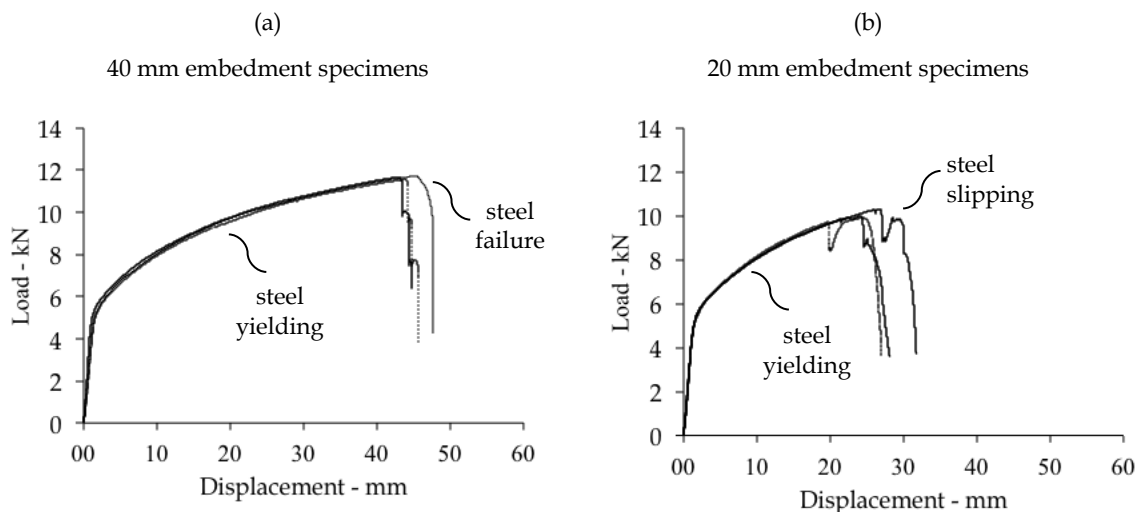
Figure 7.12: Load displacement diagrams of the *pull-out* tests on perforated steel SG embedded inserts.

7.2.3 Discussion

The results of the *pull-out* tests clearly showed a behaviour dependent on the type of interlayer. It is clear that SG specimens present a superior adhesive capacity when compared with PVB. Steel inserts laminated with this soft interlayer slip at very low stresses (1-3 MPa), clearly inferior to the high values (5 - 11 MPa) observed with the SG specimens. It is visible that no deformation of the steel occurs, especially on the perforated, which maintain the perfectly round holes.

A visual inspection of the tested specimens showed considerable deformation of the PVB instead, caused by the anchoring inside the perforated plate holes. Looking at the bar graphs in Figure 7.13, it is also clear that this different behaviour becomes more evident when reducing the embedment length. Halving the embedment length on the PVB specimens resulted in a considerable reduction of maximum strength, which in the case of the SG specimens the reduction was small. This is due to the fact that all the PVB specimens failed by debonding and slipping of the metal, while the SG specimens mainly failed by glass breakage or steel disruption.

The difference of maximum load when using perforated or non-perforated steel was minor. As we can read from the bar graph, comparing the different types of specimens, the difference was less than 10 % in each case. However in terms of failure behaviour a considerable difference is noticeable in the SG laminated specimens.
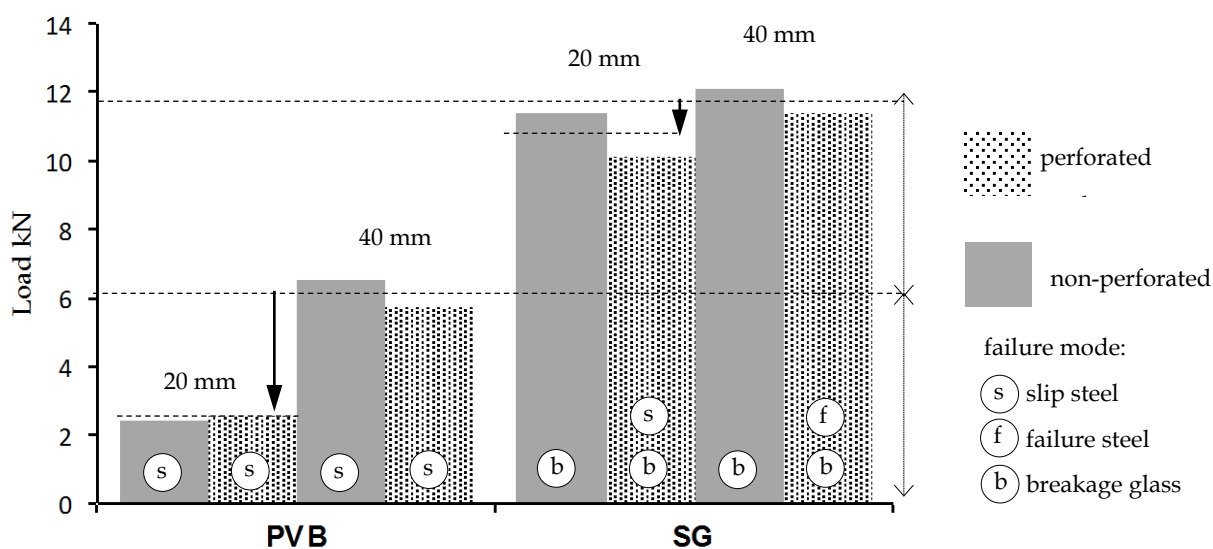
Figure 7.13. Bar graph comparing the mean maximum loads of the *pull-out* tests on PVB and SG specimens.

Non-perforated steel inserts tend to create stress concentrations along the edge of the insert and particularly on the corners. It is clear in the fragmentation of the glass, which occurs with considerable intensity in a localized area surrounding the steel insert edge (see Figure 7.14). Close to this area, aligned with the inner side of the steel insert, it is also clear an initial debonding of the interlayer caused by this stress intensification.

On the contrary, the perforated steel inserts tend to create an even distribution of stress, visible in the distributed fragmentation of the broken glass of the specimen. The capacity to distribute stresses is achieved both by the holes on the steel, which significantly increase the contact area (besides the nominal surface area), and the interlayer that fills the hollowed section thus achieving superior thickness. Additionally, the perforated plate demonstrated a higher capacity to adapt to the loading conditions, visible in the clearly distinct deformation outside of the laminate. At the end of the test it was clear that the stress on the inside plate was half of the same plate outside the laminate.

PVB

SG®

NON-PERFORATED

40mm

steel slip

6,5 kN

40mm

stress
concentration

steel yield

12,1 kN

20mm

steel slip

2,4 kN

20mm

stress

steel yield

11,4 kN

PERFORATED

40mm

steel slip

5,7 kN

40mm

even
stress
distribution

steel yield and
failure

11,7 kN

20mm

steel slip

2,6 kN

20mm

steel yield
and slip

10,1 kN
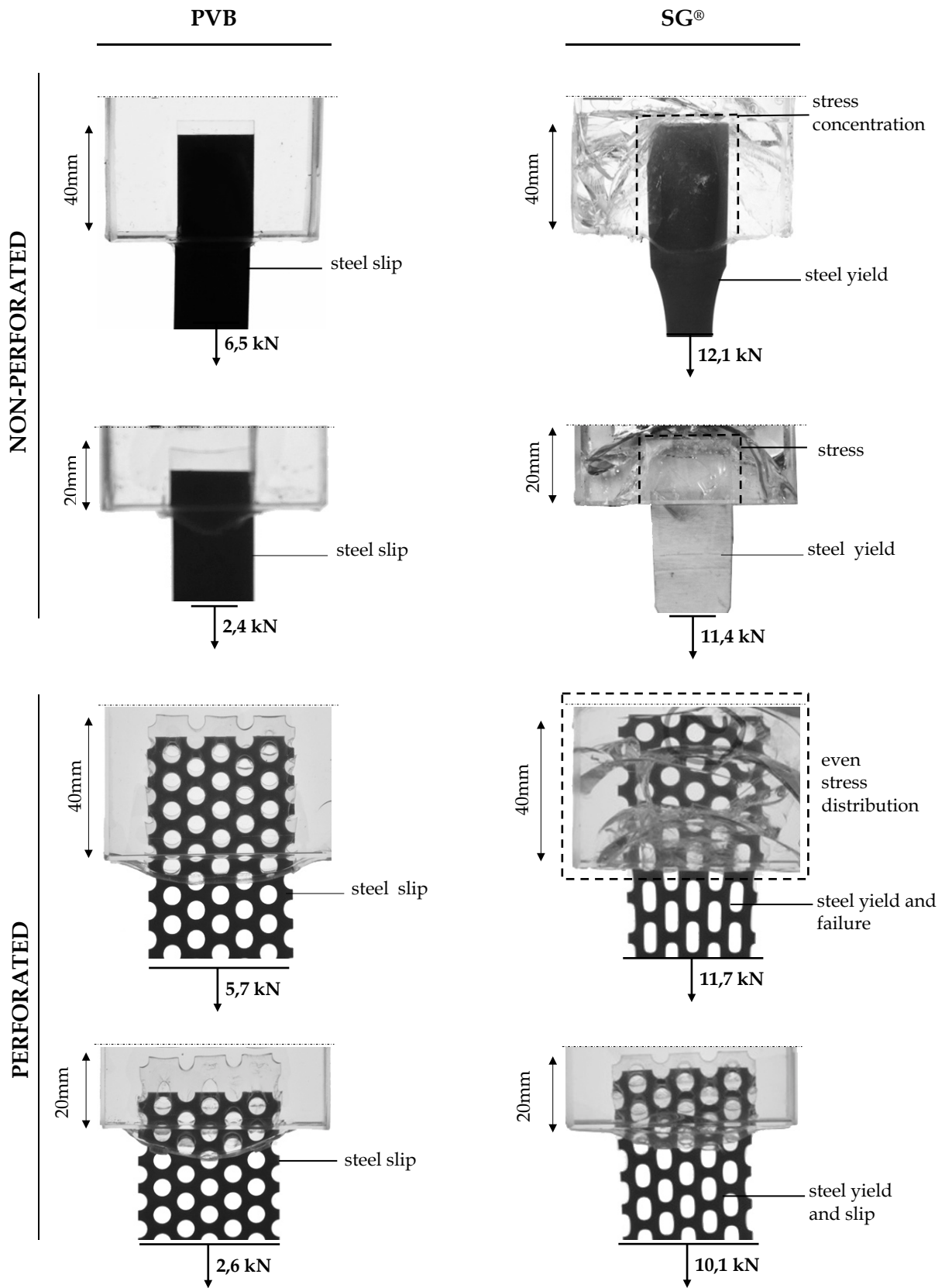
Figure 7.14. Close-up view of the *pull-out* specimens after test at the level of the embedment.

7.2.4 Conclusions

From the *pull-out* tests it is possible to conclude that the adhesive behaviour is highly dependent on the type of interlayer. Adhesive connections with reduced embedment depth can only be realized using a stiff interlayer like the SG. The low stress at which the PVB specimens failed requires a considerable increase of the adhesion area in order to be effective. Using just 40 mm of embedment length on SG laminated glass it was possible to avoid debonding and consequent slip of the steel insert. Furthermore, it is also possible to conclude that steel inserts with perforated body have a higher capacity to perform an even distribution of stress. In terms of safety of the connection it may have a decisive impact since in case of glass breakage it tends to happen in larger pieces, contrasting with the intense fragmentation observed with non-perforated inserts.

7.3 *In-between* - compressive behaviour of glass in contact with different substrates

This section addresses the experimental investigation conducted to study the compressive behaviour of glass in contact with different substrates. The parameters selected for the test comprehend the different levels of pre-stress on glass - annealed, heat-strengthened and fully tempered - and different types of substrates. With similar Young's modulus, aluminium was selected as a reference together with two transparent and three opaque polymers. This experimental investigation seeks to answer the following questions:

- What is the relation between the applied stress and deformation of the different substrates?

- How do the different substrates influence the maximum compression load?

- What is the influence of the pre-stress level in the compressive behaviour of glass?

- How different is the fracture initiation when using annealed, heat strengthened and fully tempered glass?

The selection of a wide sample of substrates, combining different mechanical characteristics, had the aim to collect insightful data concerning the items highlighted in the investigation questions. To assure comparable behaviour, all glass specimens were cut from a single sheet of 10 mm float glass and were heat strengthened in the same oven cycle. A qualitative approach was preferred in which the number of specimens per each combination was set according to the results obtained and the time available for performing the tests.

This experimental investigation was conducted in the scope of short-term scientific mission to the TU Delft, under direct supervision of Prof. Frederic Veer, from the 15th to the 30th of June 2012.

7.3.1 Test procedure

7.3.1.1 Compression test specimens

The compression test specimens comprise a single layer of 10 mm thick glass, measuring 100 mm wide and 300 mm long[1]. All the specimens were cut from a single sheet of glass and had ground, bevelled and polished edges (Figure 7.15). Three types of glass specimens were produced: annealed, heat strengthened and fully tempered. For security and post failure analysis the heat strengthened and fully tempered glass specimens were partially wrapped with one foil of self-adhesive plastic.

---

[1] 300 mm is considered the minimum length required to pass through the heat strengthening due to the space between rollers.
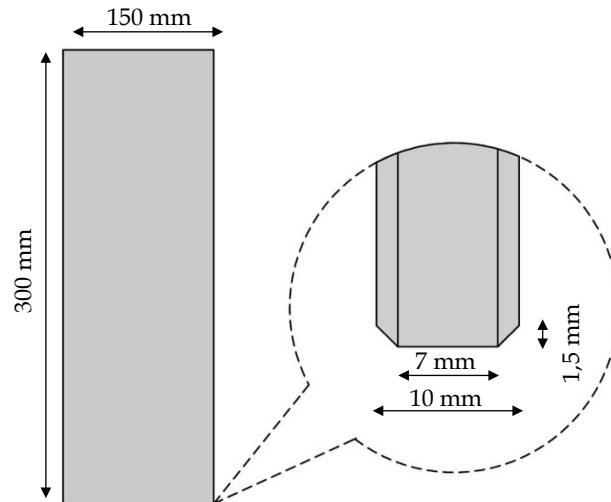
Figure 7.15: Compression test specimen geometry and detail of the glass bevelled polished edge.

Six different substrates were used: Aluminium (having the same young's modulus of glass was selected as a reference); two transparent polymers - PMMA (polymethyl methacrylate or acrylic) and PC (polycarbonate) - and three opaque polymers - POM (polyoxymethylene), PTFE (polytetrafluoroethylene) and PA6 (polyamide 6 or nylon 6) (Figure 7.16). The substrates had 10 mm thickness and were mostly square shaped with 150 mm side. Each substrate unit was used in at least three tests, with sufficient distance between each point of contact in order to avoid any previous deformation.
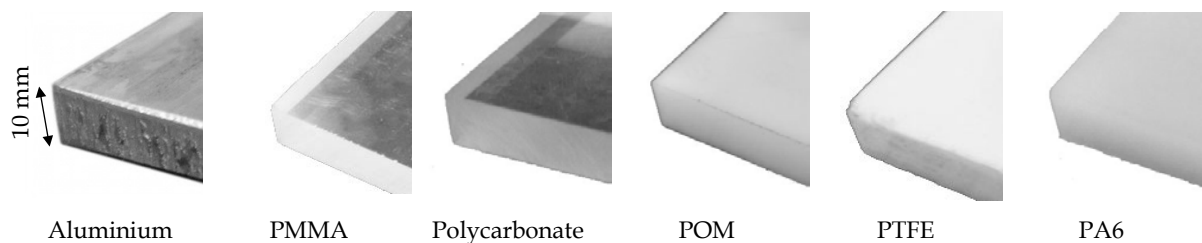
Figure 7.16: Corner detail of the selected substrates for the compression test in contact with the glass edge.

7.3.1.2   Compression test setup

A standard setup to test glass in compression with different substrates was not available. When compressing glass in the edges, premature failure by buckling is likely to happen. It would interfere with the actual compressive behaviour of glass in contact with substrates that constitutes the scope of this investigation. To avoid it, a specific setup was designed. The 100 mm x 300 mm glass specimens were hold on the upper part by a similar mechanism to a friction joint. It comprised two custom-made 10 mm steel plates and two 3 mm layers of rubber, squeezed against the glass by 6 steel bolts. An additional aluminium and rubber block, both 10 mm thick, were added to the top in order to retain certain vertical displacement as a consequence of the side rubber layers deformation during the load application (see Figure 7.17)
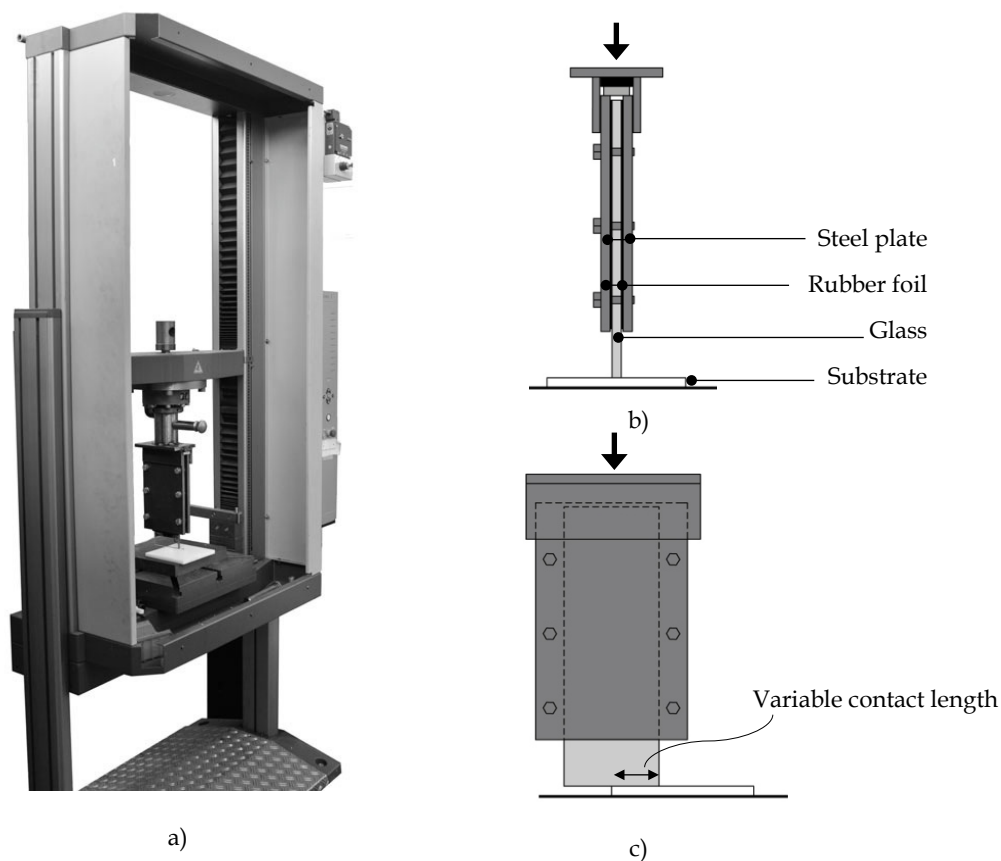
Figure 7.17: Compression test setup general view picture (a), detailed front view (b) and side view (c).

This setup sought a distributed appliance of load on the upper part of the glass specimen, thus assuring that the maximum stress would occur on the lower edge in contact with the substrate. During preliminary tests it became evident that an increase of applied stress on the glass would be needed in order to achieve its breakage before reaching the machine's maximum load capacity. The solution was to reduce the contact surface on some tests. Firstly half of the glass length (50 mm x 10 mm) was in contact, but then in certain substrates it was reduced to 40, 30 or 20 mm, thus increasing the stress and achieving the glass breakage. It can be considered as a test setup for a worst-case scenario, in which the support conditions are non homogeneous. Due to the polished bevelled geometry of the edge, the initial contact area was ≈ 47 mm x 7 mm. Only when the substrate began to deform, did the remaining chamfered thickness and width entered in contact with the substrate (see Figure 7.18). Due to the difficulty of determining this value, the total dimension was considered as nominal for comparison purpose. All specimens were tested in compression using a Zwick 100 kN Universal Machine (Figure 7.17 a). The test-loading rate was 1 mm /min. and a preload of 2 N was applied. The tests stopped when the glass or substrate showed considerable failure.
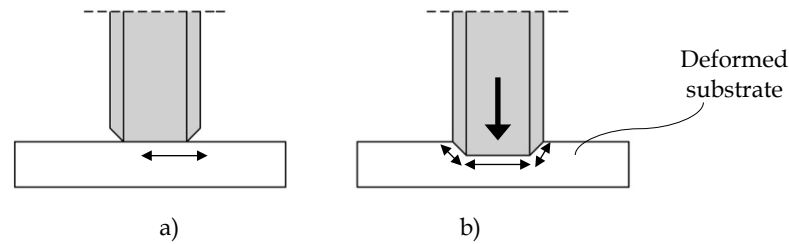
Figure 7.18: Contact surface at the beginning of loading a) and after substrate deformation (b).

7.3.2   Test results

7.3.2.1   Annealed glass

In Table 7.7 are presented the results of the compression tests with annealed glass.

Table 7.7: Results of compression tests of annealed glass with different substrates

	Contact length (mm)	Maximum load (kN)	Maximum contact stress (MPa)	mean (MPa)	Glass failure	Substrate failure
POM	50	97,7	195,4	**169,2**	yes	no
	50	62,6	125,2			
	50	93,5	187,0			
PMMA	50	91,4	182,8	**182,8**	no	yes
Al	50	110,0	220,0	**220,0**	yes*	no
	50	110,0	220,0			
PTFE	50	37,7	75,4	**71,3**	no	yes
	50	33,6	67,2			
PC	50	87,3	174,6	**197,3**	yes	no
	50	110,0	220,0		no	
PA6	50	110,0	220,0	**203,7**	yes*	no
	50	93,7	187,4		yes	

* Glass breakage appeared after test when unloading

The glass specimens in contact with POM showed considerable more crack branches when compared with the tests on Al or PC. Breakage occurred at an average stress of 169,2 MPa exhibiting between 4 and 7 crack branches. Crack initiated on the upper tensioned vertical edge, developing towards the opposite edge. One of the cracks consistently developed along the glass towards the lower edge in contact with the substrate at an angle of 45°. The tests in contact with PC and PA6 presented similar maximum average stress around 200,0 MPa and similar crack morphology as the previous tests with POM, but with reduced number of crack branches. Contrary, the glass specimens in contact with Al showed no cracks during the tests, reaching the maximum stress of 220,0 MPa. Only when unloading did the glasses broke on a single 45° branch, initiated close to the boundary of contact of the lower edge (see Figure 7.19).

POM	Al	PC	PA6
(169,2 MPa)	(220,0 MPa)	(197,3 MPa)	(203,7 MPa)
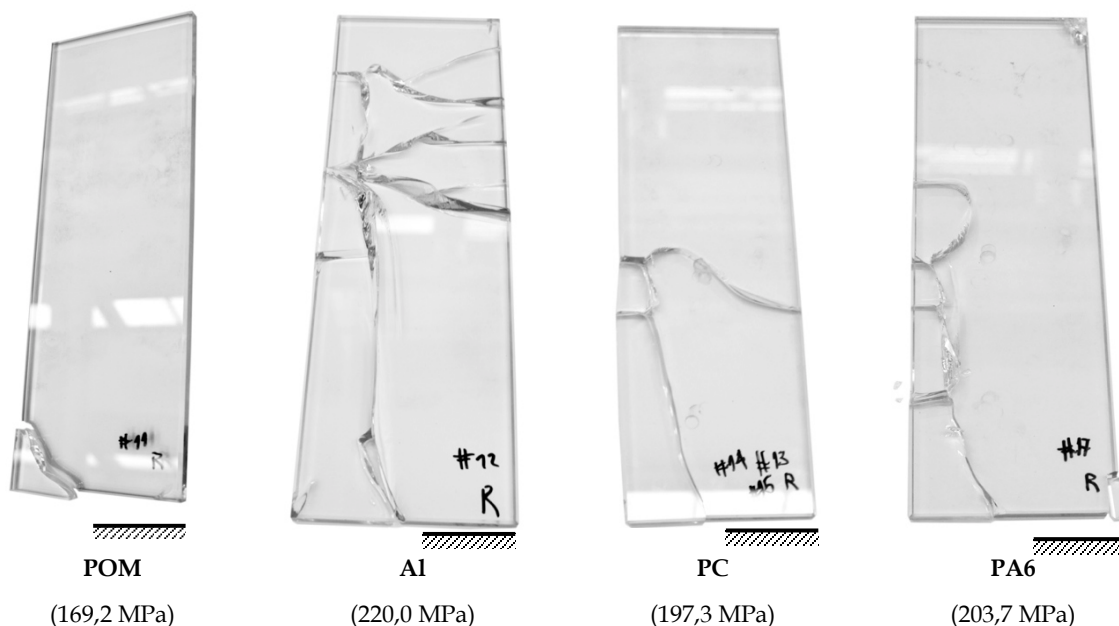
Figure 7.19: Fracture pattern of annealed glass specimens in contact with POM, Al, PC and PA6.

7.3.2.2   *Heat strengthened*

In Table 7.8 are presented the results of the compression tests with heat-strengthened glass.

Table 7.8: Results of compression tests of heat strengthened glass with different substrates

	Contact length (mm)	Maximum load (kN)	Maximum contact stress (MPa)	**mean (MPa)**	Glass failure	Substrate failure
POM	50	110	220	**220**	no	no
	50	110	220		yes*	
PMMA	50	67,3	134,6	**134,6**	no	yes
Al	50	110	220		no	no
	40	110	220		no	
	30	110	366,7	**315,6**	no	
	20	55,4	277		yes	
	20	78,6	393		yes	
	20	72,4	362		yes	
PTFE	50	28,1	56,2	**56,2**	no	yes
PC	50	110	220		no	no
	40	88,5	221,3	**216,9**	yes	no
	40	102	255		yes	yes
	20	34,3	171,5		yes	no
PA6	50	110	220	**220**	yes*	no
	50	110	220			

* Glass breakage appeared after test when unloading

For the tests with heat strengthened glass specimens, an initial 50 mm length was also used, which demonstrated to be insufficient in some cases, being applied reduced contact lengths until a minimum of 20 mm on specific tests. Similarly to what happened in the previous tests, the heat strengthened glass specimens in contact with PMMA and PTFE remained intact due to the early substrate failure.

The tests of glass in contact with POM, Polycarbonate and PA6 showed a similar average maximum stress around 220 MPa. A contact width of 50 mm was used on the POM and PA6 tests, resulting that the specimens became intact until maximum load was reached. Only when unloading did a needle shaped damage appeared on the vertical edge perpendicular to the substrate. On the tests with PC, reduced contact lengths of 40 and 20 mm were tested, reaching an estimated maximum stress of 255 MPa, which caused a severe breakage of both the glass and PC substrate. Concerning the tests with Al, a considerable maximum stress of 393 MPa was reached with 20 mm of contact length, being the average maximum stress around 315 MPa. The broken glass specimens showed a consistent pattern of around 10 branches starting on the lower edge, close to contact border, and vertically running along the glass length (see Figure 7.20).

needle shaped crack

needle shaped crack

POM   **Aluminium**   **PC**   **PA6**

(220,0 MPa)   (315,6 MPa)   (216,9 MPa)   (220,0 MPa)
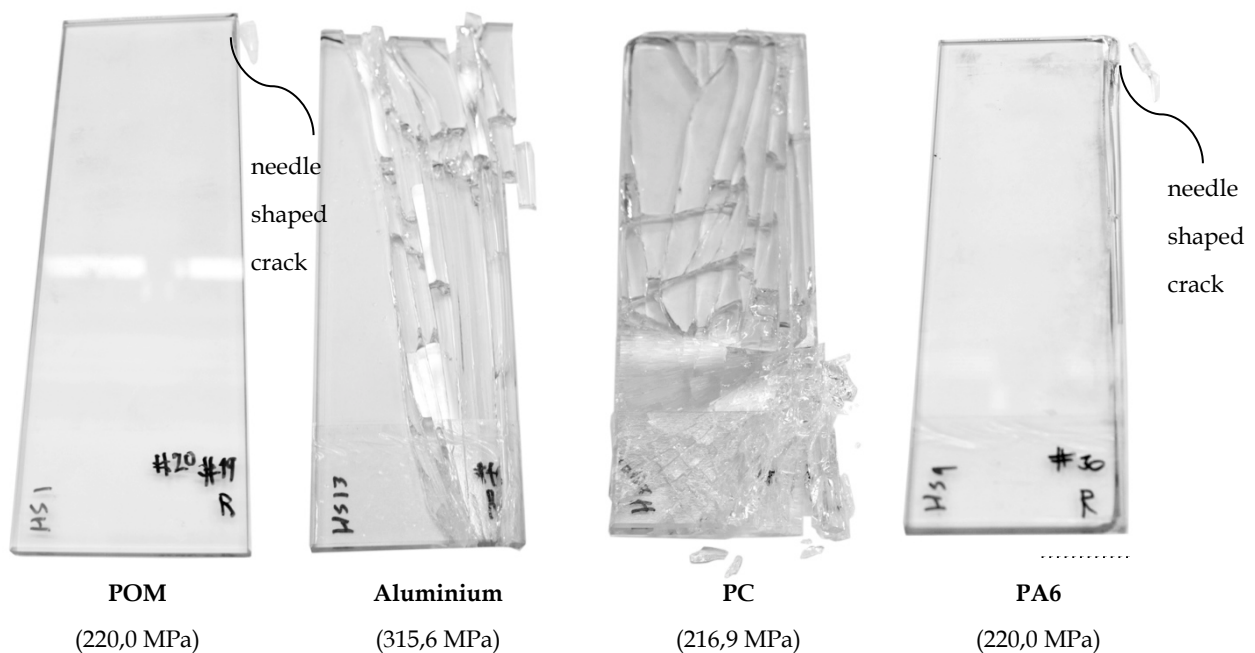
Figure 7.20: Fracture pattern of heat strengthened glass specimens in contact with POM, Al, PC and PA6.

7.3.2.3   *Fully tempered glass*

In Table 7.9 are presented the results of the compression tests with fully tempered glass.

Table 7.9: Results of compression tests of fully tempered glass with different substrates

	Contact length (mm)	Maximum load (kN)	Maximum contact stress (MPa)	**mean (MPa)**	Glass failure	Substrate failure
POM	50	57,2	114,4	**133**	yes	no
	50	75,8	151,6			
PMMA	50	69,4	138,8	**138,8**	no	yes
Al	50	109	218	**219**	yes	no
	50	110	220		yes*	
PTFE	50	35	70	**70,3**	yes*	yes
	50	35,3	70,6		no	
PC	50	100	200		yes	
	50	110	220	**151,9**	no	no
	50	17,8	35,6		yes	
PA6	50	74,9	149,8	**106,3**	yes	no
	50	31,4	62,8			

* Glass breakage appeared after test when unloading

Similarly to the previous tests, PMMA and PTFE substrates showed reduced strength and failed before any glass breakage. The failure mode of the remaining glass specimens was very similar, showing reduced crack size and intense fragmentation starting on the lower edge contact border. Meanwhile it happened at very distinct stress levels, even in contact with the same substrate. Glass in contact with POM substrates broke at an average stress of 133,0 MPa while glass in contact with Al consistently broke at a higher level of 219,0 MPa. The stress level was so high in the glass body that in conjunction with the energy release resulted in an intense fragmentation with a powder like pattern (see Figure 7.21). In contrast, the stress level that the glass specimens in contact with PCand PA6 was very disparate. Two glass specimens in contact with PC broke at around 210 MPa whilst the last broke at only 35,6 MPa. Similarly, the glass specimens in contact with PA6 showed very distinct stress levels of 149,8 MPa and 62,8 MPa.

POM   **Aluminium**   **PC**   **PA6**

(133,0 MPa)   (219,0 MPa)   (151,9 MPa)   (106,3 MPa)
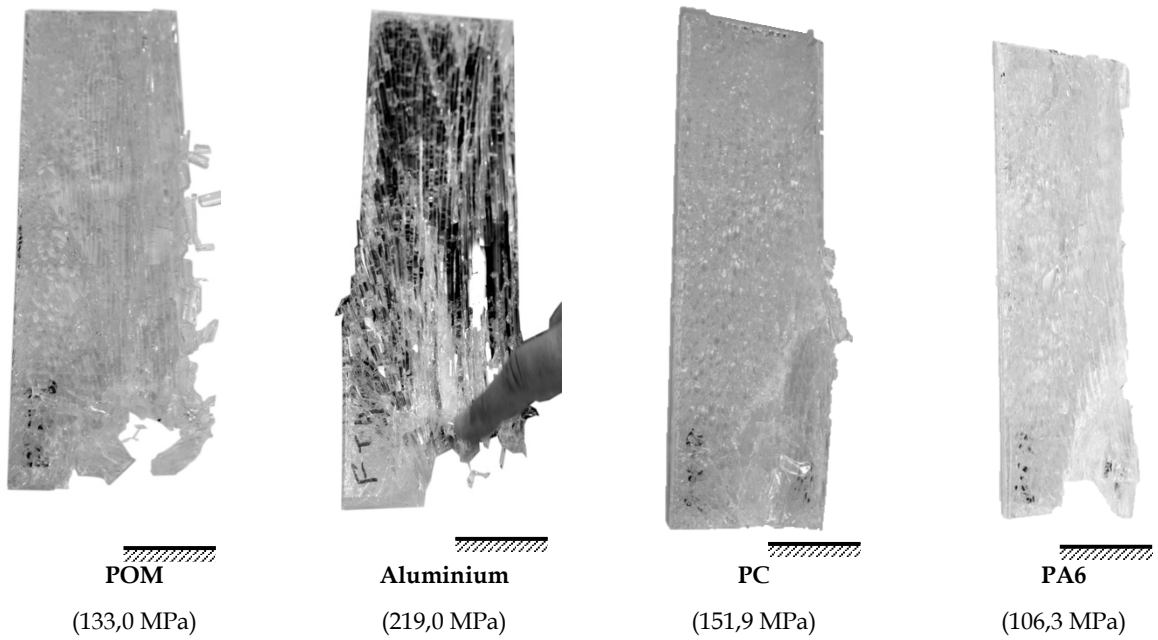
Figure 7.21: Fracture pattern of fully tempered glass specimens in contact with POM, Al, PC and PA6.

7.3.3 Discussion

The ability of the different substrates to accommodate compressive stresses in a concentrated area demonstrated to be very distinct. Figure 7.22 shows a sample of the several substrates after tests. PMMA and PTFE samples show the substrate after failure and the other samples show the deformation of the substrate when subjected to a similar stress on the range of 200 - 225 MPa.
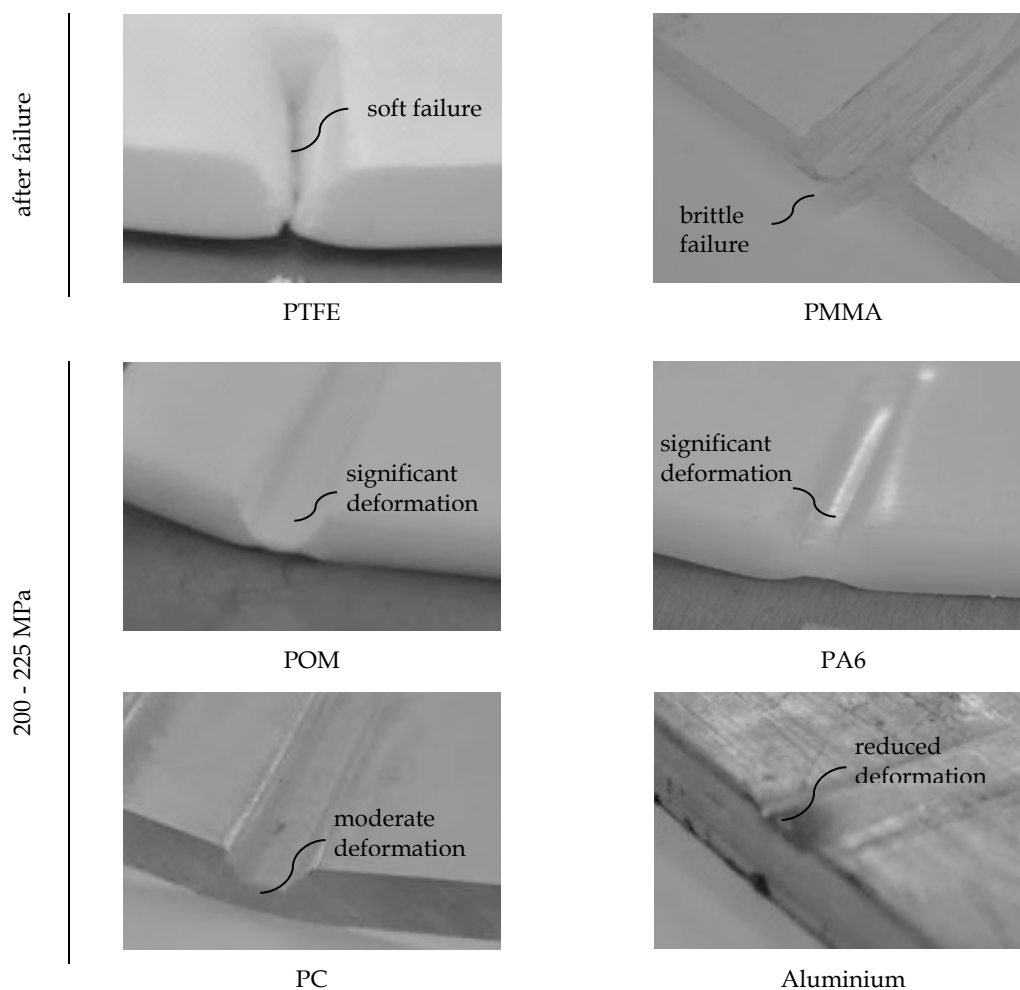
Figure 7.22: Deformation of substrates after test. PTFE and PMMA after failure and, POM, PA6, PC and Al at a similar stress, in the range of 200 - 225 MPa.

PTFE showed to be excessively soft resulting in being cut by the edge of the glasses at low stress levels around 65 MPa. For the opposite reason PMMA also showed its incapacity to accommodate localized compressive stresses since it repeatedly failed in a brittle way when stresses over 130 MPa were applied. On the contrary, aluminium substrates showed a very reduced deformation tendency during tests, even when subjected to considerable compressive stresses of 393 MPa. Among the remaining polymer substrates, PC showed a better capacity to accommodate stresses exhibiting a moderate tendency to deform. POM and PA4 did not fail in any of the tests, meanwhile showed a considerable deformation resulting that its sections after tests showed a very reduced thickness.

This fact may have benefited the behaviour of the compressive tests in contact with these substrates, since the contact surface increased from an initial phase, as described in Figure 7.18. In an after test visual inspection it was clear in both a section shrinkage of the material both on the lower and upper compressed side.
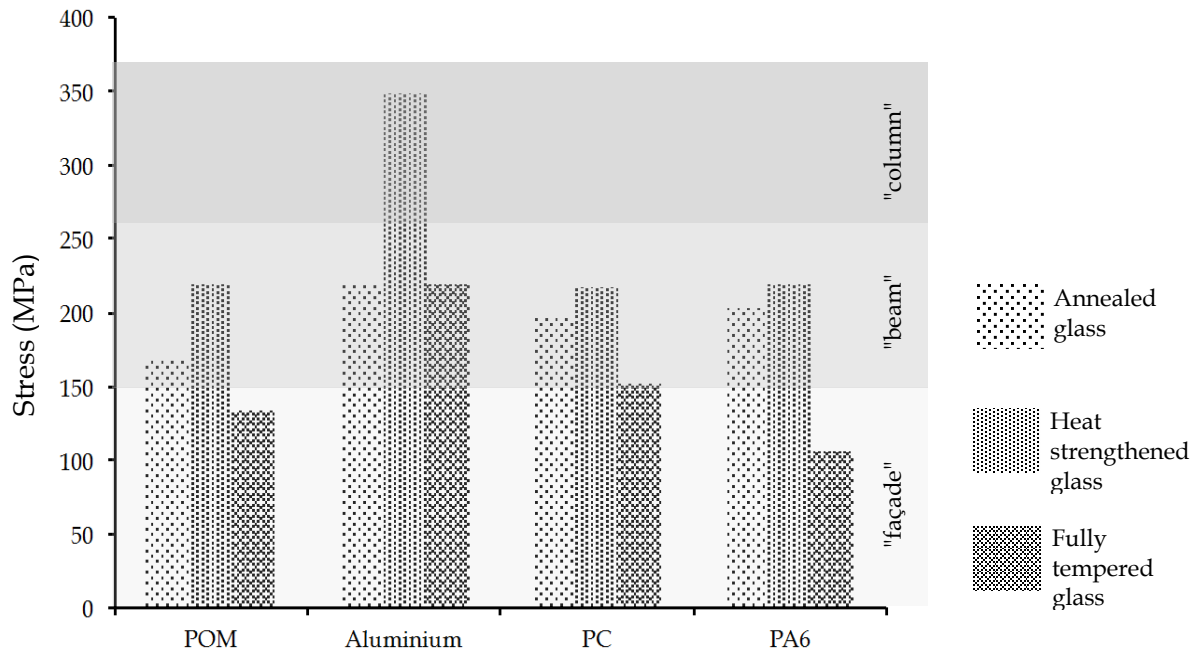
Figure 7.23: Graph bar of the compression tests results comparing the maximum stress of the substrates (PTFE and PMMA not considered) in contact with the three types of glass with qualitative classification in terms of suitable application according to estimated stress level (facade, beam or column).

Looking at Figure 7.23 it is clear that the maximum stress was achieved in all the three types of glass when Al was the substrate in contact. Particularly the compressive contact between Al and HS glass showed a prominent result. Comparing the results with the different polymers (POM, PC and PA6), the behaviour is quite similar, showing comparable maximum stresses when in contact with HS glass. It can be signalled a slight advantage when using PC comparing the results with An and FT glass.

Comparing the mean stress of the three types of glass in contact with each substrate, a first clear fact is the comparatively low stress exhibited by the FT glass in compression with all the substrates, when compared with both An and HS glass. The superior pre stress of FT glass (120 MPa[1]) anticipated a higher failure stress, meanwhile it consistently showed reduced failure stress comparing to the others. The best result obtained with FT glass is in the same range of the mean results of all the others. This shows the significant sensibility of FT glass to compressive stresses, mainly due to the uneven loading.

The increase of allowable stress in the HS specimens is visible, meanwhile showing clear variables. If when in contact with AL, the HS glass specimen accommodated a clear stress increase comparing with An glass, when in contact with POM, PC, PA6 it showed a clear approximation to the results obtained with An glass. Similarly to what was observed with FT glass, HS glass specimens exhibited a reducing stress capacity when in compressive contact.

---

[1] Characteristic tensile bending strength according to EN 572-1: 2004; prEN 13474-1: 1999

The difference between the known levels of stress capacity from bending and the measured results leads to the assumption that there must have been a correlation between the release of the toughening energy and the actual compressive stress induced during the test. The internal stress equilibrium of both HS and FT glass, when loaded in compression, is significantly affected by the uneven loading. However there isn't enough data to say what is incidental and rule. Further investigation on this topic must be performed to have a better understanding of the phenomenon.

7.3.4 Conclusions

From the experimental investigation on the mechanical behaviour of An, HS glass and FT glass in compression with POM, PMMA, PTFE, PC, PA6 and Al it is possible to conclude that Al is the most suitable material to accommodate compressive stresses when in contact with the three types of glass. It's reduced deformation allowed an even load distribution and thus achieve higher compressive stresses. PC, among the remaining substrates, exhibited the overall best results both in terms of deformation capacity and compressive behaviour. The fact that it is transparent makes it a strong choice according to the design philosophy. Both PTFE and PMMA showed to be unsuitable due to the significant softness and brittleness, respectively.

It is also concluded that the pre-stressing of glass isn't a guarantee of higher failure stress levels as expected when compared with An glass. The non-homogeneous setup chosen for the tests revealed the unreliable behaviour of pre-stressed glass when loaded in compression, especially fully tempered. Although known to be very strong when loaded in bending, it resulted to be very sensitive when loaded in compression. It consistently failed at inferior stress levels compared to An glass. Further study is required to achieve a clear understanding of the phenomenon. HS glass clearly showed the highest compressive strength in contact with all the substrates. Together with its capacity to reserve some cohesion after breakage (contrary to FT glass) and its immunity to stress corrosion (contrary to An glass) makes it the best type of glass to use in the connection technique under investigation.

7.4 *Testing the concept -* **bending behaviour of the connection**

This section addresses the experimental investigation conducted to study the concept of connecting glass panels through semi-embedded steel perforated plates, superimposed and mechanically connected with steel bolts. The *four-point bending* test has been selected as the appropriate method to evaluate the bending behaviour of the connection. During the investigation, two phases may be distinguished. The first where the geometrical configuration of the connection was studied, using an incremental progression method. In this phase two research questions were posed:

- How stiff is the connection simply bolted, when loaded in bending?

- How may its stiffness be improved?

The second phase corresponds to a more systematic approach in which a stabilized connection solution was investigated more extensively. In this case the question was:

- What determines the maximum bending strength of the improved connection solution?

This second phase was conducted after receiving the information from the previous investigation on the compressive behaviour of glass in contact with different substrates. Polycarbonate was chosen as the best transparent material to use as an intermediate layer between glass panels.

7.4.1   Test procedure

7.4.1.1   Four point bending specimens

The four-point bending test specimen consists of a beam with total size of 1047 mm × 100 mm that is composed by two symmetrical parts connected at the centre. Each part is made of two 10 mm thick rectangular shaped pieces of float glass with dimensions 500 mm × 100 mm. These are laminated using two SG® interlayers with 1,52 mm thickness. A 1 mm thick AISI 304 stainless steel plate with R5T8 perforation pattern is semi-embedded in between. It has the same height as the glass and is 78 mm wide, 40 mm of this is embedded in the laminate (see Figure 7.24).
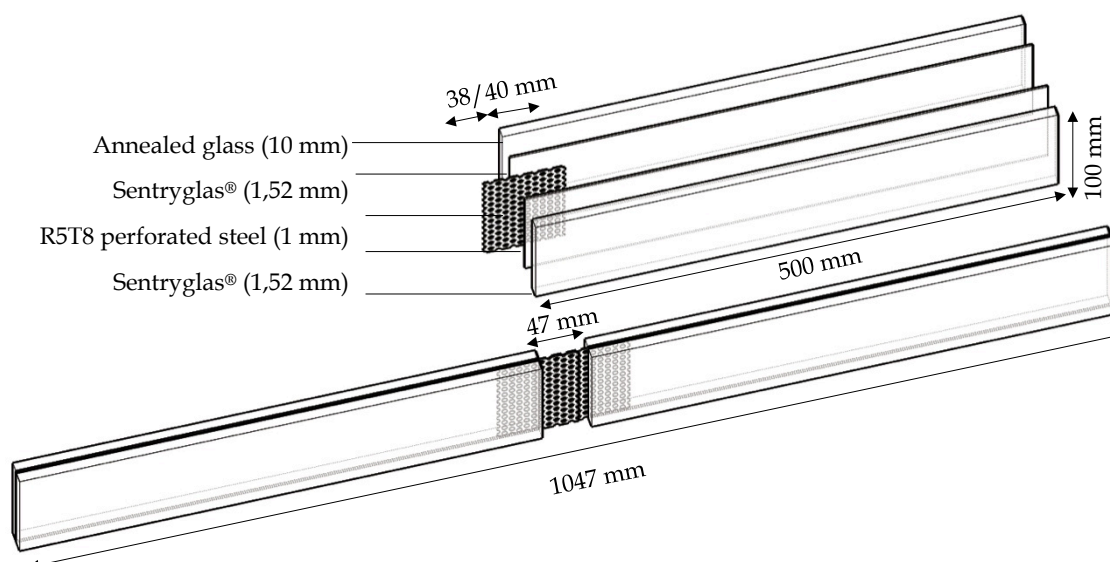
Figure 7.24. Four point bending test specimen.

The two-piece beam specimen is mechanically connected at the middle using steel M5 screws and nuts that are inserted through the plate's perforation. On the first assembly type four screws vertically displaced were used (see Figure 7.25 (1)). Three other options of assembly were tested in which complementary elements were added to increase the total stiffness: a 3mm thick steel joint cover at each side of the beam with inferior width (see Figure 7.25 (2)); two 1 mm thick 10 × 10 mm aluminium angle with the same length of the gap between the two glass laminates to be in perfect contact on the upper (compressed) part of the beam (see Figure 7.25 (3)); and two 10 × 10 mm nylon bar also with the length as the gap and placed at the upper (compressed) zone of the beam (see Figure 7.25(4).

(1)

(2)

steel bar

(3)

(4)

aluminium angle

nylon bar

(5)

polycarbonate bar (full height)
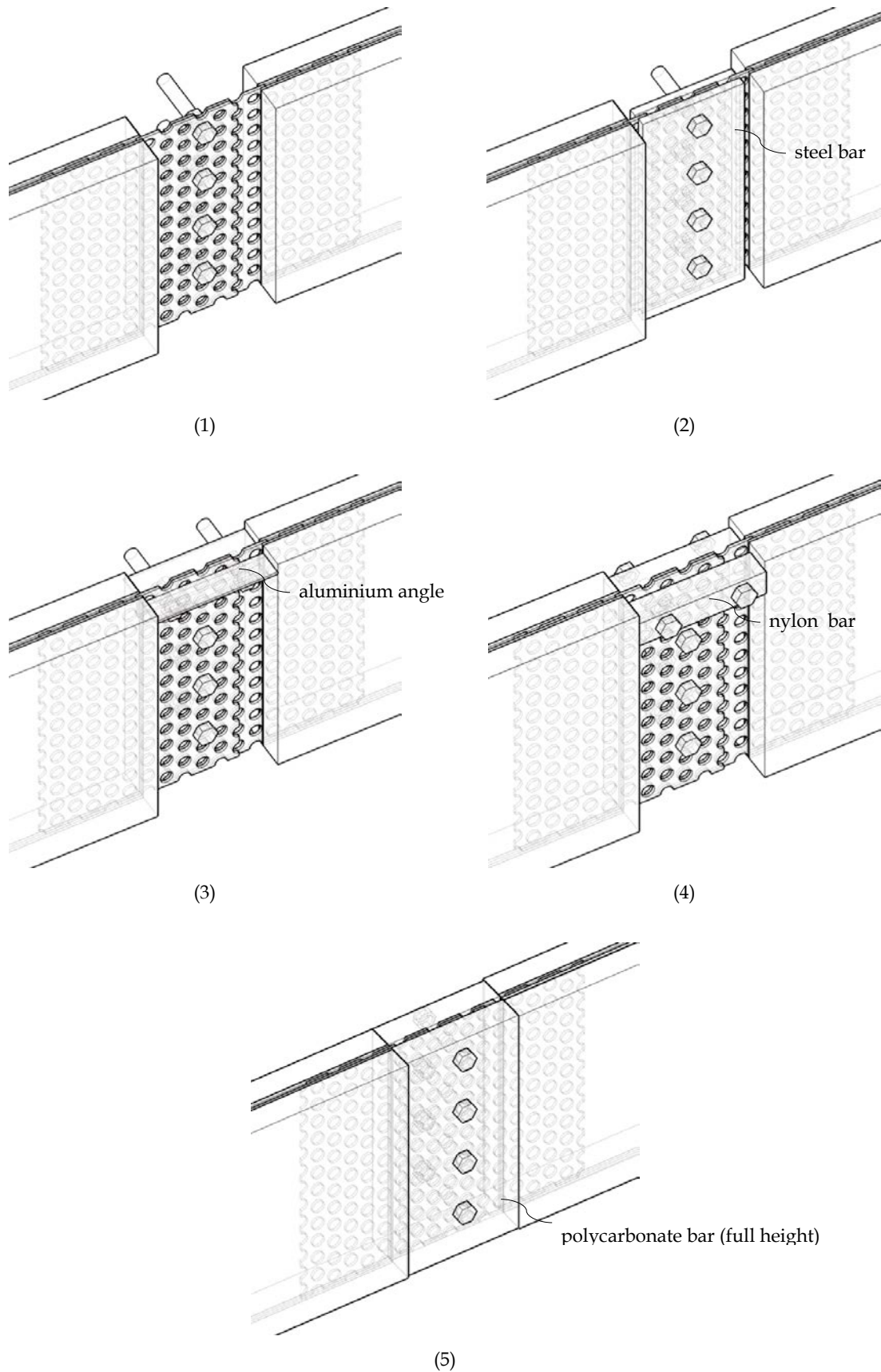
Figure 7.25. Different types of connection tested in the first phase: 1) simple; 2) with two 3 mm thick steel bar joint covers; 3) with two 1 mm thick aluminium angle; 4) with two 10 mm nylon bar; and connection tested in the second phase: (5) with two 10 mm polycarbonate bars at full height of the beam.

7.4.1.2   *Four point bending setup*

The four point bending test specimens were supported on two lower points distancing 800 mm from each other. The load was applied on two points distancing 200 mm from the centre. Additional side support frames were used with distributed points of contact to prevent buckling (see Figure 7.26) The specimens were loaded using a constant displacement rate of 2 mm / minute. For the instrumentation of the models a charge cell of AEP Transducers, with maximum capacity of 50 kN and a displacement transducer (LVDT) were used. The average room temperature during the tests was 18 ºC.
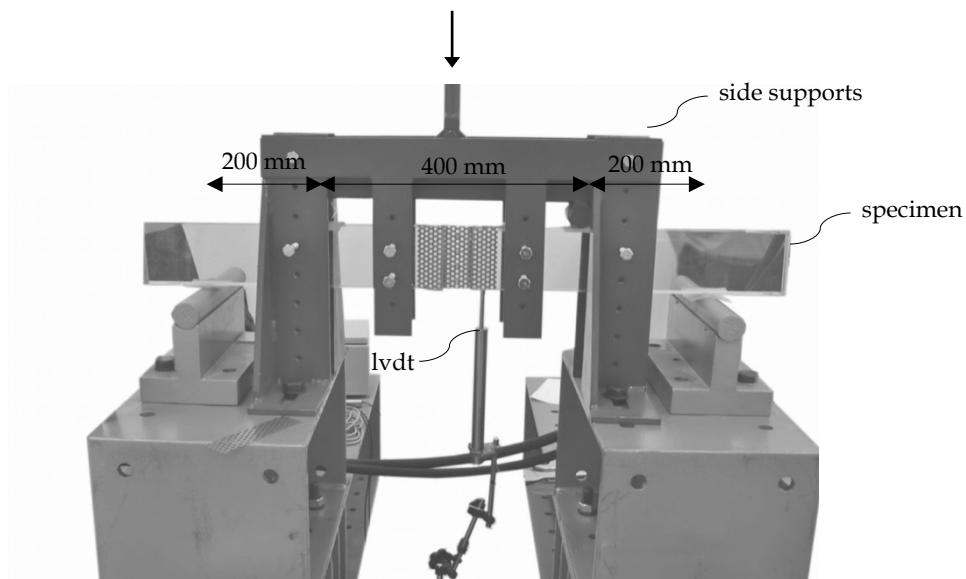
Figure 7.26. Four point bending test setup.

7.4.2   Test results

7.4.2.1   1st phase

Figure 7.27 shows the load-displacement diagrams of the four point bending tests on the different connection solutions.
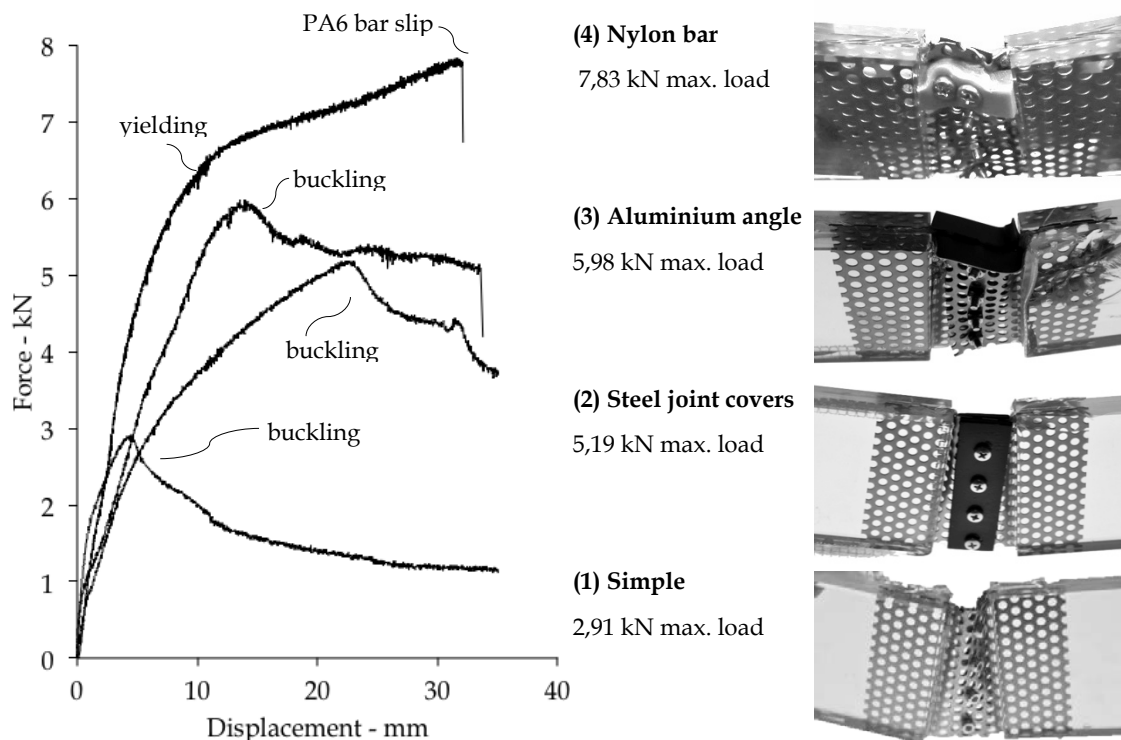
Figure 7.27. Load-displacement diagram of the preliminary four-point bending tests with different joint solution and deformation of the joint material under compressive load at the final stage of the test.

The four point bending test with the specimen simply bolted in four points showed a non-linear but constant increase of the load until almost 3 kN. At this point it started to get unstable due to the compression installed in the upper zone of the perforate steel plates and buckled. The load decreased considerably from a displacement of around 5 mm until 35 mm when the test was interrupted. Bolting two steel bars to cover and compress the overlapped perforated steel plates resulted in a similar initial behaviour, meanwhile the buckling point was increased to a load level of around 5 kN. At a vertical displacement of 22 mm it was clear that both perforated steel plates started to concede on the non-covered areas, close to the glass edge, which caused the beam to buckle.

Similarly to the previous specimen, it significantly decreased the load capacity, with the additional fact that when one of the joint covering steel plate touched a glass edge, a stress concentration occurred and the glass cracked. Adding two aluminium angles to each side of the beam, with the same length of the gap to be in perfect contact with the edge, assuring a firm screwing in the compressed upper zone visibly increased the bending stiffness of the beam. Although still failing by buckling, it happened at an increased level of 6 kN and just 8 mm of displacement. The 1 mm thick angle couldn't withstand the installed compression and started to slowly deform, initiating the buckling process of the beam.

Contrary to the previous tests, the load decrease was less severe, remaining above 5 kN until 34 mm of displacement, when the substantial deformation of the steel perforated plates pushed one of the aluminium angle edge out of place, which caused the load drop. Lastly, the specimen with two 10 mm side nylon bars screwed in contact with the upper part of the beam exhibited a continuous linear increase in applied load until around 4 kN. Afterwards, the bending stiffness continued to grow in a non-linear manner, due to an initial deformation of the nylon bars, until around 6,5 kN. At this point, the yield stress strain of the perforated steel plate was reached and it started to elongate, coupled with the compression of the nylon bars, until a maximum load of around 7,8 kN. Once again the visibly deformed steel perforated plate pushed the nylon bar out of track, causing it to slide from the glass edge, which voided the compression stress.

7.4.2.2   2nd phase

Three specimens with full height PC bars were tested in four-point bending and the load-displacement diagram is presented in Figure 7.28. At the beginning of the three tests, instability is perceptible due to the accommodation of the bolted joint, mainly the contact between PC and glass edges. Some deformation of the PC occurred at the compressed upper part to compensate the mentioned gap. Parallel to this process was the elastic deformation of the perforate steel plate, not so evident in the diagram. Also at this initial phase a small crack occurred on the lower edge of specimen (5.1) with no visible effect on loading capacity. At around 10 mm of deformation and a load of 5 kN, an approach in terms of stiffness occurred in all three specimens followed by the yielding of the perforated steel plate. It started concentrated on the holes in contact with the two lower steel bolts, expanding in a second phase to the neighbouring holes of the lower tensioned zone of the beam. In the first specimen it was visible some deformation of the perforated steel plate inside the embedded area contributing to some minor debonding. Also some deformation of the compressed PC was visible at this point.
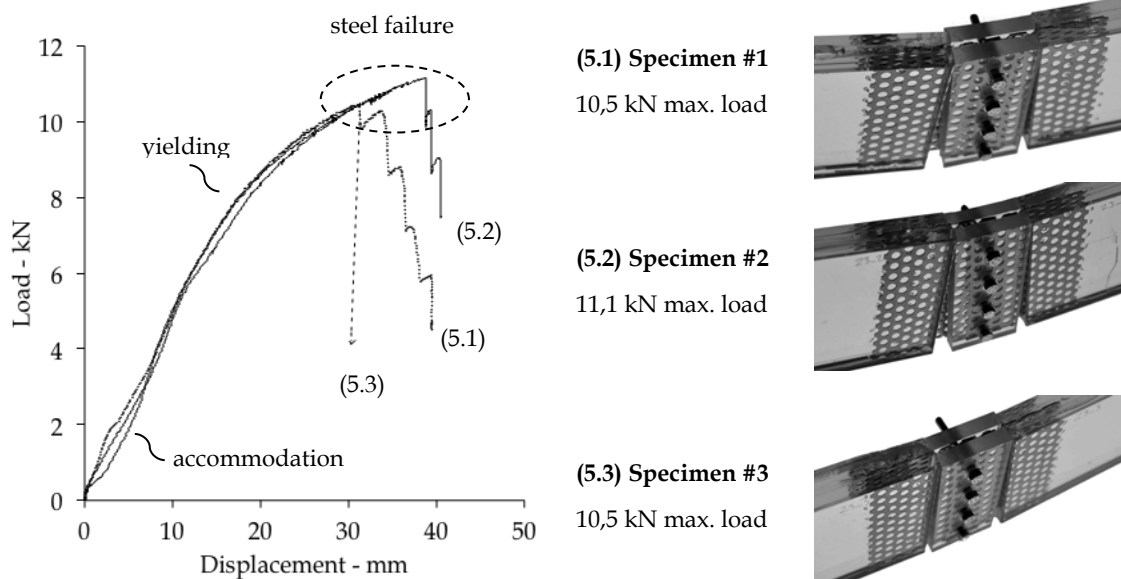
Figure 7.28. Load displacement diagram of the four-point bending test (left) and close-up view of the connection of the three specimens after test (right).

At 10,5 kN the first specimen reached the maximum load when a first hole bar of the perforated steel plate disrupted, visibly reducing the load capacity and triggering a characteristic hole-by-hole break-up process until minor load capacity remains at around 40 mm of displacement. The second specimen carried increasing load until 11,1 kN when a similar process happened. With a careful look at the diagram it is noticeable some instability before this process occurs, perhaps showing the deformation of the PC, clearly superior compared to the others in an after test visual inspection.

The third specimen reached the same maximum load as the first (10,5 kN), but instead of a perforated steel plate disruption, the failure was caused by an incidental glass breakage. It happened, on the lower edge of the beam vertically aligned with the upper support, away from the connection area. It caused a drastic reduction of load capacity and the test was interrupted. All the specimens were dismounted and the specimens were unscrewed. No damage of the steel bolts was visible. The PC showed some semi-circular carved marks on one side caused by the sliding of the rough back surface of the perforated steel plate during accommodation.

7.4.3 Discussion

The tests described illustrate a step-by-step approach to optimizing the bending efficiency achievable with the concept under investigation. The bending strength of the specimen simply screwed through the overlapped steel perforated plates clearly showed its reduced capacity to carry bending loads. The high slenderness of the connected plates caused it to buckle at a very low level of load. With the help of two steel *joint covers* to partially strengthen and stabilize the connected plates, the second specimen visibly improved the results. Buckling wasn't prevented but it happened at a clearly higher level of load.

The third solution proposed to act directly on the upper compression part of the connection by adding two slim aluminium angles in contact with the glass edges. It almost doubled the maximum load comparing with the simple solution. It had the capacity to strengthen the compression response of the applied bending moment, and failed when the aluminium deformed to a point that allowed buckling to occur.

In order to increase the compression strength and contact conditions with the glass edge, the aluminium angles were replaced by two 10 mm side nylon bars. The consequences were visible. The total stiffness considerably improved, resulting in such an increase in compressive load on the nylon bars that the tensile stress in the lower part of the steel perforated plates exceeded the yield stress. The load capacity increased in balance with compressive deformation of the nylon and plastic tensile deformation of the steel plate, which prevented buckling to occur. At this point it was clear that the concept was valid and that the results could be further improved if the intermediate material could continue to efficiently carry the compressive loads while preventing to fail due to excessive deformation.
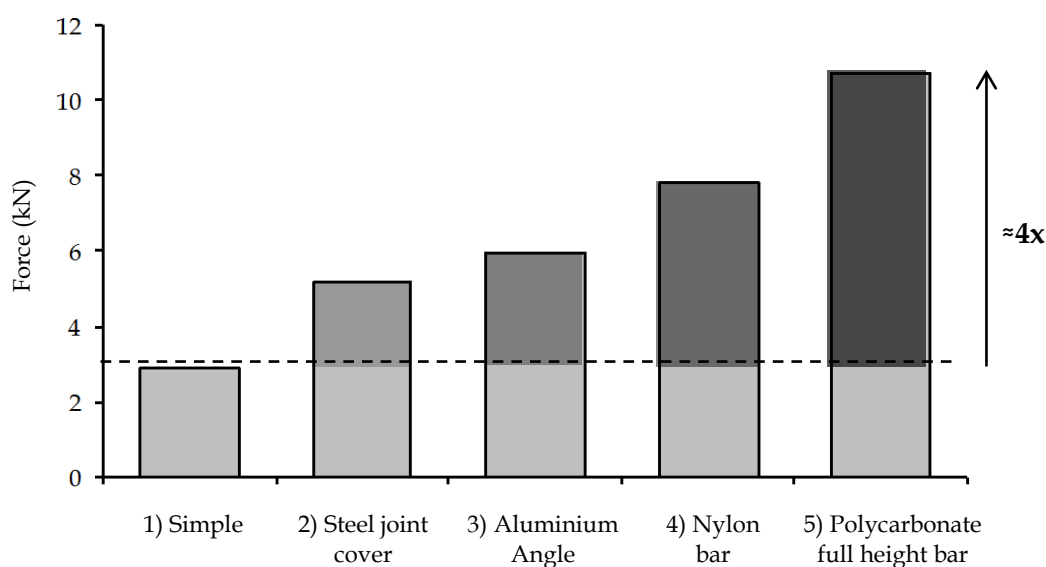
Figure 7.29. Bar graph comparing the increasing bending strength when improving the connection solution.

Finally, the improved specimens with PC bars at full height with suitably machined form proved to work very well. The bending strength increased almost four times compared with the initial simple solution (see Figure 7.29), exhibiting ductile failure behaviour, determined by the maximum tensile strength of the steel perforated plate.

7.4.4 Conclusions

From the experimental investigation on the bending behaviour of the connection it is possible to conclude that the concept of *connecting through the reinforcement* is valid when combined with a suitably machined PC layer in-between. When sufficient bending stiffness was acquired, it was possible to activate the compressive stresses at the upper zone, forcing the tensile strength on the mechanically connected steel perforated plates to be reached. Compared with the simple solution the bending strength increased almost four times, exhibiting ductile failure behaviour, determined by the maximum tensile strength of the steel perforated plate. These tests also showed the consistency on using PC in this connection solution.

8 Potential problems

8.1   Temperature effect on the adhesive behaviour

This section addresses the experimental investigation conducted to study the effect of increased temperatures on the adhesive behaviour of thin steel inserts embedded in laminated glass. Following the experimental work performed at room temperature (see Chapter 7.2) the *pull-out* test has been selected as the appropriate method. Concerning the parameters to include in the study, two temperatures were selected (40 °C and 75 °C) below and above the glass transition temperature of the chosen interlayer SG[1] (around 55/60 °C). Also the perforation of the metal insert and the embedment depth were included. The research questions for this set of experimental tests were:

- How different is the adhesive capacity between glass and thin steel elements when using a stiff interlayer at 40°C and 75°C?

- How does the use of perforated metal affect the adhesive behaviour at 40°C and 75°C?

- What is the influence of the metal embedment depth in the adhesive behaviour at 40°C and 75°C?

8.1.1   Test procedure

The test specimens were similar to the ones tested at room temperature (see section 7.2.1) combining a stiff interlayer with perforated and non-perforated steel inserts and two embedment depths (20 mm and 40 mm). To warm up the specimen a FITOCLIMA 300 EC20 climatic chamber (see Figure 8.1 (a)) was used where the specimens were conditioned for at least 6 hours before testing. To compensate for any heat loss during the mounting of the specimens in the test setup, the specimens tested at 40 °C were conditioned with additional 3 °C whilst the specimens tested at 75 °C were conditioned with additional 5 °C. Exception is made to the non-perforated specimens with 20 mm embedment depth, which were tested using a 50 kN Instrom Universal Machine with a coupled climatic chamber (see Figure 8.1 (b)). These tests were performed in collaboration with Mr. Manuel Santarsiero and Dr. Christian Louter, in the scope of the already mentioned Short Term Scientific Missions. These specimens were warmed up and tested at the exact temperatures of 40 °C and 75 °C. Additionally, a digital image correlation technique was used to detect the deformation of the specimens under investigation (see Figure 8.1 (c)). A total number of 24 specimens were tested, 12 for each temperature.

---

[1] PVB was discarded due to its low glass transition temperature, around 10-15°C (Kott and Vogel 2005)

<table>
<tr><td>(a)</td><td>(b)</td><td>(c)</td></tr>
</table>
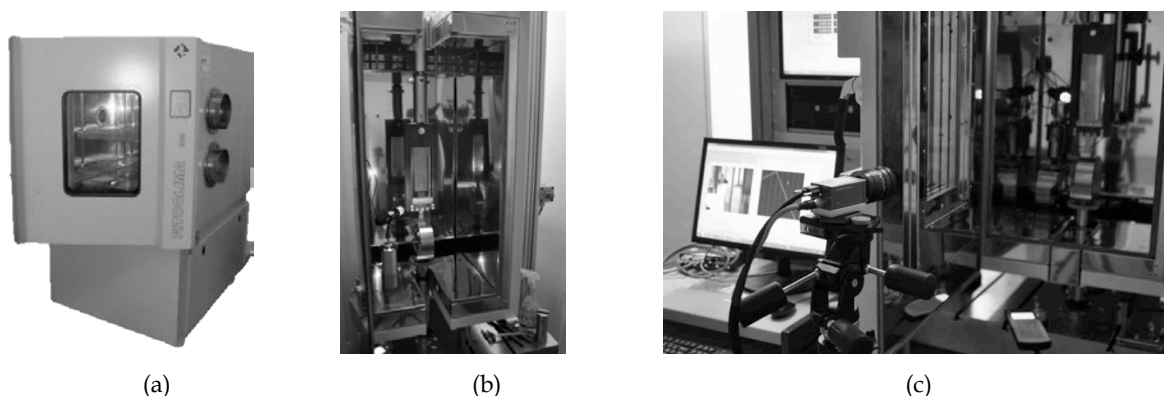
Figure 8.1. FITOCLIMA 300 EC20 climatic chamber (left) and Instrom Universal machine with coupled climatic chamber (centre) and digital image correlation system (right).

8.1.2   Test results

8.1.2.1   Pull-out tests at 40 °C

In Table 8.1 and Table 8.2 are presented the results of the pull-out tests on SG laminated steel inserts at 40 °C, and on Figure 8.2 and Figure 8.3 are presented the correspondent load-displacement curves, both non-perforated and perforated, at 20 and 40 mm of embedment. The maximum loading, correspondent displacement and maximum nominal adhesive stresses are presented. The failure of both glass and steel is referred and the load-versus-displacement curves are shown for each type of specimen.

Table 8.1. Results of the *pull-out* tests on non-perforated steel SG embedded inserts at 40 °C

	Depth (mm)	$F_{máx}$(kN)	Mean	$\tau_{máx}$(MPa)	Mean	Displacement $F_{máx}$(mm)	Glass breakage	Steel failure
		12,86		4,02		48,39	Yes	No
	40	12,10	**12,04**	3,78	**3,76**	44,18	Yes	No
		11,16		3,49		34,48	Yes	No
40 °C		7,49		4,68		10,67	Yes	No
	20	7,73	**7,64**	4,83	**4,77**	11,78	Yes	No
		7,69		4,81		11,61	No	No

Figure 8.2. Load displacement diagrams of the *pull-out* tests on non-perforated steel SG embedded inserts at 40°C
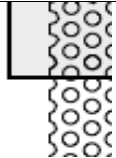
After an initial elastic deformation, the 40 mm embedded non-perforated plate tested at 40 °C start to yield and deform in a plastic way. This transition occurs at a value close to 5 kN of load and is clearly visible in the load versus displacement curve. During the subsequent plastic deformation of the metal embedment the load continues to increase until a first cracks occurs in the glass. It happened at distinct leve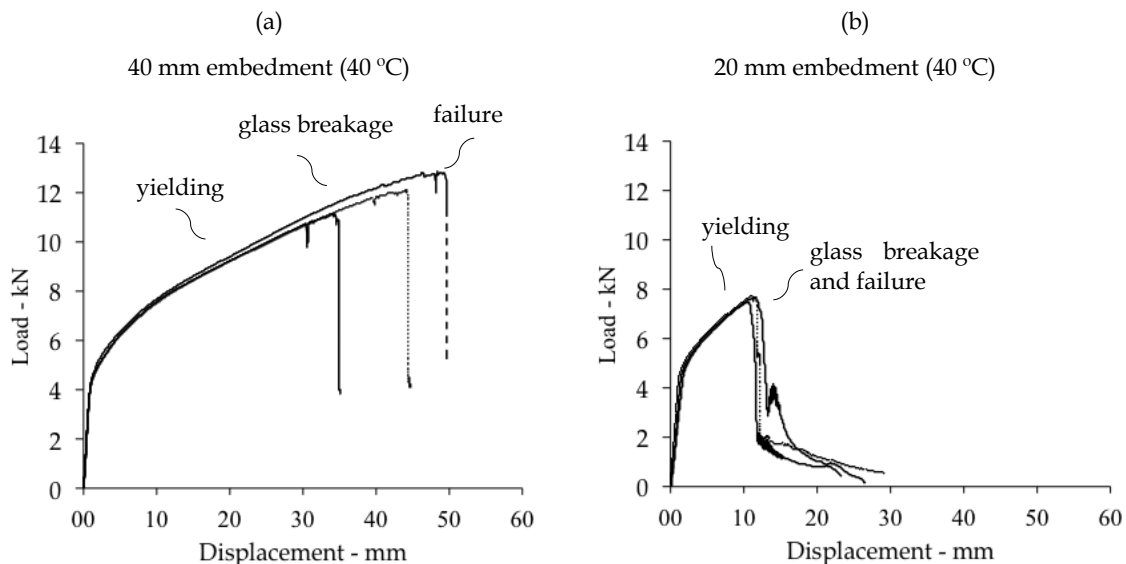ls of load in all three specimens, being 12,75 kN (sp. #1), 11,74 kN (sp. #2) and 10,40 kN (sp. #3). It caused small decreasing of load carrying capacity. Meanwhile, despite the broken glass the load capacity continued to increase until the glass breakage was such that the stiffness was lost and the load decreased abruptly. The maximum loads vary from 12,86 kN (sp. #1), 12,10 kN (sp. #2) and 11,16 kN (sp.#3).

A visual inspection of the tested specimens showed partial debonding of the steel plate that may have happened before the initial glass breakage in all three specimens. Looking with more detail at the specimen #1 load-displacement curve, it is noticeable an instability period from 11,82 kN until the first glass breakage at 12,75 kN visible by an undulating soft curve, showing increases and decreases of loading, characteristic of the debonding process. The 20 mm embedded non-perforated plate specimens tested at 40°C behaved in a very similar way compared to the 40 mm. The initial elastic deformation of the connection was succeeded by the metal plasticisation around 5 kN of load. The glass of all the three specimens broke at a certain point but, contrary to the 40 mm embedment specimens, no increase of loading occurred. It happened at an average maximum load of 7,64 kN, after which a fast decrease of load is visible.

Concerning the specimens with perforated plate tested at 40 °C, the 40 mm embedment series consistently showed elastic deformation until 5 kN of load and consequent plastic deformation of the steel. Specimen #1 showed a first glass breakage at 9,4 kN but maintained an increasing load until a maximum of 9,78 kN. At this point the load decreased abruptly due to the debonding of the metal, despite the reduced amount of glass breakage. Specimen #2 showed similar behaviour, exhibiting some glass breakage around 9,5 kN of loading, meanwhile it didn't compromise the load capacity of the connection since it kept increasing load until the maximum displacement of the machine was reached. The maximum load capacity was 11,43 kN.

Despite the glass breakage occurring close to the edge, the further embedded depth of metal plate assures that no debonding occurs. Specimen #3 exhibited the first breakages at around 9,9 kN of loading, and the maximum loading was 10,54 kN. Load decreased afterwards as a consequence of the lack of cohesion of the glass and consequent debonding.

Table 8.2. Results of the *pull-out* tests on perforated steel SG embedded inserts at 40 °C.

	Depth (mm)	$F_{máx}$(kN)	Mean	$\tau_{máx}$(MPa)	Mean	Displacement $F_{máx}$(mm)	Glass breakage	Steel failure
40 °C	**40**	9,78		4,53		29,91	Yes	No
		11,43	**10,58**	5,29	**4,90**	48,63*	Yes	No
		10,54		4,88		33,86	Yes	No
	20	6,95		6,44		8,05	Yes	No
		7,11	**6,95**	6,58	**6,44**	8,77	Yes	No
		6,80		6,30		6,03	Yes	No

* Maximum displacement of the machine was reached and the test stopped.

Figure 8.3. Load displacement diagrams of the *pull-out* tests on perforated steel SG embedded inserts at 40 °C.

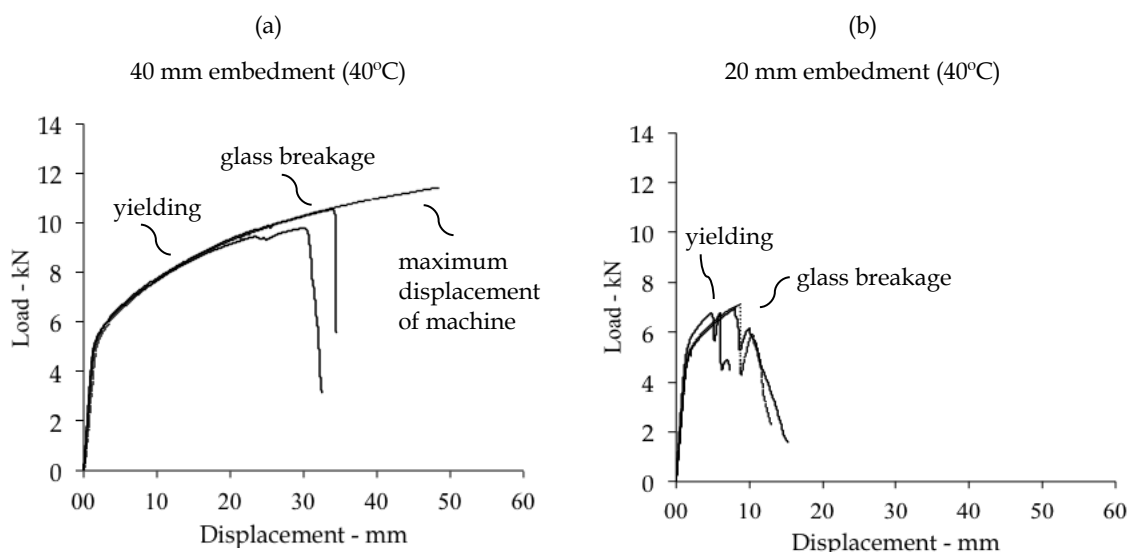The 20 mm perforated plate specimens also show elastic-plastic transition at similar load level. The metal inserts start to deform until the occurrence of glass breakage. Specimen #1 exhibited these first breakages at an early stage of the plasticization around 5,24kN of loading, but kept increasing load until a maximum of 6,95 kN, after which the load decreased significantly. Specimen #2 showed similar behaviour without the initial glass breakage, until maximum load was reached at 7,11 kN. Specimen #3 exhibited superior stiffness of the connection clearly visible on the load deformation curve. It showed maximum loading capacity of 6,80 kN, previously interrupted by a visible single branch glass breakage, which caused the final debonding of the steel insert.

8.1.2.2   Pull-out tests at 75 ºC

In Table 8.3 and Table 8.4 are presented the results of the pull-out tests on SG laminated steel inserts at 75ºC, and on Figure 8.4 Figure 8.5 are presented the correspondent load-displacement curves, both non-perforated and perforated, at 20 and 40 mm of embedment, in similar terms as the previous tests at 40ºC.

Table 8.3. Results of the *pull-out* tests on non-perforated steel SG embedded inserts at 75 ºC

	Depth (mm)	$F_{máx}$(kN)	Mean	$\tau_{máx}$(MPa)	Mean	Displacement $F_{máx}$(mm)	Glass breakage	Steel failure
		1,67		0,52		9,96	No	No
	40	2,09	**2,24**	0,65	**0,70**	2,30	No	No
		2,97		0,93		8,11	Yes	No
75ºC		1,13		0,71		4,33	No	No
	20	1,48	**1,36**	0,93	**0,85**	2,29	No	No
		1,60		0,93		7,17	Yes	No

(a)

40 mm embedment (75ºC)
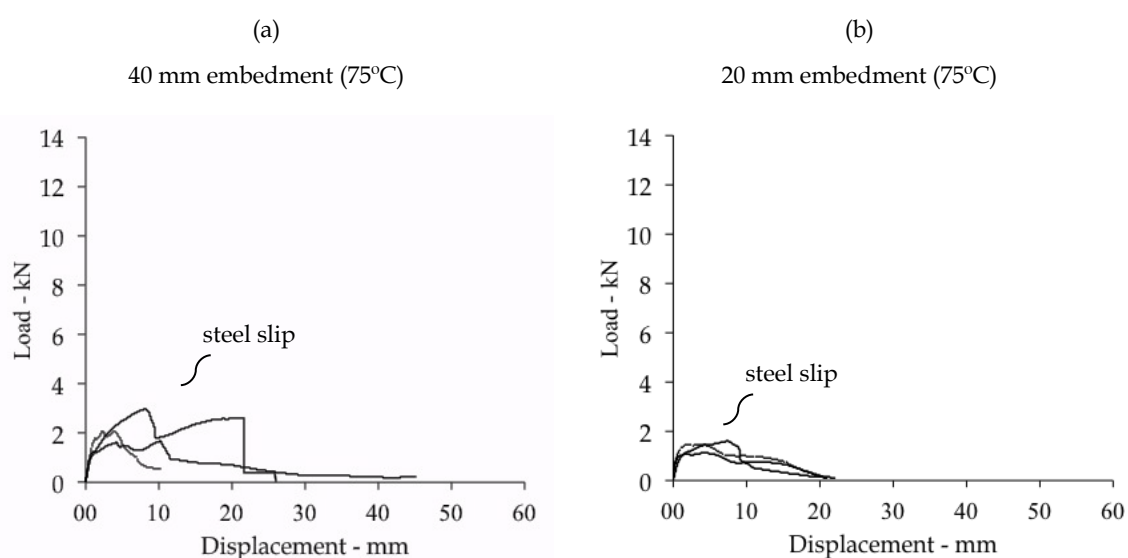
(b)

20 mm embedment (75ºC)

Figure 8.4. Load displacement diagrams of the *pull-out* tests on non-perforated steel SG embedded inserts at 75 ºC.

The pull-out non-perforated specimens tested at 75 °C consistently failed at a very low loads. With 40 mm embedment the average maximum load was only 2,4 kN, clearly before any steel deformation occur. The interlayer loses its adhesive strength and allows the steel insert to slip at this level of load. With 20 mm of embedment, it is even reduced. The average maximum load was 1,36 kN.

The perforated 40 mm embedded specimens tested at 75 °C behaved very similarly, failing at an average maximum load of 4,25 kN. It occurred after the slip of the metal due to the reduction of adhesive strength of the interlayer. The 20 mm embedded specimens also showed very similar behaviour showing more evident reduction of strength. The maximum average load was 2,77 kN.

Table 8.4. Results of the *pull-out* tests on perforated steel SG embedded inserts at 75 °C.

	Depth (mm)	$F_{máx}$(kN)	Mean	$\tau_{máx}$(MPa)	Mean	Displacement $F_{máx}$(mm)	Glass breakage	Steel failure
75 °C	**40**	4,21		1,95		3,02	No	No
		4,28	**4,25**	1,98	**1,97**	5,53	No	No
		4,27		1,98		5,54	No	No
	20	2,20		2,04		7,86	No	No
		2,75	**2,77**	2,55	**2,57**	4,87	No	No
		3,37		3,12		6,83	Yes	No

(a)

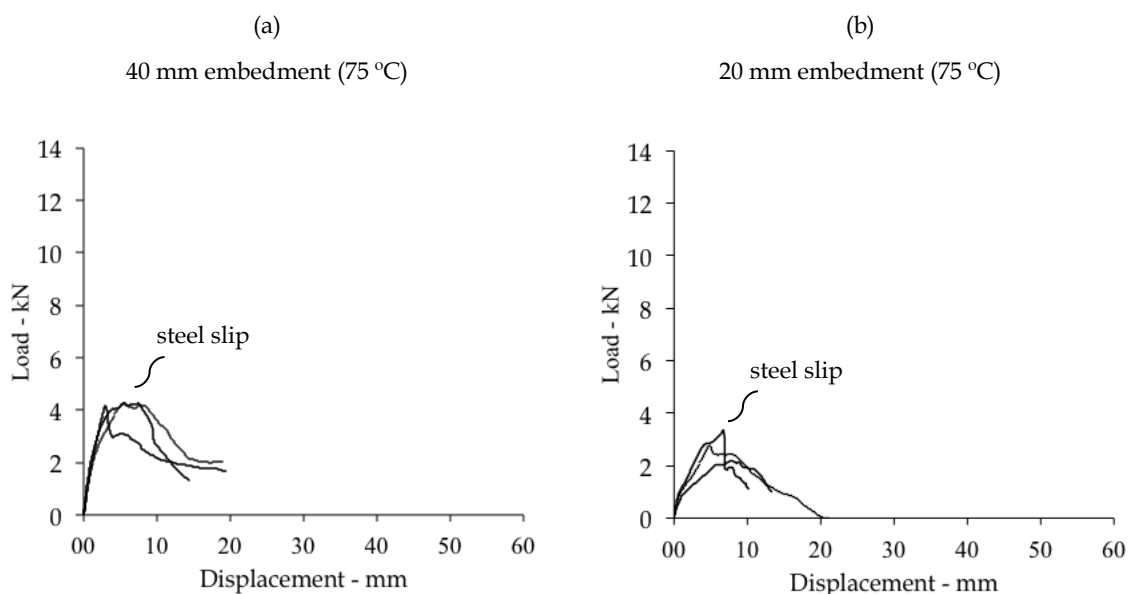40 mm embedment (75 °C)

(b)

20 mm embedment (75 °C)

Figure 8.5. Load displacement diagrams of the *pull-out* tests on perforated steel SG embedded inserts at 75 °C

8.1.3 Discussion
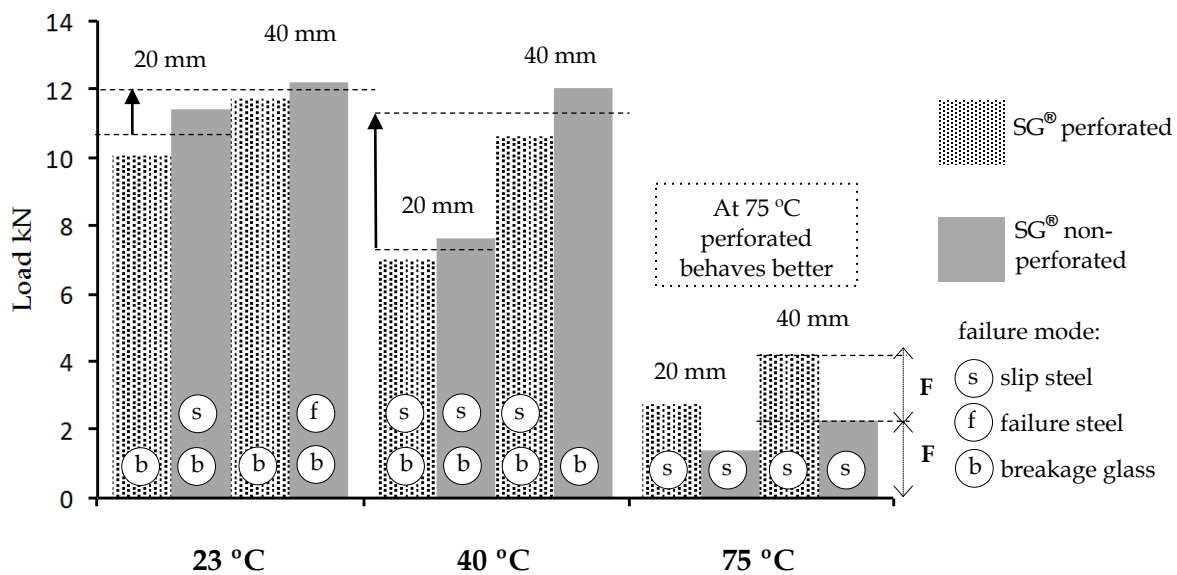
Figure 8.6. Bar graph comparing the mean maximum loads of the pull-out tests on SG specimens at 23 °C, 40 °C and 75 °C.

The results of the *pull-out* tests at different temperatures clearly showed a decrease of adhesive strength with temperature rise. At 75 °C a considerable reduction on the adhesion strength occurs both with perforated and non-perforated steel inserts. At 40 °C the reduction was less severe. Looking at the bar graph on Figure 8.6 we can see that the results with 40 mm non-perforated embedded specimens at 40 °C and 23 °C were similar. A reduction is noticed on the perforated specimens due to the fact that at 40 °C, the steel yield extended to the interior of the laminate (see Figure 8.7) allowed by a border softening of the interlayer. The yielded steel thus cut the interlayer and increased the stress inside the laminate, affecting the connection strength. This also explains the significant difference concerning the strength reduction from 40 mm to 20 mm at 23 °C and 40 °C. At the higher temperature, the interlayer softens and reduces its adhesive strength in the peripheral area close to the edge. The resulting increase of stress, visible in the breakage of glass that did not occur at 23 °C, caused the reduced embedment steel inserts, both perforated and non-perforated, to fail at lower loads.
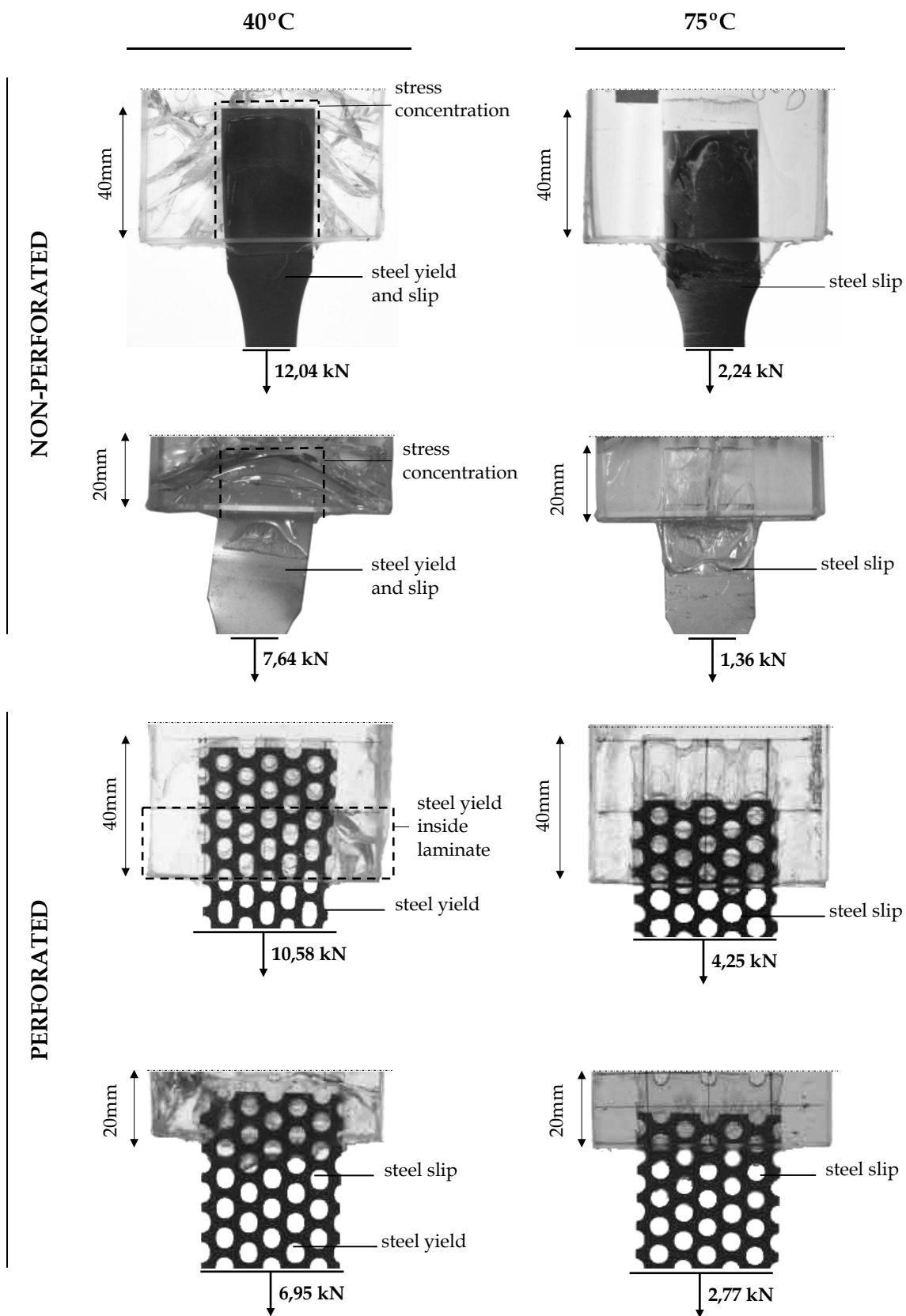
Figure 8.7. Close-up view of the *pull-out* specimens after test at 40ºC and 75ºC at the level of the embedment.

In the contrary, at 75 °C the low loads at which the specimens failed, both with perforated and non-perforated steel, didn't create any yield on steel, clearly visible by the non deformed round holes of the perforated steel plates. The failure mode in all the specimens was simply the slip of the steel. It resulted that perforated steel specimens exhibited considerably superior strength compared with the non-perforated ones due to the anchoring effect of the interlayer inside the plate holes. Both with 20 mm and 40 mm of embedment, the increase of load was almost the double.

8.1.4 Conclusions

From the experimental investigation it is possible to conclude that the strength of the connection changes considerably with temperature. At 40 °C the strength reduction is smaller and more evident at reduced embedment length due to the initial tendency of the interlayer to soften in the borders, causing stress concentrations inside the laminate. At 75 °C the strength reduction is critical both at 40 mm and 20 mm of embedment. The perforated geometry of steel showed some advantage at higher temperatures due to an anchoring effect with the interlayer, lightly compensating the loss of adhesive strength. The maximum strength doubled compared with non-perforated specimens. When temperatures over 40 °C are expected an increase of embedment depth is advised. Alternatively, another interlayer material with improved temperature behaviour (EVA) may be applied after testing.

8.2   Temperature effect on the bending behaviour

This section addresses the experimental investigation conducted to study the effect of increased temperatures on the bending behaviour of thin steel inserts embedded in laminated glass. Following the experimental work performed at room temperature (see Chapter 6.4) the *four point bending* test has been selected as the appropriate method. Concerning the parameters to include in the study, two temperatures were selected (45 ºC and 70 ºC) below and above the glass transition temperature of the chosen interlayer SG[1] (around 55/60 ºC). The research questions for this set of experimental tests were:

- *How different is the bending strength of the investigated connection at 45 ºC and 70 ºC?*

- *How does the temperature rise affects the mode of failure?*

8.2.1   Test procedure

The test setup for the four point bending tests is similar to the one used at room temperature. The difference is on the addition of a custom-made insulated box around the setup to create a temperature-controlled environment during tests. An electric fan connected to the box by insulated pipes, was responsible to heat up the inner atmosphere to the required temperature (see Figure 8.8).
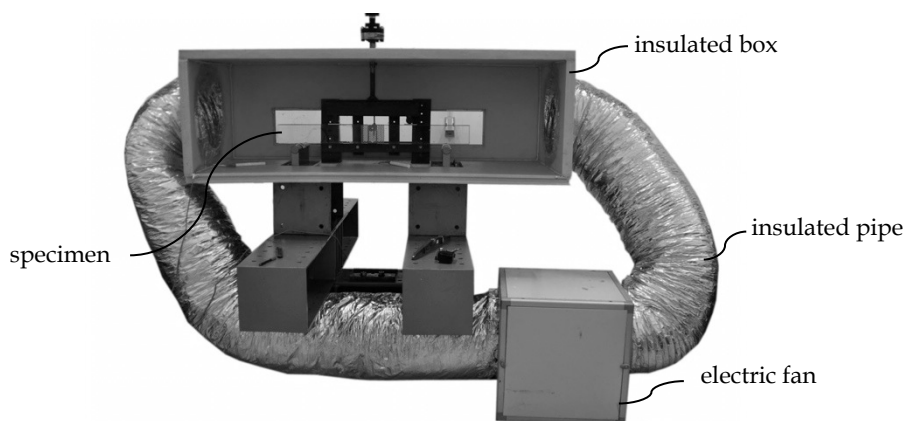
Figure 8.8. Four point bending test setup with insulated box for temperature-controlled environment.

The specimens were similar to the ones tested at room temperature in its last version. It consisted of a beam with total size of 1047 mm × 100 mm, composed by two symmetrical parts mechanically connected at the middle using steel M5 screws and nuts that are inserted through the plate's perforation and two full height polycarbonate bars on each side. These were previously conditioned at the required temperature for at least 6 hours before testing, to assure an efficient warm-up of the whole mass.

---

[1] PVB was discarded due to its low glass transition temperature, around 10-15ºC (Kott and Vogel 2005)

The loading of the specimens was made at a constant displacement rate of 2 mm/minute and the vertical deformation was measured at mid span with LVDTs with the help of an extension profile bolted at the centre of the connection. A total number of 6 specimens were tested, 3 for each temperature.

8.2.2   Tests results

8.2.2.1   Four-point bending tests at 45 ^{o}C

Specimen #1
8,5 kN max. load

Specimen #2
11,1 kN max. load

Specimen #3
10,5 kN max. load

Figure 8.9. Load displacement diagram of the four-point bending test at 45 ^{o}C (left) and photos of the three specimens after test (right).

In the four-point bending tests performed at 45 ^{o}C an initial accommodation phase was observed in two specimens, which reduced its initial stiffness. After this initial phase, specimen #1 showed plastic deformation until around 7,7 kN, when a first glass breakage occurred. It appeared close to the embedded metal edge developing in 45° angle in the direction of the upper compressed part of the beam in contact with the polycarbonate. Despite this first breakage, the load capacity grew until several successive cracks developed along in the opposite direction to the joint, causing the lost of consistency and the reduction of load capacity. The inferior maximum load achieved resulted in a minor deformation of the perforated steel plate. Meanwhile, certain debonding was visible around the metal holes on the broken glass along with some deformation of the polycarbonate was also visible in the upper part.

Specimen #2 showed considerable stiffness at the beginning of the test with a clear elastic-plastic transition until 11,1 kN was reached at around 33 mm of displacement. At this point a first glass crack arose in both glass panes close to the edge of the embedded metal. The load capacity dropped to around 10,0 kN and the glass breakage further developed in crossed directions. After 5 mm displacement a significant reduction of load capacity occurred as a consequence of local disintegration of the glass in the upper compressed zone. The deformation of the steel plate was considerably superior compared to the previous, both on the holes and on the neighbouring region, albeit without any visible steel disruption until the end of the test. Some debonding around the metal holes was clear in the broken laminated glass pane.

The third specimen showed a clear elastic-plastic transition until 10,5 kN of load and 39 mm of displacement when a strong glass break occurred close to the embedded metal edge. It developed in both glass panes until the upper compressed area in contact with the polycarbonate causing considerable disintegration. It showed a noticeable deformation of the perforated steel plate both on the holes and the adjacent area. Contrary to the other specimens, no delamination is visible as a consequence of the glass breakage.

8.2.2.2   Four-point bending tests at 70 °C

Specimen #1
4,2 kN max. load

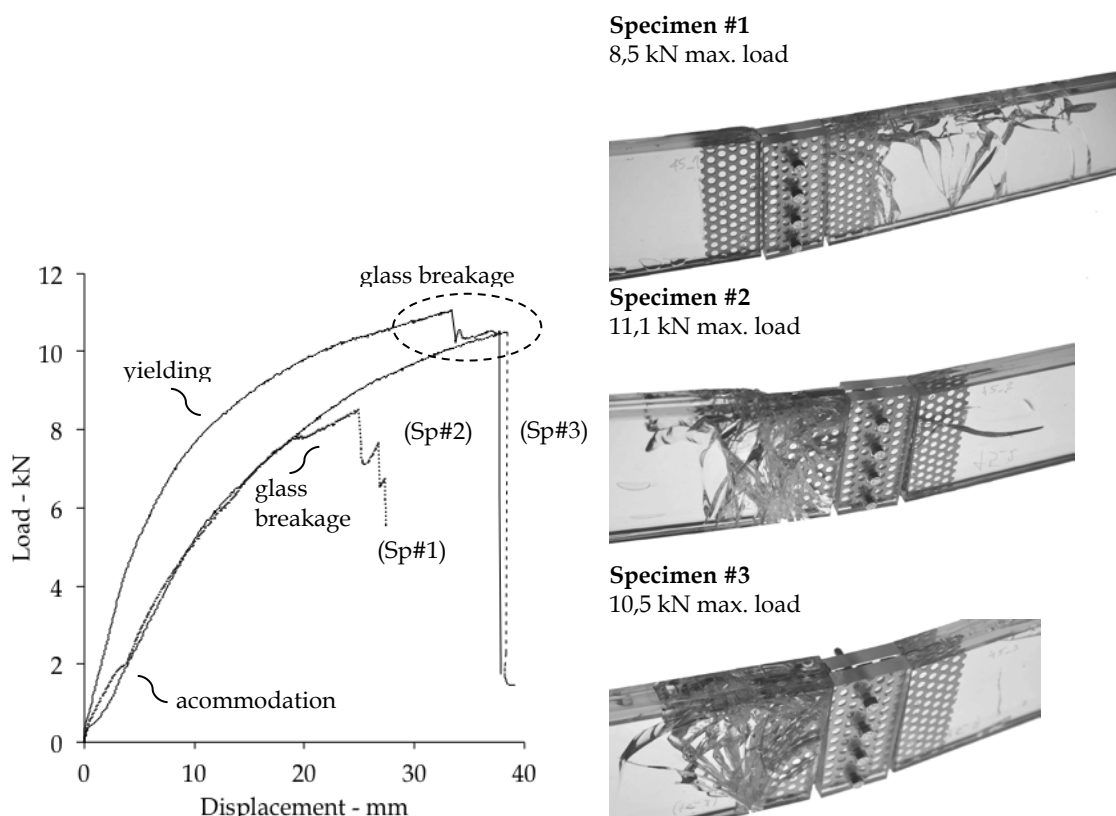**Specimen #2**
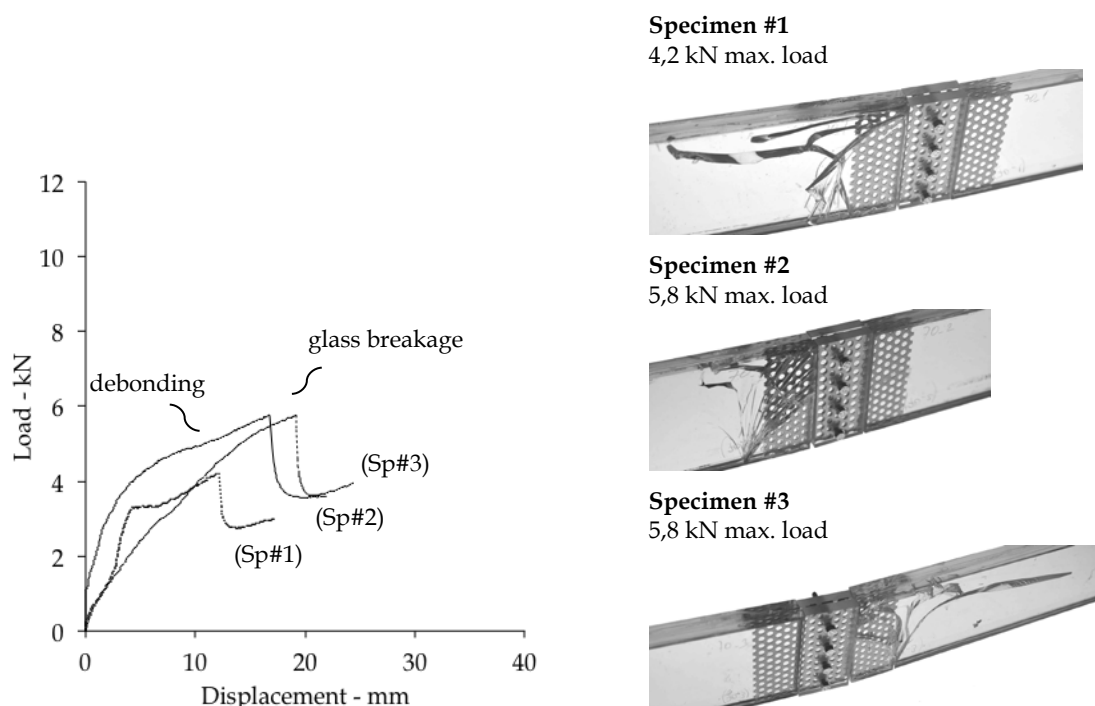5,8 kN max. load

Specimen #3
5,8 kN max. load

Figure 8.10. Load displacement diagram of the four-point bending test at 70 °C (left) and photos of the three specimens after test (right).

The tests performed at 70º C also show an initial accommodation phase, more evident on the first specimen, which after around 1,5 kN reveals an increase of stiffness until 3,2 kN of load. It is then followed by a slight reduction caused by a first small crack, which appeared in only one glass pane near the embedded metal edge. Nevertheless, the load capacity still increased until 4,2 kN after which a considerable reduction happened. It was caused by the conjunction of the further development cracks and the increased delamination of the perforated steel plate. The glass breakage revealed a densely cracked area, aligned with the embedded metal edge, and some other almost parallel bland cracks, all directed to the upper compressed zone in contact with the polycarbonate. From this point other horizontal cracks developed showing restrained development.

The specimen #2 deformed until 5,8 kN, when one glass broke and the load capacity reduced. Some deformation was visible on the lower holes of the perforated steel plate. Only one glass pane broke on the left module, again close to the embedded perforated steel plate edge. Considerable delamination was clear in the broken module in contrast to the non-broken module. The third specimen behaved very similarly to the second, with some more accommodation at the beginning, but showing the same glass breakage. It arose on the opposite side of the specimen, where visible delamination also appeared.

8.2.3 Discussion

Several phenomena occurred during tests, influenced by the temperature rising, which caused different failure mechanisms that advise a careful observation. To help on the discussion, the best results at each temperature and a closer look to the correspondent joints and failure causes are displayed in Figure 8.11.
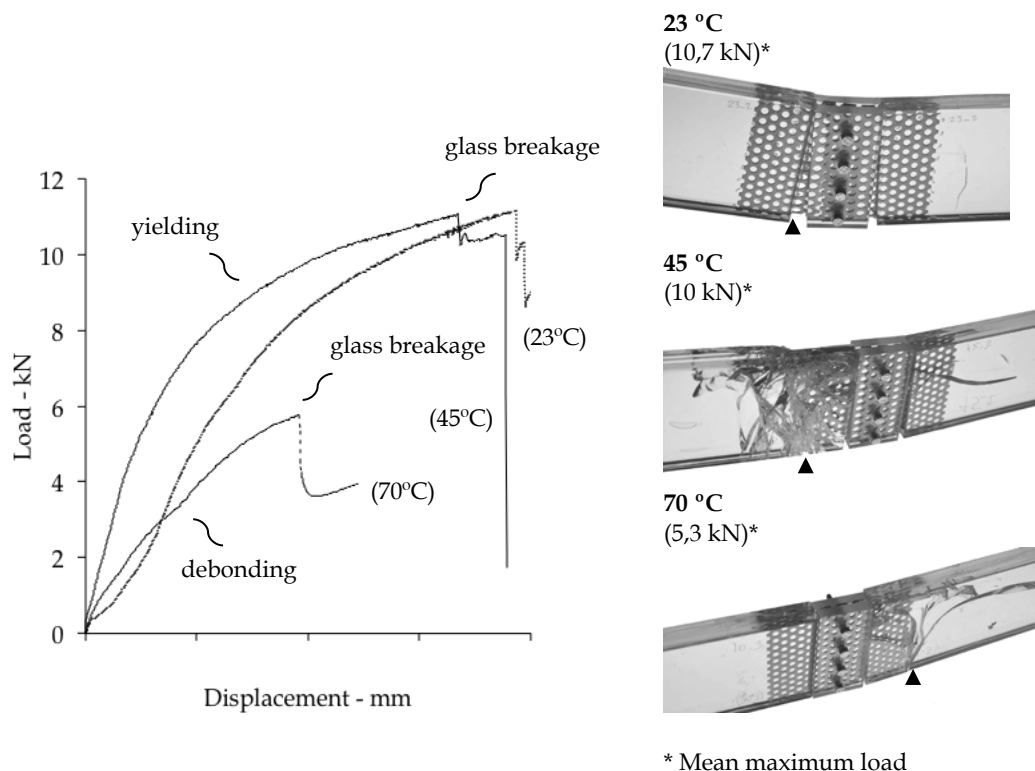
Figure 8.11. Comparison of the load-displacement curves of the best results at 23° C, 45° C and 70° C (left), and close up view of the correspondent central zone of the specimen with indication of the estimated initial failure location (right).

Comparing the tests performed at 23 °C and 45 °C, the maximum load achieved was the same (11,1 kN) but, at the lower temperature, failure was expectedly caused by the metal disruption whilst at the intermediate temperature it was caused by glass breakage, leading to the failure of the beam. At this temperature, all three specimens presented the initial crack coincident or at least very close to the edge of the embedded perforated steel plate. In most cases the installed stress caused both glass panes to break, as can be seen in Figure 8.12.
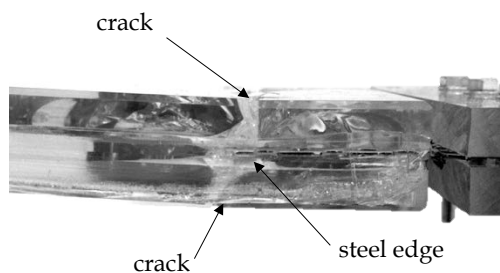
Figure 8.12. Close up view of the lower edge of specimen showing both glass broken at the metal edge area.

Looking at the specimen tested at 70 °C with best result, failure was also caused by glass breakage happening similarly close to the embedded metal edge. The difference is that it happened at only half of the applied load (5,8 kN). The typical "chicken paw" shape is the most common pattern, and no major influence is observed in its development due to the presence of the perforated steel plate. The consistency of failure modes at higher temperatures indicates that there is a localized stress happening at the transition from embed metal to full thickness of interlayer, which is amplified with temperature rising. The influence of this parameter on the adhesion resistance is more evident at 70 °C, where clear delamination occurs. Meanwhile it only happened after the glass breakage, since the non-broken part of the specimen shows no delamination both at 45 °C and 70 °C.

All the specimens were visually inspected to check if there was any steel-glass contact inside the laminate that could justify the phenomenon stress concentrations on glass at higher temperatures, but there wasn't. Attention turned then towards polycarbonate. Although its glass transition temperature is referred in literature as being around 157 °C (Ehrenstein 2001), it was believed that the low molecular weight of commercially available polycarbonate sheets might have caused a variation on this parameter. If a considerable drop in young's modulus of the polycarbonate occurred with rising of temperature, it might have been responsible for the overstress of glass. Similar four point bending tests were performed using a thicker polycarbonate bar (see Figure 8.13). Two specimens were tested at each temperature with 15 mm thick polycarbonate bars (see Figure 8.14).
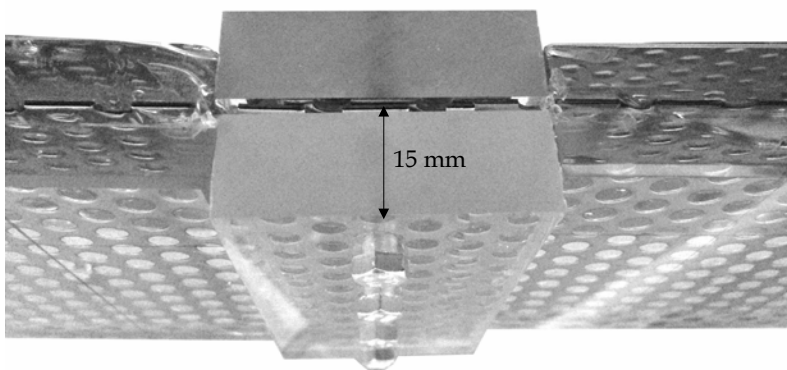
Figure 8.13. Close-up view of specimen connection with two 15 mm polycarbonate bars.
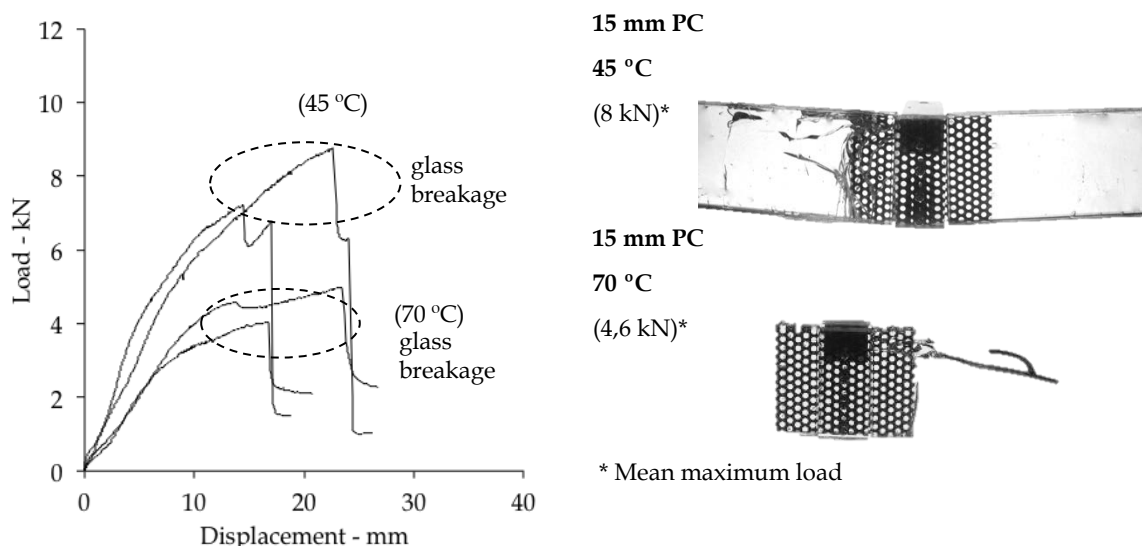
Figure 8.14. Comparison of load-displacement curves at 45 °C and 70 °C with 15 mm PC bars (left), and close up view of the correspondent central zone of the specimen after test (right).

The specimens tested with 15 mm thick PC bars continued to exhibit a localized stress concentration and consequent glass breakage. Looking at Figure 8.14 it is possible to see the load reduction when glass breakage occurs similarly to what has been observed in the previous tests.

An increase of the steel perforated plate embedment length to surpass the limitation posed by the consistent stress at both high temperatures appeared to be the way. In order to test it and get a consistent result, an increase to 210 mm of embedded steel was decided (see Figure 8.15).
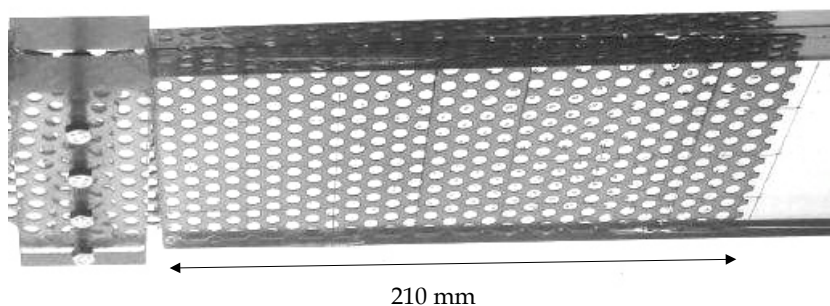
Figure 8.15. Close-up view of specimen connection with 210 mm embedded steel perforated plate.on each side

One specimen was tested at each temperature (45 °C and 70 °C) with the increased embedment length (see Figure 8.16).
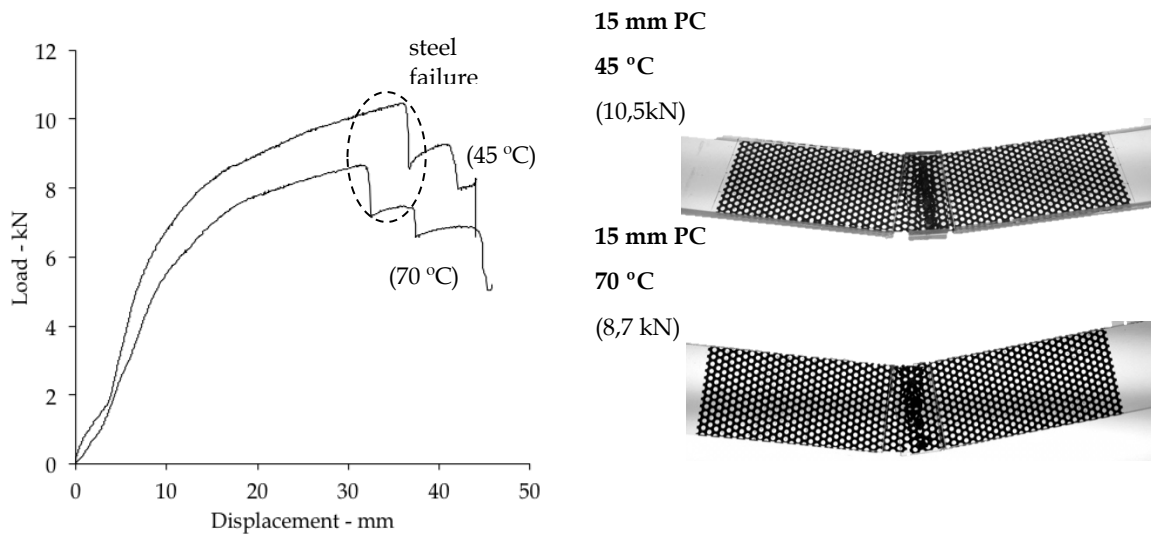
Figure 8.16. Comparison of load-displacement curves at 45° C and 70° C with 210 mm embedded steel perforated plate (left), and close up view of the correspondent central zone of the specimen after test (right).

8.2.4 Conclusions

The connection under investigation relies part of its load transfer mechanisms on polymeric materials (ionomer interlayer and polycarbonate) more prone to temperature variations. The influence of this parameter on the bending behaviour of this connection was investigated by a series of four-point bending tests at 45 °C and 70 °C.

It is possible to conclude that increasing temperature has significant influence on the bending behaviour. Contrary to what was observed at 23 °C, where ductile failure mode was accomplished through the failure of the perforated steel plate, at 45 °C and 70 °C a consistent glass breakage occurred in a localized area. This stress concentration showed tendency to increase with temperature rising. At 70 °C the connection resistance reduces to half caused by the early glass breakage, occurring at relatively low loads of 4/5 kN, and debonding of the adhesive, which demonstrated to be visibly accelerated after glass breakage. When temperatures over 45 °C are expected an increase of embedment depth is advised to surpass the glass overstress.

8.3   Time of loading effect on the bending behaviour

This section addresses the experimental investigation conducted to study the effect of time of loading on the bending behaviour of thin steel inserts embedded in laminated glass. Following the experimental work performed at room temperature (see Chapter 7.4) and effect of temperature (see Chapter 8.2) the *four-point bending* test has been selected as the appropriate method. In the investigated mechanism, two of the composing materials (ionomer interlayer and polycarbonate) are polymers, which by its nature are expected to be affected by a permanent loading over time. The research questions for this set of experimental tests were:

- *How does time of loading affect the bending behaviour of the connection?*

- *Which of the two polymeric materials show more tendency for creep deformation?*

8.3.1   Test procedure

The long duration four point bending tests were performed at room temperature using a custom-made load-controlled test setup (see Figure 8.17). The supporting conditions were similar to the short duration tests concerning the distance between each of the four supports. Meanwhile the specimen was positioned up side down to be loaded by means of a cantilever mechanism.
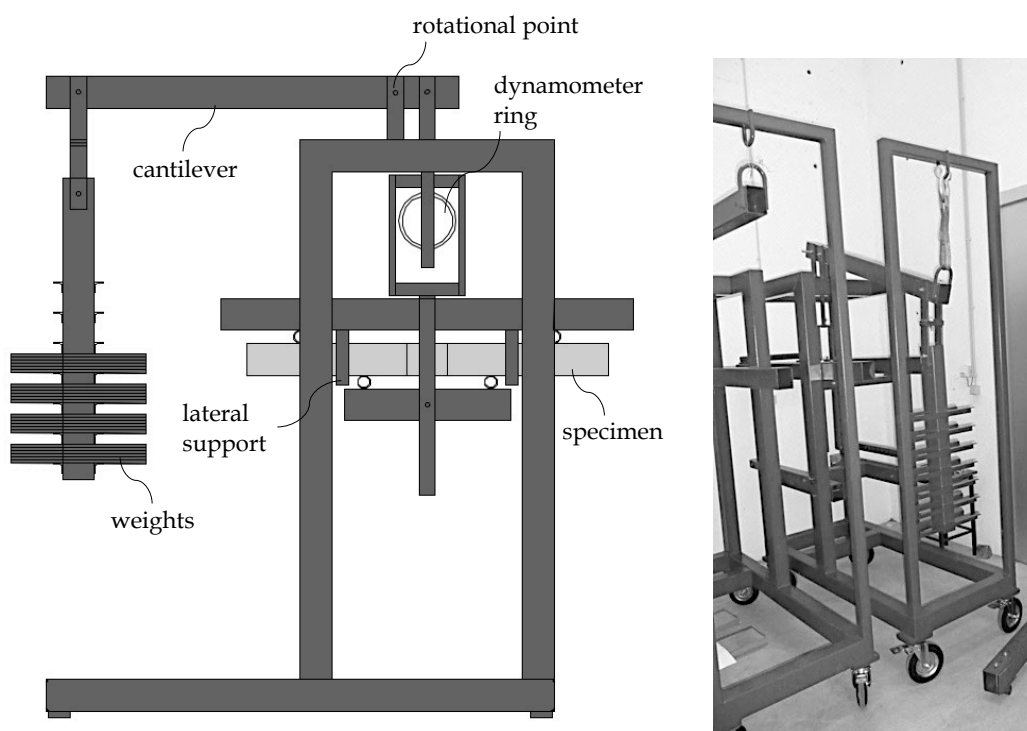

Figure 8.17. Long duration four point bending setup.

 The load is applied by placing steel weights at the counterpart of the cantilever. The cantilever ratio of 1/10 meant that for each N on the counterpart equalled to 10 N being applied on the specimen. The load was applied statically in all the specimens corresponding to 50 % (6 kN) of the predicted ultimate failure load (12 kN). The displacement was measured using a dynamometer ring. In the first hour of test the measurement records took place every 5 minutes, and then every hour during the first day. Subsequently, 3 measurements were made along every day. Additionally, frequent visual inspections were made to check the eventuality of crack initiation or propagation. A total of 3 specimens were tested in its last version with two polycarbonate bars at the full height of the beam.

8.3.2 Test results

The results of the long duration four point bending tests are presented in Table 8.5 and the correspondent time displacement diagrams are shown in Figure 8.18. A visible deformation was recorded once the static loading was applied, ranging from 4,38 mm to 8,59 mm. As discussed during the four-point bending tests with instantaneous loading, there was an accommodation phase at the beginning of the test, in which a gap between the polycarbonate and the glass edge of the specimens connection is suppressed and full contact is achieved. It is estimated that a considerable part of this initial deformation is due to this process of accommodation, which explains the different levels of deformation. Additionally, at 6 kN of load the yield stress of the steel perforated plate was reached in the instant loading tests. Therefore, it is expected that some plastic deformation of the steel may have contributed to the total initial vertical deformation.

Table 8.5. Results of the long duration four-point bending tests

	Specimen #1	Specimen #2	Specimen #3
Initial deformation (mm)	5,29	8,59	6,79
Relative deformation *	43%	70%	55%
Loading time (days)	15	12	8
Creep deformation at 7 days (mm)**	3,03	1,63	1,55

* Percentage of deformation relative to the mean deformation observed in the instant loading tests at the same level of loading.

**Difference between the deformation observed after 7 days of static loading and the initial deformation.
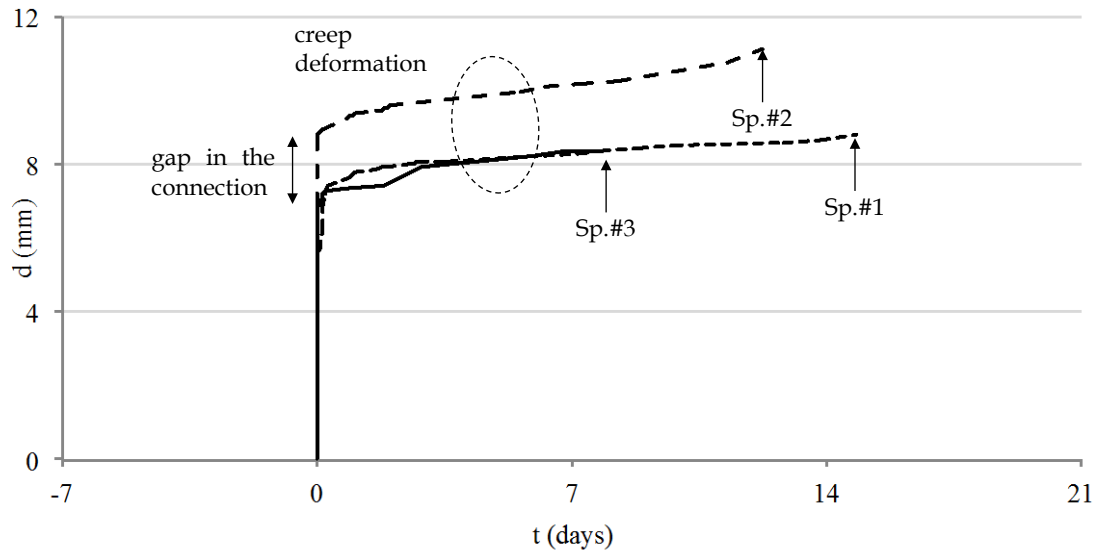
Figure 8.18. Time displacement diagram of the four-point bending test with 50% of predicted ultimate failure load

After the initial phase the specimens deformed in a relatively constant tendency for several days. At the end of 8 days a crack appeared on the edge of glass from specimen #3, close to the area of the connection under compression stresses. It further developed for some minutes until a similar crack appeared on the opposite edge, further reducing the connection strength (see Figure 8.19 (c)). Specimen #2 kept deforming until almost 11 mm of displacement when a crack appeared on one of the supports causing the failure of the beam (see Figure 8.19 (b)). Specimen #1 remained loaded for almost 14 days when failure behaviour a similar to the specimen #3 happened reducing the load capacity of the connection.

(a) Specimen #1   (b) Specimen #2   (c) Specimen #3
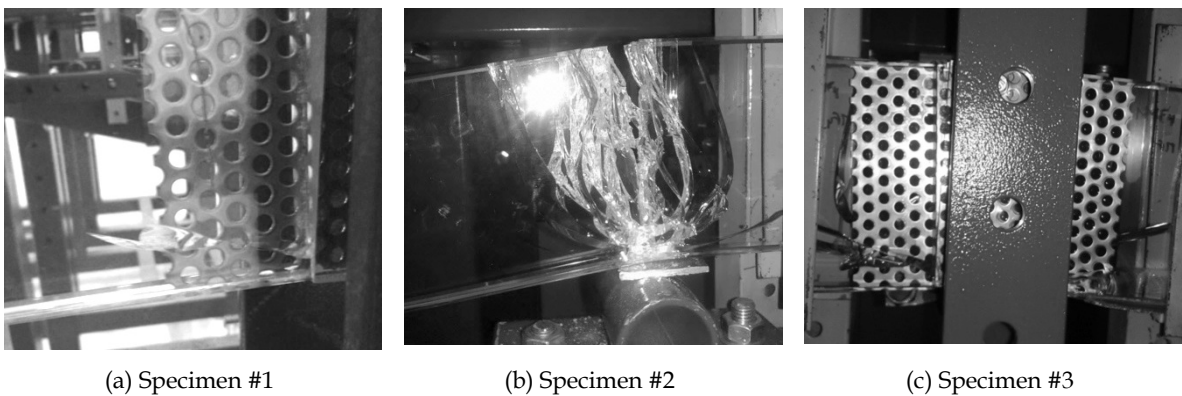
Figure 8.19. Close-up view of the initial failure crack of each specimen.

8.3.3 Discussion

The results of the long duration four-point bending tests clearly showed tendency for creep deformation. Disregarding the initial deformation, considerably influenced by the contact gaps between the different materials of the connection, the vertical deformation of the beam gradually increased in all the three specimens with a constant load. The three curves of the time-displacement diagram during the first seven days of static loading are almost parallel. The vertical deformation in this time span was around 1,6 mm in two of the specimens. No visible displacement of the steel perforated inside the laminate was observed during the tests. However, a creep deformation of the PC was observed in the compressed zone. At the end of the three tests an overstress of the glass occurred leading to the breakage. In two of the specimens it was visibly related to the balance of forces in the connection mechanism, affected by the creep deformation of the polycarbonate.

8.3.4 Conclusions

The connection under investigation relies part of its load transfer mechanisms on polymeric materials (ionomer interlayer and polycarbonate) susceptible to creep deformation. An increase of deformation with constant loading was observed. Furthermore, the polycarbonate showed more tendency for creep deformation. At this stage of the investigation, it is possible to conclude that this type of connection is suitable for elements in which no permanent loads need to be carried, such as façade or roof elements in which snow is not expected. However, the amount of data collected is not sufficient for a thorough understanding of the effect of time on the bending behaviour, requiring further study.

IV Design

9 Design of connection detail

9.1   Integrated discussion on the experimental investigation

In the previous chapters the concept of *connecting through the reinforcement* was introduced and validated by means of an extensive, yet always limited, experimental investigation. During this work, considerable information was collected and individually processed about the technological procedures involved in the fabrication as well as the structural behaviour of the connection. The relevance of such information is amplified if the related topics are treated in a combined approach, highlighting the capabilities and limitations of the system.

The present chapter provides an integrated discussion on the qualitative and quantitative information organized according to the three materials that compose the system: *Glass, Steel and Polycarbonate*; and the three load transfer mechanisms that define the functioning of the investigated connection technique: *Adhesive, Contact and Mechanical* (see Figure 9.1). The goal is to clarify the critical topics that will inform the design development of the connection detail.
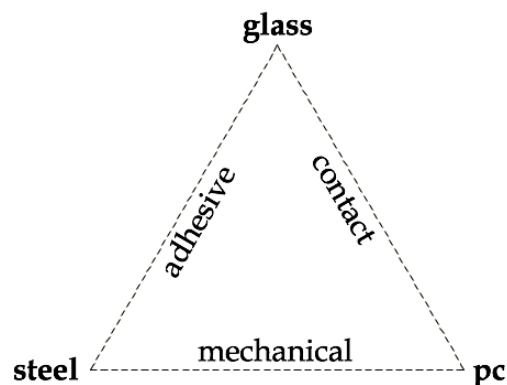
Figure 9.1. Scheme of the three main materials that compose the investigated connection and the correspondent three load transfer mechanism.

9.1.1   Technology - material processing

9.1.1.1   Glass

The glass cut, one of the first operations during fabrication, needs to secure the maximum accuracy possible. Manual methods used at an early stage of the research proved to be unsuitable. If the cut line was not perfectly orthogonal, when gridding and polishing, the misalignment would remain since these operations, when manually performed, are determined by the main element that results from cutting. Using a special gridding and polishing machine with high-accuracy, the results improved significantly.

During lamination, individual movement of glass panels caused asymmetry of the contact surfaces. When using parallel PC bars, one bar will be in contact while the other does not touch the glass. It is essential to solve this problem during the design development. The interlayer thickness that results on both sides of the embedded steel plate have a considerable influence on the internal stresses. A method to accurately place and fix the protruded steel plate in the correct position during the lamination process was investigated. It consisted on the placement of an auxiliary profile to which the protruded steel was fixed. Changing the thickness of the interlayer from 1,52 mm to 0,89 mm matches it with the steel thickness. Only then was possible to fix the plate and assure its correct position before and after lamination.

The silicone blanket lamination system used for the production of specimens, revealed to be a very simple fabrication system with several advantages to the vacuum bag method. However, it also revealed that the elasticity of the silicone blanket tend to apply a force during the application of vacuum that causes displacement of the glass panes. The auxiliary profile used to fix the protruded steel plate may be used to fix the glass in the correct position during lamination. If a belt passing over the auxiliary profile is tensioned before the application of pressure, the relative position between the two glass panes and the protruded steel is preserved (see Figure 9.2).
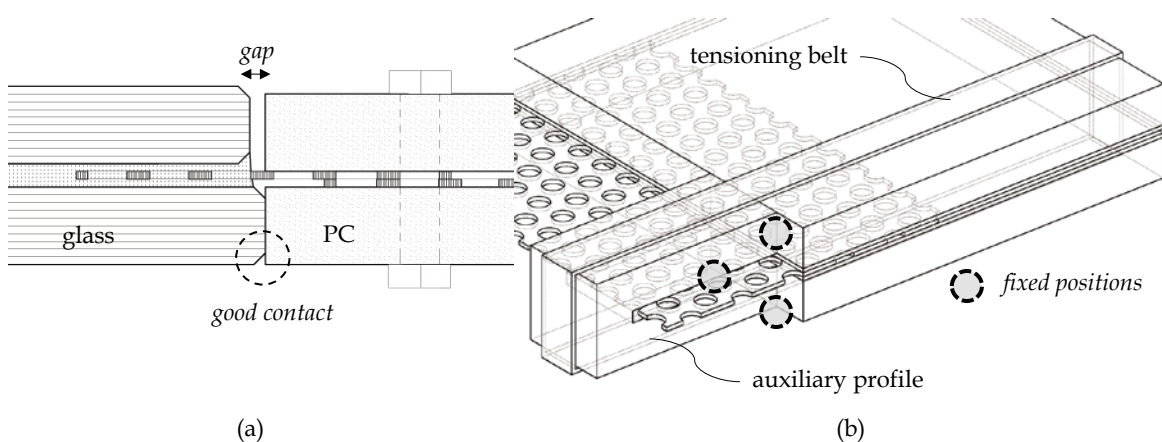
Figure 9.2. Detailed section of the glass-to-PC contact with a gap on one side caused by inadequate lamination (a) and perspective of the lamination solution with the improved configuration of the auxiliary profile to fix protruded plate and both glass edges position (b).

9.1.1.2   Steel

The preparation of the steel plates, namely the cutting operation, required considerable accuracy to preserve the perforated structure. In some operations, the cutting edge did not agree with the centre line of the holes, resulting that some plates presented weakened points of early breakage. Although at a first view, the breakage of a single web of the plate wasn't problematic, when in considerable tension stress, the event of this early breakage triggered the full disruption of the plate (Carvalho, Cruz, and Veer 2011).

It is believed that this phenomenon tends to increase with hole size and when loaded in the closed pattern direction. The larger the hole the greater the energy is released causing that the aligned sections in open pattern may disrupt more easily. Additionally, it is believed that the cutting operation of small pieces is feasible to do manually. On the contrary, if large plates with complex geometries are applied, an improved cutting method is mandatory. Laser cutting is a possible solution, requiring an accurate preparation of the steel plate in order for the machine to recognize the perforations and perform the accurate cutting line.

During the experimental investigation, an R5T8 perforation pattern steel plate was used. Through the 5 mm hole a M5 steel bolt was passed with no major concerns. It was a simple and expeditious solution to achieve a tight contact between the metal parts, however the almost inexistent tolerance is considered impracticable for real applications. Other projects already referred using metal meshes (Neugebauer 2005), which do not allow this kind of solution, applied a metal profile bonded to the mesh along the edge, to which the bolts were mechanically connected. In simple terms this solution creates another adhesive interface, however the necessity to apply a continuous opaque steel frame is not compatible with the design principle of achieving a transparent joint. It was applied in the referred project since it was embedded inside a customized yet traditional connection frame. A possible solution to solve this problem would be to preview a small size non-perforated area on the protruded reinforcement plate, where a drill could be accurately made during the pre-assembling phase, thus guaranteeing an acceptable tolerance from the individual parts (see Figure 9.3).

non-perforated
area

(a)   (b)
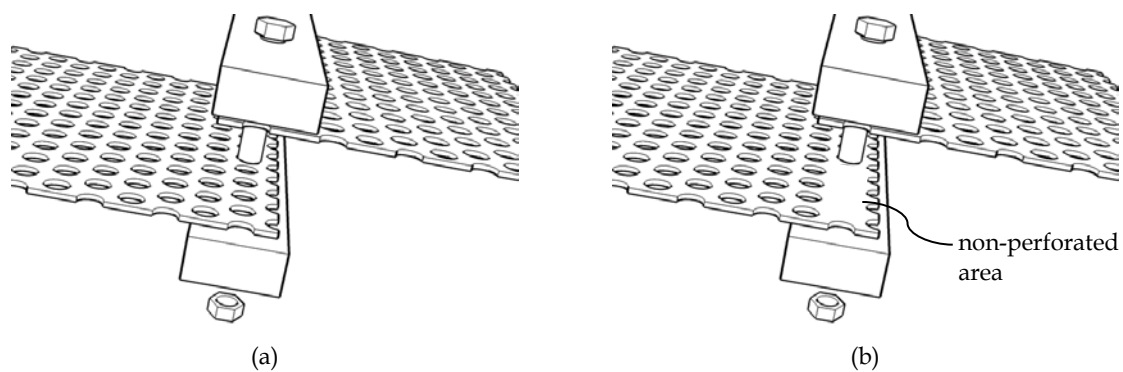
Figure 9.3. Mechanical joint of the connection using standard perforated plates (a) and customized perforated plates with a non-perforated area (b) to guarantee drilling tolerance.

9.1.1.3   Polycarbonate

The need for accuracy addressed on glass cutting, also applies to PC. When manually cut using a simple guided saw machine the accuracy was insufficient. Only when CNC milling or laser cutting was applied did the accuracy meet the required tolerances. Additionally, during bending tests the metal elongation on the tensile zone was not followed by the PC bar, which also resulted in the creation of a gap. It is prudent to apply a larger thickness of PC compared with the polished glass surface width in order to increase the tolerances. The further development of this element, namely its geometrical configuration, must address these tendency in order to foresee an efficient solution for the water tightness.
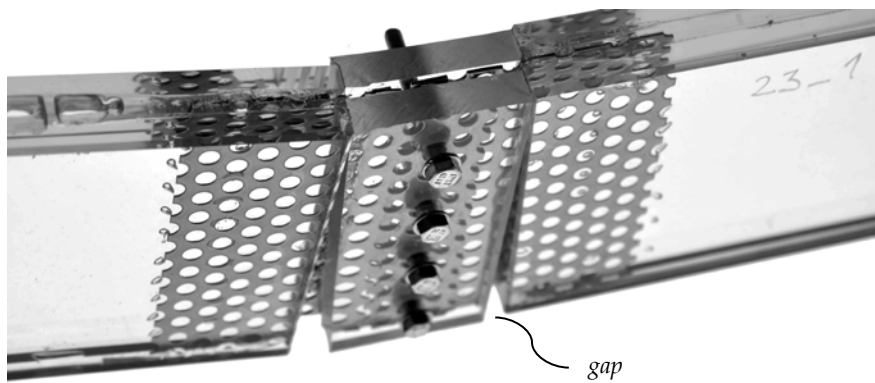
Figure 9.4. Gaps between glass and PC after loading.

9.1.2   Structure - load transfer mechanisms

9.1.2.1   Adhesive

The adhesive load transfer mechanism is responsible for connecting glass to the steel insert by means of an adhesive interlayer. The reduced thickness of the steel plate results that this load transfer mechanism is capable of bridging axial tensile loads, tensile part of bending loads and in-plane shear loads. Through the pull-out tests it was possible to observe that the adhesive behaviour of embedded thin steel elements is dependent on the type of interlayer. SG clearly showed significantly superior adhesive capacity compared to PVB. In terms of failure mechanism, on the PVB laminated specimens consistently occurred by debonding and consequent slipping of the steel, whilst on the SG laminated specimens it was caused by glass breakage or steel disruption. Only with SG was visible a deformation of the steel due to the higher stress level achieved. On the other hand the PVB specimens showed considerable deformation of the interlayer, particularly with perforated steel inserts.

The perforated body of the steel plate served as a mould to enhance the *structure* of the SG adhesive mechanism. Although the difference on maximum loads comparing perforated and non-perforated were less than 10 %, the failure behaviour was visibly different. Specimens with non-perforated plate consistently showed intense fragmentation of the glass (see Figure 9.5 (b)), while the specimens with perforated plates presented a more distributed fragmentation of the glass (see Figure 9.5 (a)). Pulled-out non-perforated plates tended to create stress concentrations along the edge of the embedded steel and particularly on the corners, while perforated plates tended to achieve an even distribution of stress, demonstrated by the larger size of broken glass fragments.

This capacity to distribute stress is achieved both by the holes of the steel, which significantly increase the contact area, and the interlayer that fills the hollowed section. It enables to configure distributed areas of superior thickness within the interlayer body (see Figure 9.5 (c)). Additionally, the perforated plate revealed higher capacity to adapt to the loading conditions, visible in the distinct deformation outside of the laminate.

The adhesive mechanism revealed to be effective on the bending tests at room temperature with 40 mm embedded perforated plates, since no debonding or glass breakage occurred. Failure was due to instability in preliminary tests and steel plate disruption, hole by hole, outside the laminate when a PC bar was applied at full height to stabilize and intermediate the contact loads.
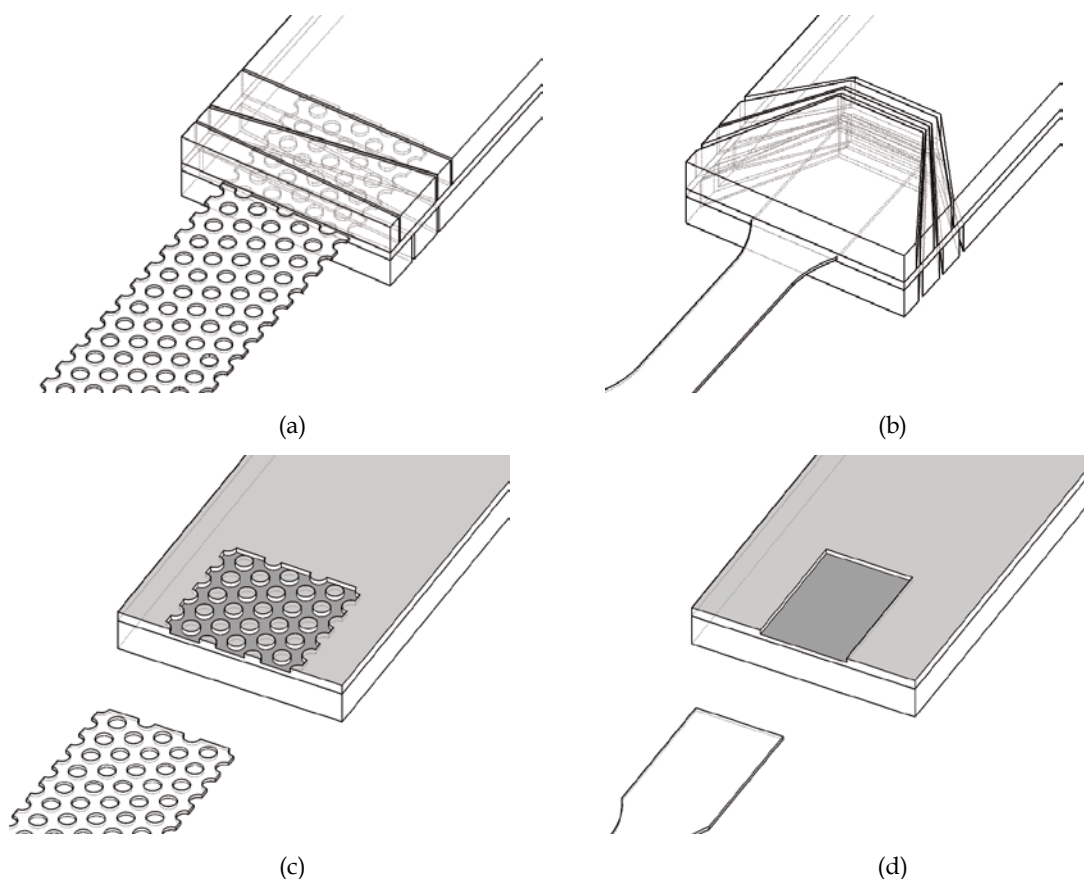
Figure 9.5. Typical crack pattern of pull-out test with perforated plate (a), non-perforated plate (b), and adhesive interlayer configuration using perforated plate (c) and non-perforated plate (d).

The experimental investigation with higher temperature showed a visible change in strength and stiffness of the interlayer, considerable influencing the behaviour of the adhesive mechanism. As shown by the pull-out tests, the strength reduction is more severe at 75 °C, resulting that failure occurred at low levels of load caused by simple slip of the metal. At 40 °C the strength reduction was more evident on the perforated plate specimens. At this temperature the steel yield extended to the interior of the laminate, allowed by a border softening of the interlayer, causing the cut of the interlayer. This fact caused an increase of stress, which considerably affected the connection strength with 40 mm and 20 mm of embedment.

Stress intensifications due to the interlayer softening were also visible in the adhesive mechanism of the bending specimens. Contrary to what was observed at room temperature, at 45 °C and 70 °C failure occurred first on the glass. This phenomenon increased in intensity with increased temperature and was caused both by the softening of the interlayer and the PC bar acting on the contact mechanism. The resulting overstress determined that the initial crack consistently appeared close to the lower edge of the embedded steel. However, debonding of the steel plate was only visible after breakage.

Comparing the maximum loads of the pull-out tests at 75 °C, an interesting phenomenon was observed. No yield of the steel was visible both on the perforated and non-perforated plates specimens, nevertheless perforated plate specimens showed significantly superior strength compared with the non-perforated plate specimens. The increase of load was almost the double, both at 20 mm and 40 mm. The adhesion reduction caused by the temperature was relatively compensated by an anchoring effect of the interlayer due to the perforated geometry of the steel-SG matrix. This fact further evidences the advantages of using perforated plate. The experimental investigation on the long duration loading revealed negligible influence on the adhesive mechanism. Similar phenomenon of failure by glass breakage occurred, as observed with high temperature, however the stress concentration occurred on the glass to PC contact, and not on the steel embedded edge as observed with high temperature bending tests.

9.1.2.2   *Contact*

The contact load transfer mechanism occurs between the edge surfaces of glass and PC. It is responsible to transmit the axial compression loads and the compression part of the bending moment. Although aluminium clearly showed the best behaviour when in compression with all types of glass, the perfect transparency of PC and the averagely best results among the other options, elected it as the final choice. PC showed a good capacity to accommodate compression stresses and a moderate tendency to deform. When in compression with annealed and fully tempered glass it showed better results compared with POM and PA6.

Important phenomena observed during compression tests was the significant sensibility of both FT glass and HS glass to uneven load application. Particularly, FT glass whose mean failure stress was very low, despite the superior pre-stress of 120 MPa. In fact the best results obtained with FT glass were at the level of the mean results of the other types of glass. HS glass had the best mean results. When in contact with Al it was clearly superior to An glass. When in contact with POM, PC and PA6 the mean results were similar. It also showed that despite the superior results, similarly to FT glass, HS glass also exhibited a reduced capacity when in uneven compression, compared to the estimated pre-stress. The internal stress equilibrium of FT glass and HS glass when loaded in compression is significantly affected by uneven loading. Meanwhile there wasn't enough data to poprely understand the phenomenon and further research was considered to be necessary.

Failure of the contact mechanism was only observed during preliminary bending tests. The reduced stiffness of the small PA6 bar and aluminium angle resulted in excessive deformation and loss of contact. On the second phase of the bending tests, the consistency on using PC to intermediate compressive loads was validated. Due to the suitable stiffness of the full height bars, the contact mechanism was preserved along the application of load. The overall bending stiffness increased by four times compared to the simple beam without any element bridging the compression loads.

The PC bar showed tendency to change its mechanical behaviour as a result of exposure to high temperature and long duration loading. Concerning the first, a possible decrease of young's modulus resulted in an increase of stress on the glass body. Consequences of this fact showed correlation with the adhesive mechanism, causing an early breakage of the glass. In the long duration loading tests, creep deformation was visible in the PC bar. This presumably caused an overstress of the glass leading to breakage, however further study is necessary on this topic.

9.1.2.3 Mechanical

The mechanical load transfer method comprises the steel perforated plates, the PC bars and the steel bolts and nuts. Two perforated steel plates are overlapped, flanked by the PC bars on each side and penetrated by the steel bolts. The screwing of the steel nut turns the mechanism effective to transfer tensile, shear and the tensile load part of the bending moment. The choice of this type of mechanism deals with the necessity to provide a simple and reversible solution, enabling both the assembly and disassembly operations to be easily and safely performed on site. During the experimental investigation the distance between bolts was considerably reduced. In the further development, larger distances were tested to acknowledge a satisfactory distance that would guarantee stability of the components when loaded and a desired simplicity and economy of means during assembly work.

The failure of this mechanism in bending always occurred through the body of the perforated plate. It never happened on the bolt or in the interface between steel plate and bolt. It was also clear the importance of the PC bar contact with the steel plate, both firmly screwed. It prevented excessive deformation, actively *clamping* the contact between the two plates, which contributed to the overall stabilization. The increased temperature and time of loading, as expected, had a negligible influence on the mechanical connection. It however was noticed that, due to a combined effect with the compressed PC bar, which showed a change in behaviour with these external factors, the metal disruption happened closer to bolts vertical alignment, after considerable plastic deformation of the beam.

9.2   Design premises and prerequisites

From the experimental investigations discussed in the previous chapter, the design of the connection detail was continuously informed. It enabled the connection solution to evolve in a consistent manner to meet all the requirements for real applications while complying with the architectural concept. These processes were conducted in parallel, although described here in consecutive sections. Below are described some of the design premises that guided the connection development.

The idea behind the will to *connect through the reinforcement* was the ability to dematerialize the connection element. The hybrid condition of the element, with the main materials embedded in one compact solution makes irrelevant the distinction between glass and connection. Visually speaking, the reinforced glass is the connection. The capacity to achieve a *smooth optical transition* between the glass elements is thus desired. The joints are considered critical points also in terms of transparency. Therefore, the connection must be designed to *reduce the joint width as much as possible*, without compromising its own transparency. The several materials that compose the connection must be *integrated as much as possible within the laminate thickness* in order to preserve the reflective integrity of the glass surface. It will also be beneficial in terms of maintenance to prevent that water or dirt might accumulate in any prominent profile. The load bearing function must be assumed by the glazing elements themselves. Therefore, the connection solutions must allow the development of self-supporting structures dispensing the need of any auxiliary opaque element.

The ductile failure behaviour achievable with the investigated concept must be preserved. The materials intervening in the connection must keep the characteristics that allowed the effective and even load transfer. Dimensional tolerances must be acquainted in terms of fabrication parameters and inevitable temperature movements. Simplicity of the design solution in order to allow considerable constructional flexibility is of interest. This means that the design solution must allow developing several glazing configurations with minor adaptations to the base detail.

The capacity to *pre-fabricate* the glass module as much as possible, leaving for the construction site just the mechanical assembly is mandatory. Additionally, both the execution and the assembly work must be kept as simple as possible. Only then is it possible to meet the high standards of quality without major changes on the production structure. It will also improve the future acceptance of the solution for real applications. If a glass panel needs to be replaced, the required disassembly must also be as simple as possible. Finally, the detail must provide good water tightness as well as space for an efficient sealing of the interlayer along the protruding steel boundary.

9.3   Morphological possibilities and detail variables

One of the critical design principles referred is the capacity to adapt to several self-supporting shapes with minor changes. There are several shapes thoroughly investigated that allow to acquire that quality. Some of the shapes develop a more efficient structural behaviour if made out of curved glass. Although perfectly possible to apply the investigated connection technique with curved glass, it is considered beyond the scope of this study and only plain flat glass solutions are developed. Some of the shapes are viable just in horizontal position, meanwhile others allow a more flexible application, as well in continuity if needed, from horizontal (overhead glazing or canopy), oblique (inclined glazing or shell) and vertical (wall or facade). In the following paragraph there is a brief description of the available possibilities, referring to works developed by other researchers, in which the application of this type of connection is considered to be viable. A simplified version of the adapted connection detail is shown.

One of the currently most investigated self-supporting shapes to be built in glass is the *dome*. Mainly in-plane compression loads occur in this shape, which contributes to its inherent stability. In the simplified adaptation of the connection detail to be applied in a dome shaped structure, the reinforcement is folded along the glass edge to an intermediate angle between the two connecting panels. The protruded reinforcement layers overlap, similarly to the *beam shaped* detail used during the experimental investigation. The polycarbonate bar is adapted to the glass edge angles, defined by the shape of the dome. The upper and lower bars have different widths and angles.

The vault shape is similar to the dome, meanwhile the loads are transmitted in only one direction. This means that the shape is less stable and needs border connection or stabilizing elements, which may be considerably slender. The design of the detail of both follows the same principles as has been described in the dome typology.

Inverted vaults are structural shapes in which mainly in-plane tensile loads are in display, which means that the reinforcement layer will have a more important role in the structure stability. Additionally the contact mechanism may be avoided, replacing the intermediate bar for a silicone joint. The connection detail follows the solutions already described for the vault, with the difference of being inverted.

Folding a thin element is an efficient measure to increase its stiffness. This design strategy is motivated by ancient techniques of origami in which paper is folded in a wide variety of shapes to acquire structural resistance despite the reduced thickness of the element. It is composed of planar, bending and shear resistant elements, presenting an ideal situation for the constructional use of glass.

The preliminary detail consists on folding the protruded reinforcement to an intermediate angle, overlap it with a similar, thus accomplishing the full folding angle. The PC bar is adapted to the glass edge angles. The flexibility of this technique allows for adaptation to different shapes and applications led to the decision of selecting it for further development using the reinforced glass connection technique.

Glass fins in facades or glass beams in overhead glazing may also be connected to the main glass panels using the investigated connection technique. On the *intersected* typology the protruded reinforcement of the main glass panels is folded at 90° whilst the reinforcement of the beam or fin is left intact. The folding edge must be separated from the glass edge of the structural glass element with the necessary distance to accommodate the polycarbonate profile.

Dome

Vault

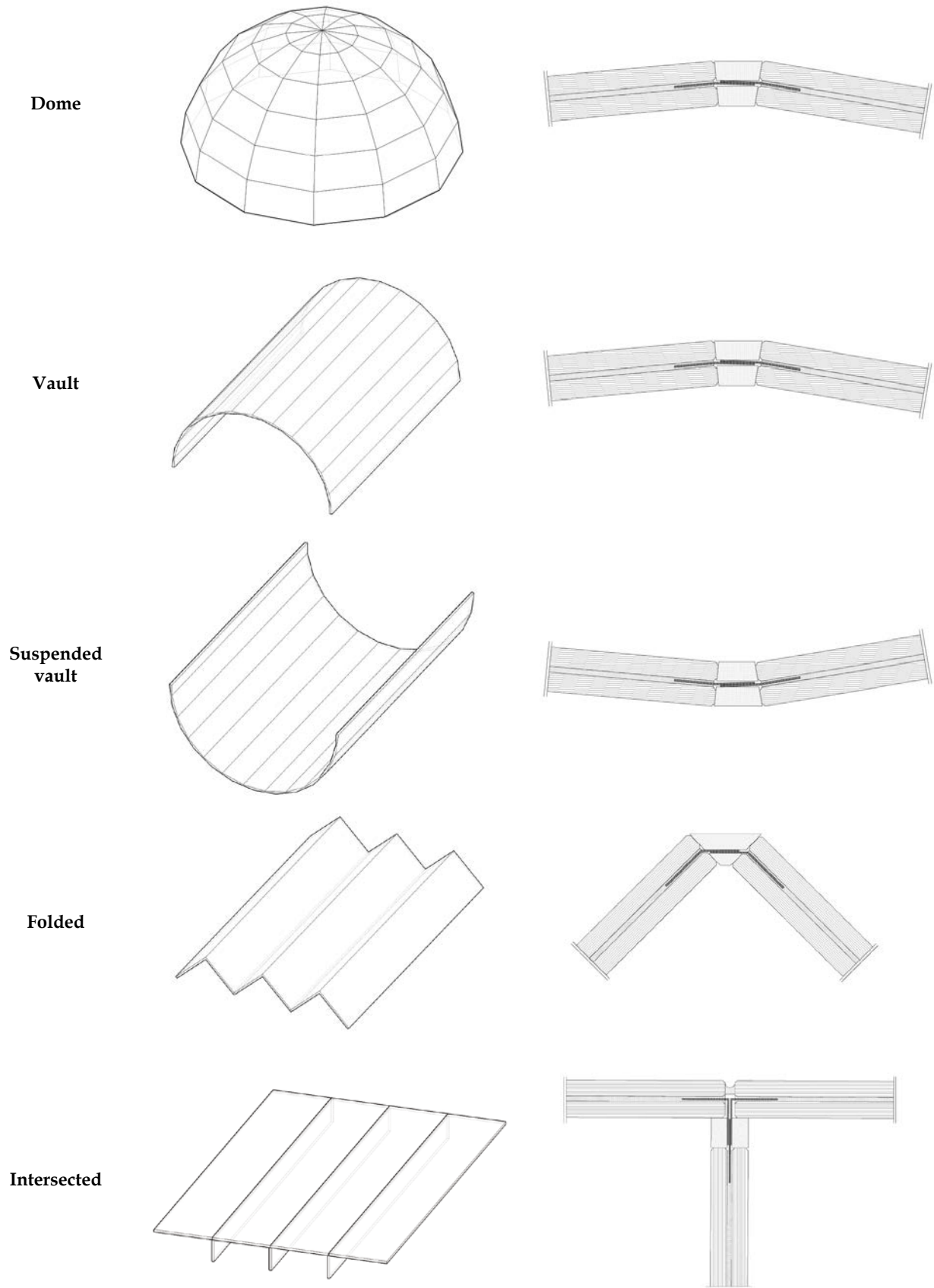**Suspended vault**

Folded

Intersected

Figure 9.6 Self-supporting shapes developable with the investigated connection technique and correspondent preliminary detail adaptation.

9.4   Design of folded geometry connection technique

The application of glass in facades and roofs with folded geometry has been applied for over two centuries. The "ridge and farrow" technique, described by Loudon as an optimized solution to build conservatories in the XIX century, was later successively applied by Joseph Paxton to cover most of the Crystal Palace's spaces.

It is considered a very efficient constructional system since the inclined panels disposed against each other provide mutual support. In terms of loads acting on a folded structure, it can be regarded as a combination of a plate and a slab, meaning that both in-plane bending moments and out of plane compressive forces are combined.

During the design process of the folded connection typology several were the problems addressed, relating to the structural, constructional and technological aspects of the connection. The combined resolution of these problems had a significant impact on the design. The five main versions of this investigation process are described above, corresponding to five design stages. At the end, the interface between the different materials was kept as simple as possible in order to fulfil the design intent of fading the joint.
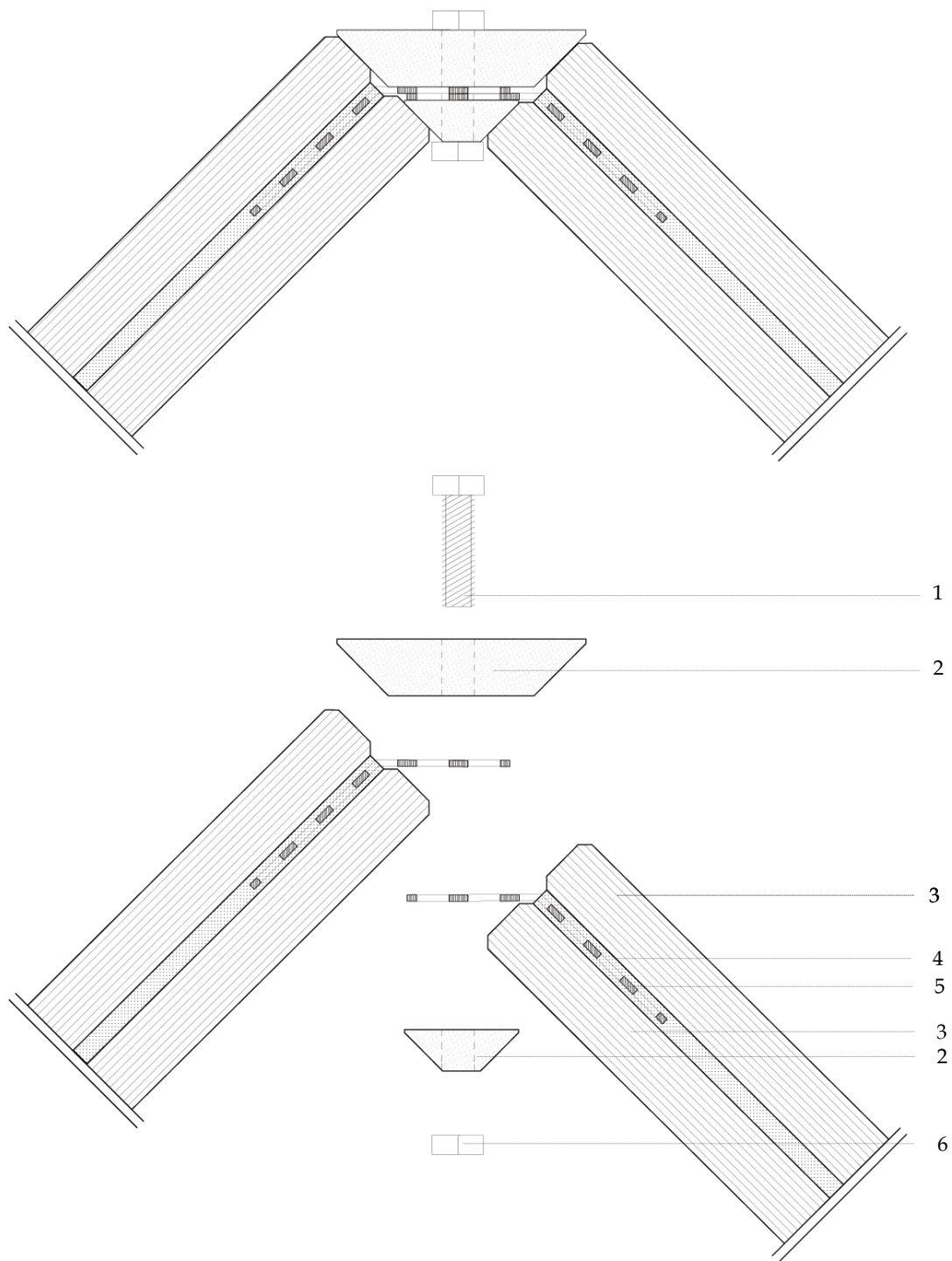
9.4.1   *Version 0*

Figure 9.7. Version #0 of the connection detail design (1 - steel bolt 8.8 M5; 2 - polycarbonate bar; 3 - annealed glass 10 mm; 4 - sentryglas interlayer 2 x 1,52 mm; 5 - stainless steel perforated plate 1 mm; 6 - steel nut).

The version 0 or "base" version is a simple transition from the straight configuration to a folded geometry. The reinforcement layer is folded at 45 º and placed in between the interlayer and glass pane with the folding line close to the end of the laminate. Each protruded reinforcement layer is then placed in overlapped position to each other in order to configure the joint where the polycarbonate bar is placed and mechanically fixed with an M5 steel bolt and nut. Due to the thickness and relative position of the glass panes, it results in an upper joint width considerably larger than the lower. A solution to avoid this fact is to displace the upper glass in relation to the lower thus acquiring similar joint widths. Additionally, when tightening the bolt it is clear that the upper polycarbonate has the tendency to tighten against the glass edges. However, the contact of the lower polycarbonate bar against the glass edge, due to the angle, has no capacity to produce a tightening mechanism similar to a shim. An improved design of this bar is tested in the next version.
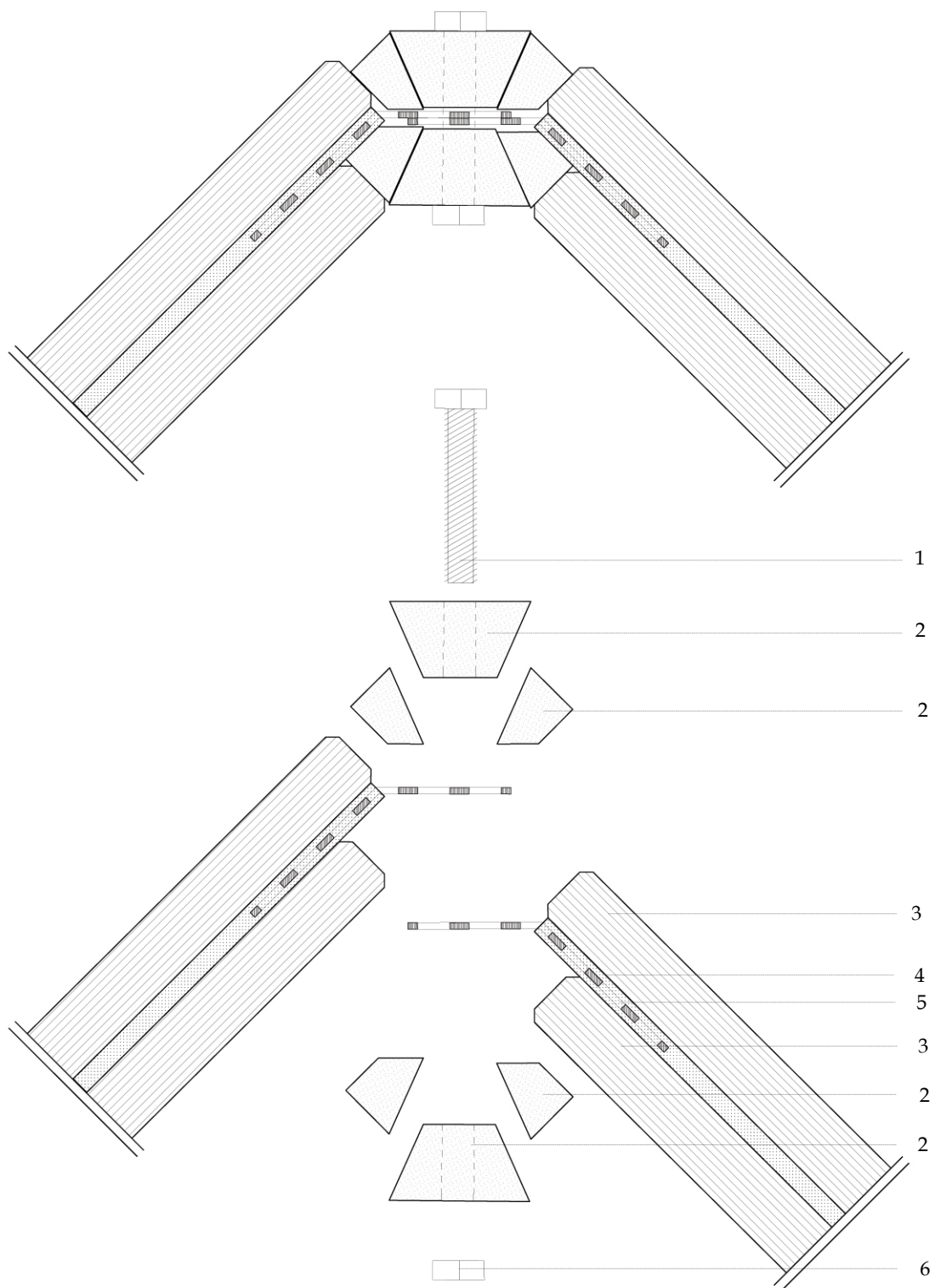
9.4.2 Version #1

Figure 9.8. Detail of the version #1 of the connection design (1 - steel bolt 8.8 M5; 2 - polycarbonate bar; 3 - annealed glass 10 mm; 4 - sentryglas interlayer 2 x 1,52 mm; 5 - stainless steel perforated plate 1 mm; 6 - steel nut).

The version #1 of the connection design presents a redesign of the PC bars to function as a shim mechanism, both at the upper and lower joints. To allow for symmetry, the glass panels are staggered at a distance of 10 mm. The folded reinforcement layer follows this reconfiguration and is placed with its folding line coincident with the lower edge of the upper glass panel. The geometrical configuration of the pieces is designed in order to execute a shim mechanism both on the upper and lower contact. A timber and aluminium prototype of this connection design was made. The adhesive mechanism is simulated using bolts and nuts to link the aluminium plates to the timber panel. This prototype allowed to empirically test the effectiveness and mechanical capacity of the solution. It was possible to understand that an excessive fragmentation of the intermediate layer (future PC bar) was prejudicial for the load transmission. As a consequence of the expected, although reduced, deformation of the elements that compose the interface, disintegration of the connection mechanism was easily achieved. A new version of the intermediate bar using a reduced number of pieces was developed as the next version.
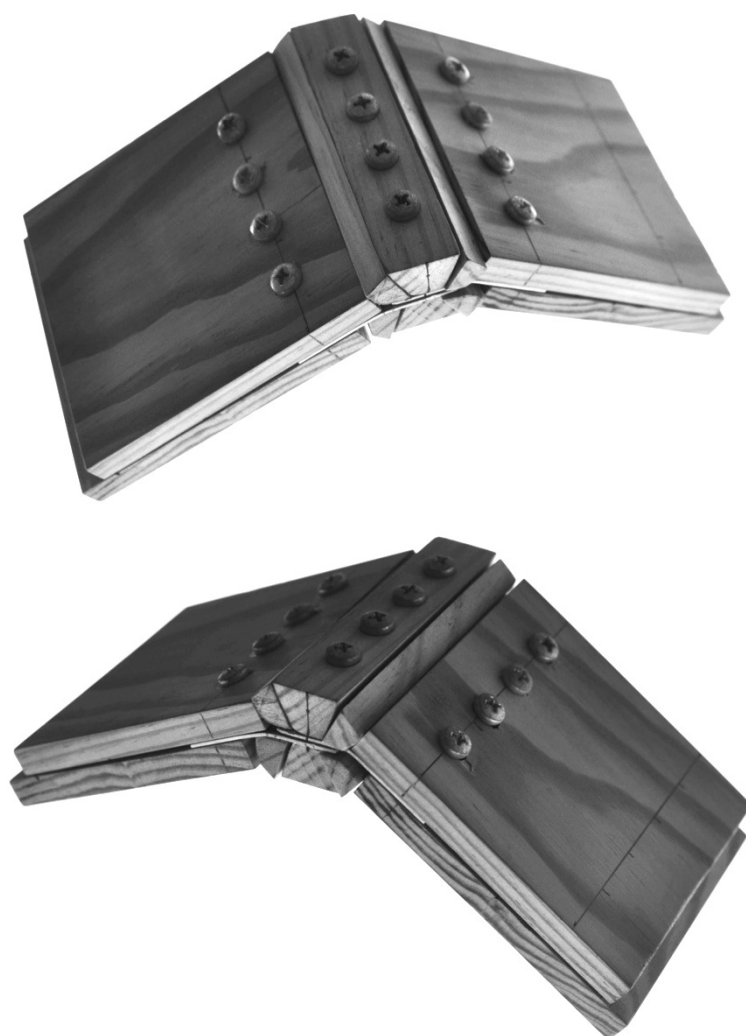

Figure 9.9. Prototype of the version #1 connection design (timber and aluminium).
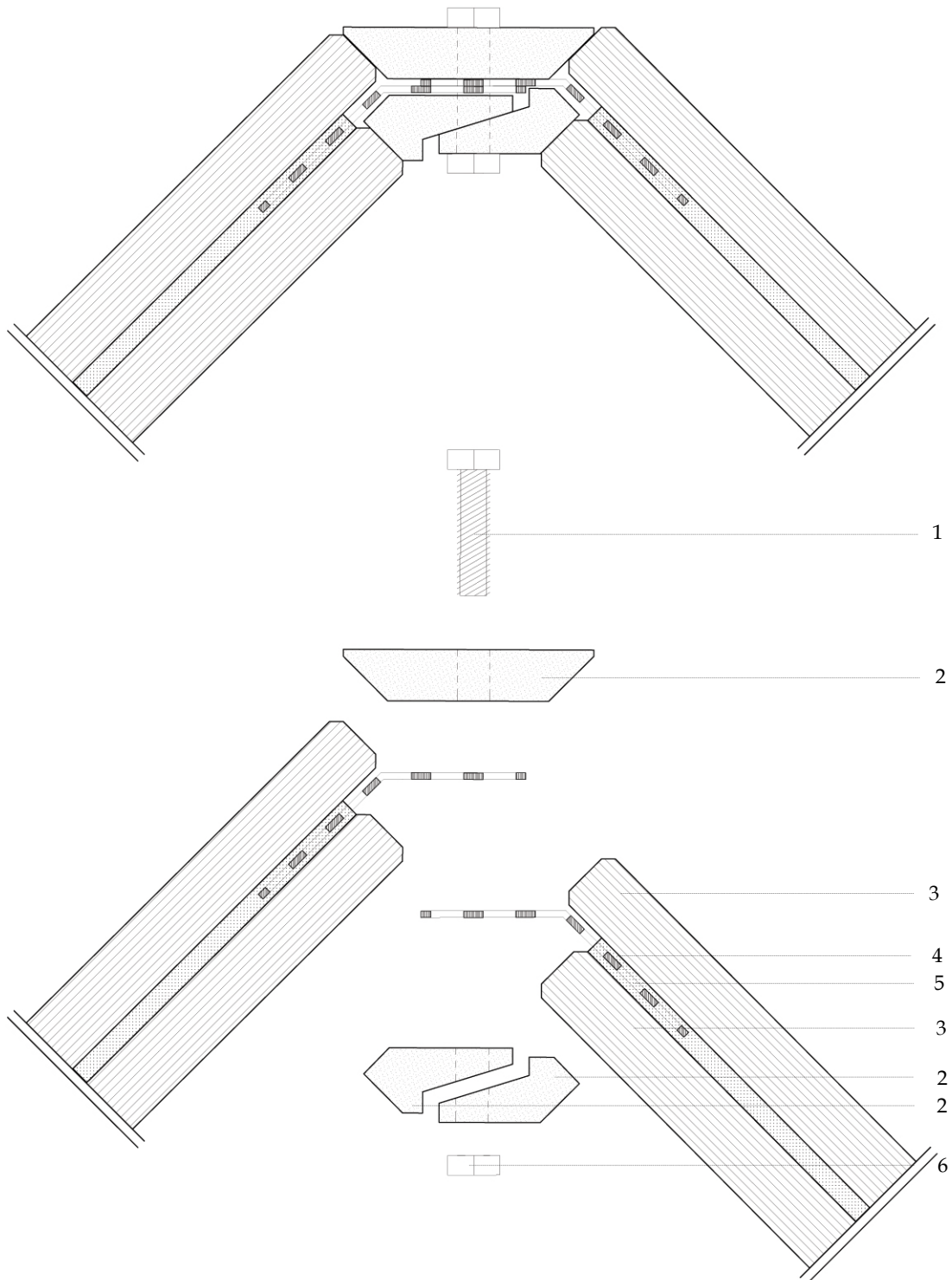
9.4.3   Version #2

Figure 9.10. Detail of the version #2 connection design - scale 1:1 (1 - steel bolt 8.8 M5; 2 - polycarbonate bar; 3 - annealed glass 10 mm; 4 - sentryglas interlayer 2 x 1,52 mm; 5 - stainless steel perforated plate 1 mm; 6 - steel nut).

On the version #2 of the connection design, the focus was mainly on the intermediate bar configuration. This layer has the purpose of intermediating the contact between the glass edges, but also, when tensioned achieve compressive pressure in order to assure full surface contact. Only then does the contact mechanism is effective and the connection is in equilibrium. It was decided to test different geometries of the PC bar for the upper and lower joints. As previously referred, the upper joint easily achieves tensioning due to the beneficial positioning of the glass edge angles. The problem remains on the lower bar, to which a new configuration was developed. It comprises two equal parts defined by a main sloping surface placed in opposite positions with both surfaces in contact. When the bolted joint is tensioned, it would work as a shim and compress to the sides in contact with the glass edges. To give room for this configuration, the joint between glass panels was enlarged. In this version, the staggered displacement of the glass panes was reduced to 7 mm.

A first reinforced glass prototype was made for this connection design version. It enabled both to test the new PC bar configuration and the actual lamination of protruded and folded reinforcement with staggered glass panels. Some of the already discussed problems on lamination arose at this stage. During the application of pressure through the combined action of vacuum and silicone blanket, the glass moved. Although the displacement was just few millimetres, which in normal laminated glass application is not problematic, for the investigated technique is critical. This lamination process is considered more suited for large glass panes where the self-weight acts as a retention mechanism to the imposed stress by the silicone blanket. Additionally, it was clear that this displacement tendency was accentuated by the asymmetrical disposition of the glass panes. When vacuum pumped, the silicone blanket tends to concentrate the elements as vertically aligned as possible, intervening in the desired staggered placement.

During fabrication a simple timber shim was used to fix and protect the metal plate from being deformed. Fixing the metal to the timber profile revealed to be insufficient since the glass had the freedom to move aided by the very low friction surface of the SG interlayer. The prototype revealed some dimensional inaccuracies after the lamination process. In order to use it, the PC bars had to be adapted to the resulting geometry. The functioning of the mechanism was tested and it demonstrated some difficulty in processing the shim movement. The significant friction of the machined PC bar prevented the sliding movement necessary to achieve contact on both sides.
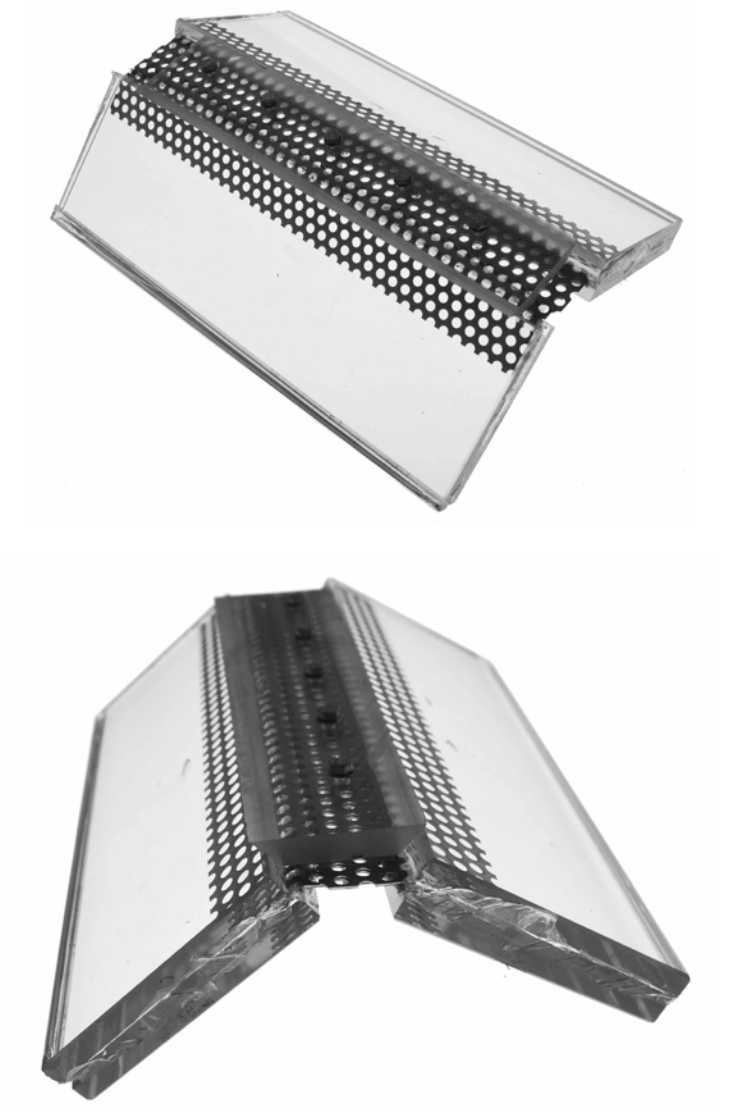
Figure 9.11. Prototype of the version #2 connection design
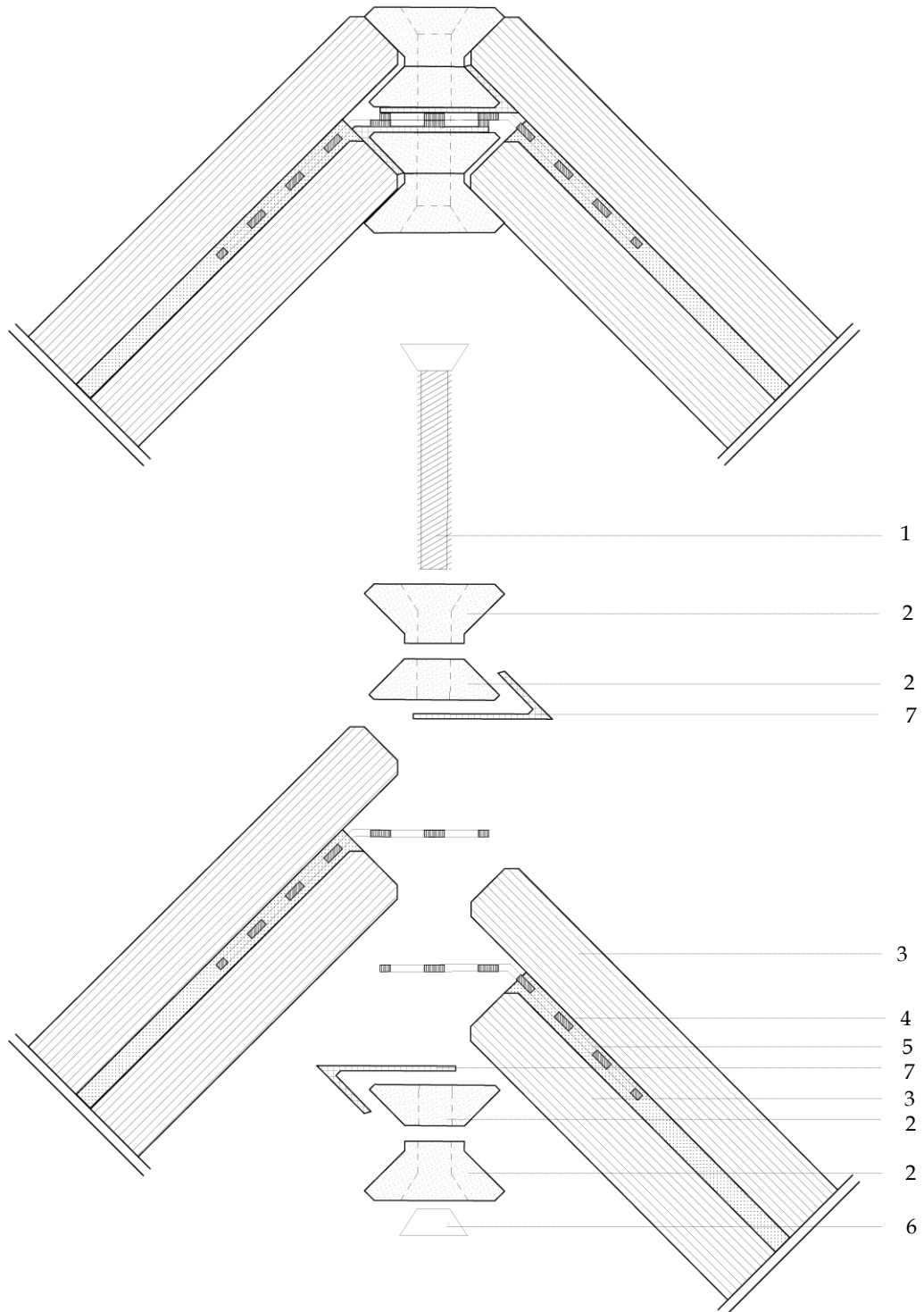
9.4.4 Version #3

Figure 9.12. Detail of the version #3 connection design - scale 1:1 (1 - steel bolt 8.8 M5; 2 - polycarbonate bar; 3 - annealed glass 10 mm; 4 - sentryglas interlayer 2 x 1,52 mm; 5 - stainless steel perforated plate 1 mm; 6 - steel nut; 7- double sided bonding tape).

The version #3 of the connection design focused on three problems discussed in the previous version, namely the excessive joint width, the inefficient tensioning mechanisms between glass edges and PC, and the unintended displacement of elements during lamination process. The PC bars geometry was developed to a new configuration based on four vertically aligned bars with symmetrical positioning (symmetry as a design principle to equalize pressure during tightening). The idea is to use the outer bars to perform structural contact with the glass edges and effectively perform the load transmission, and the inner bars to aid in the lamination process and assembly tasks. These inner bars would be applied on the individual glass panels before the lamination process by means of a transparent double sided bonding tape. This tape would fix the reinforcement layer to the PC bar, and also to the glass panel, contradicting the tendency of movement during lamination. The bonding tape was chosen for its ease of application, good adhesion to several materials, capacity to adapt different configurations and for being fully transparent.

The staggering displacement between glass panels was increased to 13 mm. It enabled to vertically align the glass edges. The position of the reinforcement layer towards the glass panels was adjusted. The folding edge was moved from the upper glass edge to the lower glass edge. It enabled to increase the available thickness to embed the upper PC bar without overtake the upper limit of the glass edge. Both the adjustment of the glass-to-glass and reinforcement-to-glass relative position enabled to stabilize four equal contact surfaces in each side, further refining the symmetry of the system (see Figure 9.12). The considerable thickness of the tape required a recess on the PC bar to accommodate it.

Laminating with a fixing element revealed visible improvements in terms of dimensional accuracy. Although not exactly at the same position as before lamination, the staggered position of the glass panes and the relative positioning of the metal layer were acceptable at a first evaluation. When testing the assembly of all pieces, it though revealed to be a difficult task. The steel bolt had to penetrate six layers of material (four PC bar holes and two steel perforated plate holes). A considerable looseness of the holes diameter was necessary to accomplish the bolt's passage. When tensioning, it became clear that the reduced displacement during lamination had significant impact on the final cohesion of the parts. In this version, the polishing of the machined PC bars was tested. After bevelling the sharp edges with a cutter, the machined surfaces were polished with a rotating brush applying a special soap during the process. These surfaces reacquired the desired transparency. Once in place, the several layers of PC bars, although smoothly polished, revealed a visual blurring. It was due to the significant number of overlapping surfaces. A total of 8 transparent surfaces comprised the connection, which when crossed by light rays caused a significant reflection, which is visually detrimental.
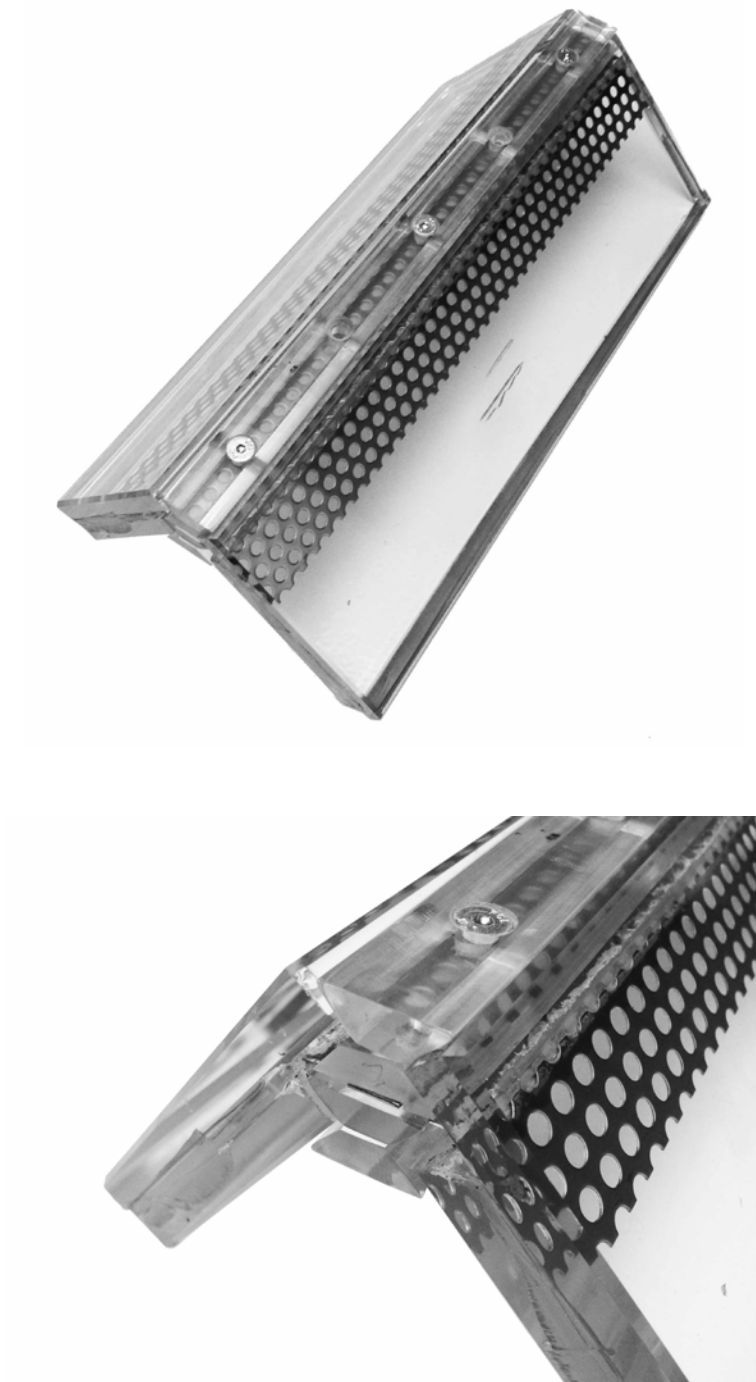
Figure 9.13. Prototype of the version #3 connection design

9.4.5   Version #4

Figure 9.14. Detail of the version #4 connection design - scale 1:1 (1 - steel bolt 8.8 M5; 2 - polycarbonate bar; 3 - annealed glass 10 mm; 4 - sentryglas interlayer 2 x 1,52 mm; 5 - stainless steel perforated plate 1 mm; 6 - steel nut).

The version #4 of the connection design seeks to solve the problems identified in the previous version, namely the capacity to fix the glass and reinforcement during lamination and avoid considerable layering of PC elements, which revealed to be inappropriate both in aesthetic and functional terms. In this version the glass and reinforcement position remained the same. The reinforcement width outside the laminate was increased to allow a slight widening of the joint.

The solution developed for the PC bar maintained the option of division in four elements, however the two elements with lamination fixing roles were considerably reduced in size in order to be embedded in the glass panes thickness, as if the missing glass from the staggering movement was replaced by two PC triangular prisms. Although previously referred in version #1 that sectioning the intermediate bar in several pieces was problematic the fact that the pieces would be bonded to glass would result in just two moveable parts. Applying a strong epoxy glue, the PC bars would be bonded to the glass and steel plate preventing movement during lamination and simplifying the following assembly work.

However, at the end the significant pressure applied during lamination broke the glue in some locations, allowing for some movement of the pieces. The PC bars were bonded again to proceed with testing. In terms of contact mechanism function they were shown to be too loose due to the lack of direct contact with the upper glass edge.

Figure 9.15. Prototype of the version #4 connection design

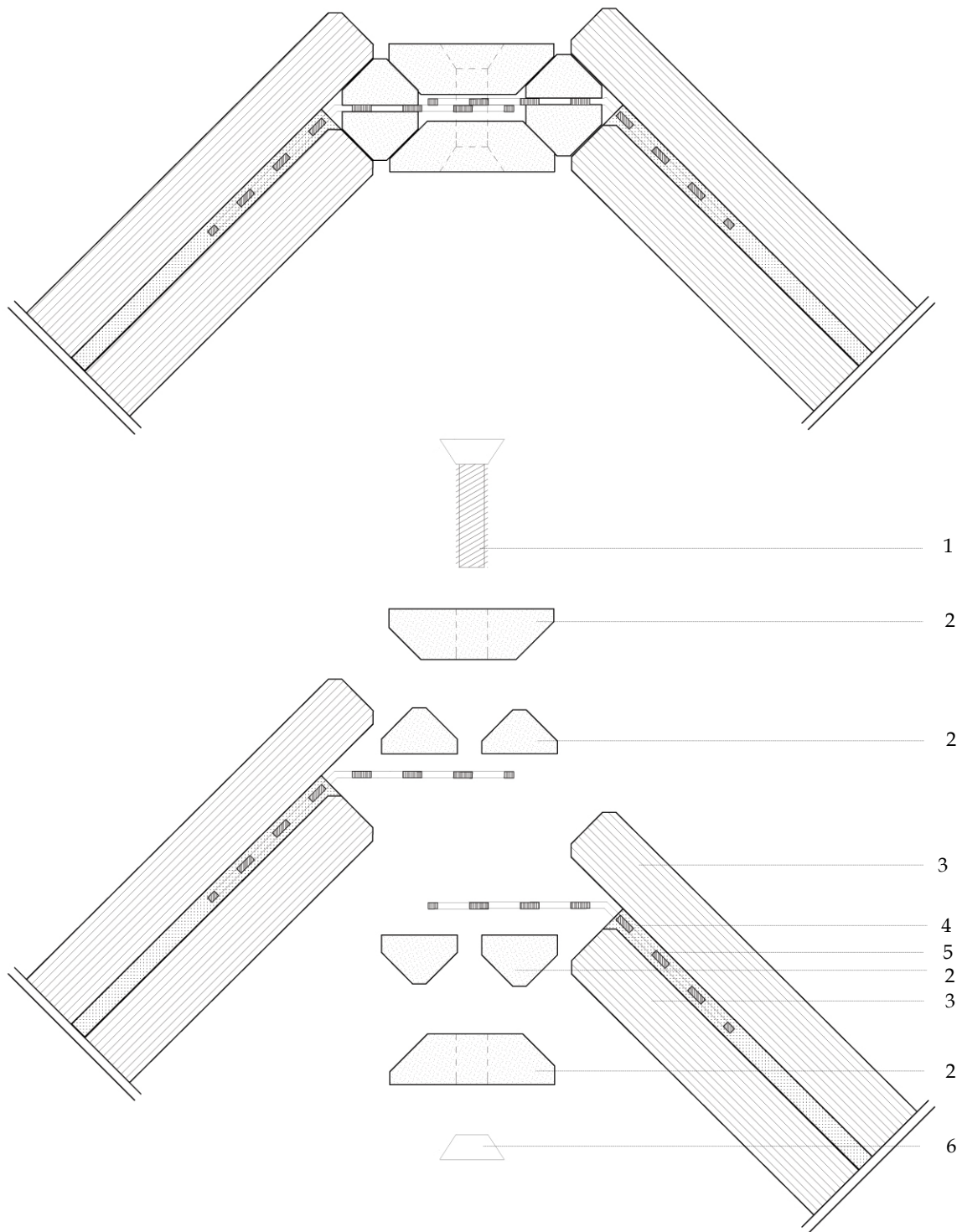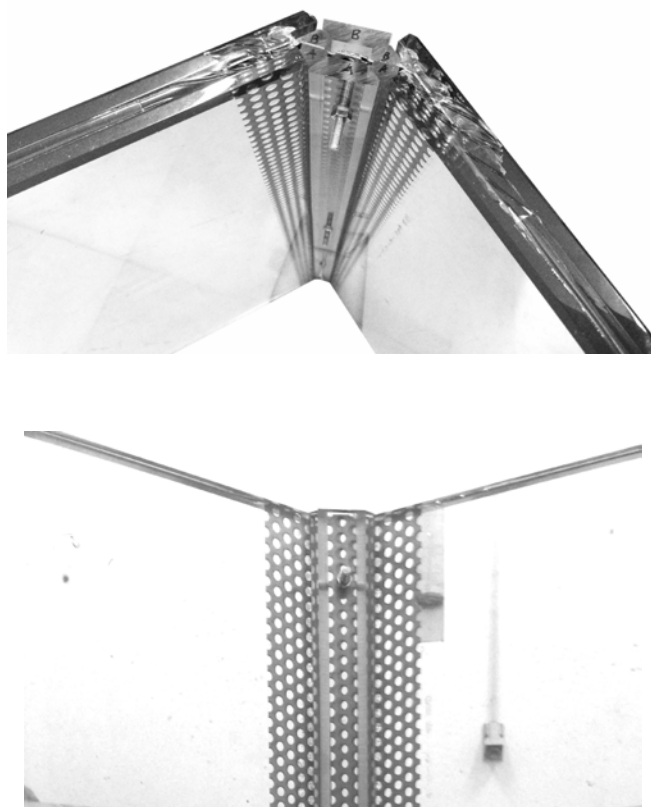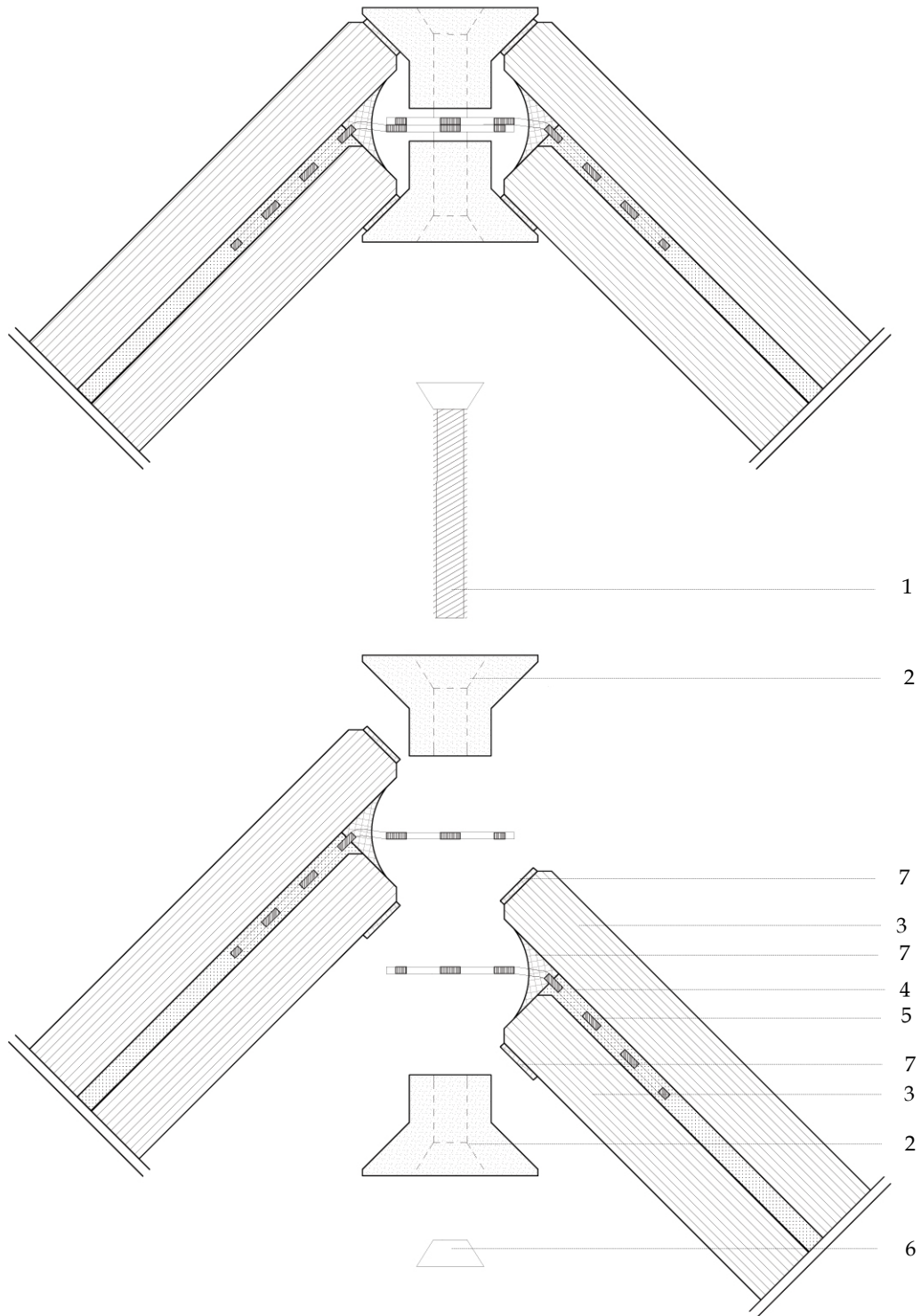## 9.4.6   Version #5

1

2

7

3

7

4

5

7

3

2

6

Figure 9.16. Detail of the version #5 connection design - scale 1:1 (1 - steel bolt 8.8 M5; 2 - polycarbonate bar; 3 - annealed glass 10 mm; 4 - sentryglas interlayer 3 x 0,89 mm; 5 - stainless steel perforated plate 1 mm; 6 - steel nut; 7 - silicone).

In the previous versions, several connection designs were developed to solve the problem of maintaining positioning during lamination while assuring an effective contact mechanism and providing an transparent view through the PC bar. The considerable complexity of most of the previous versions revealed inhibitive of accomplishing a satisfactory result. There was the conviction that the solution should be simplified as much as possible. To do so, it was decided that the lamination problem should be solved outside the scope of the connection design. Considerable efforts were employed on that task and once developed a consistent solution for it (see section 9.1.1) it was possible to submit a final version for the connection design.

Version #5 comprises two symmetrical PC bars with a simple configuration. One side of the bar presents a bevelled geometry defining the 90 $^{\circ}$ fold to be in contact with the glass edge on the upper side, and with the surface of the lower glass pane on the lower side of the connection. This geometry allows certain dimensional tolerance since there is an adaptation capacity of the elements when being tightened. The other side of the PC bar presents an orthogonal configuration to be inserted in the reduced width joint close to the the reinforcement layers. In the inner gap between the PC bar and the glass it is proposed to apply silicone for sealing the SG interlayer boundary (penetrated by the protruded reinforcement) as well as on the PC-to-glass contact to provide efficient water tightness to the system.

This design solution proved to work efficiently during the assembly and tightening operations. Since the main compression loads are transmitted on the superior glass edge, this contact showed considerable consistency. Finally, the capacity to see through the PC bar was thoroughly achieved as seen in Figure 9.17.
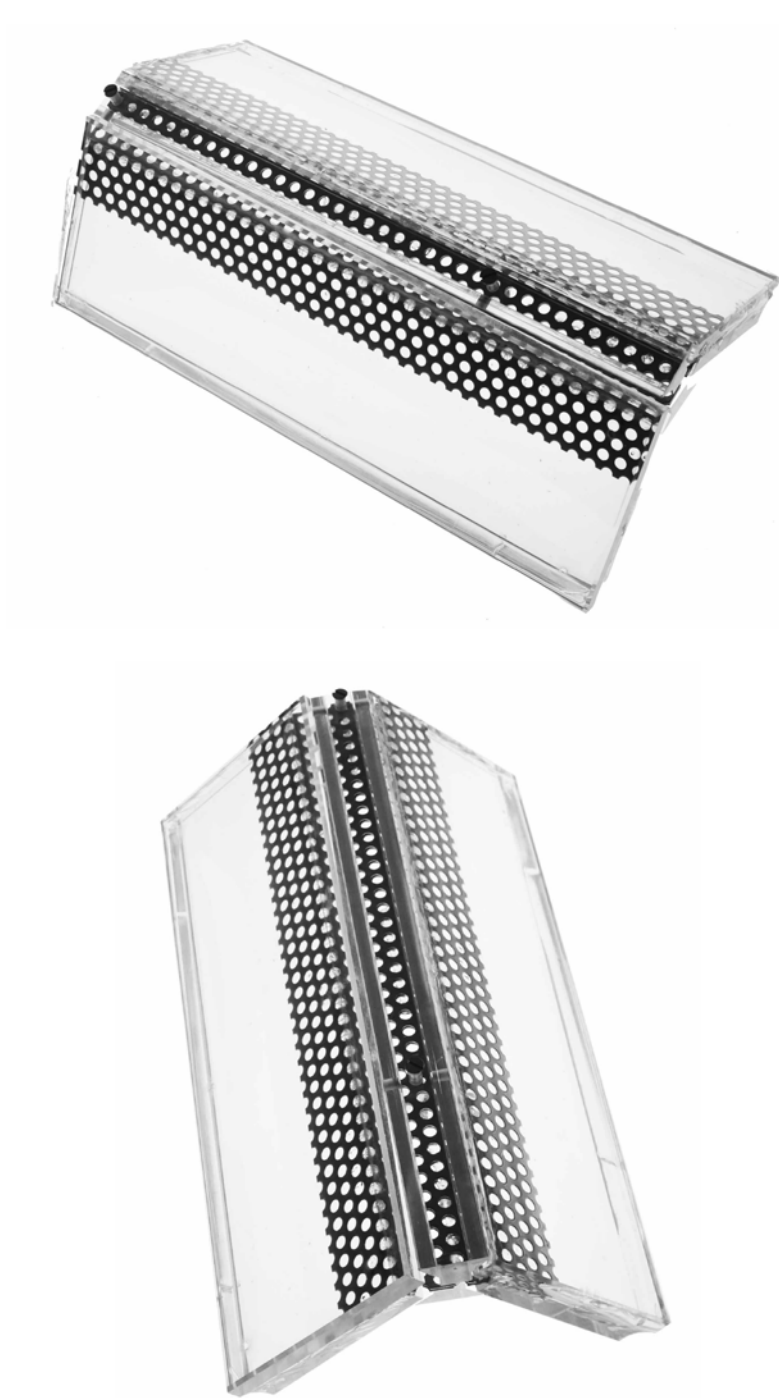
Figure 9.17. Prototype of the version #5 connection technique

10 Prototype

10.1 Layout

The concept for the prototype developed around the idea of a piece of sculpture in the University Campus of Azurém in Guimarães to be visited in an informal captivating environment. This way it was possible for both experts and non-experts to easily apprehend the different possibilities of the proposed system. Superimposition of transparent layers was a relevant feature that the prototype should display in order to enhance its phenomenological effect. Additionally, a fluid space though which people could walk around, alternating inside and outside experiences, was also a requirement. The final solution consisted on two parallel folded glass walls with 2.8 meters high (visible above the ground), slightly staggered in its relative position (see Figure 10.1). One of the walls (a) is fully "reinforced", exhibiting glass panels with perforated sheets in its entire surface, while the other (b) exhibits a freer arrangement, alternating zones with and without reinforcement. Each wall is composed by seven individual glass plates connected with the investigated technique. All the individual plates measure 2950 mm x 750 mm, with the exception of the first, which is only 1050 mm high to better show the detail. The lower part of the glass panels is embedded into the ground to a depth of 150 mm. The total structure comprises 14 panels defining an area of 5,5 m long and 2,6 m width. The flexibility of the solution allows it to be both tested on the vertical and horizontal positions. The folded geometry ensures high moment of inertia, allowing it to be self-supporting both in façades and roofs.
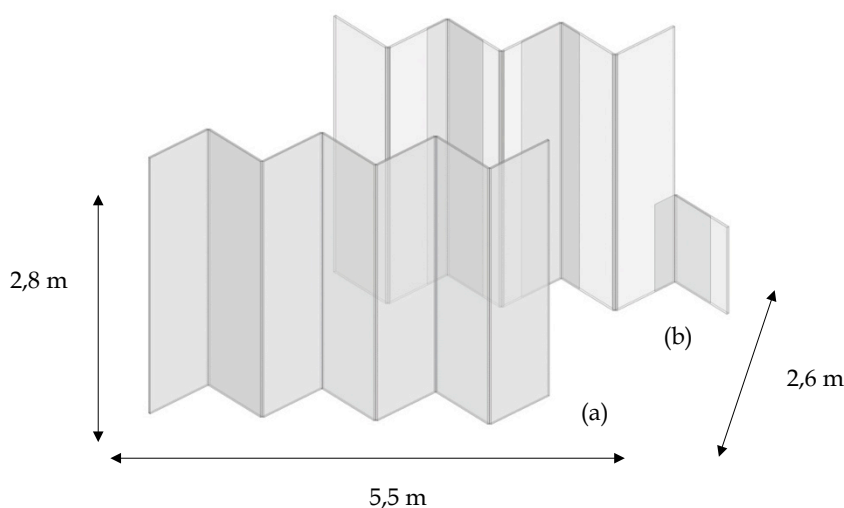

Figure 10.1. Layout of the prototype

Concerning the wall (b), three embedment widths have been determined, namely a minimal of 25 mm, a third of the glass width and two thirds of the same, measuring 250 mm and 500 mm correspondingly. The purpose is to clearly show the flexibility of the system when designing the connection and its influence to the overall design of the element. The ability to drastically reduce the amount of embedded perforated plate is tolerable by the excellent behaviour of the adhesive mechanism studied during the experimental investigation. The design of the connection used in this prototype corresponds to the latest stage of development described in the previous chapter with slight variations described below.

Firstly, the available glass for the prototype was 12 mm thick, which necessitated adapting the geometrical configuration of the intermediate bar. For several circumstantial reasons (availability of leftover material, time and ease of production, specially polishing, resistance to UV without coating, etc.) it was decided to replace polycarbonate for acrylic in the connection detail. Although the experimental investigation showed its fragile behaviour, the stress at which it happened was clearly above the expected in this application. The acrylic bar of the joint resulted with reduced width of 18 mm, perfectly polished and recessed in relation to the glass plane, contributing to the desired optical fading of the joint. In the traditional systems, it is there where the emphasis happens, which prevents a subtle definition thus transition of the planes that compose it. The connection detail and composition of each individual panel is described in Figure 10.2.
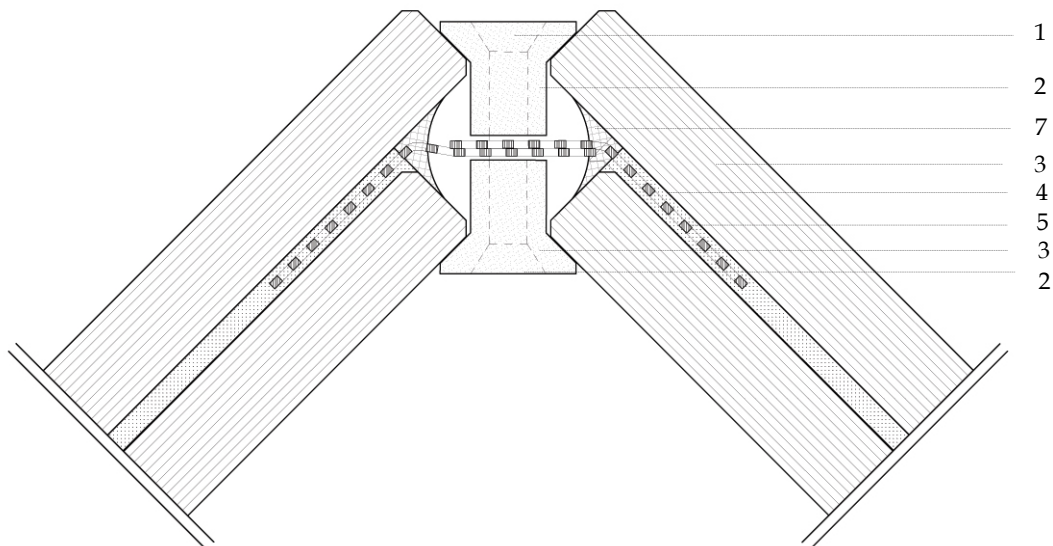

Figure 10.2. Connection detail of the prototype and description of its composition ((1 - steel bolt 8.8 M5; 2 - acrylic bar; 3 - heat strengthened glass 12 mm; 4 - sentryglas interlayer 3 x 0,89 mm; 5 - stainless steel perforated plate 1,2 mm; 6 - steel nut; 7 - silicone).

10.2 Testing

An experimental investigation on the mechanical behaviour of a folded reinforced glass component was desired to evaluate its capacity to be efficiently applied in facades and coverings. Without any known reference to test this type of structure, the test setup was designed with the practical application in mind. The out-of plan compressive behaviour is tested relating to a real application in which wind and other instant distributed loadings are expected. The application of load should be as well distributed as possible, although restricted by the specific folded geometry of the specimen. The capability for handling the specimen during tests, without any mechanical help was considered important for the completion of the tests. For this reason the length of the prototype was limited to 1 m. Although significantly smaller compared with the final prototype to be built, it was considered to be an element large enough to study the behaviour of such type of structure.

10.2.1 Test procedure

10.2.1.1 Specimen description

The out-of plan compressive test specimens have a 90° folded geometry with a total length of 1 m, comprising two symmetrical parts, each with 0,5 m of width connected at the centre (see Figure 10.3). Each part is made of two rectangular shaped pieces of 10 mm thick annealed glass, laminated with two sheets of 1,52 mm thick ionomer interlayers (SentryGlas®) to which a 1 mm thick AISI 304 stainless steel perforated plate is semi-embedded. It has the same length as the glass and is 52 mm wide, 32 mm of this is embedded in the laminate.

The steel plates were previously cleaned with isopropyl alcohol to remove oil and dust and assure good adhesion. Two polycarbonate bars with bevelled edges are placed on the upper and lower part of the connection to realize full contact between the parts once firmly screwed with M5 (8.8 ISO 4017) steel bolts, passing through the aligned perforated steel plate holes, with steel nuts and rings. Five bolts were used in each specimen, at a distance of 200 mm from each other. One of the specimens exhibited a small flaw close to the centre of the lower glass edge that was found to have some influence on the results.

(a)   (b)
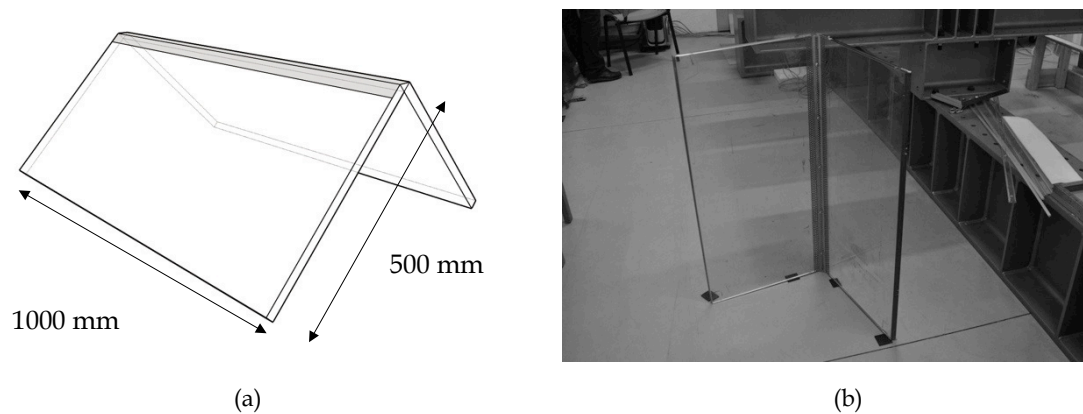
Figure 10.3. Out-of-plan compressive test setup diagram (a) and view before test (b).

10.2.1.2 *Test setup*

As mentioned before, there was no standard setup for this type of test and specimen. The test setup was thus developed in accordance with the principles considered relevant for a practical application: reduced contact area at the supports and distributed application of loading on the edge. The folded specimens were placed horizontally and supported on the four corners. A contact length of 100 mm was ensured in each corner and a cylindrical nylon profile was used as an intermediary between the laminated glass lower edge and the steel base. An "IPN 200" steel profile was placed on the upper edge to uniformly distribute the load (see Figure 10.4). The contact is done directly to the polycarbonate bar that composes the joint (see Figure 10.5 (c)).

(a)   (b)
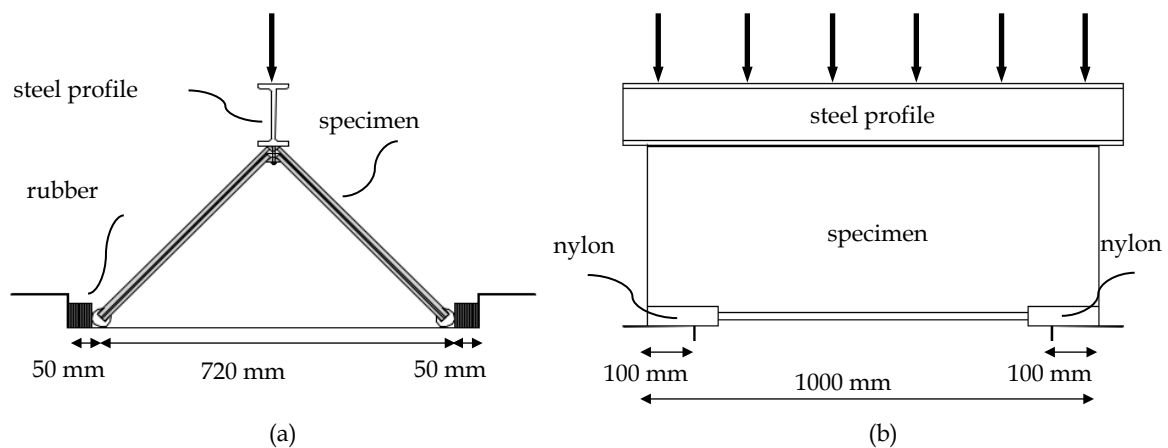
Figure 10.4. Folded glass out-of-plan compression test setup front view (a) and lateral view (b).

Due to the expected rotation of the glass panels during the test, the cylindrical shape is most suitable since it allows for rotational movement. This profile was previously machined to accommodate the laminate (see Figure 10.5 (b)). The lateral displacement of the specimen was constrained using steel profiles fixed to the main frame. Some deformation was allowed using 50 mm thick rubber blocks in between the nylon and lateral steel break.

The load was applied using a dynamic loading jack of 300 kN at a constant displacement rate of 2 mm/minute and the deformation was measured on the upper joint (vertical) and at the lateral edges (horizontal).

(a) (b) (c)
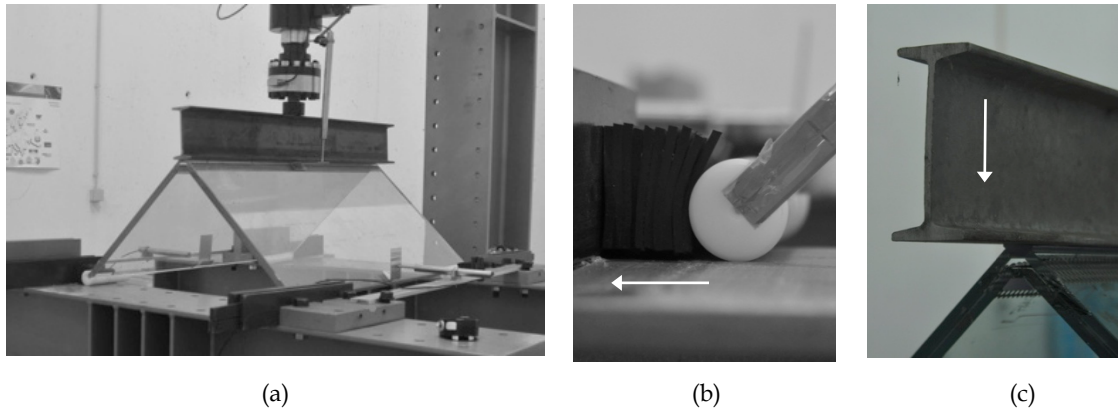
Figure 10.5. Folded glass test setup general view (a), detailed view of the lower specimen support (b) and top contact between steel frame and polycarbonate joint (c).

10.2.2 Test results

In Figure 7 the load-displacement curves of the three folded glass specimens tested are shown. The vertical displacement of the folded specimen measured on the top joint of the specimen is used. The three curves are very close to each other showing that the tests are quite reproducible. At the beginning of the test, all three specimens begin to deform, opening the folded angle and compressing the rubber layers. At a load of about 80 kN of load the first crack appeared on the specimens, starting at one of the lower supports.
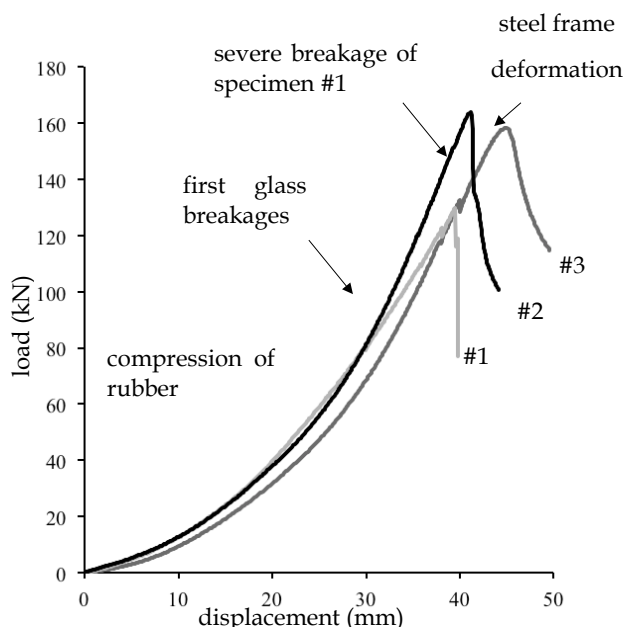
Specimen	#1	#2	#3
Max. load (kN)	129,90	163,70	152,20
Average max. load (kN)		150	
Vertical displacement at max. load (mm)	39,49	41,14	44,96
Lateral displacement at max. load (mm)	44,0	44,1	45,28

Figure 10.6. Load-displacement curves of the out-of-plan compression tests on folded glass specimens and detailed results.

In specimen #1 the first cracks appeared in both laminated glass panes at almost the same time, slowly developing along the element body (see Figure 10.7 (a)). Despite the failure of the glass, the specimen was capable of taking a considerable increase in load. At 109 kN a second crack started close to the lower support on the opposite side. The damage appeared more severe than the previous damage due to the increased load and the asymmetrical deformation already visible on the specimens. Meanwhile the load continued to increase and significant crack development and crack branching occurred, particularly close to the lower supports. Around 130 kN the fragmentation of the glass close to the initial failure was so severe that it disintegrated which considerably reduced the load carrying ability (see Figure 10.7 (b)).

(a)   (b)
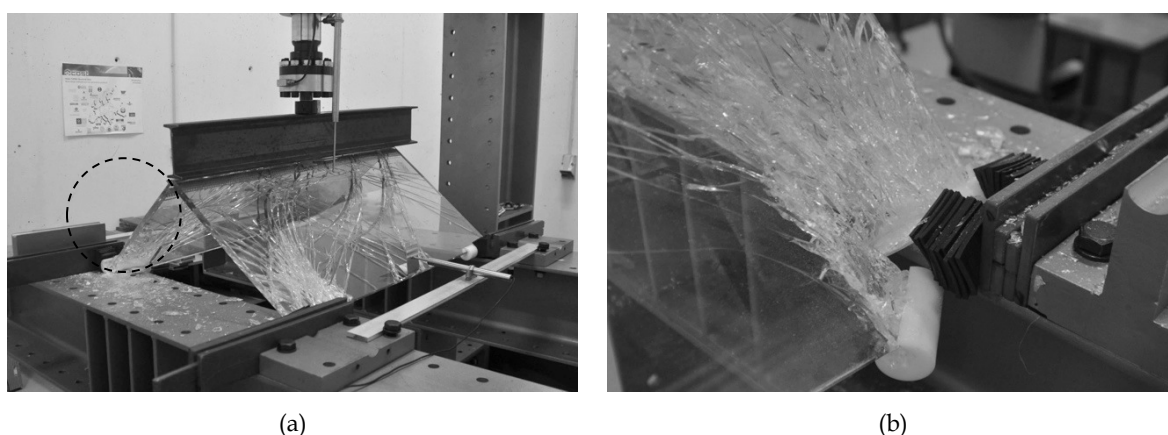
Figure 10.7. General view of specimen #1 during test (a) and close-up view of severe damage on one of the lower supports (b).

Specimen #2 also exhibited its first breakage around 85 kN, starting close to a lower support but in only one of the laminated glass panes. It stayed stable until 126 kN when the other glass pane of the laminate broke showing multiple crack development with severe crack branching (see Figure 10.8). Also in this case, despite the failure of both glass panes, the specimen was able to carry a further increase of load. Final failure happened at a load of about 160 kN, when increasing fragmentation of glass occurred, some pieces of which separated from the interlayer and were projected away. This occurred due to the extremely localized area in which it happened resulting in high stresses. Meanwhile, it didn't disintegrate, as did the previous specimen. The considerable deformation of the specimen influenced the load introduction into the specimen because the steel frame came into contact with the polycarbonate joint, which started to deform, preventing a further increase of load. This phenomenon is clear in the load-deformation curve where a soft "plastic" curve is seen at the top.

<center>(a)   (b)</center>
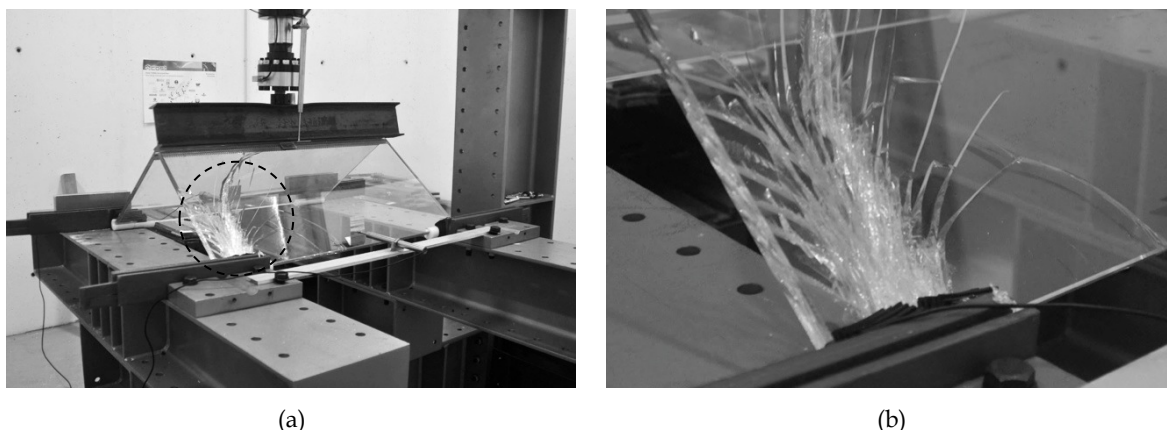
Figure 10.8. General view of specimen #2 during test (a) and close-up view of lower support exhibiting breakage of both glass layers of laminate (b).

Specimen #3 distinguished itself from the previous two by showing premature breakage of glass starting at the upper edge, close to the area of load application. Although the polycarbonate interface prevented direct contact between glass and steel, possibly flaws resulting from the glass being cut may have triggered it. It developed very slowly, exhibiting a shell like shape that grew in the horizontal direction along the glass body. At around 120 kN of load a simultaneous breakage of four glass panes occurred. It happened close to two supports on the same side of the specimen, in both laminated panes. It continued to carry increasing load resulting in new crack branches that developed from both supports. At 130 kN a third main breakage occurred, away from the support area, caused by a pre-test-damage mentioned. It meanwhile continued to carry increased loading causing considerable deformation of the specimen until around 150 kN when similarly to the previous test, the steel frame started to deform which prevented further increase of load.


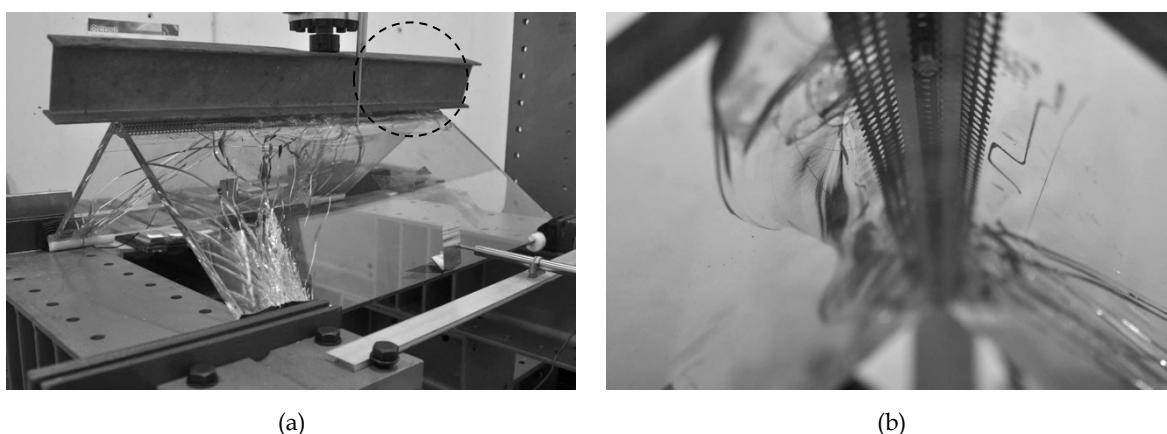<center>(a)   (b)</center>

Figure 10.9. General view of specimen #3 during test (a) and close-up view (from below) of upper edge area of the specimen exhibiting a shell shaped breakage of glass in the upper joint (b).

10.2.3 Discussion

The results of the experimental investigation clearly showed the reliable behaviour of the folded reinforced glass element when subjected to out-of-plane loads. The three specimens behaved in a very similar way, as is evident from the load displacement curves. Despite some differences in terms of failure initiation, the maximum loading achieved was very close, limited by the test setup due to excessive deformation of the upper steel profile (see Figure 10.10 (a)). This means the higher load capacities may be achieved if the test setup is improved.

The results also demonstrated the safety of the concept. Despite the glass breakage, initial and further increasing in all three specimens, the element did not collapse. In fact the load carrying capacity was found to be almost double. Only the first specimen did exhibit a partial failure of the lower support. In statistical terms from the twelve supports tested only one did fail.

Additionally, PC was found to be a suitable material to act as an intermediary for the compressive loads in the connection. In only one of the specimens did a failure occurred close to the upper edge, meanwhile the quite premature stress at which it happened indicates that a more specific cause may have been present. The gradual progress of the cracking in the three specimens is also relevant in terms of safety. It gives clear visual warning signal of the possible threat giving time to act before complete failure. Concerning the glass breakage pattern, it is clear that it is influenced by the compression applied in the upper edge. It consistently developed from the lower supports and could not reach the opposite upper edge. This unbroken area of glass (see Figure 10.10 (b)) had a significant influence in the overall cohesion of the element, further demonstrating that it is a concept leading to safety.

(a)   (b)
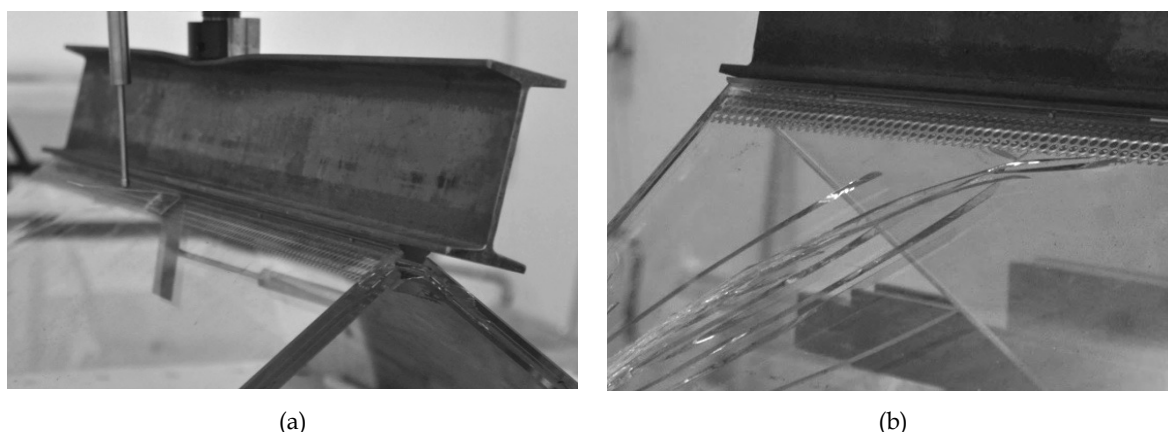
Figure 10.10. Close-up view of the deformed steel profile (a) and unbroken area of glass close to the upper edge due to compression (b).

10.2.4 Conclusions

From the results of the experimental tests to investigate the out-of-plan compressive behaviour of the connection it is possible to conclude that folded glass structures connected with the proposed technique exhibit reliable and safe behaviour. All the specimens showed considerable strength before and after breakage of several glass panes, exhibiting similar maximum load capacities. In fact, the breakage of glass did not affect the increasing of load, which in some cases almost doubled after initial failure.

10.3 Fabrication

In this section the several stages comprising the fabrication of the folded reinforced glass prototype are presented. The lamination of glass elements with protruded perforated steel inserts has been described in chapter 6, meanwhile the development of the connection design towards a folded geometry as well as the scale-up and industrial involvement, originated a beneficial development of the procedure that is next presented. Additionally, the fabrication processes of the other elements that compose the connection are also presented.

10.3.1 Auxiliary profiles

For the lamination of protruded elements auxiliary profiles are needed to fix the position of the protruding element and protect it from moving and being deformed (see Chapter 6.4.2). Laminating steel protruded plates that have been previously folded, as determined by the connection design, required a reconfiguration of the auxiliary profiles.

After testing several solutions, produced with common carpentry, it was concluded that the technology didn't provide the necessary geometric accuracy that was required. This is a determining factor since the position of the metal insert before lamination must be accurately in its final position. Therefore, production methods with higher accuracy were considered. Laser cutting was chosen as the most appropriate (see Figure 10.11 (a)). This high precision and fast production method allowed removal of the necessary auxiliary profiles from a 15 mm MDF standard board, with two similar, yet different, geometries as shown in Figure 10.11 (b) and (c). The first is for the metal facing upwards when placed on the lamination table and the other for opposite position. This profile is also responsible for the fixation of the relative position of the two glass panels due to the staggered placement determined by the design of the connection. At least four profiles were used per laminate, along the protruded metal, in order to assure uniform fixing.

(a)   (b)   (c)
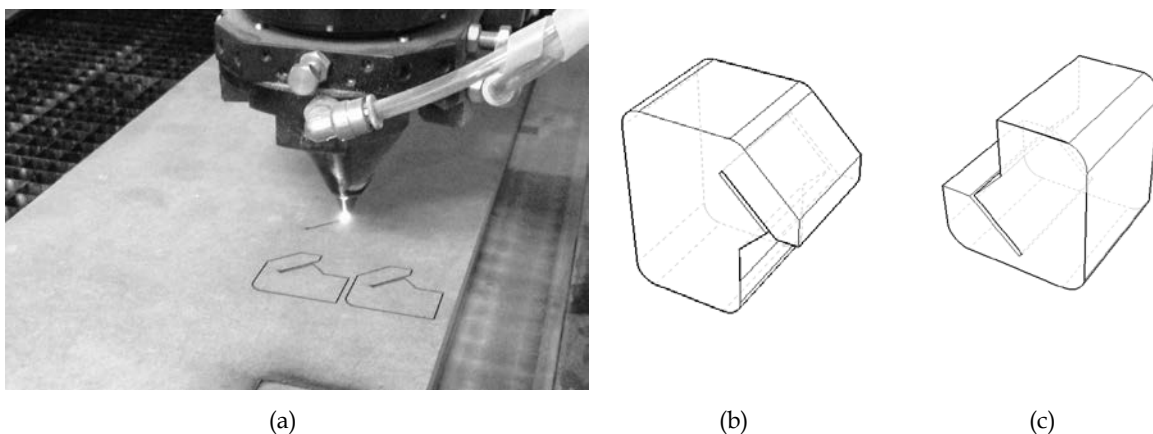
Figure 10.11. Laser cut MDF auxiliary profiles (a) and description of geometrical configuration according to the position of the protruded metal, being upwards (b) and downwards (c).

For the rest of the protruded insert length, unprotected by this profile, it was decided to use timber profiles made using carpentry as shown in (see Figure 10.12 (a)). The production of the previous profiles for the whole length of the laminate was both unnecessary and time consuming. Although less accurate, its role is of mere lower shim for protection, not significantly interfering with the positioning of the metal. Similarly, two geometries have been designed for the two different positions of the protruded element (see Figure 10.12 (b) and (c)).

(a)　　　　　　　　　　　　　(b)　　　　　　　(c)
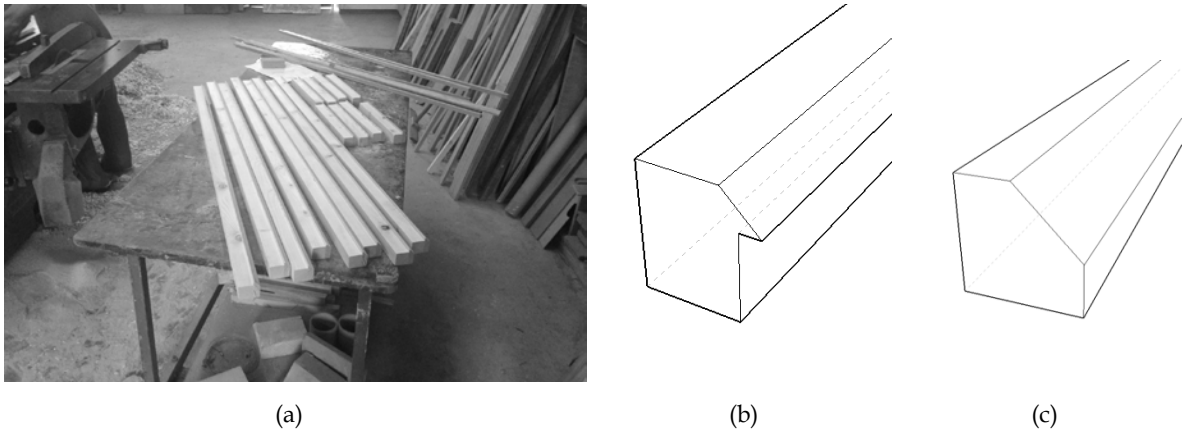
Figure 10.12. Carpentry made timber profile (a) and description of geometrical configuration according to the position of the protruded metal, being upwards (b) and downwards (c)

10.3.2 Acrylic bar

Cast acrylic and polycarbonate is usually supplied in sheet form. For the prototype 15 mm thick sheets were used, measuring 1,5 m long and 1,0 m width. To produce the connection according to the designed geometry, the acrylic sheets were milled using a 3-axis CNC milling machine. Standard 90º and 45º tip tolls were used during the process to efficiently mill the angled geometry of the bar reducing time and improving final surface quality. As a consequence of the material removal, the machined surfaces presented a mat aspect, which to reacquire the desired transparency had to be further processed.

(a)　　　　　　　　　　　　　　　　(b)
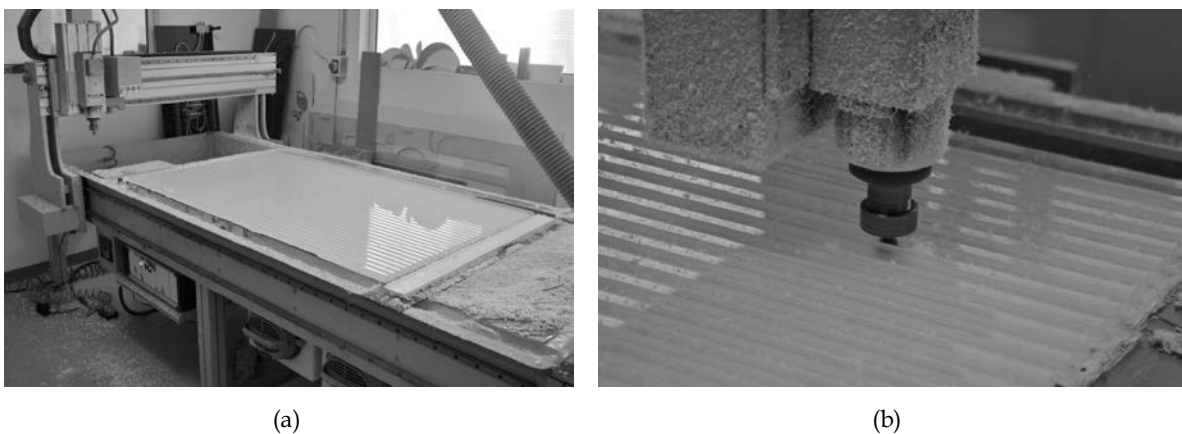
Figure 10.13. CNC milling machine used for the production of the acrylic bars (a) and standard 45º tip tool used during the process (b).

Firstly, the edges and surfaces of each acrylic bar were manually treated. It comprised two steps. Firstly, grinding was performed with a special knife to remove larger irregularities of the acrylic machined edges (see Figure 10.14 (a)). Secondly consisting on the manual sanding with middle size grain sand paper to prepare the surface for the final polishing (Figure 10.14 (b)). Both jobs were done manually done due to the intricate geometry and the necessity for very good transparency quality.

(a)   (b)

Figure 10.14. Manual grinding of the acrylic bar edges (a) and manual sanding of the surface (b).

The polishing process of the surfaces was done with a rotating machine to which a soft fabric material disc was coupled (see Figure 10.15). Before each polishing, special soaps were applied to aid the process. In the final a perfectly transparent surface was acquired. After the polishing work, the bars were drilled using a manual-milling machine to provide space for the M5 steel bolt application.

(a)   (b)

Figure 10.15. Polishing process with rotating disc machine (a) and close-up view of the process (b).

10.3.3 Steel Perforated plate

Three-meter long stainless steel perforated plates were used for the prototype. This non-standard length was necessary in order to cover the whole glass laminate without interruptions. The plates were 1,2 mm thick, 1,2 m wide and exhibited a R2T3,5 perforation pattern. The several plates were first cut to the required size using a digitally controlled shear machine (see Figure 10.16 (a)). Afterwards, the steel plates were bent at 135°, in one or both sides along a 25 mm strip, using a digitally controlled brake machine (see Figure 10.16 (b)). Afterwards, all the steel plates were degreased and cleaned using isopropyl alcohol.

(a)   (b)

Figure 10.16. Cutting of the steel plates with a shear machine (a) and bending with a brake machine (b).

10.3.4 Panels

Once properly finished and cleaned, the several materials were prepared for the layering process. It required mechanical means to position the heavy glass panels in place (see Figure 10.17 (a)). Before the placement of the first glass, two pressure tapes were laid on the table in order to perform the fixing work described below. The positioning task of both glass and folded steel perforated plates was eased by the distributed presence of the auxiliary profiles, which functioned as gauges (see Figure 10.17 (b)).

(a)   (b)
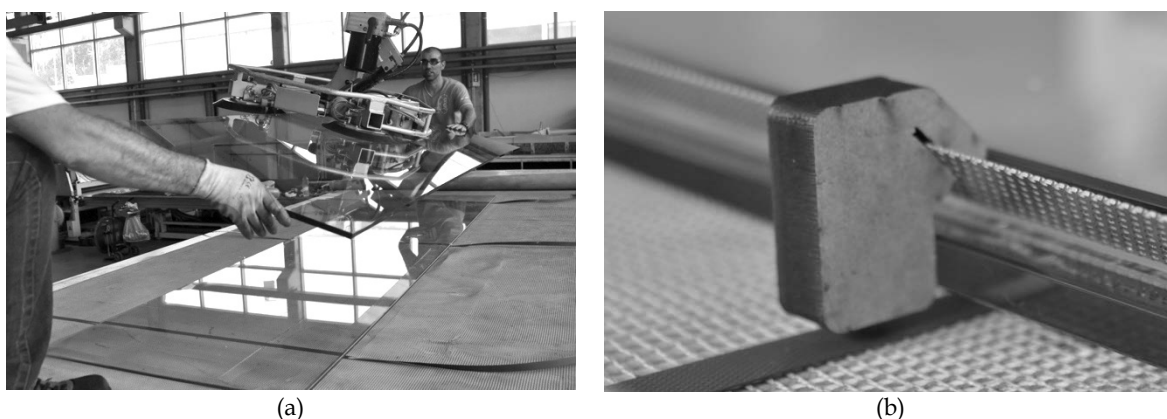
Figure 10.17. Positioning of the glass panels with mechanical means (a) and close-up view auxiliary profile in position functioning as a gauge (b).

When in position, the several layers of material were fixed according to the auxiliary profiles using a fixing pressure tape (see Figure 7.17 (a)). Then the panels were laminated using the silicone blanket lamination system as described in chapter 6.3 (see Figure 10.18 (b)),

(a)   (b)

Figure 10.18. Fixing of the different material using a pressure fixing tape (a) and preparation of silicone blanket lamination tables for the lamination cycle inside the autoclave (b).

After lamination, the panels were inspected, to assure that no residue remained and a good fit between the panels would be achieved (see Figure 10.19 (a)). Afterwards, the several panels were overlaid and prepared for transportation. The same technique used for fixing the panels during lamination, was applied for the packaging, including the auxiliary profiles, essential to protect the protruded steel plate from the pressure of the fixing strips (see Figure 10.19 (b)).
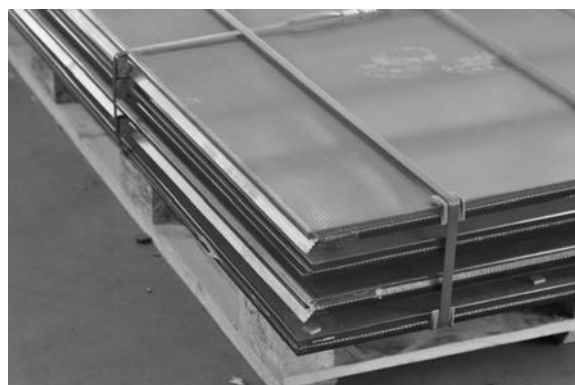
(a)   (b)

Figure 10.19. Inspection of the laminated panels (a) and packing for transportation (b).

10.4 Building the prototype

The site selected for the prototype is located on the east side of the University of Minho Azurém Campus. Flanked by the main entrance hall and the main auditorium, this site was in strategic position to exhibit the prototype during the ICSA 2013. It is a rectangular shaped garden, measuring 20 m x 5 m covered with grass in all its extent. Besides the strategic location, this specific site was chosen for the possibility to cover the auxiliary structure and achieve a more dramatic display of the system.

(a) (b)

Figure 10.20 Two view of the chosen site for erection, looking to the Campus buildings (a) and to the park (b).

Steel profile foundations were emplaced in order to receive the several glass panels in vertical position (see Figure 10.21 (a)). The main structure was placed under the ground, leaving just the clamping elements awaiting the glass panels (see Figure 10.21 (b)).

(a) (b)

Figure 10.21. Steel profile main foundation structure being placed (a) and final arrangement with visible clapping profiles (b).

The assembly work was done with the help of a 30 m arm crane, in order to lift the panels, move them to the correct position and allow a slow and directed descending (see Figure 10.22 (a)). The first wall to be assembled was the *fully reinforced*. It was decided to start with the panels of the middle and continue until the edges, in order to reduce and dissipate any relative positioning error. Meanwhile, this was found to be irrelevant and the second wall was assembled in a row, from one edge to the other (see Figure 10.22 (b)).

(a)   (b)

Figure 10.22. Placement of the panels in position using a crane (a) and assembly work of the second wall (b).

 It became clear during the assembly, a "learning by doing" process was happening. The first panels took several hours to fix in the position, while the last were placed and fixed in less than 20 minutes. The adjustment of the panels 90° position to the clamping profiles was at a certain point difficult, further delaying the process (see Figure 10.23). Meanwhile in real building application the aim is to avoid this type of assembly and simplify it. The resilience and technical expertise of Vicer employees was essential for the success of the prototype assembly. At the end, the soil was restored and covered with grass in all its extent, leaving just the glass panels at view.

(a)   (b)

Figure 10.23. Verification of the angle between the panels (a) and fixing with the clamping profiles (b).
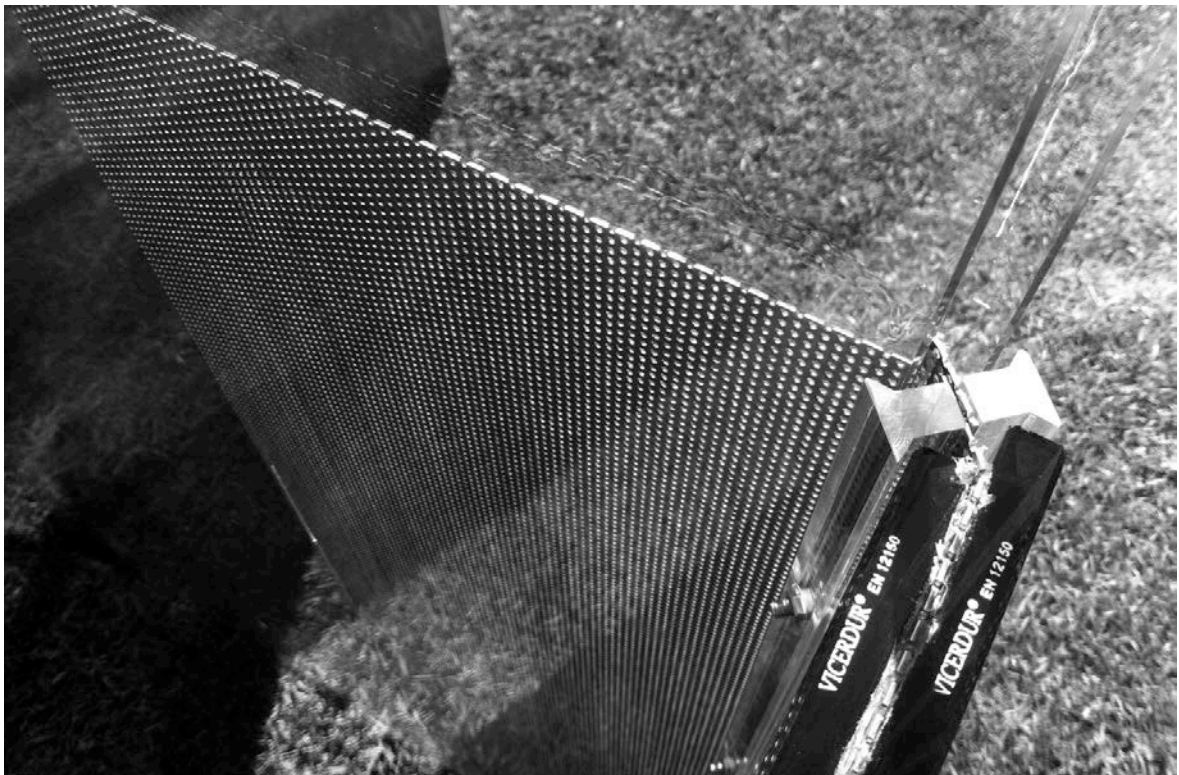
10.5 Photographic reportage

V Conclusions and recommendations

11 Conclusions

11.1 General conclusions

In the last pages that precede this final part of the thesis, the result of the multidisciplinary process that led to the development of the *(de)materializing detail* is photographically reported. A full-scale prototype comprising two parallel folded reinforced glass walls *brought to light*, through an immersive experience, the architectural potential of the solution. The different materials that compose it are characterized by different degrees of transparency and reflectance, which when closely combined give rise to a particular yet constantly mutable materiality.

The contemporary phenomenological discourse on transparency and lightness, discussed at the beginning of the thesis, besides theoretically framing the design philosophy, offers valuable tools to evaluate the pertinence of the built result. Working as a *veiling screen, the folded reinforced glass* demonstrates its capacity to subtly mediate the relationship between the observer and the distanced space. It both displays, through a combination of changing visual resources, the environmental circumstance and the reality behind. Without seeking a definite description of such resources, which would be unattainable in the least, some phenomenon are of interest to reveal the particular aesthetics of this hybrid entity: shadows combined with reflections; overlapping shadows with increased intensity, mutual reflections of glass and steel plates giving rise to lighted areas - further contrasting with neighbouring shadow; simultaneous assertive opaqueness on one side and soft transparency when illuminated from behind - all within a 23 mm thick transparent *structural line*.

The resulting formless quality of the folded reinforced glass walls, significantly depends on the application of the *(de)materializing detail* that is the focus of this investigation. This experimentally validated concept has the capacity to *dematerialize* the connection element at the same time that selectively *materializes* the glass panels within a transparent vocabulary. The final version of the connection's detail results visually faded, not only for being composed entirely by transparent materials, but also for the rigorous simplicity of configuration and disposition between the parts. Two superimposed folded steel perforated plates, anchored in-between two slightly staggered laminated glass panes, are flanked by two symmetrically bevelled PC bars. Distributed small size steel bolts and nuts give the final tightness. The joint where *everything happens* is shy of the glass surface, presenting a width of no more that the thickness of the glass panel. Priority is given to the global (i)materiality, further contributing to the tectonic indefiniteness of the glass structure.

Dissipation of the detail's presence is more pronounced on the partially reinforced panes due to the fact that the boundary of the reinforcement layer does not coincide with the joint. The overlapping reinforcement layers are perceived as one integral entity independent of the joint, further confusing the notion of limit. It demonstrates the ambivalence of the concept since the amount and nature of the reinforcement may be conceived through a multi-criteria decision, combining considerations about structure, technology, energy, aesthetics, spatial relations, etc.

The concept of the reinforced glass connection technique is based on a triangle whose vertices - main constituent materials (glass, steel and PC) - are linked by three load transfer mechanisms, being *adhesive* (glass-steel) *contact* (glass-PC), and *mechanical* (steel-PC). The design of the connection detail was supported by the parallel experimental investigation addressing the structural and technological aspects. Quantitative and qualitative data was integrated within the design process, supporting the main decisions and significantly influencing the result.

11.2 Specific conclusions

Following are the specific conclusions from the experimental investigation on the structural and technological aspects of the folded reinforced glass connection technique:

11.2.1 Structural aspects

- From the results of the experimental tests to investigate the *tensile behaviour of thin steel plates* it is concluded that the difference of perforated and non-perforated steel plates tensile strength is not significant. It is also concluded that the direction of loading in the perforated steel (open pattern or closed pattern directions) doesn't affect significantly the maximum load. A visible difference is however noticeable in the elongation at break, which in the open pattern is considerably higher due to the failure behaviour which is preceded by local plastic deformation.

- From the results of the experimental tests to investigate the *adhesive behaviour of embedded thin steel plates* it is concluded that the adhesive behaviour is highly dependent on the type of interlayer. PVB-laminated specimens failed by metal slip at considerable lower stress levels compared with SG-laminated specimens, which failure was due to glass breakage or metal disruption. This fact has relevant implications on the allowable embedment length. Adhesive connections with reduced embedment length can only be realized using a stiff interlayer like SG. Using just 40 mm of embedment length on SG laminated glass it was possible to avoid debonding and consequent slip of the steel insert. If PVB is to be used, a considerable increase of the adhesion area is required in order to be effective It is also concluded that adhesive connections with perforate steel plates have a higher capacity to perform an even distribution of stress compared with similar with non-perforated steel plates. This capacity to distribute stress is achieved both by the holes of the steel, which significantly increase the contact area, and the interlayer that fills the hollowed section. It enables to configure distributed areas of superior thickness within the interlayer body. In terms of safety of the connection it may have a decisive impact since in case of glass breakage it tends to happen in larger pieces, contrasting with the intense fragmentation observed with non-perforated inserts.

- From the results of the experimental tests to investigate the *temperature effect on the adhesive behaviour* it is conclude that the strength of the adhesive connection changes considerably with temperature. SG-laminated connections at 75 °C showed a critical strength reduction both at 40 mm and 20 mm of embedment. At 40 °C the strength reduction is smaller and more evident at reduced embedment length due to the initial tendency of the interlayer to soften in the borders, causing stress concentrations inside the laminate. When temperatures over 40 °C are expected an increase of embedment depth is advised. Alternatively, another interlayer material with improved temperature behaviour (EVA) may be applied after testing. It is also concluded that the perforated geometry of steel is advantageous at higher temperatures. The stiff interlayer filling the hollowed body creates an anchoring effect that lightly compensates the loss of adhesive strength. Comparing with non-perforated specimens, the maximum strength was almost the double.

- From the results of the experimental tests to investigate the *compressive behaviour of glass in contact with different substrates* it is concluded that PC is the most suitable material to transmit contact loads on the proposed connection technique. Although Al achieved considerably higher compressive stresses when in contact with An, HS and FT glass, the transparency of PC together with overall best results among the remaining substrates, both in terms of deformation capacity and compressive behaviour, makes it a strong choice according to the design philosophy. It is also concluded that the pre-stressing of glass isn't a guarantee of higher failure stress levels in compression (as expected) when compared with annealed glass. The non-homogeneous setup chosen for the tests revealed the unreliable behaviour of pre-stressed glass when loaded in compression, especially fully tempered. Although known to be very strong when loaded in bending, it resulted to be very sensitive when loaded in compression. It consistently failed at inferior stress levels compared to annealed glass. However, the data collected in this experimental investigation was not sufficient enough to have a comprehensive understanding of the phenomenon. Further investigation on this topic is advised. Additionally, it is concluded that heat strengthened glass is the best type of glass to use in the proposed connection technique. In addition to the highest compressive strength exhibited in contact with all the substrates, it confirmed the capacity to reserve some cohesion after breakage (contrary to FT glass) and is considered to be immune to stress corrosion (contrary to An glass).

- From the results of the experimental tests to investigate the *bending behaviour of the connection* it is concluded that the concept of *connecting through the reinforcement* is valid when combined with a suitably machined polycarbonate layer in-between. When sufficient bending stiffness was acquired, it was possible to activate the compressive stresses at the upper zone, forcing the tensile strength on the mechanically connected steel perforated plates to be reached. Compared with the simple solution (without contact load

transfer layer) the bending strength increased almost four times, exhibiting ductile failure behaviour, determined by the maximum tensile strength of the steel perforated plate.

- From the results of the experimental tests to investigate the *temperature effect on the bending behaviour of the connection* it is concluded that increasing temperature has significant influence on the bending behaviour. Contrary to what was observed at 23 °C, where ductile failure mode was accomplished through the failure of the perforated steel plate, at 45 °C and 70 °C a consistent glass breakage occurred in a localized area. This stress concentration showed tendency to increase with temperature rising. At 70 °C the connection resistance reduces to half caused by the early glass breakage, occurring at relatively low loads of 4/5 kN, and debonding of the adhesive, which demonstrated to be visibly accelerated after glass breakage. When temperatures over 45 °C are expected an increase of embedment depth is advised to surpass the glass overstress. Only then is it possible to achieve the full potential of the connection, where the maximum load capacity is determined by the steel tensile strength thus offering a desired ductile failure behaviour.

- From the results of the experimental tests to investigate the *time of loading effect on the bending behaviour* it is concluded that long duration loading has considerable impact on the structure deformation. From the experimental investigation the polycarbonate showed more tendency for creep deformation. It is also concluded that this type of connection is suitable for elements in which no permanent loads need to be carried, such as façade or roof elements in which snow is not expected. However, the amount of data collected is not sufficient for a thorough understanding of the effect of time on the bending behaviour, requiring further study.

- Finally from the results of the experimental tests to investigate the out-of-plan compressive behaviour of the connection it is possible to conclude that folded glass structures connected with the proposed technique exhibit reliable and safe behaviour. All the specimens showed considerable strength before and after breakage of several glass panes, exhibiting similar maximum load capacities. Additionally, the breakage of glass didn't affect the increasing of load, which in some cases almost doubled after initial failure.

11.2.2 Technological aspects

- From the experimental investigation on the lamination of glass with protruded steel embedded elements it is conclude that it is possible to fabricate good quality laminated glass with protruded steel embedded elements. This requires following the basic good practices for lamination, calibrating the temperature and pressure (vacuum and atmospheric pressure) parameters to the specific constitution and size of the laminate, and level the support conditions in combination with laminate structure, in order to fix the position of the protruded steel before and after autoclave cycle, counteracting the

deformation of the inner supporting conditions caused by the melting of the interlayer, necessary to adhere and fill the hollowed gaps of the perforated steel.

- From the experimental investigation on the lamination of glass with protruded steel embedded elements with folded geometry it is concluded that custom designed auxiliary profiles must be applied to fix the relative position between the protruded metal and the staggered glass panels. These profiles must be produced with high accuracy cutting methods (laser cutting) and fixed against the glass using a tensioning belt.

12 Recommendations

12.1 Introduction

The investigation on the reinforced glass connection technique inevitably addressed a limited number of parameters considered overriding for serving the integrated approach from concept to realization. Furthermore, during this process several new questions arose that are considered relevant. Following are a selection of recommendations for further study:

12.2 Reinforcement materials

A thin steel perforated plate of 1 mm thick with a RT perforation pattern was selected as the reinforcement material to be used during the whole investigation. In addition to the significant tensile strength mandatory to efficiently perform the reinforcement role, it exhibits some bending and shear resistance considered beneficial for the experimental investigation and design development. However, there are other thin reinforcement materials, such as steel wire meshes or fabrics of high strength fibres, which may be efficiently applied to the connection technique. These materials exhibit interesting transparency and reflectance phenomenon that could add value to the system. The main expected challenge is the preparation of these materials to perform the mechanical joint without compromising transparency. Additionally, non-standard perforation patterns may be investigated on thin steel plates using CNC milling technologies. Applied as protruded reinforcement, it may influence the adhesive behaviour as well as increasing the design possibilities concerning the customized perforation patterns.

12.3 Form

The simple 90°-folded geometry was selected as the basis for development of a type of reinforced glass connection technique. The study concerning the application of other geometries is of particular interest. The connection technique demonstrated considerable flexibility to adapt other geometries without compromising the main design premises. The detail variations to be applied in domes, vaults, suspended vaults or intersected panels have just been briefly referred. Additionally, within the folded geometry, other folding angles may be studied as well as considerably more complex geometric arrangement combining different types of folds. A parametrical design study is of particular interest to investigate the morphological possibilities within the system limitations, both constructional and structural. The morphological increased complexity has also technological and industrial implications that require further study.

12.4 Adhesive behaviour and interlayers material

Concerning the structural behaviour of the connection, namely the adhesive strength, it was concluded that reduced embedment depth connections of 40 mm must be applied with SG interlayer. To efficiently use PVB a considerably superior embedment depth must be provided. This value is still insufficiently investigated. Increasing the reinforcement area within a glass panel has been applied in the prototype delivering a valid result. The fact that PVB is considerably cheaper when compared with SG, makes it relevant to investigate in which cases SG could be replaced by PVB. Additionally, during high temperature tests a reduction of adhesive strength of SG was observed, advising an increase of embedment depth with temperatures over 40 ºC. An alternative interlayer material such as EVA with improved temperature behaviour may deliver good adhesion strength at this temperature range.

12.5 Compressive behaviour and pre-stress of glass

During the compression tests of glass in contact with different substrates it was observed that both fully tempered glass and heat-strengthened glass failed at very low stress compared with known values of fail stress from bending tests. It led to the assumption that there must have been a correlation between the release of the toughening energy and the actual compressive stress induced during the test. The internal stress equilibrium of both HS and FT glass, when loaded in compression, is significantly affected by the uneven loading. Nevertheless the testing sample was considered reduced to give consistent data. Further investigation on this topic must be performed to have a better understanding of the phenomenon.

12.6 Effect of time of loading

The effect of time of loading on the structural behaviour of the reinforced glass connection was just briefly addressed. It was though possible to observe that when loaded in bending the PC bar showed more tendency for creep deformation. It caused an overstress that led to glass breakage. This fact creates a limitation on the usage of this connection in permanently loaded structures. A more extended study of the effect time of loading on the adhesive and bending behaviour is advised to clarify the phenomenon and develop a possible strategy to overcome it.

12.7 Effect of humidity

The effect of humidity on the adhesive behaviour of the reinforced glass connection was not addressed on this investigation. The detail was developed with a humidity blocking measure, applying a silicone edge seal on the border of the protruded metal. However, in real applications the seal may present deficiencies that may lead to humidity contaminations. The consequences of this fact on the adhesive behaviour may be further investigated.

12.8 Analytical and numerical modelling

The experimental research gave rise to a considerable body of data that may be used to develop and calibrate accurate numerical models that may allow parametrical studies and the consequent development of analytical models and simplified design rules.

Bibliography

Bibliography

Achleitner, Friedrich. 1999. "The Conditioning of Perception or The Kunsthaus Bregenz as an Architecture of Art." In *Peter Zumthor Kunsthaus Bregenz*, Hatje Cantz Publishers, 50–55.

Andreau, Paul. 2011. "Musée de La Mer , Sea Sphere Osaka - Japon." http://www.paul-andreu.com/pages/pages fiches/67-Sea Sphere d'Osaka.html (September 2, 2011).

Asahi Glass. 2011. *Lamimetal - Laminated Glass with Punched Metal*. Asahi Glass Ltd Co.

Bagger, A. 2010. "Plate Sheel Structures of Glass - Studies Leading to Guidelines for Structural Glass." Technical University of Denmark.

Bagger, A., J. Jonsson, and H. Almegaard. 2008. "Bending Stresses in Facetted Glass Shells." In *Challenging Glass*, eds. F. Bos, C. Louter, and F. Veer. Delft: IOS Press, 313–22.

Bagger, A., J. Jonsson, H. Almegaard, and T. Wester. 2007. "Facetted Shell Structure of Glass." In *Glass Performance Days*, Tampere, 111–14.

Banham, R. 1996. "Modern Monuments." In *A Critic Writes: Essays by Reyner Banham*, A centennial book, Berkeley: University of California Press, 261–64.

Baudrillard, Jean, and Jean Nouvel. 2005. *The Singular Objects of Architecture*. Minneapolis: University of Minnesota Press.

Belis, Jan, Dieter Callewaert, Didier Delincé, and Rudy Impe van. 2009. "Experimental Failure Investigation of a Hybrid Glass/steel Beam." *Engineering Failure Analysis* 16(4): 1163–73.

Bennison, S.J., C.A. Smith, A. Van Duser, and Anand Jagota. 2001. "Structural Performance of Laminated Safety Glass Made with 'Stiff' Interlayers." In *Glass Processing Days*, Tampere, 283–87.

Blau, Eve. 2007. "Transparency and the Irreconcilable Contradictions of Modernity." *PRAXIS* (9): 50–59.

———. 2009. "Tensions in Transparency. Between Information and Experience: The Dialectical Logic of SANAA's Architecture." *Harvard Design Magazine* (29): 29–37.

Bucak, Ö, and M Meissner. 2005. *Trag- Und Resttragfähigkeitsuntersuchungen an Verbundglas Mit Den Zwisschenlage SentryGlas Plus –Abschlussbericht*. München.

Carvalho, Paulo L. L., Paulo J. S. Cruz, and Fred A. Veer. 2011. "Perforated Steel Plate to Laminated Glass Adhesive Propreties." In *Glass Performance Days*, Tampere, 281–85.

Cruz, Paulo J. S., and José Pequeno. 2008. "Timber-Glass Composite Structural Panels: Experimental Studies & Architectural Applications." In *Challenging Glass*, eds. Freek Bos, Christian Louter, and Fred A. Veer. Delft: IOS Press, 449–58.

———. 2009. "Timber-Glass Composite Structural Panels: Tectonics, Sustainability & Integrated Energetic System Solutions." In *Glass Performance Days*, Tampere, 123–26.

Dallard, Pat, Mark Facer, Shigeru Hikone, Ryoichi Hirose, Arata Oguri, and Jin Sasaki. 2001. "Osaka Maritime Museum." *The Arup Journal* (01): 21–27. http://www.arup.com/_assets/_download/download39.pdf.

Davidson, Cynthia. 1994. "Reflections on Transparency: An Interview with Terence Riley." In *Light Construction Reader*, ed. Todd Gannon. New: The Monacelli Press, 47–50.

Dupont. 2009. "DuPontTM SentryGlas® Architectural Safety Glass Interlayer." http://www2.dupont.com/SafetyGlass/en_US/assets/pdfs/sentryglas_brochure.pdf.

Ehrenstein, G. 2001. *Polymeric Materials: Structure-Properties-Applications*. ed. Hanser. Munich.

El-Magd, E., A. Kranz, and R. Risch. 2001. "Geometrisch Bedingtes Anisotropieverhalten von Lochblechen." *Materialwissenschaft und Werkstofftechnik* 32(11): 821–26.

Feirabend, S. 2008. "Reinforced Laminated Glass." In *Challenging Glass*, eds. Freek Bos, Christian Louter, and Fred A. Veer. Delft: IOS Press, 469–78.

———. 2010. "Steigerung Der Resttragfähigkeit von Verbundsicherheitsglas Mittels Bewehrung in Der Zwischenschicht." Universität Stuttgart, Germany.

Feirabend, S., and W. Sobek. 2009. "Improved Post-Breakage Behavior of Laminated Glass due to Embedded Reinforcement." In *Glass Performance Days*, Tampere, 726–29.

Fierro, Annette. 2003. *The Glass State: The Technology of the Spectacle, Paris 1981-1998*. MIT Press.

Foster, N. 2013. "Willis Faber & Dumas Headquarters." http://www.fosterandpartners.com/projects/willis-faber-dumas-headquarters/.

Frampton, K. 2007. *Modern Architecture: A Critical History (World of Art)*. 4th ed. London: Thames & Hudson, Limited.

Frampton, Kenneth. 1969. "Maison de Verre." *Perspecta: The Yale Architectural Journal* (12): 77–126.

———. 1986. "Pierre Charreau: An Eclectic Architect." In *Light Construction Reader*, ed. Todd Gannon. New York: The Monacelli Press, 375–86.

———. 1995. *Studies in Tectonic Culture: The Poetics of Construction in Nineteenth and Twentieth Century Architecture*. ed. John Cava. Cambridge, Massachussets: The MIT Press.

Futagawa, Yukio, Bernard Bauchet, and Marc Vellay. 1988. *La Maison de Verre*. Tokyo: A.D.A. Edita.

Gannon, Todd, ed. 2002. *The Light Construction Reader*. New York: The Monacelli Press.

Georgiadis, Sokratis. 1995. "Introduction." In *Building in France, Building in Iron, Building in Ferroconcrete*, Santa Monica: Getty Center for the History of Art and the Humanities, 1–53.

Giedion, Sigfried. 1967. *Space, Time and Architecture: The Growth of a New Tradition*. Fifth edit. Cambridge, Massachussets: Harvard University Press.

———. 1995. *Building in France, Building in Iron, Building in Ferroconcrete*. Santa Monica: Getty Center for the History of Art and the Humanities.

Graham, Dan. 1999. *Two-Way Mirror Power: Selected Writings by Dan Graham on His Art*. ed. Alexander Alberro. Cambridge, Massachussets: The MIT Press.

GRANTA. 2012. "CES Edupack Selector."

Haldimann, Mathias, Andreas Luible, and Mauro Overend. 2008. *Structural Use of Glass*. Zurich: IABSE.

Hinckley, J, and J Robinson. 2005. *The Big Book of Car Culture: The Armchair Guide to Automotive Americana*. Minnesota: Motorbooks.

Hitchcock, H R, and P Johnson. 1997. *The International Style*. New York: W.W. Norton.

IPA. 1993. "Designers, Specifiers and Buyers Handbook for Perforated Metals." Designers, Specifiers and Buyers Handbook for perforated metals.

Ito, Toyo. 2006. *Arquitectura de Límites Difusos*. Barcelona: Gustavo Gili.

Jencks, C. 1977. *The Language of Post-Modern Architecture*. First. New York: Rizzoli.

Johnson, P, and M Wigley. 1988. *Deconstructivist Architecture*. New York: Museum of Modern Art.

Kepes, Gyorgy. 1969. *El Lenguage de La Vision*. Buenos Aires: Editiones Infinito.

Koolhass, Rem. 1998. *S,M.L.XL*. Second edi. ed. Jennifer Sigler. New York: The Monacelli Press.

Kott, A., and T. Vogel. 2005. "Remaining Structural Capacity of Broken Laminated Safety Glass." In *Glass Processing Days*, Tampere, 403–7.

Krauss, Rosalind. 1994. "The Grid, /The Cloud/, and The Detail." In *The Presence of Mies*, ed. Detlef Mertins. New York: Princeton Architectural Press, 133–48.

Louter, C. 2011. "Fragile yet Ductile - Structural Aspects of Reinforced Glass Beams." Delft University of Technology, TUDelft.

Mertins, Detlef, ed. 1994. *The Presence of Mies*. New York: Princeton Architectural Press.

Milheiro, Ana Vaz. 2007. A minha casa é um avião. Coleção arquitectura *A Minha Casa É Um Avião*. 1ª ed. Lisboa: Relógio D'Água Editores.

Moholy-Nagy, Laszlo. 1933. "How Photography Revolutionizes Vision." In *The Listener*, London, 688–90.

Moholy-Nagy, László. 1956. *Vision in Motion*. 5th ed. Chicago: Paul Theobald and Company.

Molderings, Herbert. 2009. "'Revaluating the Way We See Things'. The Photographs, Photograms and Photoplastics of Lászlo Moholy-Nagy." In *László Moholy-Nagy Retrospective*, eds. Ingrid Pfeiffer and Max Hollein. London: Prestel, 36–43.

Moneo, Rafael. 2001. "Introduction." In *Fear of Glass: Mies Van Der Rohe's German Pavillion in Barcelona*,.

Moravánszky, Ákos. 2010. "Mies-En-Scène." In *SANAA: Kazuyo Sejima, Ryue Nishizawa; Intervention in the Mies Van Der Rohe Pavillon*, ed. Xavier Costa. Barcelona: Fundacio Mies van der Rohe / Actar, 30–37.

Moreno, Cristina Días, and Efrén García Grinda. 2004. "Fragments of a Conversation with Kazuyo Sejima and Ryue Nishizawa: Liquid Playgrounds." *El Croquis 121/122*.

Nelson, Paul. 1933. "La Maison de La Rue Saint-Guillaume." *L'Architecture d'aujourd'hui*: 9–11.

Neugebauer, Jürgen. 2005. "A Special Fixation With Which The Broken Laminated Safety Glass Is Prevent From Falling." In *Glass Processing Days*, Tampere, 8–12.

———. 2013. "Stainless Steel Fabric as a Connection System for Bomb Blast Glass." In *COST Action TU0905, Mid-Term Conference on Structural Glass*, eds. J. Belis, C. Louter, and D. Mocibob. London: Taylor and Francis, 493–98.

Nordeson, Guy. 2009. "Infrathin." In *Engineered Transparency - The Technical, Visual and Spatial Effects of Glass*, eds. Michael Bell and Jeannie Kim. New York: Princeton Architectural Press, 72–77.

O'Callaghan, James. 2005. "A Case Study of the Apple Computer Stores - Glass Structures 2001 - 2005." In *Glass Processing Days*, Tampere, 406–9.

———. 2007. "An All Glass Cube in NY City." In *Glass Performance Days*, Tampere, 98–101.

O'Callaghan, James, and Charles Bostick. 2012. "The Apple Glass Cube: Version 2.0." In *Challenging Glass 3*, eds. Freek Bos, Christian Louter, Rob Nijsse, and Fred Veer. Delft: IOS Press, 57–65.

Picon, Antoine. 2009. "Glass at the Limits." In *Engineered Transparency - The Technical, Visual and Spatial Effects of Glass*, eds. Michael Bell and Jeannie Kim. New York: Princeton Architectural Press, 69–71.

Pimlott, M. 1997. "Dan Graham and Architecture." In *Dan Graham: Architecture*, eds. Dan Graham, Adachiara Zevi, Brian Hatton, and Mark Pimlott. London: Architectural Association Publications, 48–53.

Puller, K. 2012. "Untersuchung Des Tragverhaltens von in Die Zwischenschicht von Verbundglas Integrierten Lasteinleitungselementen." Universität Stuttgart.

Puller, K., and W. Sobek. 2012. "Load-Carrying Behaviour of Metal Inserts Embedded in Laminated Glass." In *Challenging Glass 3*, eds. F. Bos, C. Louter, R. Nijsse, and F. Veer. Delft: IOS Press, 307–14.

Puller, Krestin, Jurgen Denonville, and Werner Sobek. 2011. "An Innovative Glass Connection Technique Using an Ionomer Interlayer." In *Glass Performance Days*, Tampere, 638–41.

Quetglas, J. 2001. *Fear of Glass: Mies Van Der Rohe's German Pavillion in Barcelona*. Birkhäuser-Publishers for Architecture.

Rice, Peter, and Hugh Dutton. 1995. *Structural Glass*. Second. London: E & FN Spon.

Riley, Terence. 1995. *Light Construction*. New York: The Museum of Modern Art.

Rowe, Colin, and Robert Slutzky. 1963. "Transparency: Literal and Phenomenal" eds. Todd Gannon and Jeffrey Kipnis. *Perspecta* 8: 44–54.

Van Russelt, M. 1997. "How to Make a Good Laminated Safety Glass for Windscreens." In *Glass Performance Days*, Tampere, 475–79.

Scheerbart, Paul. 2000. *Glasarchitektur*. Berlin: Gebr. Mann Verlag.

Schittich, C, and D Balkow. 1999. *Glass Construction Manual*. Munich: Birkhauser.

Segura, Alfonso Diaz. 2003. "The Maison de Verre. The Sensuality of Veiled Things." *Via Arquitectura* 12: 14–23.

Sejima, K, and R Nishizawa. 2010. *SANAA: Kazuyo Sejima, Ryue Nishizawa ; [intervention in the Mies Van Der Rohe Pavillon]*. ed. Xavier Costa. Barcelona: Fundacio Mies van der Rohe / Actar.

Solà-Morales, Ignasi. 2003. "Arquitectura Inmaterial." In *Territórios*, Barcelona: Gustavo Gili, 138–49.

Speranzini, Emanuela, and Paolo Neri. 2007. "On the Bending of GFRP Reinforced Glass Elements." In *Asia-Pacific Conference on FRP in Structures*, ed. S. T. Smith. Hong-Kong, 311–16.

Starobinsky, Jean. 1989. "Poppea's Veil." In *Light Construction Reader*, ed. Todd Gannon. New York: The Monacelli Press.

Stelzer, I. 2010. "High Performance Laminated Glass." In *Challenging Glass 2*, eds. Freek Bos, Christian Louter, and Fred A. Veer. Delft: IOS Press, 467–74.

Stelzer, Ingo, Stephen J. Bennison, and M. Hx Qin. 2008. "High- Performance Laminated Glass for Structurally Efficient Glazing." In *International Symposium on the Application of Architectural Glass (ISAAG)*, Munich, 65–77.

Tschumi, Bernard. 1995. "Light Construction Symposium." In *Light Construction Reader*, ed. Todd Gannon. New York: The Monacelli Press, 53–69.

———. 2012. *Architecture Concepts - Red Is Not a Color*. New York: Rizzoli.

———. 2013. "Glass Video Gallery, Groningen 1990." http://www.tschumi.com/projects/17/#.

Veer, Fred. 2005. "10 Years of ZAPPI Research." In *Glass Processing Days*, Tampere, 424–28.

Veer, Fred A., H. Rijgersberg, D. Ruytenbeek, C. Louter, and J. Zuidema. 2003. "Composite Glass Beams, the Third Chapter." In *Glass Processing Days*, Tampere, 307–10.

Vidler, Anthony. 1992. "Transparency." In *The Architectural Uncanny: Essays in the Modern Unhomely*, The MIT Press, 217–26.

Weller, Bernhard, and Michael Kothe. 2011. "Ageing Behaviour of Polimeric Interlayer Materials and Laminates." In *Glass Performance Days*, Tampere, 240–43.

Wellershoff, F. 2011. "Blast Enhanced Cable Facades." In *Glass Performance Days*, Tampere, 617–21.

Wellershoff, F., G. Lori, M. Zobec, and K. Osterland. 2013. "Structural Design of Blast Enhanced Cable Net Facades." In *COST Action TU0905, Mid-Term Conference on*

Structural Glass, eds. J. Belis, C. Louter, and D. Mocibob. London: Taylor and Francis, 121–31.

Wigginton, Michael. 1996. *Glass in Architecture*. Phaidon Press.

Willareth, Philippe, and Daniel Meyer. 2011. "A New Folding Glass Roof for the Historic City Swimming Hall Zurich." In *Glass Performance Days*, Tampere, 622–24.

Wurm, Jan. 2007. *Glass Structures - Design and Construction of Self-Suporting Skins*. Basel: Birkhauser.

Figure sources

Figure sources

Chapter 2

2.1 (a)   http://www.essential-architecture.com/LO/LO-009.htm

2.1 (b)   http://rosswolfe.files.wordpress.com/2013/05/paxton-1851.jpg?w=904

2.2 (a)   Giedion, Sigfried. 1995. *Building in France, Building in Iron, Building in Ferroconcrete*. Santa Monica: Getty Center for the History of Art and the Humanities.

2.2 (b)   Giedion, Sigfried. 1995. *Building in France, Building in Iron, Building in Ferroconcrete*. Santa Monica: Getty Center for the History of Art and the Humanities.

2.3 (a)   Giedion, Sigfried. 1967. *Space, Time and Architecture: The Growth of a New Tradition*. Fifth edit. Cambridge, Massachussets: Harvard University Press.

2.3 (b)   Giedion, Sigfried. 1967. *Space, Time and Architecture: The Growth of a New Tradition*. Fifth edit. Cambridge, Massachussets: Harvard University Press.

2.4 (a)   El Croquis 121/122 "Sanaa (Kazuyo Sejima + Ruyo Nishizawa)", p.155.

2.4 (b)   Riley, Terence. 1995. *Light Construction*. New York, The Museum of Modern Art. p. 45.

2.5 (a)   http://www.oma.eu/projects/1989/très-grande-bibliothèque

2.5 (b)   http://www.oma.eu/projects/1989/très-grande-bibliothèque

2.6   http://images.artnet.com/artwork_images_970_359941_jordi-bernado.jpg

2.7 (a)   http://blog.styleboston.tv/wpcontent/uploads/2011/07/DanGraham_GreekCross.jpg

2.7 (b)   http://www.plugin.org/exhibitions/2013/dan-graham-performance-cafe-perforated-sides

2.8   http://www.docomomo.fr/batiment/maison-verre-paris

2.9 (a)   Maison du Verre - François Halard - Thames & Hudson 2007, p19.

2.9 (b)   Photogram from "La Maison de Verre - A film by Robert Vickery 1970/97, courtesy of AA Photo Library Collection", https://vimeo.com/60453259

2.9 (c)   Photogram from "La Maison de Verre - A film by Robert Vickery 1970/97, courtesy of AA Photo Library Collection", https://vimeo.com/60453259

2.10   Mertins, Detlef, ed. 1994. *The Presence of Mies*. New York: Princeton
            Architectural Press, p. 5, 7, 9, 11, 13.

2.11 (a)   http://www.moma.org/collection/object.php?object_id=787

2.11 (b)   http://25.media.tumblr.com/tumblr_lq2w6azX6F1qgpvyjo1_1280.jpg

2.11 (c)   http://www.moma.org/collection_images/resized/648/w500h420/CRI_5648
            .jpg

2.11 (d)   http://www.moma.org/collection/object.php?object_id=660

2.12   http://www.pinterest.com/pin/232005818276823782/

2.13 (a)   Quetglas, J. 2001. *Fear of Glass: Mies Van Der Rohe's German Pavillion in
            Barcelona*. Birkhäuser-Publishers for Architecture, p. 130.

2.13 (b)   Quetglas, J. 2001. *Fear of Glass: Mies Van Der Rohe's German Pavillion in
            Barcelona*. Birkhäuser-Publishers for Architecture, p. 131.

2.13 (c)   Quetglas, J. 2001. *Fear of Glass: Mies Van Der Rohe's German Pavillion in
            Barcelona*. Birkhäuser-Publishers for Architecture, p.85.

2.14   Quetglas, J. 2001. *Fear of Glass: Mies Van Der Rohe's German Pavillion in
            Barcelona*. Birkhäuser-Publishers for Architecture, p. 57.

2.15 (a)   Molderings, Herbert. 2009. "'Revaluating the Way We See Things'. The
            Photographs, Photograms and Photoplastics of Lászlo Moholy-Nagy." In
            László Moholy-Nagy Retrospective, eds. Ingrid Pfeiffer and Max Hollein.
            London: Prestel, p. 50.

2.15 (b)   Giedion, Sigfried. 1995. *Building in France, Building in Iron, Building in
            Ferroconcrete*. Santa Monica: Getty Center for the History of Art and the
            Humanities, p. 144.

2.15 (c)   Giedion, Sigfried. 1995. *Building in France, Building in Iron, Building in
            Ferroconcrete*. Santa Monica: Getty Center for the History of Art and the
            Humanities, p. 144.

2.16 (a)   http://www.all-art.org/art_20th_century/moholy-nagy3.html

2.16 (b)   http://mondo-blogo.blogspot.pt/2011/11/get-into-laszlo-moholy-nagy.html

2.16 (c)   Moholy-Nagy, László. 1956. *Vision in Motion*. 5th ed. Chicago: Paul Theobald
            and Company, p. 193

2.16 (d)   Molderings, Herbert. 2009. "'Revaluating the Way We See Things'. The
            Photographs, Photograms and Photoplastics of Lászlo Moholy-Nagy." In
            László Moholy-Nagy Retrospective, eds. Ingrid Pfeiffer and Max Hollein. London:

Prestel, p. 75.

2.17 (a)   Moholy-Nagy, László. 1956. *Vision in Motion*. 5th ed. Chicago: Paul Theobald and Company, p. 239.

2.18 (a)   https://www.flickr.com/photos/evandagan/3228388769

2.18 (b)   https://www.flickr.com/photos/evandagan/3228389475

2.19 (a)   Sejima, K, and R Nishizawa. 2010. *SANAA: Kazuyo Sejima, Ryue Nishizawa ; [intervention in the Mies Van Der Rohe Pavillon]*. ed. Xavier Costa. Barcelona: Fundacio Mies van der Rohe / Actar, p. 17.

2.19 (b)   Sejima, K, and R Nishizawa. 2010. *SANAA: Kazuyo Sejima, Ryue Nishizawa ; [intervention in the Mies Van Der Rohe Pavillon]*. ed. Xavier Costa. Barcelona: Fundacio Mies van der Rohe / Actar, p. 44.

Chapter 3

3.1 (a)   Franz Wimmer, http://www.art-magazin.de/cityguide/muenchen/36301/sammlung_goetz_szenetipp_muenchen

3.1 (b)   Sasha Cisar, http://www.bustler.net/index.php/article/swiss_peter_zumthor_awarded_with_2009_pritzker_prize

3.2 (a)   http://architecture.mapolismagazin.com/ateliers-jean-nouvel-fondation-cartier-museum-contemporary-art-paris

3.2 (b)   Kei Koyama, http://www.domusweb.it/en/architecture/2011/10/25/jane-s-carousel.html

3.3   Tomio Ohashi, http://www.pritzkerprize.com/sites/default/files/2013-w-03.jpg

3.4 (a)   Nordeson, Guy. 2009. "Infrathin." In *Engineered Transparency - The Technical, Visual and Spatial Effects of Glass*, eds. Michael Bell and Jeannie Kim. New York: Princeton Architectural Press, 72–77.

3.4 (b)   http://www.nordenson.com/project.php?id=7&img=2&l=name&sup=

3.5 (a)   http://www.tschumi.com/media/files/01918.jpg

3.5 (b)   http://www.tschumi.com/media/files/01915.jpg

3.6 (a)   http://kkmm.de/content/99-projekte/1-paradiese/3-diashow/02b.Bicton-Gardens-Interior.jpg

3.6 (b)   http://www.anexetermum.com/wp-

content/uploads/2012/09/roseglasswindow.jpg

3.7 (a)   Fierro, Annette. 2003. *The Glass State: The Technology of the Spectacle, Paris 1981-1998*. MIT Press, p. 113.

3.7 (b)   Fierro, Annette. 2003. *The Glass State: The Technology of the Spectacle, Paris 1981-1998*. MIT Press, p. 120.

3.8 (a)   Peter Zumthor Kunsthaus Bregenz, Hatje Cantz, p. 36.

3.8 (b)   Peter Zumthor Kunsthaus Bregenz, Hatje Cantz, p. 33.

3.8 (c)   Peter Zumthor Kunsthaus Bregenz, Hatje Cantz, p. 32.

3.9   http://www.jmhdezhdez.com/2012/01/sendai-mediatheque-toyo-ito-mediateca.html

3.10 (a)   http://www.fosterandpartners.com/data/projects/0102/construction/img8.jpg

3.10 (b)   http://www.fosterandpartners.com/data/projects/0102/drawings/img11.jpg

3.11 (a)   Rice, Peter, and Dutton, Hugh. 1995. *Structural Glass*. Second. London: E & FN Spon, p. 60.

3.11 (b)   Rice, Peter, and Dutton, Hugh. 1995. *Structural Glass*. Second. London: E & FN Spon, p. 33.

3.12 (a)   O'Callaghan, James. 2007. "An All Glass Cube in NY City." In *Glass Performance Days*, Tampere, p. 99.

3.12 (b)   Jobs, et al., United States Design Patent, USD478,999 S, August 26, 2003, p. 11.

3.12 (c)   Jobs, et al., United States Design Patent, USD478,999 S, August 26, 2003, p. 11.

3.13 (a)   O'Callaghan, James, and Charles Bostick. 2012. "The Apple Glass Cube: Version 2.0." In *Challenging Glass 3*, eds. Freek Bos, Christian Louter, Rob Nijsse, and Fred Veer. Delft: IOS Press, 60.

3.13 (b)   Glass Performance Days 2013, p. 370.

3.14 (a)   http://www.paul-andreu.com/pages/pages%20fiches/67-Sea%20Sphere%20d'Osaka.html

3.14 (b)   http://www.glass-ranger.com/img/g_15b.jpg

3.14 (c)   Asahi Glass. 2011. *Lamimetal - Laminated Glass with Punched Metal*. Asahi Glass Ltd Co.

3.15 (a)   http://materialsandsources.com/okatech-insulating-glass-with-metal-interlayer-from-okalux/

3.16 (a)   http://www.stylepark.com/en/architecture/between-sunscreen-and-transparency-everything-for-books/308350

3.16 (b)   Thomas Hawk, http://www.stylepark.com/en/architecture/between-sunscreen-and-transparency-everything-for-books/308350

3.17 (a)   http://www.wernick.eu.com/wp-content/uploads/2012/02/Des-Moines-1f.jpg

3.17 (b)   http://www.wernick.eu.com/wp-content/uploads/2012/02/Farshid-Assassi-Ph.-Des-Moines-3.jpg

3.17 (c)   http://www.bdonline.co.uk/Pictures/120xAny/P/Pictures/web/o/c/f/okatechlouvrediag_bw_copy.jpg

Chapter 4

4.1 (a)   Carvalho, Paulo

4.1 (b)   Carvalho, Paulo

4.2   Carvalho, Paulo

4.3 (a)   Louter, C. 2011. "Fragile yet Ductile - Structural Aspects of Reinforced Glass Beams." Delft University of Technology, TUDelft, p. 23.

4.3 (b)   Louter, C. 2011. "Fragile yet Ductile - Structural Aspects of Reinforced Glass Beams." Delft University of Technology, TUDelft, p. 23.

4.4 (a)   Louter, C. 2011. "Fragile yet Ductile - Structural Aspects of Reinforced Glass Beams." Delft University of Technology, TUDelft, p. 22.

4.4 (b)   Louter, C. 2011. "Fragile yet Ductile - Structural Aspects of Reinforced Glass Beams." Delft University of Technology, TUDelft, p. 262.

4.5 (a)   Cruz, Paulo J. S., and José Pequeno. 2008. "Timber-Glass Composite Structural Panels: Experimental Studies & Architectural Applications." In *Challenging Glass*, eds. Freek Bos, Christian Louter, and Fred A. Veer. Delft: IOS Press, p. 456.

4.5 (b)   Cruz, Paulo J. S., and José Pequeno. 2008. "Timber-Glass Composite Structural Panels: Experimental Studies & Architectural Applications." In *Challenging Glass*, eds. Freek Bos, Christian Louter, and Fred A. Veer. Delft: IOS Press, p. 456.

4.6   Speranzini, Emanuela and Neri, Paolo. 2009. "Structural Behaviour of "Reinforced Glass", In *Glass Performance Days*. Tampere. p. 355.

4.7 (a)   Feirabend, S. 2008. "Reinforced Laminated Glass." In *Challenging Glass*, eds. Freek Bos, Christian Louter, and Fred A. Veer. Delft: IOS Press, p. 472.

4.7 (b)   Feirabend, S. 2008. "Reinforced Laminated Glass." In *Challenging Glass*, eds. Freek Bos, Christian Louter, and Fred A. Veer. Delft: IOS Press, p. 477.

4.8   Carvalho, Paulo

4.9   Carvalho, Paulo

4.10   Adapted from Bagger, Anne. 2010. "Plate Sheel Structures of Glass - Studies Leading to Guidelines for Structural Glass." Technical University of Denmark, p. 84.

4.11 (a)   Adapted from documents provided by Willareth, Phillipe.

4.11 (b)   Willareth, Philippe, and Daniel Meyer. 2011. "A New Folding Glass Roof for the Historic City Swimming Hall Zurich." In *Glass Performance Days*, Tampere, p. 623.

4.12 (a)   Adapted from Neugebauer, Jürgen. 2005. "A Special Fixation With Which The Broken Laminated Safety Glass Is Prevent From Falling." In *Glass Processing Days*, Tampere, p. 10.

4.12 (b)   Adapted from Neugebauer, Jürgen. 2013. "Stainless Steel Fabric as a Connection System for Bomb Blast Glass." In *COST Action TU0905, Mid-Term Conference on Structural Glass*, eds. J. Belis, C. Louter, and D. Mocibob. London: Taylor and Francis, 493–98.

4.13   Adapted from Wellershoff, F., G. Lori, M. Zobec, and K. Osterland. 2013. "Structural Design of Blast Enhanced Cable Net Facades." In *COST Action TU0905, Mid-Term Conference on Structural Glass*, eds. J. Belis, C. Louter, and D. Mocibob. London: Taylor and Francis, p. 124.

4.14 (a)   Adapted from Puller, K. 2012. "Untersuchung Des Tragverhaltens von in Die Zwischenschicht von Verbundglas Integrierten Lasteinleitungselementen." Universität Stuttgart, p. 77.

4.14 (b)   Adapted from Puller, K. 2012. "Untersuchung Des Tragverhaltens von in Die Zwischenschicht von Verbundglas Integrierten Lasteinleitungselementen." Universität Stuttgart, p. 88.

4.14 (c)   Adapted from Puller, K. 2012. "Untersuchung Des Tragverhaltens von in Die Zwischenschicht von Verbundglas Integrierten Lasteinleitungselementen." Universität Stuttgart, p. 92.

4.15 (a)   Belis, Jan, Dieter Callewaert, Didier Delincé, and Rudy Impe van. 2009.

"Experimental Failure Investigation of a Hybrid Glass/steel Beam."
Engineering Failure Analysis 16(4), p. 1165.

4.15 (b)   Louter, C. 2011. "Fragile yet Ductile - Structural Aspects of Reinforced Glass
Beams." Delft University of Technology, TUDelft, p. 36.

Chapter 5

5.1   Carvalho, Paulo

5.2 (a)   http://www.krepcio.com/vitreosity/archives/Photo-crownglass.jpg

5.2 (b)   http://explorepahistory.com/kora/files/1/2/1-2-1322-25-ExplorePAHistory-
a0k9s0-a_349.jpg

5.3   Carvalho, Paulo

5.4   Carvalho, Paulo

5.5   Haldimann, Mathias, Andreas Luible, and Mauro Overend. 2008. *Structural
Use of Glass*. Zurich: IABSE.

5.6   Carvalho, Paulo

5.7   Carvalho, Paulo

5.8   Feirabend, S. 2010. "Steigerung Der Resttragfähigkeit von
Verbundsicherheitsglas Mittels Bewehrung in Der Zwischenschicht."
Universität Stuttgart, Germany. p.18.

5.9   Carvalho, Paulo

5.10   IPA. 1993. "Designers, Specifiers and Buyers Handbook for Perforated Metals."
Designers, Specifiers and Buyers Handbook for perforated metals, p. 93.

5.11   IPA. 1993. "Designers, Specifiers and Buyers Handbook for Perforated Metals."
Designers, Specifiers and Buyers Handbook for perforated metals, p. 49.

5.12   IPA. 1993. "Designers, Specifiers and Buyers Handbook for Perforated Metals."
Designers, Specifiers and Buyers Handbook for perforated metals, p. 12.

Chapter 6

6.1 - 6.22   Carvalho, Paulo

Chapter 7

7.1 - 7.30   Carvalho, Paulo

Chapter 8

8.1 - 8.19   Carvalho, Paulo

Chapter 9

9.1 - 9.18   Carvalho, Paulo

Chapter 10

10.1 - 10.35   Carvalho, Paulo

Appendix

Patent nº PT 106772 B

Reinforced glass modular system

During the development of the *reinforced glass connection technique* a close contact was established with the University of Minho Intellectual Property department (TecMinho) to evaluate the feasibility to patent the solution. During this process a provisional patent request was prepared and submitted on January 2013. It confirmed that the proposed invention was original and could be industrially developed, thus was considered patentable. The patent request for national invention with the number 106772 was conceived in 2015-02-03 and published on the PI 26/2015 bulletin in 2015-02-06. Following is the final version of the patent (in Portuguese).

---

inpi instituto nacional
da propriedade industrial
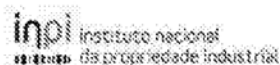
(11) Número de Publicação: **PT 106772 B**

(51) Classificação Internacional:
B32B 17/00 (2006.01)

(12) **FASCÍCULO DE PATENTE DE INVENÇÃO**

---

(54) Epígrafe: **SISTEMA MODULAR DE VIDRO REFORÇADO**

(57) Resumo:

A PRESENTE INVENÇÃO REFERE-SE A UM SISTEMA DE LIGAÇÃO PARA ESTRUTURAS DE VIDRO. COM BASE NOS CONCEITOS DE LIGAÇÃO EMBEBIDA E VIDRO REFORÇADO, É PROPOSTO UM NOVO TIPO DE LIGAÇÃO, QUE TIRA PROVEITO DA ELEVADA RESISTÊNCIA À COMPRESSÃO DO VIDRO E DA CONSIDERÁVEL RESISTÊNCIA À TRAÇÃO DO REFORÇO DE AÇO PARA CONSEGUIR UMA SOLUÇÃO DE LIGAÇÃO DISCRETA SEMITRANSPARENTE PARA USO ESTRUTURAL. O SISTEMA MODULAR DE VIDRO REFORÇADO PROPOSTO É COMPOSTO POR TRÊS COMPONENTES PRINCIPAIS: VIDRO LAMINADO, REFORÇO E PERFIL MACIO. MAIS CONCRETAMENTE, REFERE-SE A UM SISTEMA QUE COMPREENDE UM OU MAIS MÓDULOS CADA QUAL COMPREENDIDO POR PELO MENOS DOIS PANOS DE VIDRO (2) LAMINADOS EMBEBENDO UMA CAMADA INTERCALAR ADESIVA (3) E UMA CAMADA DE REFORÇO (4) MAIS COMPRIDA QUE PELO MENOS UM BORDO DOS PANOS DE VIDRO (2), EM QUE CADA MÓDULO ESTÁ CONECTADO ATRAVÉS DA JUNÇÃO DA CAMADA DE REFORÇO (4) DE CADA MÓDULO COM UMA CAMADA INTERMÉDIA (5) COM PERFURAÇÕES DE APARAFUSAMENTO (6, 7) DA REFERIDA JUNÇÃO.
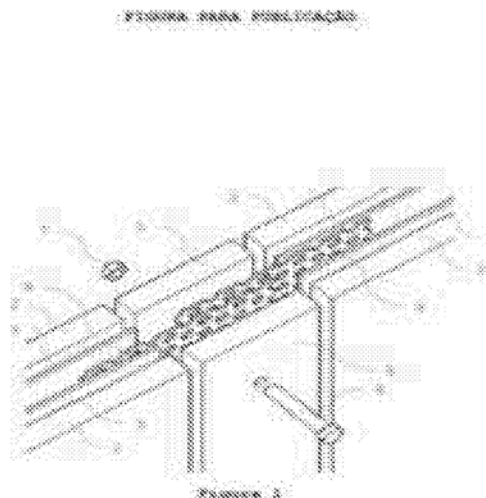
RESUMO

Sistema modular de vidro reforçado

A presente invenção refere-se a um sistema de ligação para estruturas de vidro. Com base nos conceitos de ligação embebida e vidro reforçado, é proposto um novo tipo de ligação, que tira proveito da elevada resistência à tracção do reforço de aço para conseguir uma solução de ligação discreta semi-transparente para usos estrutural. O sistema modular de vidro reforçado proposto é composto por três componentes principais: vidro laminado, reforço e perfil macio. Mais concretamente, refere-se a um sistema que compreende um ou mais módulos cada qual compreendido por pelo menos dois panos de vidro (2) laminados embebendo uma camada intercalar adesiva (3) e uma camada de reforço (4) mais comprida que pelo menos um bordo dos panos de vidro (2), em que cada módulo com uma camada intermédia (5) com perfurações de aparafusamento (6,7) da referida junção.

DESCRIÇÃO

Sistema modular de vidro reforçado e método de fabrico do mesmo

Domínio da Invenção

A presente invenção refere-se genericamente a estruturas de vidro. Em particular, consiste num sistema modular de vidro reforçado para uso em fachadas, coberturas ou divisórias de edifícios. Esta invenção destina-se à área de arquitectura e engenharia civil (construção civil).

Antecedentes da invenção

A utilização de elementos de vidro como parte integrante de estruturas em edifícios tem conhecido um grande incremento nas últimas décadas. No entanto a fragilidade do vidro e o seu comportamento imprevisível é ainda um desafio para o seu uso estrutural. A falta de conhecimento e normalização leva a que as metodologias vigentes recorram a um sobredimensionamento das estruturas para que em caso de quebra de um elementos os restantes que compõem a estrutura sejam capazes de garantir a estabilidade da estrutura. Este tipo de redundâncias estruturais leva a que as estruturas de vidro sejam consideradas especiais, principalmente pelo custo associado. Recentemente têm sido desenvolvidas várias soluções de estruturas de vidro reforçadas com elementos de aço (ou outros materiais com elevada resistência à tração), que à semelhança do que se obteve no betão, o comportamento frágil é redimido pelo efeito mecânico conjunto com o reforço. No caso do vidro não se evita a sua quebra, porém permite-se controlar os efeitos de uma eventual quebra, evitando o colapso total sem recorrer a um sobredimensionamento da estrutura. Este comportamento pós-rotura melhorado evita o referido sobredimensionamento da estrutura, com vantagens quer em termos de peso como de custo.

A solução específica de vidro reforçado com chapas ou malhas metálicas perfuradas de reduzida espessura embebidas no laminado oferece a possibilidade de utilizar elementos de vidro temperado para assim conceber elementos de maior dimensão. Este é tipo de vidro que oferece uma maior resistência antes de quebra, no entanto em caso de quebra, a energia libertada devido ao tratamento térmico leva a uma desintegração do elemento em pedaços de pequena dimensão. Elementos de vidro temperado, mesmo que laminado, oferecem uma resistência pós-rotura reduzida, principalmente a temperaturas elevadas. Quando reforçados com chapas ou malhas metálicas perfuradas, a transparência é garantida devido à perfuração e a capacidade estrutural pós-rotura melhora consideravelmente.

Quando se aborda a questão de ligação estrutural entre elementos de vidro, o binário transparência-fragilidade torna-se mais evidente. A incapacidade de absorver concentrações de tensão aconselha um aumento da área de contato para assim transferir uniformemente as cargas. No entanto, a opacidade dos elementos de ligação comuns é incompatível com a desejada transparência. A solução mais comum passa pela utilização de elementos de ligação metálicos com tamanho tendencialmente reduzido. O desenvolvimento recente de soluções adesivas trouxe novas oportunidades, ao oferecer métodos fortes e seguros de ligação adesiva vidro-vidro e metal-vidro. As excelentes propriedades adesivas de intercalares ionoméricos permitiram o desenvolvimento de um novo tipo de ligação em que o elemento metálico é embebido entre os intercalares poliméricos. A transferência de cargas deste tipo de ligação torna-se mais gradual ao combinar os mecanismos de adesão e contacto.

James O'Challaghan apresentou uma solução que se encontra disposta nas lojas Apple e que consiste numa solução de ligação em que o elemento metálico está embebido entre camadas de vidro laminado para utilização entre outros, em degraus de escadas de vidro. Esta solução apresenta um formato semicircular no lado interior para reduzir as tensões internas, e recto do outro para ficar faceado e totalmente embebido em relação ao bordo do vidro, sendo laminada na terceira camada de vidro do laminado.

Uma questão da incompatibilidade em relação ao material usado para a inserção metálica é referenciada como problema durante a laminação, devido à considerável espessura do mesmo. Diferentes tipos de aço e alumínio causaram a quebra do vidro durante o processo de laminagem em autoclave e em alguns casos após a montagem. Foi selecionado titânio por ter um coeficiente de expansão térmico e propriedades de condução próximas do vidro, apesar do elevado custo do material. Comparada com esta solução, a reduzida espessura da inserção de metal da invenção, evita a necessidade de utilizar mais do que dois vidros, reduz o problema de diferentes coeficientes de expansão térmica dos materiais que compreendem o sistema e evita a necessidade de recortar e afundar o vidro intermédio de forma a prever espaço para embeber a peça metálica.

Anne Bagger apresenta uma solução de ligação em que uma chapa é embebida no bordo do vidro intermédio usando silicone estrutural, sendo as faces constituídas por três vidros laminados com intercalar adesivo Sentry Glas. As soluções testadas são referidas como possuindo um pano de vidro intermédio mais espesso, sendo 20 mm refundado de forma a criar um canal contínuo periférico onde uma chapa de alumínio com 4 mm, e com uma largura de 50 mm, é colada utilizando silicone estrutural. Comparada com esta solução, a principal desvantagem, para além da necessidade de prever no mínimo três camadas de vidro, prende-se com o sistema construtivo. Metade da ligação tem que ser colada em obra, tornando-se bastante susceptível a problemas de adesão. É igualmente bastante difícil substituir um painel em caso de quebra. Igualmente ao caso anterior, a considerável espessura do elemento metálico embebido obriga a usar no mínimo três camadas de vidro.

Existe também uma solução criada por Phillip Willareth que consiste numa ligação para uma nova cobertura "de geometria dobrada" para o complexo de piscinas da cidade histórica de Zurique instalada durante o verão de 2011. Duas unidades de vidro laminado compreendendo cada uma dois painéis de vidro e um intercalar ionomérico (SentryGlas) são acopladas por tiras de metal perfurado embebidas no intercalar sem recuo do bordo do vidro.

As tiras metálicas de acoplamento foram quinadas ao longo de uma linha pré-perfurada, depois do processo de laminagem, para conceder a configuração desejada e preparar a unidade de vidro dobrada para instalação. Este sistema apresenta algumas limitações. Uma vez que os painéis são ligados por apenas uma tira metálica que é quinada após o processo de colagem, este sistema limita a dois o número máximo de painéis a serem ligados.

Também o transporte e montagem em obra requerem meios complexos devido à tridimensionalidade imposta pelos painéis à saída da fábrica. Em caso de quebra de um dos painéis, torna-se impossível de ser substituído individualmente, significando que o sistema acoplado tem que ser substituído, significando um custo superior. A espessura significativa da tira de metal, necessária para garantir a resistência às cargas de compressão, tensão e torção, e assim evitar o contacto entre os bordos do vidro, obriga por um lado a utilização de uma significativa espessura de intercalar para absorver a espessura da tira de metal; e contraindica por outro a sua extensão a todo o elemento de vidro para assim funcionar como reforço. Esta limitação estende-se aos materiais possíveis de utilizar para ligação, que terão que ter uma significativa rigidez, desconsiderando assim malhas metálicas e tecidos de fibra.

Apresenta-se também uma solução desenvolvida por Jurgen Neugebauer que consiste numa solução de retenção para ligação desenvolvida com o objectivo de aumentar a capacidade resistente residual para envidraçados em coberturas, na qual um mecanismo de retenção é incorporado. É proposto embeber um malha no intercalar de PVB, entre os painéis de vidro próximo dos bordos, sendo um dos lados da malha estendida para o exterior do vidro de forma a poder ser fixa à substrutura. Em caso de quebra do vidro, as forças de membrana aumentam, o que tende a puxar o vidro para fora do sistema de suporte, forçando a ligação a tornar-se efetiva. O objectivo é assegurar que em caso de quebra do vidro laminado, este mantém-se fixo e é impedido de colapsar.

Uma limitação desta solução prende-se com o facto de recorrer ao reforço para adicionar funções a uma solução de ligação comum, nomeadamente o melhoramento do desempenho pós rotura de panos de vidro e prevenção de queda. Não é feito nenhum melhoramento significativo ao elemento de ligação propriamente dito, de forma a reduzir a quantidade de metal estrutural necessário para suportar o vidro.

Ligação embebida e reforço do vidro com elementos metálicos finos são dois conceitos que a presente invenção combina com um elemento macio de contacto, de forma a explorar a máxima capacidade dos materiais que a compõem, possibilitando uma redução das espessuras das diversas camadas e por conseguinte a quantidade de material aplicado. Por outro lado, o detalhe construtivo permite um fabrico e aplicação modular, com vantagens adicionais em termos de custo.

Descrição Geral

A invenção refere-se a um sistema de ligação para estruturas de vidro. A ligação é considerada um ponto crítico das estruturas de vidro devido ao facto de ser neste ponto onde a concentração de tensões acontece, podendo levar à rotura. A possibilidade de embeber elementos metálicos no interior de uma unidade de vidro laminado permite alcançar uma melhor distribuição de tensões, porém a maioria das soluções existentes recorre a elementos metálicos de elevada espessura de forma a concentrar nesse elemento a transferência de todas as cargas. Esta característica leva à necessidade de prever camadas adicionais de vidro ou de intercalar apenas com o propósito de prever o espaço necessário para o embebimento eficaz do elemento metálico.

A presente invenção distingue-se desta filosofia ao prever uma distribuição da transferência de carga pelo reforço, de metal ou fibra, e pelo próprio vidro recorre a camada macia que intermedeia o contacto direto vidro-vidro.

Esta solução permite utilizar elementos de reforço de reduzida espessura, contribuindo para uma redução considerável do peso da estrutura. Por seu lado, a reduzida espessura torna viável a extensão do reforço a toda a superfície melhorando o comportamento pós-rotura. Adicionalmente os painéis são concebidos modelarmente, através do desenvolvimento de solução de ligação aparafusada, que torna o sistema construtivo mais flexível através da fácil execução em obra, evitando operações de colagem fora de fábrica, e permitindo a fácil substituição de painéis em caso de quebra.

Com base nos dois conceitos complementares expostos - ligação embebida e vidro reforçado - é proposto um novo tipo de ligação, que tira proveito da elevada resistência à compressão do vidro e da considerável resistência à tração do reforço de aço para conseguir uma solução de ligação discreta semi-transparente para uso estrutural. A possibilidade de estender o reforço para toda a superfície do vidro assegura um melhor comportamento pós-ruptura. Neste caso, ao ser desenvolvida a ligação através do reforço, este comportamento é ampliado pelo facto de se garantir uma ancoragem aos painéis adjacentes, compensando assim o comportamento viscoelástico dos intercalares poliméricos a temperaturas mais elevadas.

O sistema modular de vidro reforçado é composto por três componentes principais: vidro laminado, reforço e perfil macio. Esta solução procura um uso optimizado relativamente às características mecânicas de cada material, de forma a reduzir espessuras e assegurar a robustez estrutural. Em seguida são descritos com detalhe os elementos que compõem a invenção, as variações e intervalos possíveis. Em todos os elementos, pelo menos uma dimensão não é definida uma vez que depende da estrutura que se pretende construir, não sendo limitativa para a invenção em questão.

Relativamente ao elemento vidro, podem ser aplicados todos os tipos de vidro "flutuado", ou seja, vidro corrente para o sector da construção, quer no estado recozido ou com tratamento térmicos, nomeadamente termo-endurecido ou temperado.

Em termos de espessuras de vidro, cada painel simples (antes da laminação) deverá ter entre 6 mm e 25 mm. Considera-se preferencial que ambos os painéis tenham a mesma espessura uma vez que assim garante-se uma mais equilibrada distribuição dos esforços internos, mas poderão ser aplicados painéis com espessuras diferentes.

Relativamente ao tipo de intercalar a utilizar para tornar efetiva a colagem vidro-vidro e vidro-reforço, pode ser aplicado o PVB, EVA ou ionomérico. A aplicação de cada um destes intercalares terá implicações na profundidade de embebimento do reforço de acordo com as condições de carga, uso e ambientais, a definir em cada caso. Em termos de espessura do elemento de laminagem/colagem, este depende sempre da espessura do elemento de reforço, devendo ser sempre superior. Só assim se garante a existência de material de colagem entre o vidro e reforço, condição essencial para a qualidade da colagem. Estima-se que o intervalo de aplicação seja entre 1 mm e 6 mm correspondendo à gama de espessuras necessárias para embeber o reforço .

Relativamente ao reforço, podem ser aplicadas chapas metálicas perfuradas de aço inoxidável, malhas metálicas de fio fino de aço inoxidável ou tecido de fibra de alta resistência. A espessura total dos elementos de reforço deverá estar compreendida entre 0,5 mm e 4 mm. A partir desta espessura considera-se que o reforço deixa de ter espessura reunida uma vez que é necessário adicionar um terceiro vidro para obter a espessura interna necessária para o embeber. Relativamente à percentagem de perfuração/abertura dos elementos de reforço o sistema permite a aplicação de todo o espectro oferecido pela indústria, desde elevada abertura até reduzida abertura (dependendo da resistência de cada material e profundidade de embebimento a calcular em cada caso), passando por elementos sem aberturas, elementos misto com e sem aberturas ou elementos com aberturas customizadas aplicando padrões fabricados por encomenda. No caso das chapas metálicas, estas devem ser quinadas previamente ao processo de laminagem com ângulos compreendidos entre 90º e 150º.

Relativamente ao tipo de camada intermédia macia, poderá ser aplicado policarbonato, acrílico, nylon, POM ou alumínio. Estes elementos deverão ter uma espessura mínima de 6 mm e máxima de 30 mm, correspondendo às espessuras admissíveis de vidro que deverá ser semelhante, e ser maquinados com geometria de acordo com os desenhos anexos.

A posição do reforço em relação ao painel de vidro, nomeadamente a profundidade de embebimento deverá ser igual ou superior a 20 mm, estando limitada pela dimensão do próprio painel de vidro, podendo preenche-lo na totalidade.

Elementos de fixação, como por exemplo parafusos, porcas e silicone com propósito de selagem, são elementos complementares que permitem que o mecanismo de ligação seja efetivo. Os parafusos deverão ser de aço com dimensão de acordo com os restantes elementos que compõem a ligação (reforço e camada macia) estando compreendido entre 15 mm e 70 mm para o comprimento e 3 mm e 12 mm para o diâmetro. A distância entre os parafusos deverá estar compreendida entre 50 mm e 300 mm.

A solução foi concebida para ser montada em geometrias não complanares - "dobrada", "intersectada" ou em "casca" e assim adquirir rigidez tridimensional. A consequência estrutural de torna-se autoportante permite prescindir da necessidade de prever qualquer elemento estrutural auxiliar (p.ex. estrutura de aço de contraventamento), economizando material empregue e contribuindo para a distinção e refinamento estético relevante na comercialização de soluções de estruturas de vidro.

Em cada tipologia, a camada macia intermédia é concebida de acordo com o ângulo da disposição geométrica desejada e número de painéis: "intersectado" - mais do que dois painéis com 90°; "dobrado" - 2 painéis com ângulo 0° ≤ 120°; e "casca" com dois painéis com ângulo no intervalo de 120°≤ 180°.

Faz parte desta invenção o método de fabrico dos painéis de vidro laminado com reforço integrado e projectado para o exterior. Uma vez devidamente limpos, os vários materiais (com exceção do policarbonato) são dispostos em camadas e preparados para o processo de colagem.

O método usado preferencialmente é a laminação com manta de silicone (também pode ser usado o método de saco de vácuo, embora a um custo superior) que combina alta temperatura, para derreter a camada intermédia, pressão e vácuo para assegurar o pleno contacto entre as camadas e retirar o ar do interior. O facto de a chapa perfurada ser saliente em relação ao vidro, obriga à previsão de um conjunto de peças especiais em MDF cortadas a laser, de forma a se adaptarem com rigor à geometria específica. Por um lado calçam a chapa, evitando a deformação do metal pelo silicone tencionado, por outro asseguram a correta posição da chapa em relação ao vidro, evitando que se desloque ou afunde por gravidade durante o derretimento da película polimérica. Juntamente com estas, são aplicados perfis em madeira intercalados de forma a proteger o reforço nos locais onde não é abrangido pelos perfis especiais.

Breve descrição das figuras

Figura 1 - Axonometria explodida de pormenor de sistema de ligação com reforço de chapa perfurada em que (2) corresponde a placas de vidro, (3) intercalares adesivos, (5) camada intermédia macia, (6) parafuso, (7) porca e (9) um elemento de reforço em chapa perfurada.

Figura 2 - Axonometria explodida de pormenor de sistema de ligação com reforço de chapa mista em que (2) corresponde a placas de vidro, (3) intercalares adesivos, (5) camada intermédia macia, (6) parafuso, (7) porca (10) um elemento de reforço em chapa mista.

Figura 3 - Axonometria explodida de pormenor de sistema de ligação com reforço de tecido de fibra ou malha de arame em que (2) corresponde a placas de vidro, (3) intercalares adesivos, (5) camada intermédia macia, (6) parafuso, (7) porca e (11) um elemento de reforço em tecido de fibra ou malha de arame.

Figura 4 - Axonometria de módulo de vidro reforçado em solução dobrada em que (1) corresponde ao painel modular, (2) placas de vidro, (3) intercalares adesivos e (4) elemento de reforço.

Figura 5 - Axonometria explodida de módulo de vidro reforçado em solução dobrada em que (2) corresponde a placas de vidro, (3) intercalares adesivos e (4) elemento de reforço.

Figura 6 - Axonometria de sistema modular de vidro reforçado em solução "dobrada" em que (1) corresponde ao painel modular, (5) camada intermédia macia e (6) parafuso.

Figura 7 - Axonometria explodida de sistema modular de vidro reforçado em solução "dobrada" em que (2) corresponde a placas de vidro, (3) intercalares adesivos, (4) elemento de reforço (5) camada intermédia macia e (6) parafuso.

Figura 8 - Axonometria de pormenor de ligação de módulos de vidro reforçado em solução "dobrada" em que (2) corresponde a placas de vidro, (3) intercalares adesivos, (4) elemento de reforço (5) camada intermédia macia, (6) parafuso e (8) silicone.

Figura 9 - Axonometria explodida de pormenor de ligação de módulos de vidro reforçado em solução "dobrada" em que (2) corresponde a placas de vidro, (3) intercalares adesivos, (4) elemento de reforço (5) camada intermédia macia, (6) parafuso e (7) porca.

Figura 10 - Axonometria de elemento construtivo (horizontal ou vertical) utilizando sistema modular de vidro reforçado em solução "dobrada".

Figura 11 - Axonometria de elemento construtivo (horizontal ou vertical) utilizando sistema modular de vidro reforçado em solução "casca".

Figura 12 - Axonometria de elemento construtivo (horizontal ou vertical) utilizando sistema modular de vidro reforçado em solução "intersectada".

Figura 13 - Axonometria de perfil auxiliar de laminação em MDF cortado a laser.

Figura 14 - Axonometria de perfil auxiliar de laminação em madeira.

Descrição detalhada da invenção

A invenção consiste num painel modular (1) composto por duas placas de vidro (2), dois intercalares adesivos (3) e um elemento de reforço (4).

A sua eficácia da invenção consiste na combinação de três mecanismos de transferência de carga, de acordo com o interface em questão (Fig. 1):

- Adesivo entre o vidro laminado e o reforço, por meio de pelo menos dois intercalares poliméricos. O reforço é semi-embebido entre dois painéis de vidro antes da laminação a uma profundidade mínima de 20 mm. Esta profundidade permite garantir uma colagem eficaz durante o fabrico e assim garantir uma correta transferência de cargas.

- Mecânico entre o reforço e o perfil macio intermediário, utilizando parafusos e porcas de aço. Os parafusos atravessam os perfis macios intermediários (previamente furados) e o reforço afim de fixar firmemente ambos os materiais.

- Contacto entre o vidro e o perfil macio intermediário com o auxílio de silicone apenas para fins de selagem.

A invenção permite desenvolver estruturas com diferentes geometrias sem alterar a composição da mesma. Faz parte desta invenção três soluções de disposição geométrica autoportantes com elevada inércia, com o objectivo de conceber as estruturas de vidro sem a necessidade de prever uma estrutura auxiliar opaca. Considera-se que a definição de uma estrutura definida apenas por elementos transparentes é uma característica importante em termos de diferenciação e viabilidade comercial. Portanto, o desenvolvimento do detalhe construtivo teve a preocupação de ensaiar soluções que possam ser montadas de forma não-complanar e, assim, alcançar a necessária rigidez tridimensional.

O detalhe construtivo para uma solução dobrada a 90° é mostrado nas Figuras 5 e 6. Os painéis de vidro são ligeiramente escalonados, a fim de se adaptarem à geometria angular e reduzir o espaço da junta para o mínimo de 20 mm, necessário para a integração dos perfis macios intermediários. A unidade do painel de vidro e a reduzida espessura do conjunto laminado foram considerados desde o início como as forças motrizes para a concepção do detalhe construtivo. Todos os outros materiais seriam integrados tanto quanto possível. A solução resultante oferece a vantagem adicional de reduzir a necessidade de manutenção e limpeza.

Em cada tipologia o perfil macio intermediário é concebido de acordo com o ângulo da disposição geométrica desejada e número de painéis: "intersectado" - mais do que dois painéis com 90°; "dobrado" - 2 painéis com ângulo 0° ≤ 120°; e "casca" com dois painéis com ângulo no intervalo de 120°≤ 180°. O elemento metálico apresenta uma reduzida espessura o que permite reforçar o elemento de vidro ao mesmo tempo que faz parte do mecanismo de ligação. A sua reduzida espessura evita a necessidade de sobre-dimensionar a espessura do intercalar ou a necessidade de camadas de vidro adicional de forma a ser possível absorver a espessura do metal e embebê-lo.

O sistema resultante é também caracterizado por uma elevada flexibilidade construtiva permitindo ligar painéis de acordo com diferentes tipologias, resultando em várias geometrias possíveis com aplicação horizontal (cobertura), vertical (parede ou fachada) ou oblíqua (envidraçado inclinado ou "casca").

O pormenor desenvolvido para o sistema de ligação requer um elevado grau de precisão para ser estruturalmente eficaz. Embora os três materiais principais - vidro, chapa aço e policarbonato - sejam fornecidas em folha, são necessários métodos e tecnologias distintas de corte, moldagem e acabamento, com as tolerâncias e limitações correspondentes. De seguida é feita uma descrição dos vários passos necessários ao fabrico da invenção:

1- Os vidros fornecidos em tamanho "jumbo" (6 x 3,21 m) são cortados com ferramenta de diamante controlada por CNC. Um primeiro corte é feito segundo uma medida intermédia, uma vez que deverá ser prevista uma margem mínima de 2 mm para permitir a moagem e polimento. Só então é que o tamanho final é obtido.

2- As chapas perfuradas de aço com espessura reduzida (menos do que 2 mm) são geralmente fornecidas em 2 x 1 m de dimensão. A chapa é cortada para o tamanho pretendido e posteriormente quinada segundo um ângulo de correspondente.

3- O perfil macio intermediário, também fornecido em folha, é primeiro maquinado com uma fresadora CNC, para adquirir a geometria pretendida e posteriormente polido com sabão especial para readquirir a desejada transparência (no caso do policarbonato ou acrílico). No final executa-se as furações por onde passam os parafusos.

4- Uma vez devidamente limpos, os vários materiais (com exceção do perfil macio intermediário) são dispostos em camadas e preparados para o processo de colagem. O método preferencial a usar é a laminação com manta de silicone que combina alta temperatura, para derreter o intercalar adesivo, pressão e vácuo para assegurar o pleno contacto entre as camadas e retirar o ar do interior.

5- O facto de a chapa perfurada ser saliente em relação ao vidro, tornou necessário a previsão de um conjunto de peças especiais em MDF cortadas a laser, de forma a se adaptarem com rigor à geometria específica. Por um lado calçam a chapa, evitando a deformação do metal pelo silicone tencionado, por outro asseguram a correta posição da chapa em relação ao vidro, evitando que se desloque ou afunde por gravidade durante o derretimento da película polimérica.

Uma vez terminado o processo de laminação, os painéis estão prontos para aplicação em obra. A sua aplicação consiste em:

1 - Colocação de pelo menos dois painéis em posição, sobrepondo as faces exteriores dos elementos de reforço que se encontram semi-embedidos.

2- Vedação com silicone transparente em todo o perímetro dos painéis de vidro, com especial atenção nas zonas com reforço semi-embebido.

3 - Colocação dos perfis macios intermediários em posição.

4 - Fixação dos vários elementos com a aplicação dos parafusos através da furação previamente feita nos perfis macios intermediários.

Estas tarefas deverão ser repetidas pelos vários painéis modulares que compõem a estrutura.

Reivindicações:

1. Sistema modular de vidro reforçado caracterizado por compreender módulos constituídos por dois panos de vidro laminados com intercalares adesivos, elementos finos de reforço semi-embebidos mais compridos que os panos de vidro, em que cada módulo está conectado através de elementos de fixação localizados na sobreposição da parte exterior dos elementos de reforço, juntamente com perfis macios a intermediar o contacto entre bordos de vidro, com perfurações para acomodar os parafusos e porcas.

2. Sistema de ligação de vidro, de acordo com a reivindicação anterior, caracterizado por o perfil macio ter a mesma espessura que o pano de vidro.

3. Sistema de ligação de vidro, de acordo com a reivindicação anterior, caracterizado por o contacto entre o perfil macio e o vidro ser feito por silicone.

4. Sistema de ligação de vidro, de acordo com a reivindicação anterior, caracterizado por o perfil macio ser de Policarbonato, Acrílico, Alumínio, Pom ou Nylon.

5. Sistema de ligação de vidro, de acordo com a reivindicação 1, caracterizado por o adesivo intercalar ser ionomérico, PVB, EVA ou Epoxy.

6. Sistema de ligação de vidro, de acordo com a reivindicação anterior, caracterizado por preferencialmente ser usado um intercalar adesivo ionomérico.

7. Sistema de ligação de vidro, de acordo com a reivindicação 1, caracterizado por o reforço ter uma profundidade de embebimento igual ou superior a 20 mm.

8. Sistema de ligação de vidro, de acordo com a reivindicação anterior, caracterizado por o reforço ser escolhido entre chapas metálicas, tecidos de fibra ou malhas de arame.

9. Sistema de ligação de vidro, de acordo com a reivindicação anterior, caracterizado por o material de reforço ser perfurado, não perfurado ou misto.

10. Sistema de ligação de vidro, de acordo com as reivindicações 7 - 9, caracterizado por preferencialmente ser utilizadas chapas metálicas como reforço.

11. Sistema de ligação de vidro, de acordo com a reivindicação anterior, caracterizado por as chapas metálicas terem uma espessura de 0,5 - 4 mm.

12. Sistema de ligação de vidro, de acordo com as reivindicações 1 a 11, caracterizado por o ponto de junta de cada módulo permitir a ligação de dois ou mais módulos.

13. Sistema de ligação de vidro, de acordo com as reivindicações 1 a 12, caracterizado por obter-se painéis de diferentes geometrias com posições horizontais, verticais ou oblíquas.

14. Sistema de ligação de vidro, de acordo com a reivindicação anterior, caracterizado por a geometria horizontal ser cobertura envidraçada ou de abóbada.

15. Sistema de ligação de vidro, de acordo com a reivindicação 13, caracterizado por a geometria vertical ser de parede ou fachada.

16. Sistema de ligação de vidro, de acordo com a reivindicação 13, caracterizado por a geometria oblíqua ser envidraçado inclinado ou cúpula.

17. Sistema de ligação de vidro, de acordo com as reivindicações 1 - 16, caracterizado por os módulos serem ligados com geometria dobrada, intersectada ou cúpula, entre outros.

18. Sistema de ligação de vidro, de acordo com as reivindicações 1 - 17 caracterizado por cada módulo ser substituído independentemente.
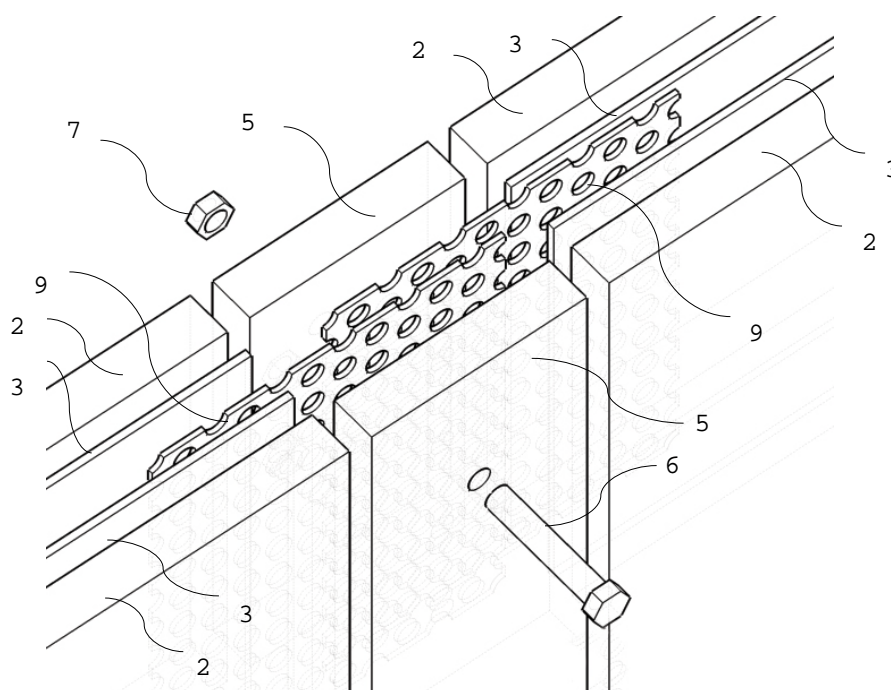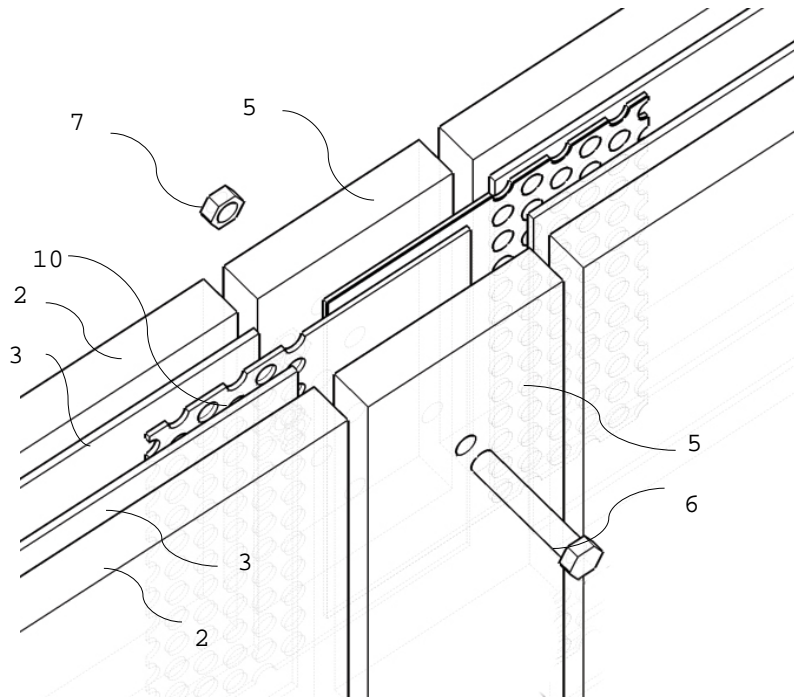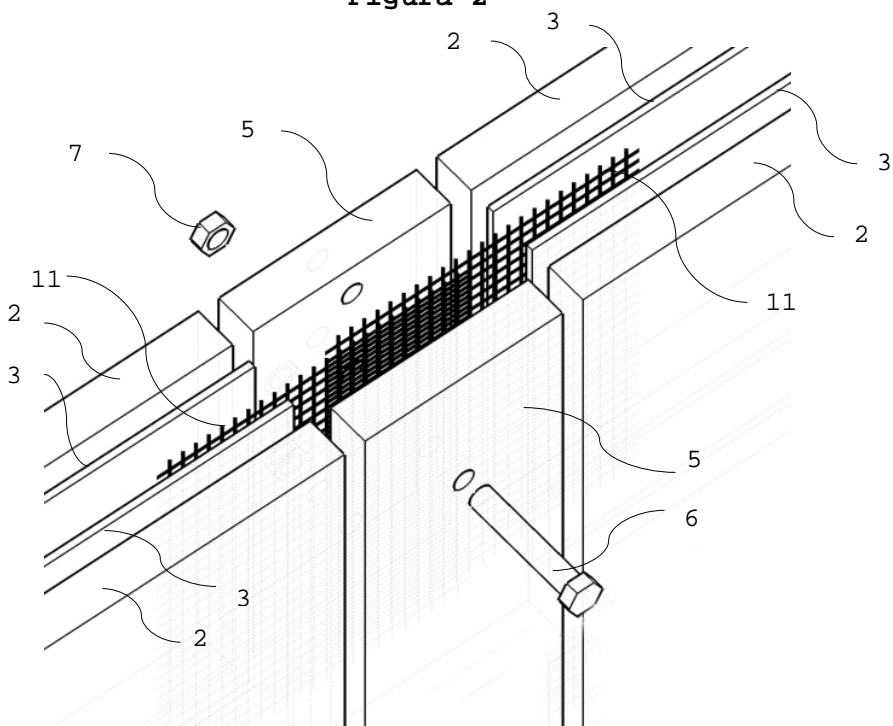
Figuras

Figura 1

Figura 2
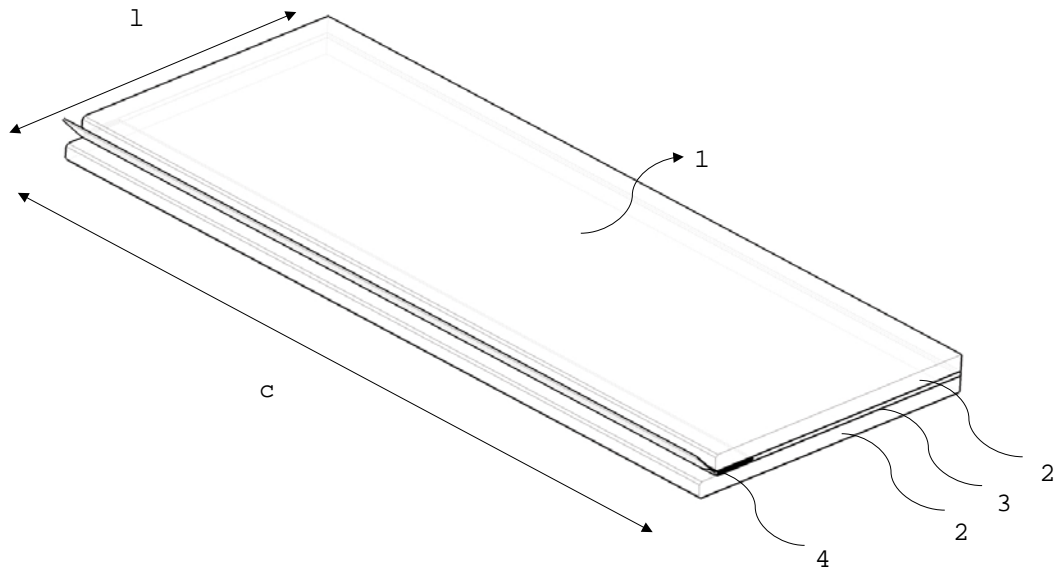

Figura 3

Figura 4
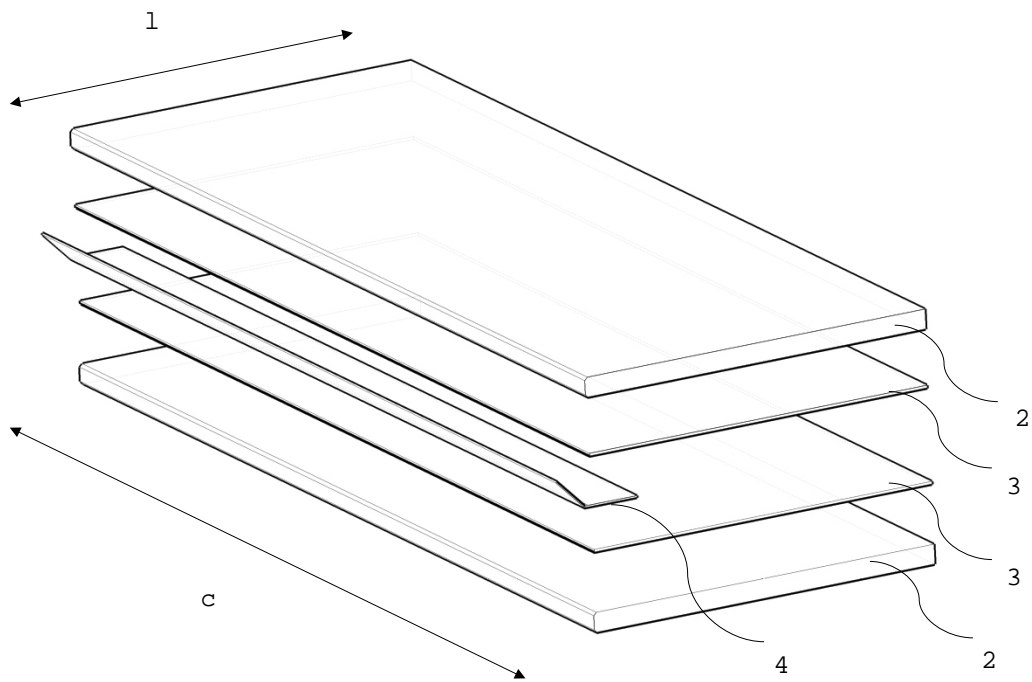
Figura 5
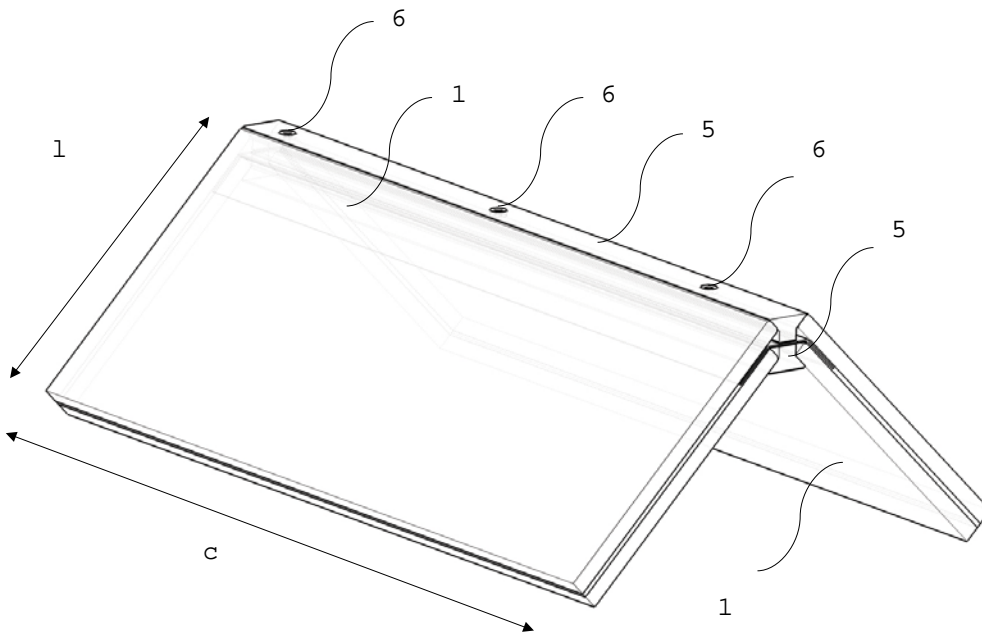
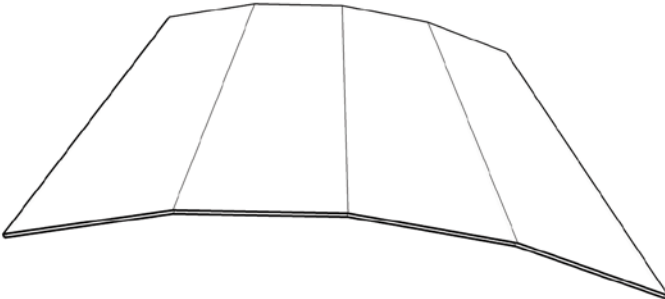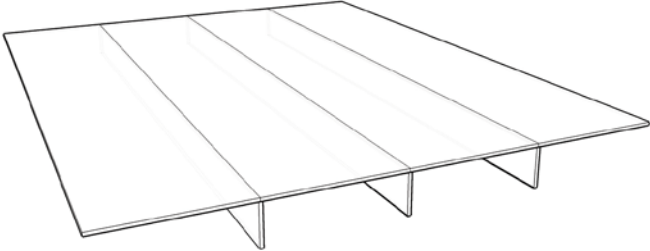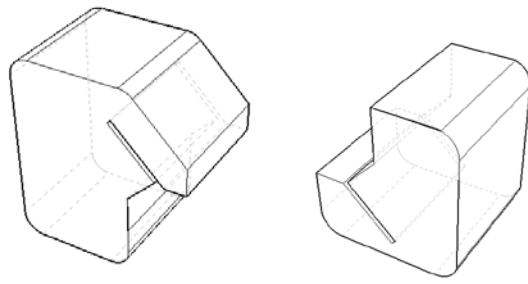**Figura 6**
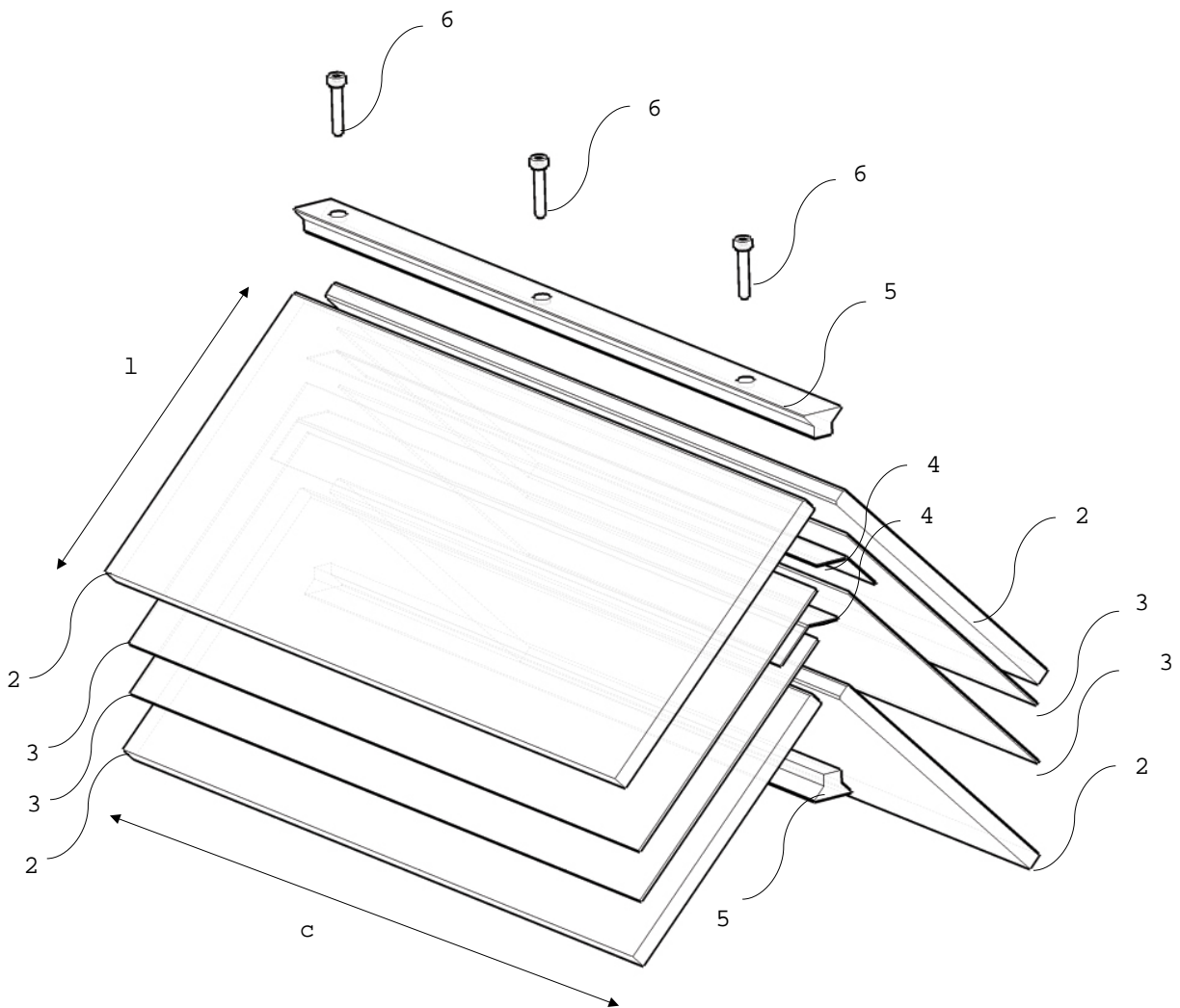
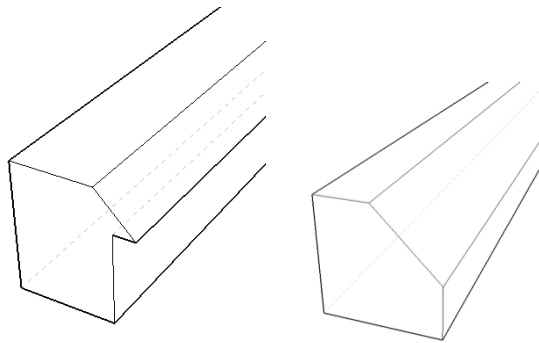**Figura 7**
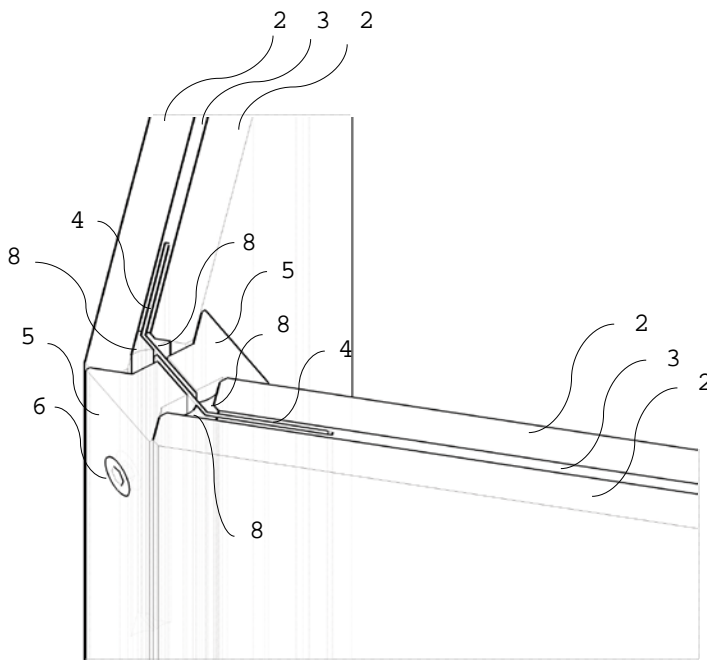
Figura 8
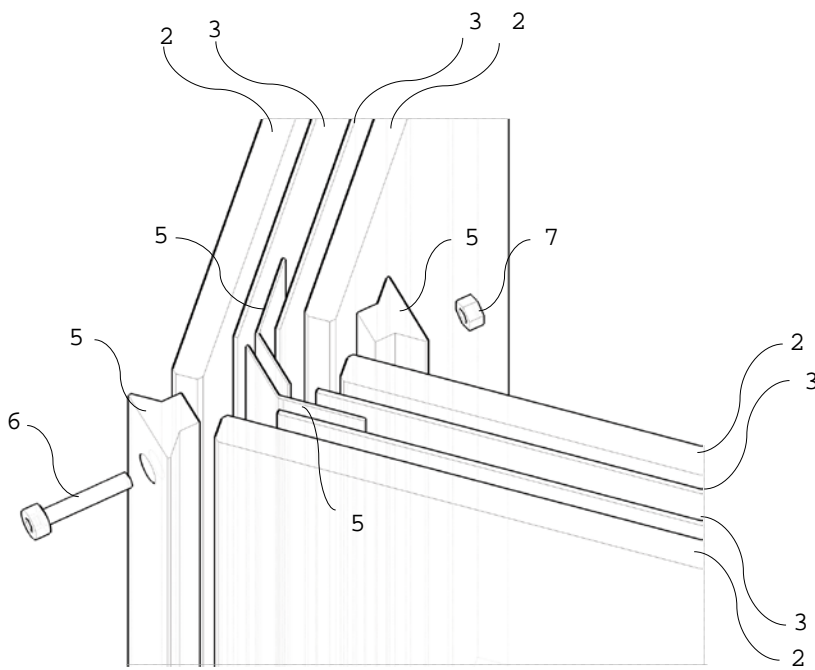
Figura 9
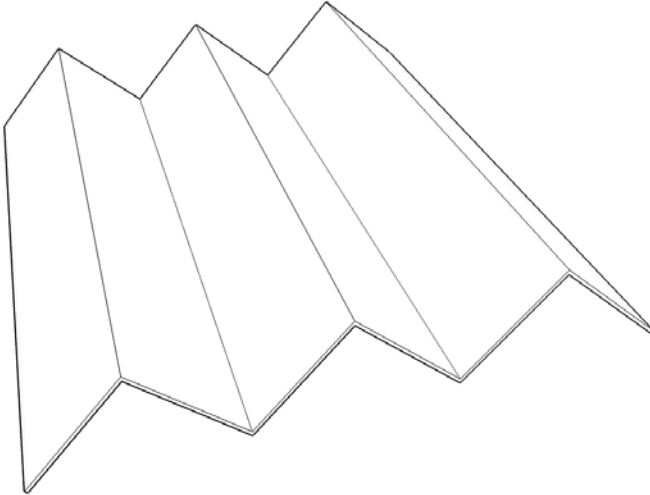
Figura 10

Figura 11

Figura 12

Figura 13

Figura 14

Curriculum Vitae

Paulo Lopes Lago de Carvalho

Born on the 15th of April 1982 in Porto, Portugal.

Graduated from the School of Architecture of the University of Minho in 2005 with honours.

Trainee and assistant at the architectural office of Prof. Arch. Manuel Fernandes de Sá in Porto, from 2005 to 2008, working and coordinating design projects of different programmes and scales.

Co-founder of Prod Arquitectura Lda. in 2008, an architectura and design atelier based in Viana do Castelo, where he develops applied research and design activity.

Research fellow in the SipdECO project "Development of eco-efficient partition wall solutions" in 2009 at ISISE - University of Minho.

PhD researcher at the School of Architecture of the University of Minho since 2010, in the field of Construction and Technology, under the supervision of Prof. Paulo Cruz and co-supervision of Dr. Fred Veer.

Invited assistant at the Integrated Master Course of Architecture at the University of Minho from 2011 to 2013, where he was the regent of the curricular unit "Seminar - Innovation and Technology".

Guest professor at the School of Architecture at the University of Minho teaching courses on construction and product design.

Member of the European COST Action TU0905 "Structural Glass" from 2011 to 2014, at the Task Group 13 -"Hybrid components" from the Working Group 4 - "Novel Glass Assemblies" (www.glassnetwork.org).

Visiting researcher at EPFL - ICOM (Switzerland) in June 2013, hosted by Dr. Christian Louter.

Visiting researcher at TU Delft (Netherlands) in June 2012 and November 2013, hosted by Dr. Fred Veer.

Prizes and recognitions

Merit scholarship (2005) granted by the Ministry of Science, Tech. and Higher Education.

Merit prize (2003 and 2004) granted by the University of Minho.

Research scholarship in the scope of the "Sipdeco" project (January to September 2009).

PhD scholarship granted by Fundação Ciência e Tecnologia FCT (SFRH_BD_62061_2009).

Patents and design registrations

Patent - "*Reinforced glass modular system*", accepted on (submitted on January 2014), Prof. Paulo Cruz, Arch. Paulo Carvalho.

Community Design Registration - "*Oblong glass fixing*", No 002023127-0001, Registered 11/04/2012, Prof. Paulo Cruz, Arch. Paulo Carvalho.

Research projects

FCT project - "*S-GLASS - Structural Performance & Design Rules of Glass Beams Externally Reinforced*". (University of Minho and University of Coimbra), coordination: Paulo Cruz, Funding: FCT - PTDC/ECM/116609/2010, period: April 2012 - March 2015.

 Qren project - "*METAL GLASS - High Performance Safety Glass*". VICER, Vidraria Central de Ermesinde Lda. and Universidade do Minho, coordination Paulo Cruz, period: March 2012 - August 2013.

Main publications

Carvalho, P.L., Cruz, P.J.S., Veer, F.A. " Connecting through reinforcement - design, testing and construction of a folded reinforced structure". Journal od Façade Design and Engineering 2 (2014) 109-122, DOI 10.3233/FDE-140013, IOS Press.

Carvalho, P.L.L., Cruz, P.J.S., Veer, F.A. "Design, Testing and Construction of a folded reinforced glass". Challenging Glass 4 Conference & Cost Action Tu0905 Final Conference, Lausanne, February 2014.

Carvalho, P.L.L., Cruz, P.J.S., Veer, F.A. "Reinforced Glass Connection - Concept, test and detail." ICSA 2013 – Second Int. Conf. Structures and Architecture, Guimarães, July 2013.

Carvalho, P.L.L., Cruz, P.J.S., Veer, F.A. "Connecting through reinforcement – Experimental analysis of the temperature dependent behaviour". COST Action TU0905, Mid-term Conference on Structural Glass, Porec, April 2013.

Carvalho, P.L.L., Cruz, P.J.S., Veer, F.A. "Connecting through reinforcement – Experimental analysis of a glass connection using perforated steel plates. Challenging Glass 3 – Conference on Arch. and Struc. Applications of Glass, TU Delft, June 2012.